

Volume III

Final
Report

September 1972

Book 1
Design Analysis
and Trade Studies

Astronomy Sortie Missions Definition Study

(NASA-CR-129677) ASTRONOMY SORTIE MISSION
DEFINITION STUDY, VOLUME 3: BOOK 1:
DESIGN ANALYSIS AND TRADE STUDIES Final
Report (Bendix Corp.) Sep. 1972 382 p

00/99 Unclas
16540

MARTIN MARIETTA

Itek

Bendix

Contract NAS8-28144
DPD No. 282
DR No. MA-04

AM 1002-1004

Volume III

Final
Report

September 1972

Book 1

**ASTRONOMY
SORTIE MISSION
DEFINITION STUDY**

**DESIGN ANALYSIS AND
TRADE STUDIES**

Prepared for:

National Aeronautics and Space Administration
George C. Marshall Space Flight Center
Huntsville, Alabama

**BENDIX CORPORATION
NAVIGATION AND CONTROL DIVISION
Denver, Colorado 80201**

**ITEK CORPORATION
OPTICAL SYSTEMS DIVISION
Lexington, Massachusetts 02173**

**MARTIN MARIETTA CORPORATION
DENVER DIVISION
Denver, Colorado 80201**

FOREWORD

This document is submitted in accordance with the Data Procurement Document Number 282, Data Requirements Number MA-04 under the George C. Marshall Space Flight Center Contract NAS8-28144.

This is Book 1 of Volume III of the Astronomy Sortie Missions Definition Study Final Report. This volume is the Design Analysis and Trade Studies and it includes the results of the mission and systems analyses, subsystem analyses, and the preliminary design tasks.

Comments or requests for additional information should be directed to:

Dale J. Wasserman/PD-MP-A
Astronomy Sortie Mission Definition Study
Contracting Officer's Representative
George C. Marshall Space Flight Center
Marshall Space Flight Center, Alabama 35812

or

William P. Pratt/8102
Astronomy Sortie Missions Definition Study
Martin Marietta Denver Division Study Manager
Denver, Colorado 80201

PREFACE

The realization of a fully operational Space Shuttle will open the door for unparalleled research opportunities in space astronomy. One mode of operation currently envisioned for the Space Shuttle is the short-duration sortie mission. The sortie mission would consist of a low earth orbit of approximately seven days' duration. During this seven days, research would be conducted by an experiment crew utilizing a scientific payload located in the Space Shuttle cargo bay.

For research in astronomy, the Space Shuttle sortie mission offers significant advantages. Several of the more important are (1) the ability to escape the Earth's atmosphere and, therefore, open up the entire electromagnetic spectrum to research, (2) the elimination of atmospheric perturbations and, thus, the ability to use the spatial resolution of the telescopes, which is currently limited to approximately one-half arc-second for ground-based telescopes, and (3) the ability to continually observe the sun during the seven-day mission without obscurations. Combining these scientific advantages with the large payload capability of the Space Shuttle, the low-cost operation of the Space Shuttle, the availability of an experiment crew on-orbit with the experiments, the frequent space flight opportunities, and the ability to return the experiment to Earth for refurbishment and retrofit offer the scientific community a unique opportunity for further research in the field of astronomy.

While the opportunities for advances in space astronomy research are clear, it is evident that significant planning is required by NASA to ensure an orderly and timely program that not only satisfies the astronomy objectives but also provides the most return for the smallest investment. The primary purpose of this study was to provide NASA with an overview of the astronomy sortie mission requirements.

The specific objectives of the study were to:

- 1) Evaluate the responsiveness of the sortie mission concept to stated scientific objectives;
- 2) Develop conceptual designs and interfaces for sortie missions including telescopes, mounts, controls, displays, and support equipment;

- 3) Develop a system concept encompassing the sortie mission from mission planning through postflight engineering and scientific documentation;
- 4) Provide funding estimates, development schedules, and supporting research and technology requirements for Shuttle sortie hardware.

The approach used in performing the study consisted of the following sequence:

- 1) Analyzing and conceptually designing the alternative candidate astronomy sortie mission program that maximized the utilization of common features;
- 2) Analyzing the astronomy sortie mission program to ensure compatibility between interfacing systems, evaluating overall performance and ensuring mission responsiveness, and developing a complete mission profile;
- 3) Analyzing the support subsystems to a depth sufficient to establish feasibility, compatibility with other subsystems, adequate performance, physical characteristics, interface definition, reliability level, and compatibility with manned operations;
- 4) Conceptually designing the selected astronomy sortie mission program, which included defining the significant design features, dimensions and interfaces on layout drawings, and defining the telescope system physical characteristics and support requirements;
- 5) Providing funding estimates, development schedules, and supporting research and technology requirements.

The final report of the study is contained in four volumes of which this volume is Volume II, Book 1. They are:

Volume I - *Astronomy Sortie Missions Definition Study Final Report: Executive Summary*

This volume summarizes the significant achievements and activities of the study effort.

Volume II - *Astronomy Sortie Missions Definition Study Final Report:*

Book 1 - *Astronomy Sortie Program Technical Report*

Book 1 of this volume includes the definition of telescope requirements, preliminary mission and system definitions, identification of alternative sortie programs, definition of alternative sortie programs, evaluation of the alternative sortie programs, and selection of the recommended astronomy sortie mission program. This volume identifies the various concepts approached and documents the rationale for the concept and approaches selected for further consideration.

Volume II - *Astronomy Sortie Missions Definition Study Final Report:*

Book 2 - *Appendix*

Book 2 of this volume contains the *Baseline Experiment Definition Documents (BEDDs)* that were prepared for each of the experiments considered during the study.

Volume III - *Astronomy Sortie Missions Definition Study Final Report:*

Book 1 - *Design Analyses and Trade Studies*

Book 1 of this volume includes the results of the design analyses and tradeoff studies conducted for candidate concepts during the selection of recommended configurations as well as of the design analyses and tradeoff studies conducted for the selected concept.

Volume III - *Astronomy Sortie Missions Definition Study Final Report*

Book 2 - *Appendix*

Book 2 of this volume contains the backup or supporting data for the design analyses and tradeoff studies that are summarized in Volume III, Book 1.

Volume IV - *Astronomy Sortie Missions Definition Study Final Report: Program Development Requirements*

This volume contains the planning data for subsequent phases and includes the gross project planning requirements; schedules, milestones, and networks; supporting research and technology; and cost estimates.

CONTENTS

	<u>Page</u>
I. INTRODUCTION	I-1 and I-2
II. MISSION AND SYSTEM ANALYSES	II-1
A. Guidelines and Assumptions	II-1
B. Pointing and Control System Requirements	II-10
C. Facility, Personnel and Support Hardware Requirements	II-39
D. Timelines	II-49
E. Mission Analysis	II-52
F. Maintainability and Reliability	II-75
G. Logistics Support	II-88
H. Utilization of Man	II-93
I. System Performance	II-96 thru II-99
III. SUBSYSTEM ANALYSIS	III-1
A. Thermal Control System Analysis	III-1
B. Structural Analysis	III-52
C. Stabilization and Control Subsystem Analysis	III-85
D. Electronic Subsystem Analysis	III-118
E. References	III-151
IV. PRELIMINARY DESIGN	IV-1
A. System Layout Drawings	IV-1
B. Subsystem and Instrument Drawings	IV-16 thru IV-50
V. INTERFACES	V-1
A. Space Shuttle Interfaces	V-1
B. Sortie Lab and Pallet Interfaces	V-13
C. References	V-19
VI. IR TELESCOPE ON-ORBIT DETECTOR ACCESS	VI-1
A. Ground Rules and Assumptions	VI-1
B. Analysis	VI-2
C. Recommended Configuration	VI-20

Figure

II-1	Solar Payload Configuration	II-6
II-2	Stellar Payload Configuration	II-7
II-3	Baseline Support Hardware	II-8
II-4	Grumman Shuttle Orbiter Configuration	II-11
II-5	Local Vertical X-POP and X-IOP Candidate Shuttle Orbiter Attitudes	II-13
II-6	Sketch of X-IOP Stabilized Shuttle Orbiter	II-15
II-7	Sketch of X-POP Stabilized Shuttle Orbiter with a Double Gimbal Experiment Pointing System	II-19
II-8	Sketch of X-IOP Stabilized Shuttle Orbiter	II-25
II-9	RCS Weight Comparison	II-31
II-10	Shuttle Orbiter Baseline Experiment Payload	II-34
II-11	Impact of Proposed Shuttle Orbiter Stabilization Systems on the Experiments	II-37
II-12	Preliminary Operations Concept	II-40
II-13	Payload Processing Facility at MSFC	II-41
II-14	Manpower Requirements per Turnaround Cycle	II-47
II-15	Turnaround Schedule	II-50
II-16	Payload Refurbishment Cycle	II-51
II-17	Telescope and Array Refurbishment Cycles	II-51
II-18	Beta Angle Relationships	II-53
II-19	Inclination Required for 90-deg Beta Angle	II-57
II-20	Altitude Required for Continuous Sun	II-58
II-21	Altitude Required for 400-km Atmosphere	II-59
II-22	Beta Angle Variations as a Function of Inclination	II-61
II-23	Doppler Shift as a Function of Inclination	II-61
II-24	Photoheliograph Constraint on Inclination	II-63
II-25	Celestial Sphere Availability (45 deg Moon Constraint)	II-66
II-26	Celestial Sphere Availability (5 deg Moon Constraint)	II-67
II-27	Celestial Sphere Availability (New Moon)	II-68
II-28	Stellar Viewing Variation with Sun and Moon Position	II-70
II-29	Look Angle Constraint Impact on Celestial Viewing	II-70
II-30	Cone of Continuous Visibility	II-72
II-31	Array Time in South Atlantic Anomaly	II-74
III-1	Orbiter/Payload Configuration	III-3
III-2	Pallet/IR Payload Nodal Layout	III-4
III-3	Node 1661; Transient Heating, Polar Orbit, IR Telescope Payload	III-5
III-4	Node 1665; Transient Heating, Polar Orbit, IR Telescope Payload	III-6

III-5	Orbiter Orientation and Earth Orbit Views	III-8
III-6	IR Telescope Transient Heat Flux Distribution	III-9
III-7	MTRAP Options	III-10
III-8	IR Telescope Transient Equivalent Space Sink Temperatures	III-13
III-9	Pallet Experiment Mounts Equivalent Space Sink Temperatures	III-14
III-10	Array Equivalent Space Sink Temperatures	III-15
III-11	Pallet and Sortie Lab Equivalent Space Sink Temperatures	III-16
III-12	Insulation Detail at Tubular Supports	III-20
III-13	Insulation Detail at Rear Access Cover	III-21
III-14	Forward Termination of Multilayer Insulation	III-22
III-15	Pressure-Enthalpy Vent Process Diagram for Neon	III-24
III-16	Liquid Orientation and Vent System	III-25
III-17	Flow Diagram for Construction of IRT Thermal Model	III-28
III-18	Optics Assembly and Instrument Chamber	III-29
III-19	IR Telescope Nodal Layout	III-31
III-20	Nodal Model of Primary Mirror	III-34
III-21	Heat Leak Imposed Neon Boiloff	III-37
III-22	IR Telescope Transient Temperatures	III-37
III-23	Thermal Control Concepts	III-40
III-24	Stratoscope III Equivalent Network for Radiation	III-44
III-25	100-cm Photoheliograph Heat Flow	III-48
III-26	2.45- and 4.0-cm Coronagraph Heat Flow	III-48
III-27	Coordinate System	III-54
III-28	IR Telescope	III-57
III-29	Experiment Mounts	III-63
III-30	Wide Coverage X-Ray Detector Mount	III-69
III-31	Gamma-Ray Spectrometer Housing and Mount	III-71
III-32	Common Mount Assembly	III-73
III-33	Telescope Gimbal	III-77
III-34	Array Platform	III-81
III-35	Number of Stars Per Square Milliradian as a Function of Photographic Star Magnitude, M_p , or Brighter	III-90
III-36	Probability P of Two Stars of Magnitude $M_p = 8$ or Brighter Lying in an $a \times a$ FOV	III-92
III-37	Probability P of Two Stars of Magnitude $M_p = 10$ or Brighter Lying in an $a \times a$ FOV	III-92
III-38	Probability P of Two Stars of Magnitude $M_p = 12$ or Brighter Lying on a $a \times a$ FOV	III-93
III-39	Probability P of Two Stars of Magnitude $M_p = 14$ or Brighter Lying in an $a \times a$ FOV	III-93

III-40	Probability P of Two Stars of Magnitude $M_p = 16$ or Brighter Lying in an $a \times a$ FOV	III-94
III-41	Probability P of Two Stars of Magnitude $M_p = 18$ or Brighter Lying in an $a \times a$ FOV	III-94
III-42	Required Fine Attitude Error Sensor Field of View as a Function of Star Magnitude, M_p	III-95
III-43	Flexible Suspension Gimbal System (Concept IA) . . .	III-97
III-44	Wide Angle Spherical Gas Bearing Configurations (Concepts IB-1, IB-2, IB-3)	III-98
III-45	Gas Bearing Gimbal System (Concept IC)	III-100
III-46	Coarse External - Internal IMC System (Concept IIA) .	III-100
III-47	Wide Angle Spherical Gas Bearing, Two-Pad Configuration (Concept IIB)	III-102
III-48	Orientation of Body 2 with Respect to Body 1	III-104
III-49	Block Diagram of Telescope Fine Statilization System	III-105
III-50	Experiment Mass Motion Disturbance Torque T_D	III-107
III-51	Baseline Telescope Deployment, Pointing, and Fine Stabilization System	III-110
III-52	Functional Block Diagram of ASM Stabilization and Control Subsystem	III-114
III-53	ASM Payload Control and Display Console	III-129
III-54	C&D Console Interface Diagram	III-130
III-55	Vertical Reach and Viewing Envelope	III-135
III-56	Lateral Work and Visual Envelope	III-136
III-57	Data Management Interface Components	III-144
III-58	Single Frame Transmission Time	III-146
III-59	Power Distribution Interface Diagram	III-150
IV-1	Payload vs Shuttle Orbiter cg Constraints	IV-2
IV-2	Payload Accommodations	IV-5
IV-3	Payload 1-2	IV-7
IV-4	ASM Payloads 3AB, 3AC, 3AD and 3AE	IV-11
IV-5	ASM Payloads 4AB, 4AC, 4AD and 4AE	IV-13
IV-6	Orbiter Payload Bay Reference Datum System	IV-15
IV-7	ASM C&D Console Outline Drawing	IV-17
IV-8	ASM C&D Console	IV-18
IV-9	ASM C&D Console Upper Panel Layout	IV-19
IV-10	ASM C&D Console Lower Panel Layout	IV-20
IV-11	ASM CMG Outline Drawing	IV-21
IV-12	ASM Elevation Axis Pointing/Stabilization Actuator	IV-22
IV-13	ASM Azimuth Table Pointing Actuator	IV-23
IV-14	ASM Deployment Actuator	IV-24
IV-15	ASM Azimuth Gimbal Axis Stabilization Actuator	IV-25

IV-16	ASM Roll Pointing/Stabilization Actuator	IV-26
IV-17	ASM Elevation Pointing Actuator	IV-27
IV-18	Sun Sensor Optical-Mechanical Assembly	IV-28
IV-19	IMU Package	IV-29
IV-20	X-Ray Telescope	IV-31
IV-21	Inner and Outer Coronagraphs	IV-33
IV-22	25 CM XUV Spectroheliograph	IV-34
IV-23	Solar Telescope Group	IV-35
IV-24	100 CM Photoheliograph	IV-37
IV-25	Stratoscope III - 120 CM Telescope	IV-38
IV-26	Mass Properties Data, Photoheliograph	IV-40
IV-27	Mass Properties Data, Solar Group	IV-41
IV-28	Mass Properties Data, Stratoscope III	IV-42
IV-29	Mass Properties Data, IR Telescope	IV-43
IV-30	Mass Properties Data, High-Energy Arrays	IV-44
IV-31	ASM Solar Payload 1-2 System Schematic	IV-45
IV-32	ASM Stellar Payloads 3AB, 3AC, 3AD, and 3AE System Schematic	IV-47
IV-33	ASM Stellar Payloads 4AB, 4AC, 4AD, and 4AE System Schematic	IV-49
V-1	Shuttle Payload Capability	V-3
V-2	Shuttle Cargo Bay Acoustic Environment	V-5
V-3	Shuttle Thermal Environment	V-7
V-4	Telescope Temperature During Ascent	V-8
V-5	Center of Gravity Constraint	V-11
V-6	Baseline Sortie Lab and Pallet	V-14
VI-1	IR Telescope Configuration No. 1	VI-3
VI-2	IR Telescope Configuration No. 2	VI-5
VI-3	IR Telescope Configuration No. 3	VI-7
VI-4	IR Telescope Configuration No. 4	VI-9
VI-5	IR Telescope Configuration No. 5	VI-11
VI-6	Gas Bearing Support Concept for IR Telescope	VI-13
VI-7	IR Telescope Observation Time	VI-15

Table

II-1	Baseline Payload Combinations	II-3
II-2	Baseline Flight Schedule	II-4
II-3	X-POP and X-IOP Experiment Pointing Methods	II-14
II-4	Viewing Constraints and Momentum Requirements for the Five Experiment Pointing Methods	II-28
II-5	Advantages and Disadvantages of Orbiter ACPS	II-32
II-6	Advantages and Disadvantages of Low-Thrust RCS	II-32
II-7	Advantages and Disadvantages of CMG System	II-33
II-8	Pointing and Stabilization Requirements	II-36
II-9	Payload Support Equipment	II-43

II-10	Telescopes and Arrays Support Equipment	II-45
II-11	Manpower Requirements	II-46
II-12	Direct Labor Manpower for Astronomy Sortie Program.	II-48
II-13	Effect of Doppler Shift on Solar Instruments	II-62
II-14	Solar Payload Orbit Parameters	II-64
II-15	Stellar Payload Orbit Parameters	II-71
II-16	Summary of Critical Single Failure Points from FMEA	II-77
II-17	Subsystem/Experiment Estimated Failure Rates	II-78
II-18	Estimated Failure Rates for Baseline Payload Groups	II-79
II-19	Estimated Critical Failures and Flight Reliability With and Without Recommended Improvements	II-82
II-20	Estimated Cost Savings for Incorporation of Redun- dancy and Inflight Maintenance to Reduce Critical Failure Risk	II-82
II-21	Maintainability Requirements	II-84
II-22	Redundancy Requirements	II-87
II-23	Maintenance Spares Estimate	II-89
II-24	Operational Consumables Requirements	II-92
II-25	Solar Payloads	II-96
II-26	Stellar Payloads	II-97
III-1	IR Telescope Thermal Environment Summary	III-17
III-2	Electrical Heat Loads	III-18
III-3	Thermophysical Properties	III-18
III-4	Thermal Model Nodal Information	III-32
III-5	Neon Boiloff Summary	III-35
III-6	Temperature Effects Summary	III-36
III-7	Solar Telescope Allowable Temperature Limits	III-46
III-8	Solar Telescope Heat Balance Summary	III-50
III-9	Orbiter Loads	III-53
III-10	Material Properties	III-54
III-11	IR Telescope Weight	III-65
III-12	Experiment Mount Weights	III-83
III-13	Summary of Experiment Mount Weights for Payload Combinations	III-84
III-14	Baseline ASM Telescope Pointing and Stabilization (Azimuth and Elevation) Requirements	III-86
III-15	Experiment Pointing and Stabilization Concepts	III-99
III-16	Experiment Pointing and Stabilization Concept Tradeoffs	III-103
III-17	ASM Gimbal System Actuators and Characteristics	III-113
III-18	Function and Purpose of GN&C Subsystem Digital Computer Programs	III-117
III-19	Control and Display Commonality Matrix: Telescopes	III-120

III-20	Control and Display Commonality Matrix: High-Energy Arrays	III-121
III-21	Mission Dedicated Console Requirements	III-123
III-22	Common/Dedicated Console Requirements	III-125
III-23	C&D Console to CIU Interface	III-131
III-24	C&D Electrical Power Requirements	III-133
III-25	C&D Console Mass Properties	III-138
III-26	Digital Data Rates, Storage, and Telemetry Requirements	III-143
III-27	Electrical Power Requirements for Mission Payloads	III-148
V-1	Payload Bay Wall Thermal Environment	V-6
V-2	On-Orbit Thermal Characteristics	V-10
V-3	IR Telescope Thermal Environment Summary	V-10
V-4	Telemetry Requirements	V-12
V-5	Payload Power Requirement	V-16
V-6	Digital Data Requirements	V-18
VI-1	Operation Parameters	VI-16

I. INTRODUCTION

This volume includes the detailed analyses and trade studies that were performed on the Astronomy Sortie program defined in Volume II, Book 1 of this report. The major chapters of this volume are the Mission and Systems Analyses, Subsystem Analyses, Preliminary Design, Interfaces and an evaluation of on-orbit access to the IR detectors. The contents of each chapter is summarized below.

Mission and Systems Analyses - This includes those analyses that were performed to establish the basic mission and system requirements for the Astronomy Sortie program. The mission analyses include the definition of an operational concept, the establishment of mission profiles and timelines, and the selection of the preferred orbital parameters for the astronomy payloads. The system analyses include the definition of the facilities, personnel, and support hardware necessary to support the Astronomy Sortie program over the 12-year duration, the definition of the maintenance, reliability, and logistic requirements, and the evaluation of the overall Astronomy Sortie program performance.

Subsystem Analysis - The detailed analyses for each of the subsystems required for the Astronomy Sortie mission are covered. Special emphasis was placed on the design of the IR telescope, the common mount for the telescopes and arrays, and the stabilization and control system. The specific subsystems that are covered include the thermal control, structural, stabilization and control and electronic subsystems. The definition in this chapter is to a depth that establishes the feasibility of the Astronomy Sortie mission concept.

Preliminary Design - The preliminary design chapter includes the payload layout drawings, the telescope and subsystem drawings, and the systems schematics for those concepts selected as a result of the subsystem analysis.

Interfaces - As a result of the analyses performed, the issues that are most important to the success or failure of the Astronomy Sortie program are the capabilities and constraints of the interfacing elements--the Space Shuttle, Sortie Lab, and Pallet. These elements are major drivers on the operation of the experiments and the design of the astronomy support hardware. For this reason the interfaces for these elements are collected in one chapter to allow visibility of the interface requirements that were derived or assumed during this study.

IR Telescope On-Orbit Detector Access - Several alternatives were investigated for providing on-orbit access to the IR telescope detectors. Although, the results of this investigation suggest that no on-orbit access should be provided for the IR detectors, further study is required to establish the preferred approach.

II. MISSION AND SYSTEM ANALYSES

Mission and system analyses were performed on the approved astronomy sortie mission program concept to ensure compatibility with the interfacing systems; to ensure mission responsiveness; to develop a complete mission profile; and to evaluate overall performance.

A. GUIDELINES AND ASSUMPTIONS

The Astronomy Sortie mission program concept, defined in Volume II, Book 1 of this report, was the approved baseline for the more detailed analyses that are reported on in this volume. The Astronomy Sortie mission program concept was derived during the first three months of the study based on preliminary analyses of several alternatives and was approved by the NASA/MSFC, COR as the baseline for the remainder of the study. The approved Astronomy Sortie mission concept is summarized in this section.

1. Experiments

The experiments that were baselined consisted of the following telescopes and arrays:

Solar Telescopes

- 100-cm photoheliograph,
- 25-cm XUV spectroheliograph,
- 32-cm X-ray telescope,
- 2.45- and 4.0-cm coronagraphs;

Stellar Telescopes

- 120-cm Stratoscope III,
- 100-cm IR telescope;

High-Energy Arrays

Wide coverage X-ray detector,
Narrow-band spectrometer/polarimeter,
Large modulation collimator,
Large area X-ray detector,
Collimated plane crystal spectrometer,
Gamma-ray spectrometer,
Low background gamma-ray detector.

2. Payload Groupings

The above experiments were grouped into nine different payloads as shown in Table II-1. The primary consideration in the experiment grouping was the physical size of the telescopes and arrays and the volume available in the Shuttle cargo bay. Four different payloads are shown for the Stratoscope III and the IR telescopes. In each case, the primary experiment is the telescope (i.e., Stratoscope or IR), with the secondary experiment being the particular group of high-energy arrays.

3. Baseline Flight Schedule

The baseline flight schedule is shown in Table II-2. This schedule was provided by the NASA/MSFC, COR at the start of the study and was modified to reflect the baseline payload groupings.

4. Operations Concept

The operations concept established for the Astronomy Sortie missions uses three major areas of payload-oriented activities, the Payload Integration Center (PIC) located at MSFC, the Space Astronomy Control Facility (SACF), and the installations required for Shuttle and mission operations and support. The PIC provides the sustaining engineering for the telescopes, arrays, Sortie Labs and pallets throughout the Astronomy Sortie program. This sustaining engineering includes all those activities that are necessary to ensure the delivery of a flight-ready payload to the Shuttle launch site. The SACF would be responsible for all experiment operations and for coordinating the space astronomy activities with the established

Table II-1 Baseline Payload Combinations

Experiment Groups	Payloads	Stratoscope III Payloads				IR Payloads			
	Solar Payloads	3AB	3AC	3AD	3AE	4AB	4AC	4AD	4AE
<u>Telescope Groups</u>									
1. PHG	X								
2. XUV SHG + X-Ray + Coronagraphs	X								
3. Stratoscope III		X	X	X	X				
4. IR Telescope						X	X	X	X
<u>Array Groups</u>									
A. Wide Coverage X-Ray		X	X	X	X	X	X	X	X
B. Narrow Band Spectrometer/Polarimeter		X				X			
C. γ -Ray Spectrometer + Low Background γ -Ray Detector			X				X		
D. Large Modulation Collimator				X				X	
E. Large Area X-Ray Detector + Collimated Plane Crystal Spectrometer					X				X
<p>PHG = 100-cm photoheliograph. XUV SHG = 25-cm XUV Spectroheliograph. X-Ray = 32-cm X-Ray Telescope.</p> <p>Note: Combinations are based on the 2.26 m (84 in.) inside diameter telescope mounting tube adopted for remainder of study.</p>									

Table II-2 Baseline Flight Schedule

Payload	Calendar Year												Total
	79	80	81	82	83	84	85	86	87	88	89	90	
Solar 1-2	X	XX	XXX	XXX	XXX	XX	26						
Strato- scope III	3AB			X		X	X		X	X	X		6
	3AC					X	X	X		X	X	X	6
	3AD					X	X		X	X		X	6
	3AE					X		X	X		X	X	6
IR	4AB		X		X	X		X	X		X	X	8
	4AC	X			X	X	X		X	X		X	8
	4AD			X	X		X	X		X	X	X	8
	4AE			X		X	X	X	X		X		7
Total	2	3	5	7	8	81							

and continuing ground-based research. This facility would have extensive capabilities in astronomy and would accommodate the ground-based scientific personnel that would support all mission phases throughout the Astronomy Sortie program. The Shuttle launch and landing site would be responsible for loading the payload, monitoring the payload status after installation, and unloading the payload after the mission is completed.

5. Operational Configuration

Figures II-1 and II-2 show the configuration concepts that were approved for the remainder of the study. Major features include the use of the Sortie Lab, a standard pallet, and a common mount for telescopes and arrays.

The solar payload configuration shown reflects the Space Shuttle in an X-perpendicular-to-the-orbit-plane (X-POP) inertial attitude with a beta angle of 90 deg (the angle between the sun line and the orbit plane). For this type of an inertial attitude and beta angle it would be necessary to deploy the entire payload out of the cargo bay to view the sun.

The stellar payload configuration shown would require deploying the telescopes and arrays out of the pallet to enable viewing of a hemisphere with the telescope and array mounts.

6. Support Hardware

The support hardware defined for the Astronomy Sortie mission program is shown pictorially in Fig. II-3.

The Sortie Lab is a standard facility that provides the pressurized volume from which the experiment crew operates the telescopes and arrays. The Sortie Lab also provides the subsystem support (i.e., power, data, C&D, etc) required by the experiments and experiment support hardware. This minimizes the amount of experiment-peculiar support hardware required for the Astronomy Sortie program.

The pallet is a standard pallet available in modular increments to provide the desired lengths. The pallet serves as the strongback for mounting experiments and experiment support hardware.

The deployment yoke is used to deploy the telescopes and arrays out of the cargo bay to provide clear access for hemispherical viewing.

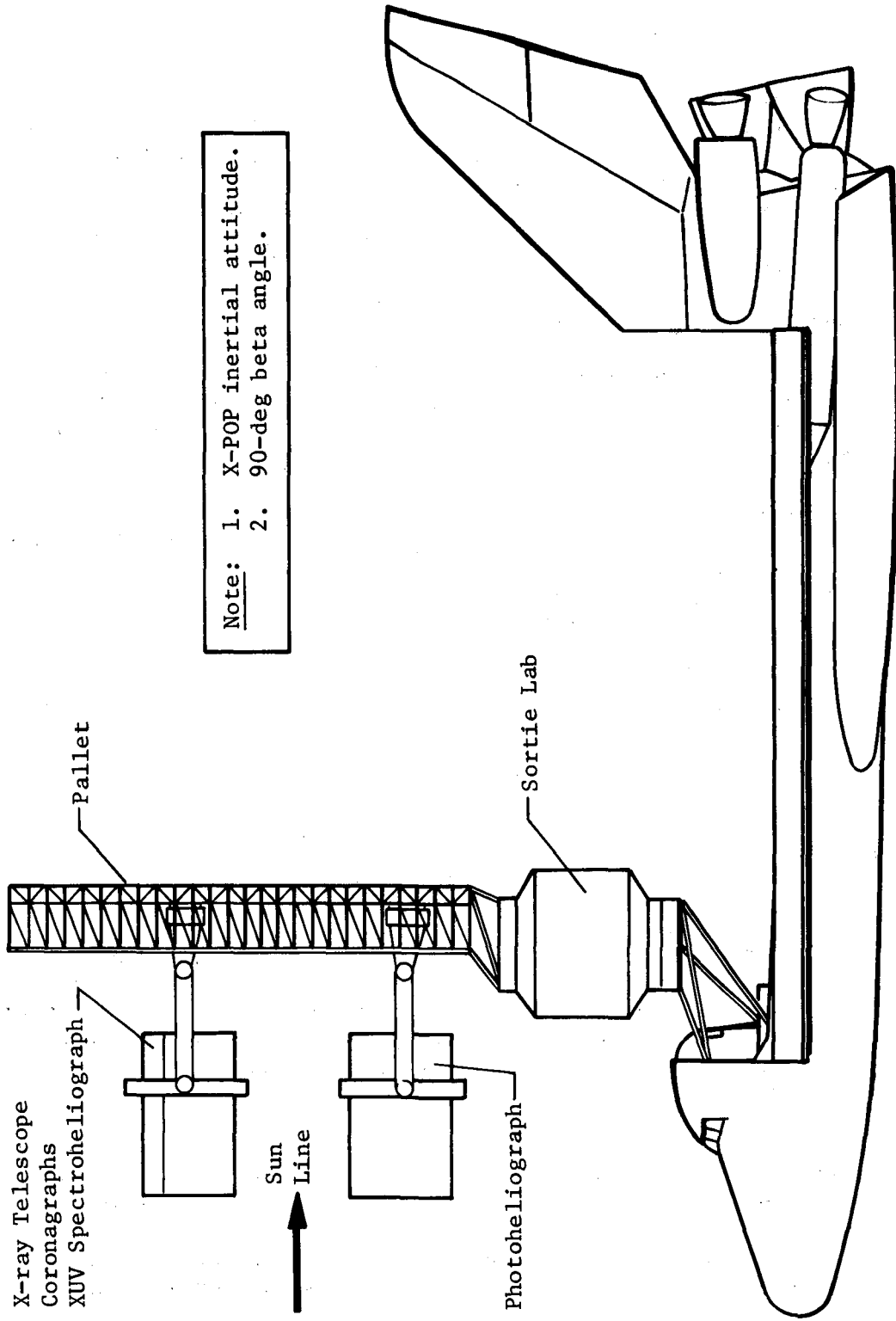


Fig. II-1 Solar Payload Configuration

Note:
1. X-POP inertial attitude.
2. Wide-angle gimbals provide hemispherical coverage.

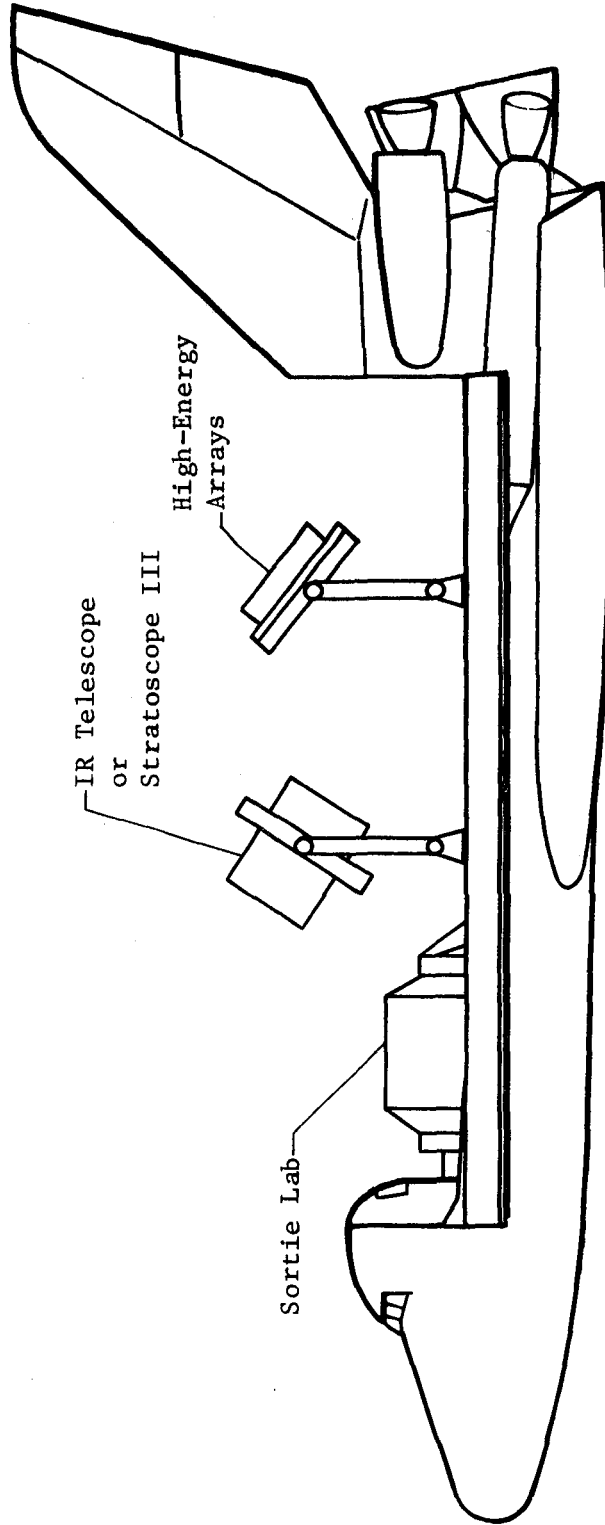


Fig. II-2 Stellar Payloads Configuration

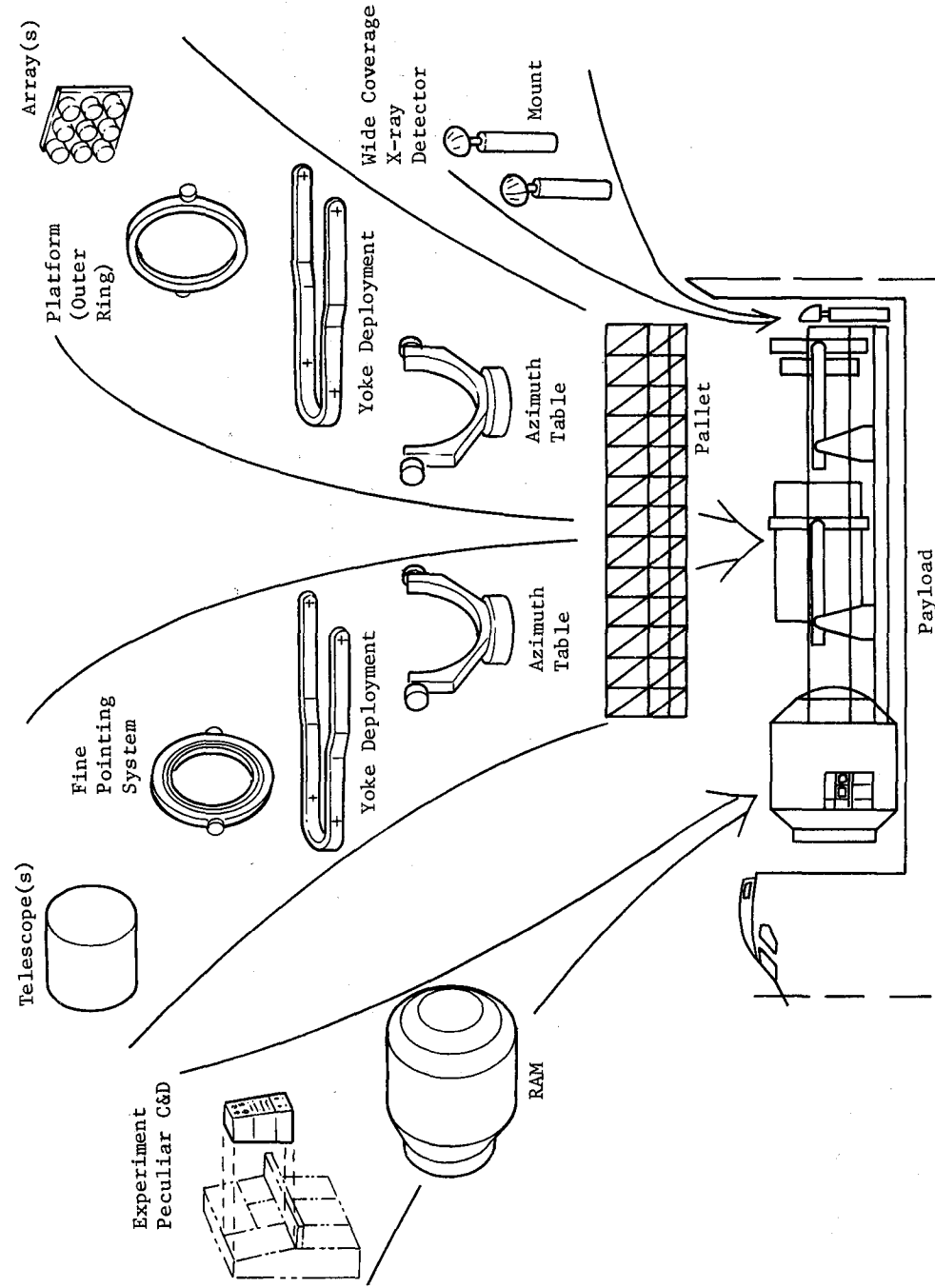


Fig. II-3 Baseline Support Hardware

Hemispherical coverage is provided by the azimuth table and elevation gimbal. The elevation gimbal interfaces with the deployment yoke and the fine pointing system and is shown on the outer ring of the fine pointing system.

The fine pointing system is a three-axis fine pointing and stabilization system required for the telescopes. The arrays do not have the stringent fine pointing and stabilization requirements and do not require the fine pointing system. The fine pointing system shown has an inside diameter of 2.13 m (84 in.) and with the use of special adapters, can accommodate a variety of telescope diameters.

7. Shuttle Interfaces

The baseline Astronomy Sortie mission program concept defined in Volume II assumes the following Space Shuttle operational interfaces: (1) the Space Shuttle can maintain any inertial attitude for the duration of the seven-day sortie mission; (2) 24 hr a day launch capability exists; and (3) the air breathing engine system (ABES) is not required for the Astronomy Sortie missions.

B. POINTING AND CONTROL SYSTEM REQUIREMENTS

The Astronomy Sortie missions (ASM) are designed to use the Shuttle Orbiter as an earth-orbiting base for performing various astronomy missions. In this report, the various candidate methods and attitude control systems for stabilizing the Shuttle Orbiter during the seven-day baseline mission are investigated. The resources such as fuel required by these systems and their impact on the ASM experiments are determined and discussed.

The Shuttle Orbiter model used in this report is the Grumman configuration shown in Fig. II-4. The Shuttle Orbiter inertias used are:

$$I_{xx} = 1.41 \times 10^6 \text{ kg-m}^2 \quad (1.04 \times 10^6 \text{ slug-ft}^2)$$

$$I_{yy} = 8.22 \times 10^6 \text{ kg-m}^2 \quad (6.05 \times 10^6 \text{ slug-ft}^2)$$

$$I_{zz} = 8.55 \times 10^6 \text{ kg-m}^2 \quad (6.30 \times 10^6 \text{ slug-ft}^2)$$

$$I_{xy} = I_{xz} = I_{yz} = 0$$

The Shuttle Orbiter is assumed to be stabilized in a 500 km (270 n mi) circular orbit.

1. Candidate Shuttle Orbiter Attitudes

The following four candidate Shuttle Orbiter attitudes are considered in this report.

- 1) An inertial attitude with the vehicle's longitudinal axis (X_v axis) perpendicular to the orbital plane (X-POP);
- 2) An attitude in which the vehicle's longitudinal axis is perpendicular to the orbital plane with a transverse axis (Z_v axis) pointing to local vertical (X-POP ZLV);
- 3) An inertial attitude with the vehicle's longitudinal axis in the orbital plane (X-IOP);
- 4) An attitude in which the vehicle's longitudinal axis is in the orbital plane with a transverse axis (Z_v axis) pointing to local vertical (X-IOP ZLV).

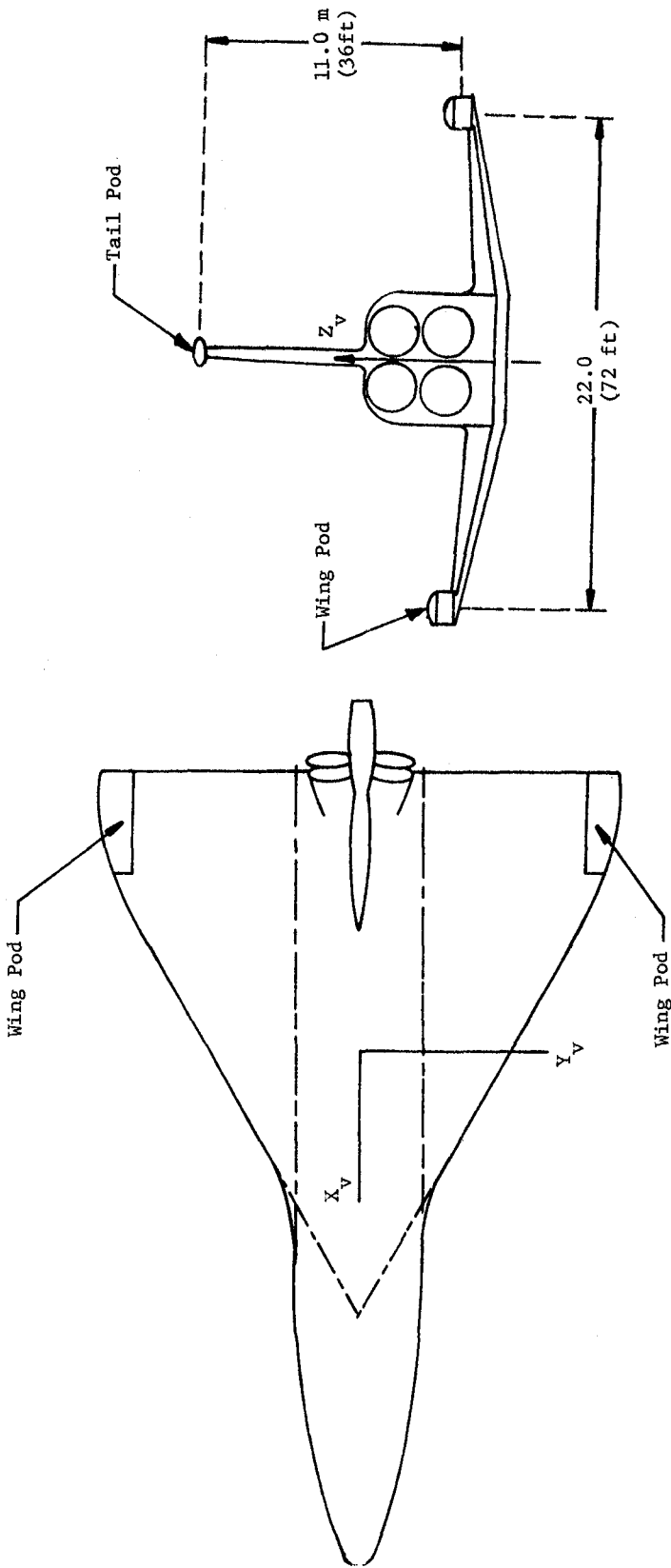


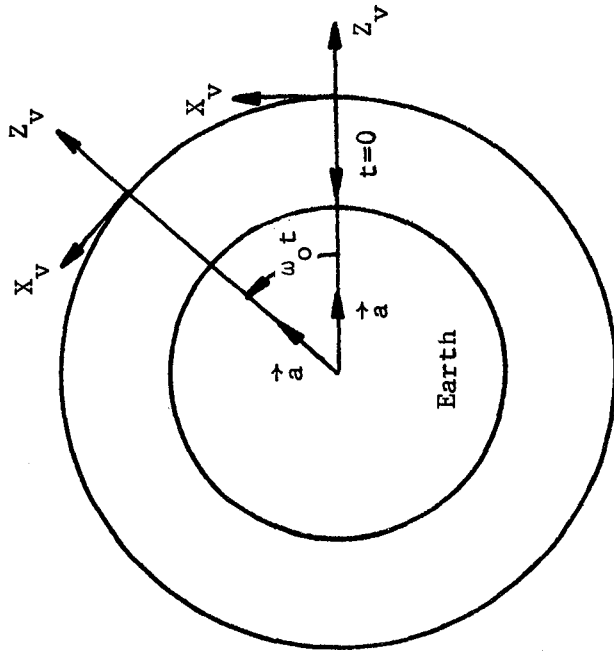
Fig. II-4 Grumman Shuttle Orbiter Configuration

The impact of these attitudes on both the Shuttle Orbiter stabilization and control system and the experiment pointing and stabilization systems are determined. Two Shuttle Orbiter stabilization and control systems are considered, a reaction control system (RCS) and a control moment gyro (CMG) system.

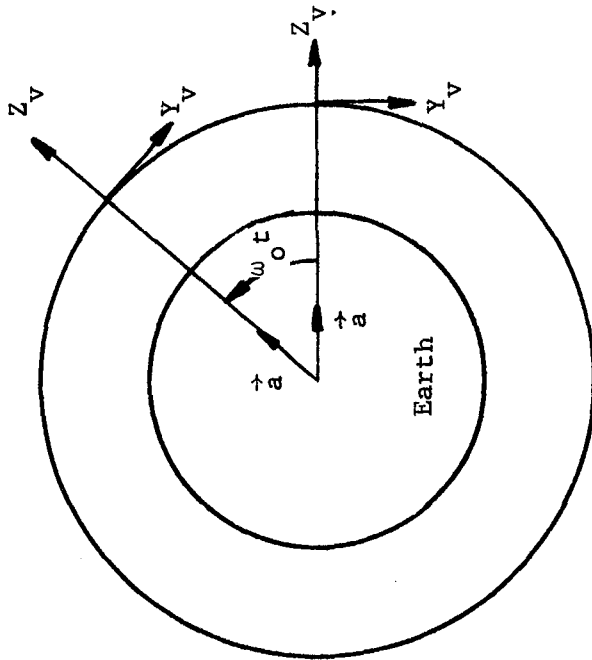
a. X-POP ZLV and X-IOP ZLV Attitudes - For the two candidate local vertical attitudes, X-POP ZLV and X-IOP ZLV, shown in Fig. II-5 the Shuttle Orbiter is continuously rotating at the orbital rate ω_v about the X_v and Y_v axes, respectively. The resulting torque environments are low since the normally large gravity gradient disturbance torques acting on an inertially oriented vehicles are ideally zero. This zero-gravity gradient torque environment is a result of the Orbiter's principal Z axis being pointed along the earth's gravitational vector acting on the Orbiter. From the standpoint of the Orbiter's stabilization system, this low torque environment is an advantage because it can result in a fuel savings for the RCS stabilization system and a reduced momentum storage requirement for a CMG system. The chief disadvantage of these two attitudes is that none of the baseline ASM experiments can be hardmounted to the Orbiter since all of the experiments must remain inertially pointed. The experiments would require an additional wide angle stabilization system to remove the Orbiter's rotational motion ω_v , thus significantly increasing the complexity of the overall experiment stabilization system. For the above reason, these two ZLV attitudes are eliminated as potential Shuttle Orbiter attitudes for the ASM experiments.

b. Inertial X-POP and X-IOP Attitudes Experiment Pointing System - There are five methods for pointing the ASM experiments using these two inertial attitudes, three for a X-IOP and two for a X-POP stabilized Shuttle Orbiter. These five methods are listed in Table II-3. Three of these systems partially or entirely point the experiments by maneuvering the Shuttle Orbiter. Because the Shuttle Orbiter must be maneuvered, these three systems impose special maneuvering requirements on the Orbiter's stabilization system.

For a X-IOP attitude, the Shuttle Orbiter's X axis is constrained to the orbital plane, thus reducing its rotational degrees of freedom from three to two. The Orbiter can be maneuvered about its X axis and its axis normal to the orbital plane and still remain in a X-IOP attitude.



X-IOP ZLV



X-POP ZLV

Fig. II-5 Local Vertical X-POP and X-IOP Candidate Shuttle Orbiter Attitudes

Table II-3 X-POP and X-IOP Experiment Pointing Methods

X-IOP Stabilized Shuttle Orbiter	
Method 1:	The experiment pointing is performed by maneuvering the Shuttle Orbiter. The experiment is mounted along one of the Orbiter transverse axis and is pointed by maneuvering the Orbiter about its X axis and axis normal to the orbital plane.
Method 2:	The experiment is partially pointed by the Orbiter and a single wide angle gimbal. The experiment is pointed in elevation by rolling the Orbiter about its X axis and in azimuth by a single wide-angle gimbal.
Method 3:	The experiment is pointed in azimuth and elevation with respect to the orbiter by using two wide-angle gimbals.
X-POP Stabilized Shuttle Orbiter	
Method 4:	The experiment is partially pointed by the Orbiter and a single wide angle gimbal. The experiment is pointed in azimuth by rolling the Orbiter about its X axis and in elevation by a single wide-angle gimbal.
Method 5:	The experiment is pointed in azimuth and elevation with respect to the Orbiter by using two wide-angle gimbals.

Method 1 - Assume that the ASM experiments are mounted along the Orbiter Z axis. The experiments can be pointed in the celestial sphere by maneuvering the Orbiter about its two remaining rotational degrees of freedom, its X axis and its axis normal to the orbital plane. The advantage of this pointing scheme is that no wide angle gimbal system is needed to point the experiments with respect to the Orbiter. Its disadvantage is that the experiments and the Shuttle Orbiter are pointed as one unit. The Orbiter's stabilization control system must maneuver the combined Orbiter and experiments by imparting an angular momentum H to the vehicle. To compute H, the following assumptions are made:

- 1) The Shuttle Orbiter is initially oriented as shown in Fig. II-6 with its X and Z axes in the orbital plane;
- 2) The experiments are pointed by two distinct Shuttle Orbiter maneuvers, first a maneuver about its Y axis and then one about its X axis;
- 3) These maneuvers are performed at a moderate rate of ω_m of 1.745×10^{-3} radians/s (6 deg/min).

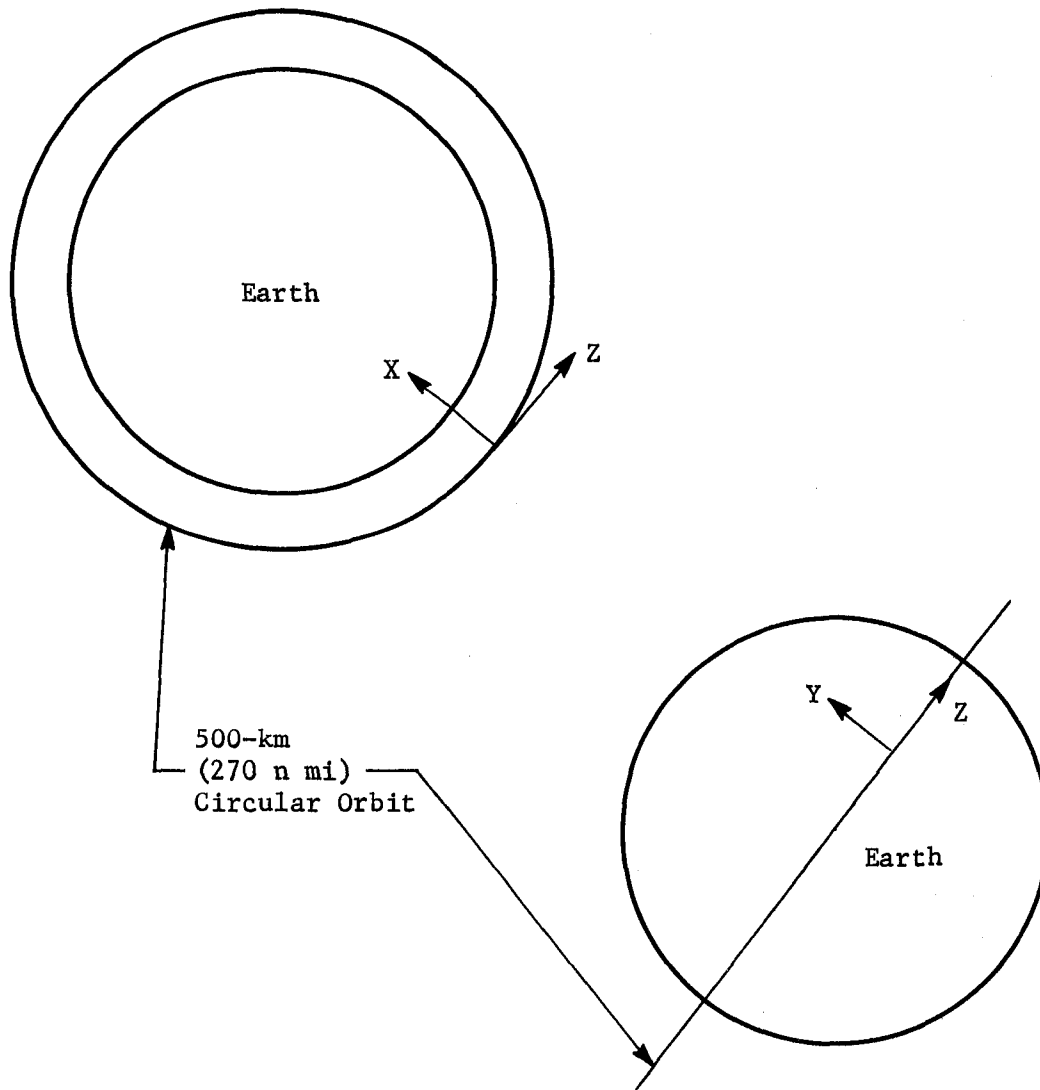


Fig. II-6 Sketch of X-IOP Stabilized Shuttle Orbiter

The Y and X axis angular momentums that must be imparted to the Orbiter to perform these experiment pointing maneuvers are:

$$H_y = I_{yy} \omega_m = 1.43 \times 10^4 \text{ N-m-s (1.06 x 10}^4 \text{ ft-lb-sec)}$$

$$H_x = I_{xx} \omega_m = 2.46 \times 10^3 \text{ N-m-s (1.81 x 10}^3 \text{ ft-lb-sec)}$$

The proposed Orbiter CMG stabilization system must be sized so that its momentum maneuver capability $H_{CMG}^{(m)}$ equals H_y , the largest of the above momentums.

$$H_{CMG}^{(m)} = H_y = 1.43 \times 10^4 \text{ N-m-s (1.06 x 10}^4 \text{ ft-lb-sec)}$$

Assume the CMGs are the same as those that will be used on Skylab. A single Skylab ATM CMG has a momentum capability of 3120 N-m-s (2300 ft-lb-sec). To provide a momentum capability of $H_{CMG}^{(m)}$, five ATM CMGs would be required.

For the low-thrust RCS to point the experiment it would have to impart to the Orbiter a momentum $H_{RCS}^{(m)}$ that equals

$$H_{RCS}^{(m)} = 2(H_x + H_y) = 3.35 \times 10^4 \text{ N-m-s (2.48 x 10}^4 \text{ ft-lb-sec)}$$

Half of $H_{RCS}^{(m)}$ is used to put the Orbiter in motion and the other half is required to stop it. When the experiments are pointed at a new target in the celestial sphere, the above momentum $H_{RCS}^{(m)}$ is expended. The RCS must be sized to produce a total experiment pointing momentum equal to $nH_{RCS}^{(m)}$ where n equals the number of times the experiments must be pointed during a mission.

Method 2 - By adding one wide-angle gimbal to the telescope, the telescope can be pointed in azimuth using the gimbal and in elevation by rolling the Orbiter about its X axis. There is no loss in pointing capability since the experiments can still be pointed anywhere in the celestial sphere. The advantage of adding this single gimbal is that the necessity of maneuvering the Shuttle Orbiter about its axis normal to the orbital plane is eliminated.

The Orbiter's stabilization system must only supply the momentum H_x required to maneuver the Shuttle Orbiter about its longitudinal axis. For the proposed CMG system, $H_{CMG}^{(m)}$ equals

$$H_{CMG}^{(m)} = H_x = 2.46 \times 10^3 \text{ N-m-s (1.81} \times 10^3 \text{ ft-lb-sec)}$$

To provide $H_{CMG}^{(m)}$, the momentum capability of less than one ATM CMG would be required. For the proposed RCS system, $H_{RCS}^{(m)}$ equals

$$H_{RCS}^{(m)} = 2H_x = 4.92 \times 10^3 \text{ N-m-s (3.62} \times 10^3 \text{ ft-lb-sec)}$$

By adding the single wide-angle gimbal to the experiments, $H_{RCS}^{(m)}$ is reduced by approximately seven. Since the amount of fuel expended by the RCS per maneuver is directly proportional to $H_{RCS}^{(m)}$, the amount of fuel needed to point the experiment is also reduced by a factor of seven.

Method 3 - The addition of a second wide-angle gimbal to point the experiments in elevation eliminates the necessity of maneuvering the Shuttle Orbiter. The pointing capability of this system compared to the previously described methods is reduced from a spherical to a hemispherical one. This reduction in pointing coverage is not as great as it may first appear since approximately half of the celestial sphere is always occulted by the earth. The speed at which the experiments can be slewed to a new point in the celestial sphere using two wide-angle gimbals should be faster than for the two previously described schemes. For these other systems, the speed at which the experiments can be pointed is limited by the maximum allowable Shuttle Orbiter maneuver rate since experiment pointing is performed entirely or partially by maneuvering the Orbiter.

For a X-POP attitude, the Shuttle Orbiter's Y and Z axes are constrained to the orbital plane thus reducing the Orbiter's rotational degrees of freedom from three to one. The Orbiter can only be maneuvered about its X axis.

Method 4 - Since both the Orbiter's Y and Z axes are constrained to the orbital plane, the experiment pointing system needs at least one wide-angle gimbal to obtain a spherical pointing capability. The addition of one wide-angle gimbal allows the experiments to be pointed anywhere in the celestial sphere by pointing the experiments in azimuth by rotating the Orbiter about its X axis and in elevation by using the wide-angle gimbal. The Shuttle Orbiter's stabilization control system points the experiments in azimuth by imparting an X axis angular momentum H_x to the vehicle.

This system is identical to the X-IOP single wide-angle gimbal system; the only difference is that the experiment pointing roles of the Orbiter and the wide-angle gimbal are reversed due to the change in Orbiter attitude. The resultant momentum maneuver requirements $H_{CMG}^{(m)}$ and $H_{RCS}^{(m)}$ placed on the Orbiter stabilization system are also the same as for the X-IOP system.

$$H_{CMG}^{(m)} = H_x = I_{xx} \omega_m = 2.46 \times 10^3 \text{ N-m-s (1.81} \times 10^3 \text{ ft-lb-sec)}$$

$$H_{RCS}^{(m)} = 2H_x = 4.92 \times 10^3 \text{ N-m-s (3.62} \times 10^3 \text{ ft-lb-sec)}$$

Method 5 - The addition of a second wide-angle gimbal to point the experiments in azimuth as well as in elevation eliminates the necessity of maneuvering the Shuttle Orbiter. This system is identical to the X-IOP double gimbal system except that Orbiter is now stabilized in a X-POP attitude. All conclusions that are made about this X-POP system also apply to the double gimbal X-IOP system. Just as in the X-IOP case, the system pointing capability is reduced from a spherical to a hemispherical coverage. Assume that the Shuttle Orbiter is in the X-POP attitude described in Fig. II-7. Note two celestial targets, a primary and a secondary, are depicted. The ASM experiments can be pointed using the two wide-angle gimbals anywhere in the hemisphere described by the shaded areas. The primary period θ_E is the position of the orbit when the primary target can be viewed from the Shuttle Orbiter. During the rest of the orbit, the primary target is occulted by the earth. By properly selecting a secondary target and properly orienting the Shuttle Orbiter as shown in Fig. II-7, the ASM experiments can be pointed by the wide-angle gimbals at the secondary target while the primary target is occulted.

* Primary Target

θ_E , Primary Experimentation
 Period = 1.244π (59.1 min)

* Secondary Target

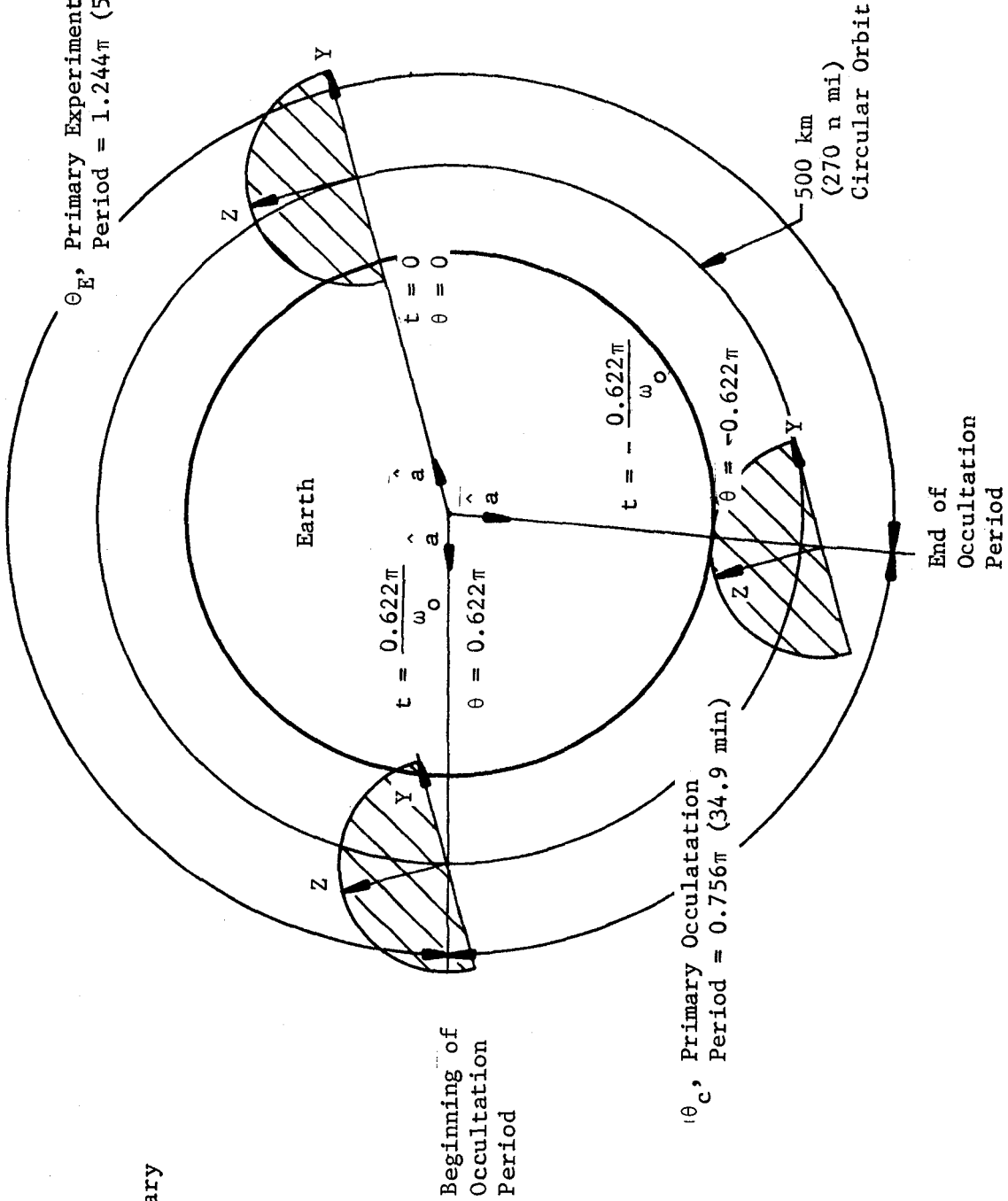


Fig. II-7 Sketch of X-POP Stabilized Shuttle Orbiter With a Double Gimbal Experiment Pointing System

Assume that:

- 1) The primary and secondary targets are 0.83π radians (150 deg) apart;
- 2) The slew capability of the two ASM wide angle gimbals is 1.745×10^{-2} radians/s (1 deg/sec);
- 3) The Shuttle Orbiter maneuver rate capability about its X axis is 1.745×10^{-3} radians/s (6 deg/min);
- 4) The occultation period θ_c lasts for 34.9 min.

For the single wide-angle gimbal that points the experiments in azimuth by maneuvering the Orbiter about its X axis, up to 25 minutes are necessary to point the experiment from the primary to the secondary target. Since the occultation period lasts for only 34.9 min and another 25 min would be needed to point the experiment back to the primary target, it is not feasible to experiment during the occultation period with this system or any system that wholly or partially points the experiments by maneuvering the Orbiter. By adding an additional wide-angle gimbal, the ASM experiments can be slewed from the primary to the secondary target in 2.5 min. The addition of the second wide-angle gimbal now makes it feasible to experiment during the occultation period. This second gimbal increases system complexity, but it can also significantly increase the total allowable experimentation time. For an RCS Orbiter stabilization system, another benefit of a double wide-angle gimbal experiment pointing system is that the Orbiter maneuvering requirements are minimized, thus reducing the amount of fuel used by the RCS. This fuel reduction makes the system lighter and also minimizes the experiment contaminates that an RCS would produce.

c. Shuttle Orbiter Stabilization System Momentum Requirements for X-POP and X-IOP - The Shuttle Orbiter external torque environment is assumed to be due only to gravity gradient torques. A CMG stabilization system must be capable of storing the resultant gravity gradient angular momentum \vec{H}_{gg} . The CMG system is sized to store both the accumulated momentum \vec{H}_a due to constant axial torques and peak cyclic momentum $\left| \vec{H}_c \right|_p$. The CMG gravity gradient momentum storage requirement H_{CMG} equals

$$H_{CMG} = \left| \vec{H}_a \right| + \left| \vec{H}_c \right|_p .$$

An RCS stabilization system counteracts the gravity gradient torques acting on the Orbiter by expelling fuel at a rate directly proportional to the rectified gravity gradient momentum H_{gr} .

X-POP Stabilized Shuttle Orbiter - The Shuttle Orbiter is assumed to be stabilized in the X-POP attitudes shown in Fig. II-7. Assume the Orbiter is misaligned from its true X-POP attitude by two small Y and Z axis rotational errors, ϵ_y and ϵ_z , and that ϵ_y and ϵ_z are equal ($\epsilon_y = \epsilon_z = \epsilon$). The resultant X-POP gravity gradient torque equations are:

$$T_{gx} = \frac{3\omega_o^2}{2} (I_{zz} - I_{yy}) \sin 2\omega_o t$$

$$T_{gy} = \frac{3\omega_o^2}{2} (I_{zz} - I_{xx}) \epsilon \left[1 - \cos 2\omega_o t - \sin 2\omega_o t \right]$$

$$T_{gz} = \frac{3\omega_o^2}{2} (I_{yy} - I_{xx}) \epsilon \left[1 + \cos 2\omega_o t - \sin 2\omega_o t \right]$$

ω_o in the above equations is the orbital rate and equals 1.10×10^{-3} radians/s for a 500 km (270 n mi) circular orbit.

Integrating the above torque equations results in the gravity gradient momentum that the CMGs must store.

$$H_{gx} = \int T_{gx} dt = -\frac{3\omega_o}{4} (I_{zz} - I_{yy}) \cos 2\omega_o t$$

$$H_{gy} = \int T_{gy} dt = \frac{3\omega_o}{4} (I_{zz} - I_{xx}) \epsilon \left[2\omega_o t - \sin 2\omega_o t + \cos 2\omega_o t \right]$$

$$H_{gz} = \int T_{gz} dt = \frac{3\omega_o}{4} (I_{yy} - I_{xx}) \epsilon \left[2\omega_o t + \sin 2\omega_o t + \cos 2\omega_o t \right]$$

The axial components of \vec{H}_a and \vec{H}_c are

X axis: $H_{ax} = 0$

$$H_{cx} = -\frac{3\omega_o}{4} (I_{zz} - I_{yy}) \cos 2\omega_o t$$

Y axis: $H_{ay} = \frac{3\omega_o}{2} (I_{zz} - I_{xx}) \varepsilon t$

$$H_{cy} = \frac{3\omega_o}{4} (I_{zz} - I_{xx}) \varepsilon \left[\cos 2\omega_o t - \sin 2\omega_o t \right]$$

Z axis: $H_{az} = \frac{3\omega_o^2}{4} (I_{yy} - I_{xx}) \varepsilon t$

$$H_{cz} = \frac{3\omega_o}{4} (I_{yy} - I_{xx}) \varepsilon \left[\sin 2\omega_o t + \cos 2\omega_o t \right]$$

The magnitude of the accumulated momentum $|\vec{H}_a|$ equals

$$|\vec{H}_a| = \sqrt{H_{ax}^2 + H_{ay}^2 + H_{az}^2} = \frac{3\omega_o}{2} \varepsilon t \sqrt{(I_{zz} - I_{xx})^2 + (I_{yy} - I_{xx})^2}$$

Assume that ε equals 1.745×10^{-2} radian (1 deg). The momentum $|\vec{H}_a|$ accumulated during the primary experimentation period θ_E shown in Fig. II-7 ($t = 3550$ sec) equals

$$|\vec{H}_a| = 1200 \text{ N-m-s (883 ft-lb-sec)}$$

The magnitude of the cyclic moment \vec{H}_c equals

$$|\vec{H}_c| = \sqrt{H_{cx}^2 + H_{cy}^2 + H_{cz}^2}$$

Since the Shuttle Orbiter inertias I_{yy} and I_{zz} are approximately equal, $|\vec{H}_c|$ can be approximated by

$$\left| \vec{H}_c \right| = \frac{3\omega_o}{4} \left\{ \left[\left(I_{zz} - I_{yy} \right)^2 + \epsilon^2 \left(I_{zz} - I_{xx} \right)^2 + \epsilon^2 \left(I_{yy} - I_{xx} \right)^2 \right] \cos^2 2\omega_o t + \epsilon^2 \left[\left(I_{zz} - I_{xx} \right)^2 + \left(I_{yy} - I_{xx} \right)^2 \right] \sin^2 2\omega_o t \right\}^{\frac{1}{2}}$$

The peak cyclic momentum $\left| \vec{H}_c \right|_p$ corresponds to t equal to zero.

$$\left| \vec{H}_c \right|_p = \frac{3\omega_o}{4} \left[\left(I_{zz} - I_{yy} \right)^2 + \epsilon^2 \left(I_{zz} - I_{xx} \right)^2 + \epsilon^2 \left(I_{yy} - I_{xx} \right)^2 \right]^{\frac{1}{2}}$$

$$\left| \vec{H}_c \right|_p = 314 \text{ N-m-s (231 ft-lb-sec)}$$

The CMG gravity gradient momentum storage requirement H_{CMG} equals

$$H_{CMG} = \left| \vec{H}_a \right| + \left| \vec{H}_c \right|_p$$

$$= 1514 \text{ N-m-s (1113 ft-lb-sec)}$$

The rectified angular momentums H_{gr} accumulated during one orbit due to the gravity gradient torques are

$$H_{grx} = \int_0^{\frac{2\pi}{\omega_o}} \left| T_{gx} \right| dt = 6\omega_o \left(I_{zz} - I_{yy} \right)$$

$$H_{gry} = \int_0^{\frac{2\pi}{\omega_o}} \left| T_{gy} \right| dt = \frac{3(4 + \pi)}{2} \epsilon \left(I_{zz} - I_{xx} \right)$$

$$H_{grz} = \int_0^{\frac{2\pi}{\omega_o}} \left| T_{gz} \right| dt = \frac{3(4 + \pi)}{2} \epsilon \left(I_{yy} - I_{xx} \right)$$

Again assume that ϵ equals 1.745×10^{-2} radian (1 deg). The accumulated momentums that the RCS must counteract each orbit are

$$H_{grx} = 2245 \text{ N-m-s (1650 ft-lb-sec)}$$

$$H_{gry} = 1470 \text{ N-m-s (1080 ft-lb-sec)}$$

$$H_{grz} = 1400 \text{ N-m-s (1030 ft-lb-sec)}$$

The total rectified gravity gradient momentum that the X-POP Shuttle Orbiter stabilization RCS must absorb equals

$$\begin{aligned} H_{gr} &= H_{grx} + H_{gry} + H_{grz} \\ &= 5115 \text{ N-m-s (3760 ft-lb-sec)} \end{aligned}$$

X-IOP Stabilized Shuttle Orbiter - Assume that the Shuttle Orbiter is stabilized in the X-IOP attitude shown in Fig. II-8. The X-IOP gravity gradient torque equations are

$$T_{gx} = \frac{3\omega_o^2}{2} (I_{zz} - I_{yy}) \sin \lambda \cos \lambda (1 - \cos 2\omega_o t)$$

$$T_{gy} = \frac{3\omega_o^2}{2} (I_{zz} - I_{xx}) \cos \lambda \sin 2\omega_o t$$

$$T_{gz} = \frac{3\omega_o^2}{2} (I_{yy} - I_{xx}) \sin \lambda \sin 2\omega_o t$$

λ is the angle subtended by the Orbiter's Y axis and its projection onto the orbital plane.

Integrating the above gravity gradient torque equations results in the momentum that the CMG stabilization system must store.

$$\begin{aligned} H_{gx} &= \int T_{gx} dt \\ &= \frac{3\omega_o}{4} (I_{zz} - I_{yy}) \sin \lambda \cos \lambda (2\omega_o t - \sin 2\omega_o t) \end{aligned}$$

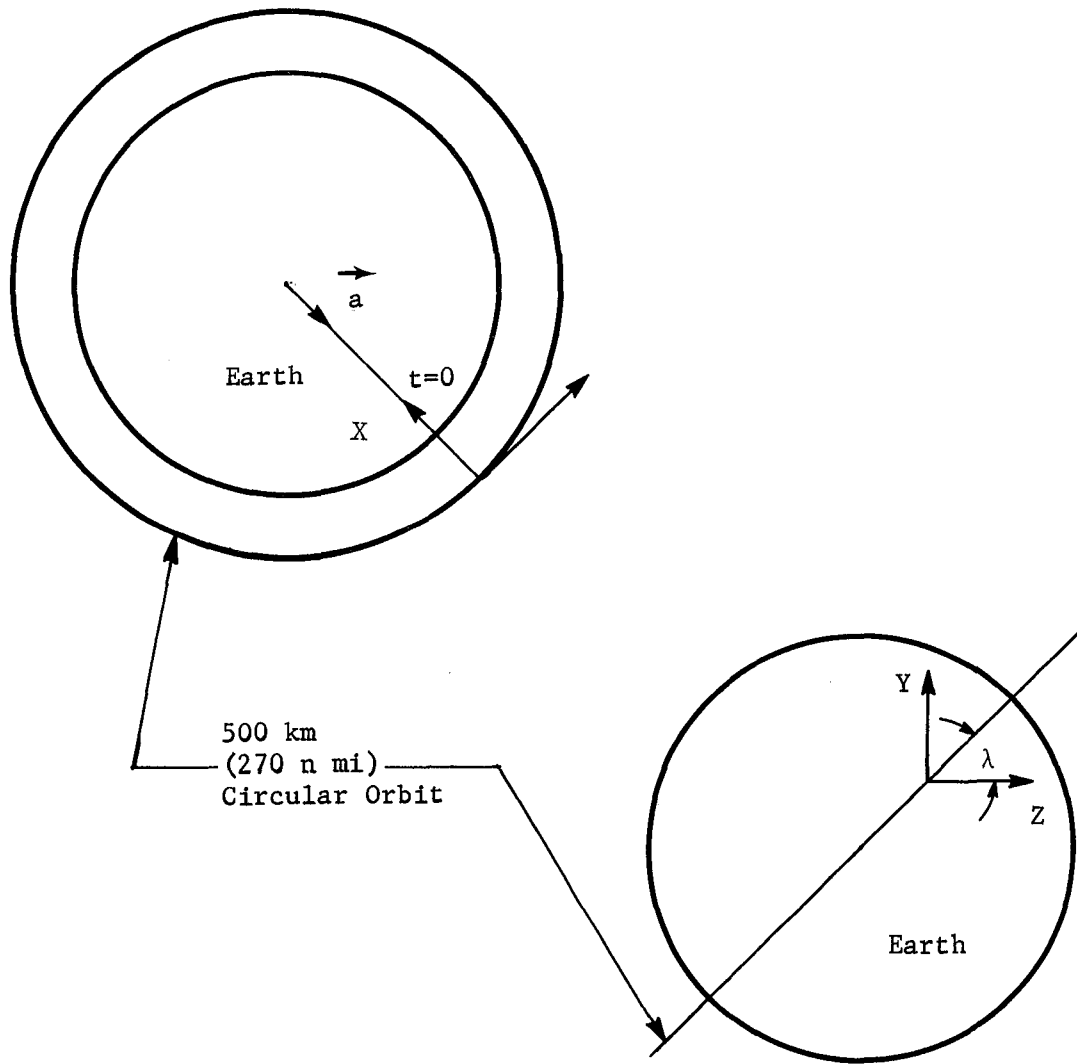


Fig. II-8 Sketch of X-IOP Stabilized Shuttle Orbiter

$$\begin{aligned}
 H_{gy} &= \int T_{gy} dt \\
 &= -\frac{3\omega_0}{4} (I_{zz} - I_{xx}) \cos \lambda \cos 2\omega_0 t
 \end{aligned}$$

$$\begin{aligned}
 H_{gz} &= \int T_{gz} dt \\
 &= \frac{3\omega_0}{4} (I_{yy} - I_{xx}) \sin \lambda \cos 2\omega_0 t.
 \end{aligned}$$

The axial components of \vec{H}_a and \vec{H}_c are

$$\text{X axis: } H_{ax} = \frac{3\omega_0^2}{2} (I_{zz} - I_{yy}) (\sin \lambda \cos \lambda) t$$

$$H_{cx} = \frac{3\omega_0}{4} (I_{zz} - I_{yy}) \sin \lambda \cos \lambda \sin 2\omega_0 t$$

$$\text{Y axis: } H_{ay} = 0$$

$$H_{cy} = -\frac{3\omega_0}{4} (I_{zz} - I_{xx}) \cos \lambda \cos 2\omega_0 t$$

$$\text{Z axis: } H_{az} = 0$$

$$H_{cz} = \frac{3\omega_0}{4} (I_{yy} - I_{xx}) \sin \lambda \cos 2\omega_0 t$$

To maximize H_{CMG} , let λ equal 0.81 radians (46.4 deg). The magnitude of the accumulated momentum \vec{H}_a equals

$$\left| \vec{H}_a \right| = H_{ax} = \frac{3\omega_0^2}{2} (I_z - I_y) (\sin \lambda \cos \lambda) t$$

The momentum $\left| \vec{H}_a \right|$ accumulated during the primary experimentation period ($t = 3550$ sec) equals

$$\left| \vec{H}_a \right| = 1100 \text{ N-m-s (811 ft-lb-sec)}$$

The magnitude of the cyclic momentum \vec{H}_c equals

$$\left| \vec{H}_c \right| = H_{cx}^2 + H_{cy}^2 + H_{cz}^2$$

The peak cyclic momentum $\left| \vec{H}_c \right|_p$ corresponds to t equal to zero.

$$\left| \vec{H}_c \right|_p = \frac{3\omega_o}{4} \left[(I_{zz} - I_{yy})^2 \cos^2 \lambda + (I_{yy} - I_{xx})^2 \sin^2 \lambda \right]^{1/2}$$

$$\left| \vec{H}_c \right|_p = 5740 \text{ N-m-s (4230 ft-lb-sec)}$$

The CMG gravity gradient momentum storage requirement H_{CMG} equals

$$H_{CMG} = \left| \vec{H}_a \right| + \left| \vec{H}_c \right|_p$$

$$H_{grx} = \int_0^{\frac{2\pi}{\omega_o}} \left| T_{gx} \right| dt = 3\omega_o \pi (I_{zz} - I_{yy}) \sin \lambda \cos \lambda$$

$$H_{gry} = \int_0^{\frac{2\pi}{\omega_o}} \left| T_{gy} \right| dt = 6\omega_o (I_{zz} - I_{xx}) \cos \lambda$$

$$H_{grz} = \int_0^{\frac{2\pi}{\omega_o}} \left| T_{gz} \right| dt = 6\omega_o (I_{yy} - I_{xx}) \sin \lambda$$

To maximize H_{gr} , let λ equal 0.81 radians (46.4 deg). The accumulated momentums that the RCS must counteract each orbit are

$$H_{grx} = 1760 \text{ N-m-s (1295 ft-lb-sec)}$$

$$H_{gry} = 32,500 \text{ N-m-s (24,000 ft-lb-sec)}$$

$$H_{grz} = 32,500 \text{ N-M-s (24,000 ft-lb-sec)}$$

d. *Comparison of the Five X-POP and X-IOP Experiment Pointing Systems* - Table II-4 contains the experiment viewing constraints and momentum associated with the five methods for pointing the ASM experiments listed in Table II-3. The momentum requirements are listed for both a CMG and a RCS stabilization system. The recommended pointing system is a X-POP stabilized Shuttle Orbiter with two wide-angle gimbals for pointing the experiments with respect to the Orbiter, Method 5. Method 5 was selected because it maximizes the total mission experimentation time by allowing the experiments to be pointed at a secondary target while the primary celestial target is occulted by the earth and because it minimizes the momentum requirements of the Orbiter's stabilization system. By minimizing the momentum requirements of the Shuttle Orbiter's stabilization system, the volume, weight, power, and cost of the stabilization system is also minimized.

Table II-4 *Viewing Constraints and Momentum Requirements for the Five Experiment Pointing Methods*

Method	Orbiter Attitude	Viewing Constraints		Momentum Requirements, N-m-s			
		Pointing Coverage	Experimentation during Earth Occultation of Primary Target	CMG		RCS	
				Maneuvering	Stabilization	Maneuvering	Stabilization
1	X-IOP	Spherical	No	1.43×10^4	6.84×10^3	3.35×10^4	6.676×10^4
2	X-IOP	Spherical	No	2.46×10^3	6.84×10^3	4.92×10^3	6.676×10^4
3	X-IOP	Hemi-spherical	Yes	0	6.84×10^3	0	6.676×10^4
4	X-POP	Spherical	No	2.46×10^3	1.514×10^3	4.92×10^3	5.115×10^3
5	X-POP	Hemi-spherical	Yes	0	1.514×10^3	0	5.115×10^3

2. Candidate Shuttle Orbiter Stabilization Systems

The Space Shuttle is principally an earth-to-orbit and an orbit-to-earth transport and is not being designed as an accurately stabilized base for on-orbit experimentation. The Shuttle Orbiter baseline attitude control propulsion system (ACPS) is a monopropellant hydrazine reaction control system (RCS) with a minimum attitude deadband of ± 8.75 mrad (± 0.5 deg). When one of the attitude deadband limits is reached, an impulse of torque is imparted to the affected axis, sending it toward the other deadband limit. For the ± 8.75 mrad ACPS attitude deadband, the axis of the Shuttle Orbiter will continuously limit cycle between their attitude deadband limits. The environmental torques acting on the Shuttle Orbiter are not large enough to decelerate these axes sufficiently to prevent them from limit cycling. The amount of fuel required by the ACPS to stabilize the Shuttle Orbiter within its minimum altitude for a seven-day ASM mission is 2600 kg (5700 lb). This fuel requirement is computed in Appendix A1, Volume III, Book 2. This large ACPS fuel consumption, beside making the Shuttle Orbiter stabilization system heavy, is a source of experiment contamination that could degrade or cause the termination of the ASM experiments.

Two additional Shuttle Orbiter stabilization systems are being considered to augment the Orbiter's baseline ACPS. The two candidates are:

- 1) A low thrust RCS;
- 2) A double gimbal CMG system.

The Shuttle Orbiter's ACPS places the Orbiter in a X-POP attitude and then relinquishes control to one of the above proposed Orbiter stabilization systems. Both of these additional stabilization systems are sized in Appendix A1, Volume III, Book 2.

The Shuttle Orbiter CMG stabilization system sized in this report consists of three Skylab ATM CMGs. Due to the safety factor designed into this system if one CMG fails, the two remaining CMGs can still satisfactorily meet the ASMs Shuttle Orbiter stabilization requirements. The resultant reliability of this system is therefore high. The CMGs are desaturated by using a gravity gradient desaturation system during the period of the orbit when the primary ASM celestial target is occulted by the earth. The resulting gravity gradient desaturation maneuvers are small and will not prevent the ASM experiments from being pointed at a secondary target during this CMG desaturation period. This CMG system also uses a psurdo-axis-of-inertia alignment scheme to minimize the accumulated momentum stored in the CMGs. Two small

rotational maneuvers are performed about the Orbiter's Y and Z control axes at the end of the desaturation interval in an attempt to minimize the momentum that must be desaturated during the next desaturation period. Depending on how well this pseudo-axis-of-inertia alignment scheme performs, it may not be necessary to desaturate the CMGs every orbit. The CMG desaturation and pseudo-axis alignment maneuvers are computed using CMG momentum samples that are measured during the orbit. No additional hardware is needed to perform these maneuvers; however the digital computer housed in the Sortie Lab is required for computing the desaturation and pseudo-axis alignment maneuvers.

The optimal low thrust RCS sized in Appendix A1, Volume III, Book 2, is a 17.4 N (4 lbf) thrust bipropellant (MMH or UDMH and N_2O_4) system with a 80 msec pulse width. The system thrust level and fuel requirements were computed for a X-POP inertially stabilized Shuttle Orbiter. The thrust level was sized so that it would be small enough to prevent excessive limit cycling, thus minimizing fuel consumption but large enough to ensure that the vehicle will not exceed its attitude deadbands. Figure II-9 compares the weight of the proposed CMG system and the various low thrust RCSs sized. Note that for the baseline seven-day ASM mission, the bipropellant RCS weighs about one-third as much as the CMG system. If the mission is extended from seven days to 30 days, the weight of the RCS approaches or exceeds the weight of the CMG system, depending on the type of RCS fuel used.

Tables II-5 thru II-7 list the advantages and disadvantages of the three candidate ASM Shuttle Orbiter stabilization systems: (1) the baseline Orbiter ACPS; (2) the low thrust RCS; and (3) the proposed CMG system, respectively.

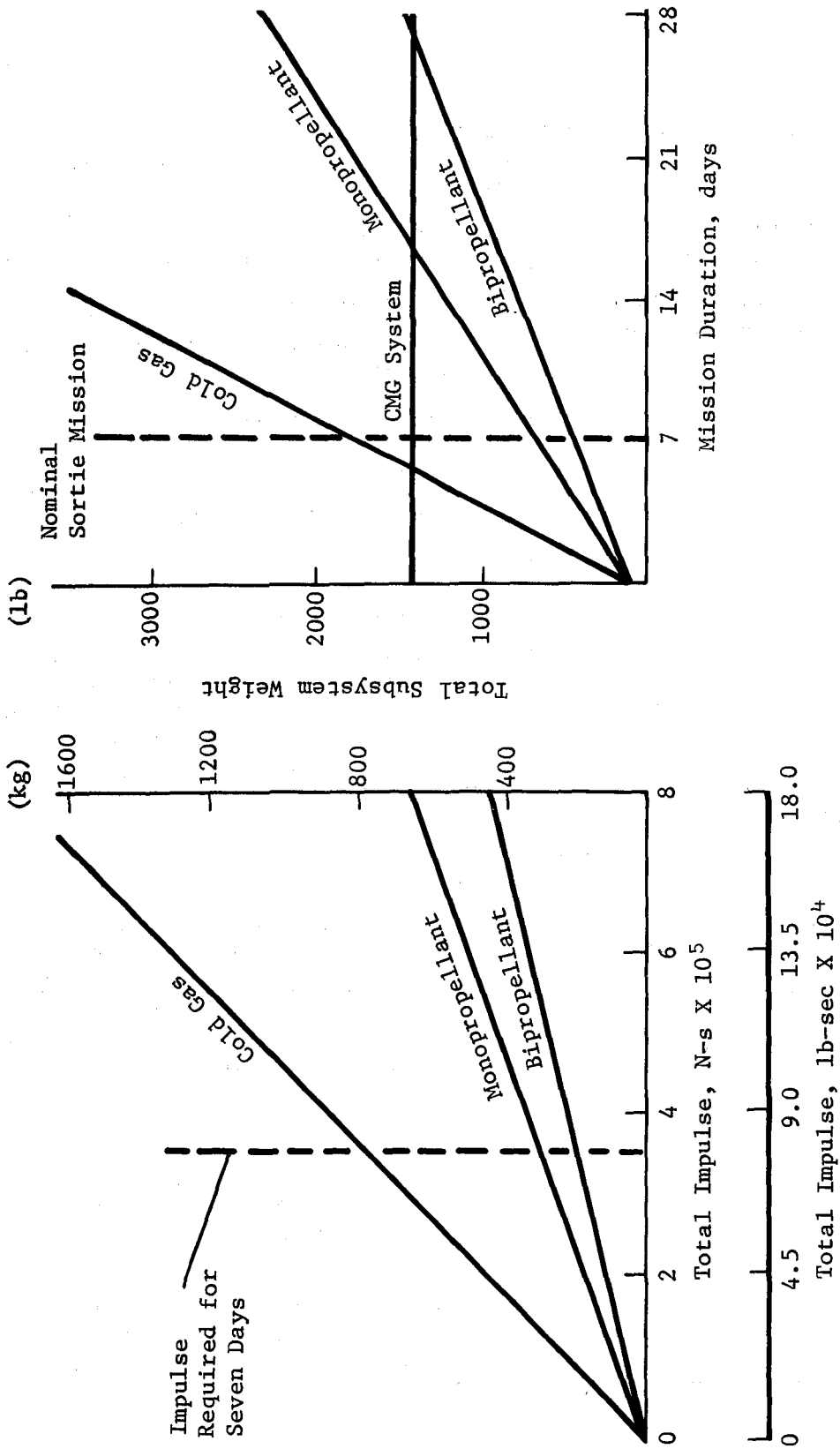


Fig. II-9 RCS Weight Comparison

Table II-5 Advantages and Disadvantages of Orbiter ACPS

Advantages	Disadvantages
<ol style="list-style-type: none"> 1. No new system required (system exists on Orbiter) 2. Not restricted to an inertial X POP attitude (all-attitude capability) 	<ol style="list-style-type: none"> 1. Large fuel consumption 2600 kg (5700 lb) per mission. 2. Source of experiment contamination. 3. Additional tanks required for fuel storage. 4. Additional tanks stored in the bay of the Orbiter makes payload integration more complex 5. Hazardous materials, fuel, introduced to Orbiter bay. 6. Has only a coarse vehicle stabilization capability ± 8.75 mrad (± 0.5 deg). 7. Firing large ACPS thrusters may cause large coupling disturbance torques to be transmitted through the ASM experiment fire stabilization system (see Appendix B3, Volume III, Book 2).

Table II-6 Advantages and Disadvantages of Low-Thrust RCS

Advantages	Disadvantages
<ol style="list-style-type: none"> 1. Lowest system weight per baseline mission 190 kg (420 lb). 2. Lowest system cost. 	<ol style="list-style-type: none"> 1. Requires an additional system to be added to the Shuttle Orbiter. 2. Source of experiment contamination. 3. Integration of low thrust RCS to Orbiter complicates turnaround operations. 4. Restricted to an inertial X-POP attitude. 5. Has only a moderate vehicle stabilization capabilities ± 3.5 mrad (± 0.2 deg). 6. Hazardous materials introduced to Orbiter bay (assumes fuel stored in Orbiter bay).

Table II-7 Advantages and Disadvantages of CMG System

Advantages	Disadvantages
<ol style="list-style-type: none"> 1. Virtually contamination free system (eliminates RCS contaminates). 2. Integrated with payload prior to payload integration with Orbiter (does not directly interface with Orbiter). 3. Reuse system many times (minimum expendables). 4. Capability of providing a base Orbiter stability of approximately 0.3 mrad (1 min). 5. Weight and system requirements approximately the same for 7- or 30-day mission (does not affect mission duration growth potential). 	<ol style="list-style-type: none"> 1. Requires an additional system to ASM payload. 2. Weight of system is 642 kg (1416 lb). 3. Restricted to inertial X-POP attitude. 4. CMG power requirement is 150 W.

3. Impact of Shuttle Orbiter Stabilization System on the ASM Experiments

The baseline ASM experiment payload consists of a telescope(s), a high-energy array(s), a wide coverage X-ray detector, and an ASM Sortie Lab. Figure II-10 is a sketch of this ASM experiment payload in the Shuttle Orbiter bay. The wide coverage X-ray detector is hardmounted to the ASM pallet. The telescope(s) and high-energy array(s) are mounted on separate wide-angle pointing systems, as shown in Fig. II-10. Each experiment pointing system consists of two wide-angle gimbals; these two wide-angle gimbals permit the experiments to be pointed with respect to the Shuttle Orbiter anywhere in the hemisphere whose center is defined by the Shuttle Orbiter's positive Z axis. After the Shuttle Orbiter is stabilized in an inertial X-POP attitude, the telescope(s) and the high-energy array(s) are deployed as shown in Fig. II-10 by extending these experiments and their wide-angle gimbals out of the Shuttle Orbiter bay. The experiments are deployed so that the sides of the bay will not interfere with the operations of the experiments. The telescope(s) and high-energy array(s) are pointed by slewing their attached wide angle gimbals to the desired orientation. The wide-angle gimbals are then locked and the experiments are stabilized either by the Shuttle Orbiter or an additional fine stabilization system.

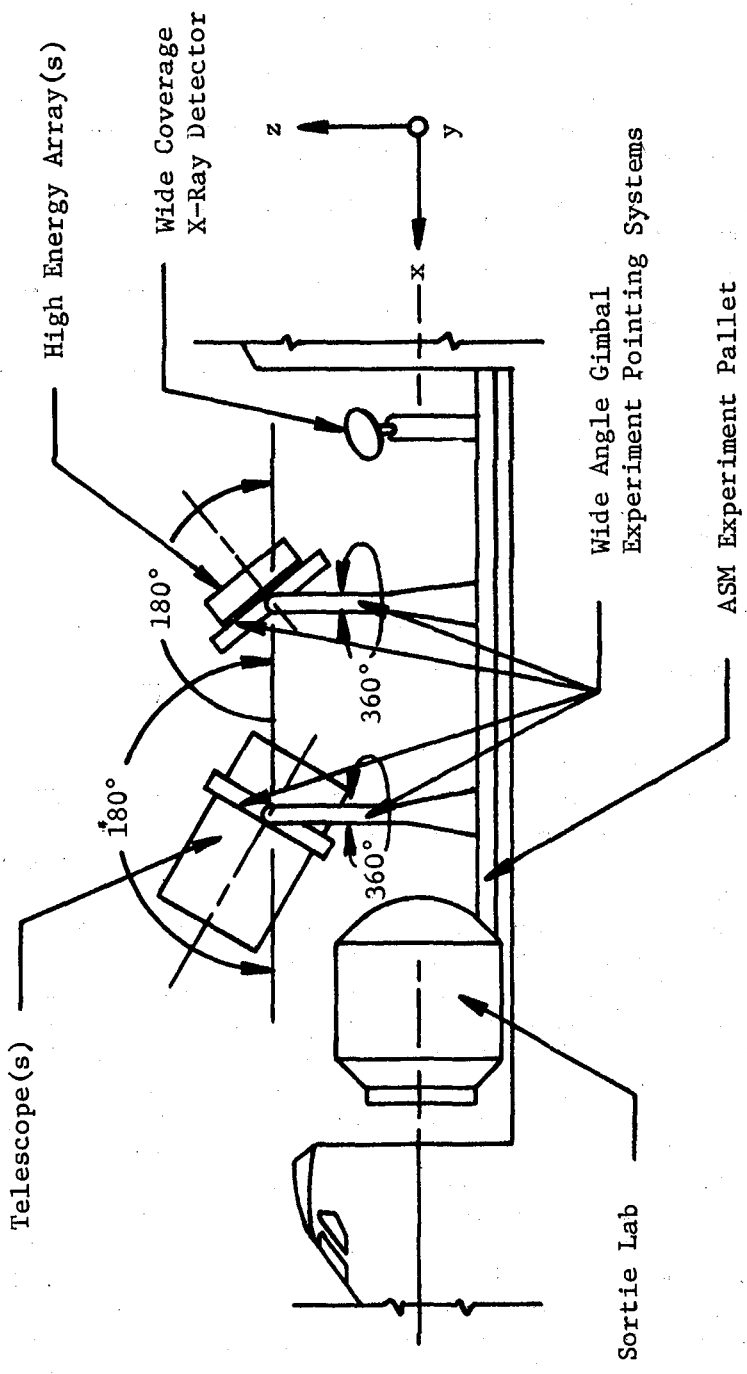


Fig. II-10 Shuttle Orbiter Baseline Experiment Payload

The Shuttle Orbiter is stabilized in its inertial X-POP attitude by using either a low-thrust RCS or a double gimbal CMG system. From the standpoint of performance, the most significant difference between the two stabilization systems is that the low-thrust RCS is a discrete system and the CMG system is a continuous one. For the RCS when one of the Orbiter's control axes attitude error ϵ equals one of the limits of the attitude deadband, θ_0 or $-\theta_0$, a discrete torque impulse $F\Delta t\ell$ is imparted to the Shuttle Orbiter about its affected axis sending the axis back through the deadband away from the impinged deadband limit. F , the thrust level of the RCS engines, Δt , the effective RCS impulse duration; and ℓ , the effective system moment arm, are constants. Therefore, the RCS imparts a constant amplitude control torque impulse to the Shuttle Orbiter every time one of the control axes approaches one of the limits of the attitude deadbands. On the other hand, a CMG stabilization system imparts a continuous control torque proportional to the continuously monitored Shuttle Orbiter attitude error. The magnitude and direction of the CMG control torque are regulated in an attempt to eliminate the attitude errors. A CMG stabilization system is inherently more accurate than a RCS because an RCS attempts to confine the Shuttle Orbiter's axial attitude errors ϵ between two limits, θ_0 and $-\theta_0$, while a CMG system continuously tries to eliminate all attitude errors.

Table II-8 lists the most stringent external body pointing and stabilization requirements associated with the ASM telescopes, high-energy arrays, and wide coverage X-ray detector. The estimated Shuttle Orbiter stabilization capabilities of the proposed low thrust RCS and CMG stabilization systems are 4 mrad (0.2 deg) and 0.3 mrad (1 $\overline{\text{min}}$), respectively. As an ASM follow-on effort, a detailed simulation of the Shuttle Orbiter and its selected ASM Shuttle Orbiter stabilization system should be performed to confirm or update the above stabilization performance estimate.

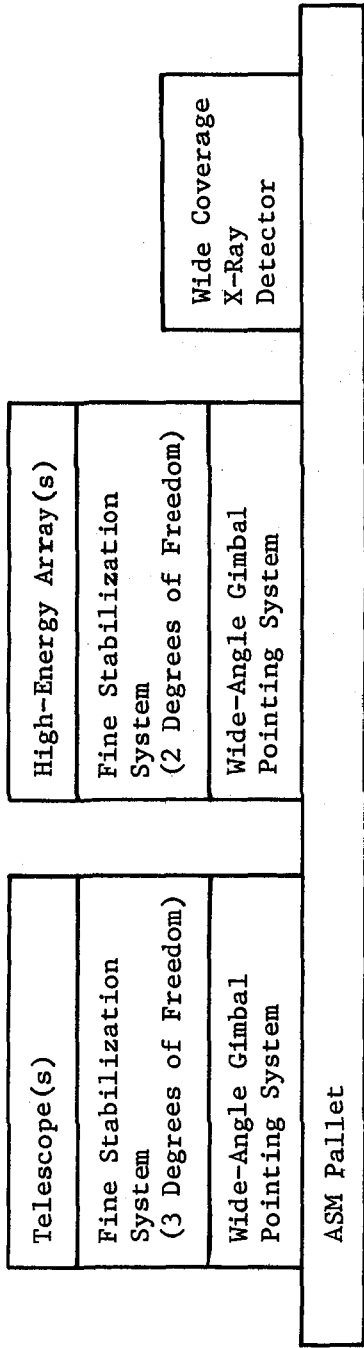
The telescope and high-energy array experiments are pointed by stabilizing the Shuttle Orbiter in an appropriate inertial X-POP attitude so that the desired celestial target is within the hemispherical field of view of the experiments' wide angle pointing systems. The wide-angle pointing system then slews the telescope(s) and the high-energy array(s) to the desired point in the celestial hemisphere. The estimated stabilization characteristics of the low-thrust RCS and CMG systems should be sufficient to permit the experiments to lock onto the desired celestial targets with the required accuracies listed in Table II-8.

Table II-8 Pointing and Stabilization Requirements

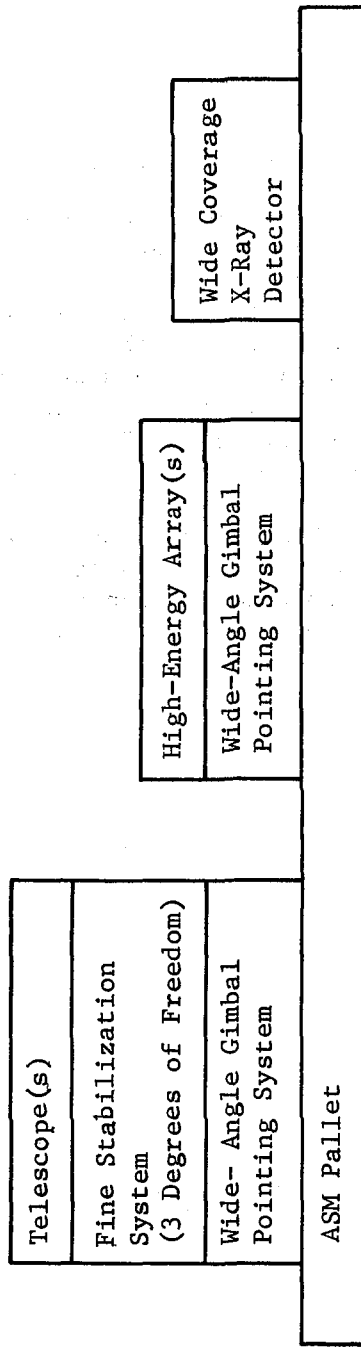
Experiment	Pointing	Stabilization		
		Pitch	Yaw	Roll
Telescope	10 μ rad (2 $\overline{\text{sec}}$)	0.5 μ rad (0.1 $\overline{\text{sec}}$)	0.5 μ rad (0.1 $\overline{\text{sec}}$)	25 μ rad (5 $\overline{\text{sec}}$)
High-Energy Array	0.3 mrad (1 $\overline{\text{min}}$)	0.3 mrad (1 $\overline{\text{min}}$)	0.3 mrad (1 $\overline{\text{min}}$)	0.1 rad (6 deg)
Wide Coverage X-Ray Detector	--	8.75 mrad (30 $\overline{\text{min}}$)	8.75 mrad (30 $\overline{\text{min}}$)	8.75 mrad (30 $\overline{\text{min}}$)

Figure II-11 illustrates the impact that the proposed low-thrust RCS and the CMG Shuttle Orbiter stabilization systems have on the ASM experiments. For both candidate Shuttle Orbiter stabilization systems, the wide coverage X-ray detector stability requirements listed in Table II-8 can be met hardmounted to the Shuttle Orbiter. To meet the stability requirements of the ASM telescopes, an additional fine stabilization system must be added to the telescopes. This additional stabilization system must have three rotational degrees of freedom to completely isolate the telescopes from all Shuttle Orbiter perturbations in pitch, yaw, and roll. For the ASM high-energy arrays, an additional stabilization system is needed only for the RCS stabilized Shuttle Orbiter. This stabilization system needs only two degrees of freedom since the arrays' roll stabilization requirements can be met by the Shuttle Orbiter. The same actuators that are used to point the high-energy arrays can also be used to stabilize the arrays. Only such additional instrumentation and hardware as a fine attitude error sensor and a rate gyro package need to be added to the basic pointing system to furnish the required stabilization. For the CMG stabilized Shuttle Orbiter, the high-energy arrays require no additional stabilization system because the stability of the Shuttle Orbiter is sufficient. The high-energy arrays can be pointed open loop using the two wide-angle gimbals. The appropriate gimbal commands are computed and then inputted to the wide angle gimbal actuators.

If the Shuttle Orbiter CMG stabilization system cannot meet its 0.3 mrad (1 min) stability design goal, but can meet a reduced stabilization in the range from 0.6 to 0.9 mrad (2 to 3 $\overline{\text{min}}$), the stability requirements for the high-energy arrays must be reevaluated, some of the arrays still are not compatible with this reduced Shuttle Orbiter stabilization capability, an additional stabilization system for these affected arrays will have to be added. In this event, there would be little or no difference between the low-thrust RCS and CMG ASM experiment pointing and stabilization systems.



Low Thrust RCS Stabilized Shuttle Orbiter



Double Gimbal CMG Stabilized Shuttle Orbiter

Fig. II-11 Impact of the Proposed Shuttle Orbiter Stabilization Systems on the Experiments

4. Recommended ASM Experiment Pointing System

The base line ASM experiment payload consists of three elements: a telescope complement, a set of high-energy arrays, and a wide coverage X-ray detector. The recommended ASM experiment pointing system consists of stabilizing the Shuttle Orbiter in an inertial X-POP attitude using three ATM CMGs. The telescope complement and high-energy arrays are then pointed in azimuth and elevation with respect to the Shuttle Orbiter using separate two-degree-of-freedom wide-angle gimbals. The pointing requirements of the wide coverage X-ray detector can be met hardmounted to the Orbiter.

A CMG Shuttle Orbiter stabilization system was selected principally on the basis of experiment contamination. A CMG system produces virtually no contaminants. Conversely, an RCS is a possible major source of experiment contamination; this is the main reason it was not selected.

C. FACILITY, PERSONNEL, AND SUPPORT HARDWARE REQUIREMENTS

A detailed analysis was performed for each phase of the operational concept to determine the facility, personnel, and support hardware required for the ASM program. The operational concept was divided into six distinct operation phases (Fig. II-12). Each phase was analyzed to determine those functions that would be performed during that phase and the facilities, personnel, and support hardware that would be required to satisfy the function.

The six operational phases analyzed were: Phase I - Pack, Ship, Deliver to Launch Site; Phase II - Receipt-to-Launch at Launch Site; Phase III - Ascent and Orbital Flight; Phase IV - Deorbit, Safe, Remove, Inspect, and Service Payload; Phase V - Pack, Ship, Deliver to Payload Integration Center (PIC); and Phase VI - Refurbish, Integrate, and Service Payload at PIC. The worksheets derived from the detailed analyses are included in Appendix A2 of Volume III, Book 2, and are the basis for the summaries presented below.

1. Facility Requirements

A facility concept for the PIC is shown in Fig. II-13. This concept combines all of the facilities in one building called the Payload Processing Facility (PPF). No attempt was made to determine if the existing facilities at MSFC would satisfy these requirements, because the objective of this task was to just identify the requirements. A building having about 90,000 sq ft of floor space and providing an entrance-and-exit airlock large enough for the integrated payload, several class 100,000 clean work areas, offices, and general utilities services is required. Utilities requirements include electrical power, lighting, and commodities services and handling. Commodities that are required include gaseous nitrogen, liquid nitrogen, liquid neon, and liquid helium. The facility should provide a 50-ton overhead crane in the payload assembly area and smaller cranes in the work areas.

Although the facility requirements at the Shuttle launch and landing site were identified in the detailed analyses, they are not summarized, because the results of the Implementation of Research and Applications Payloads at the Shuttle Launch Site Study (Contract NAS10-7685) indicated that the existing facilities would be adequate for the astronomy payloads.

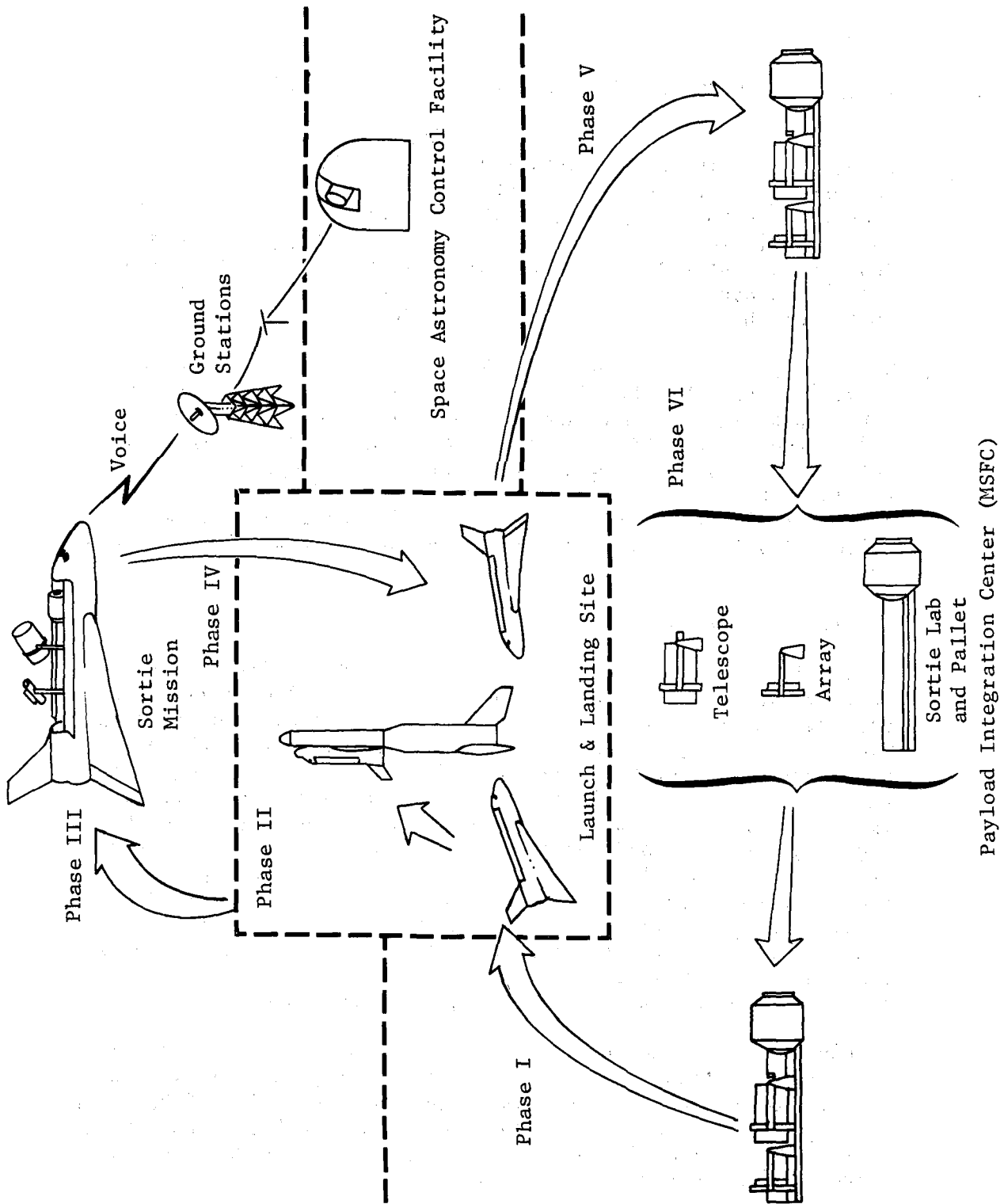
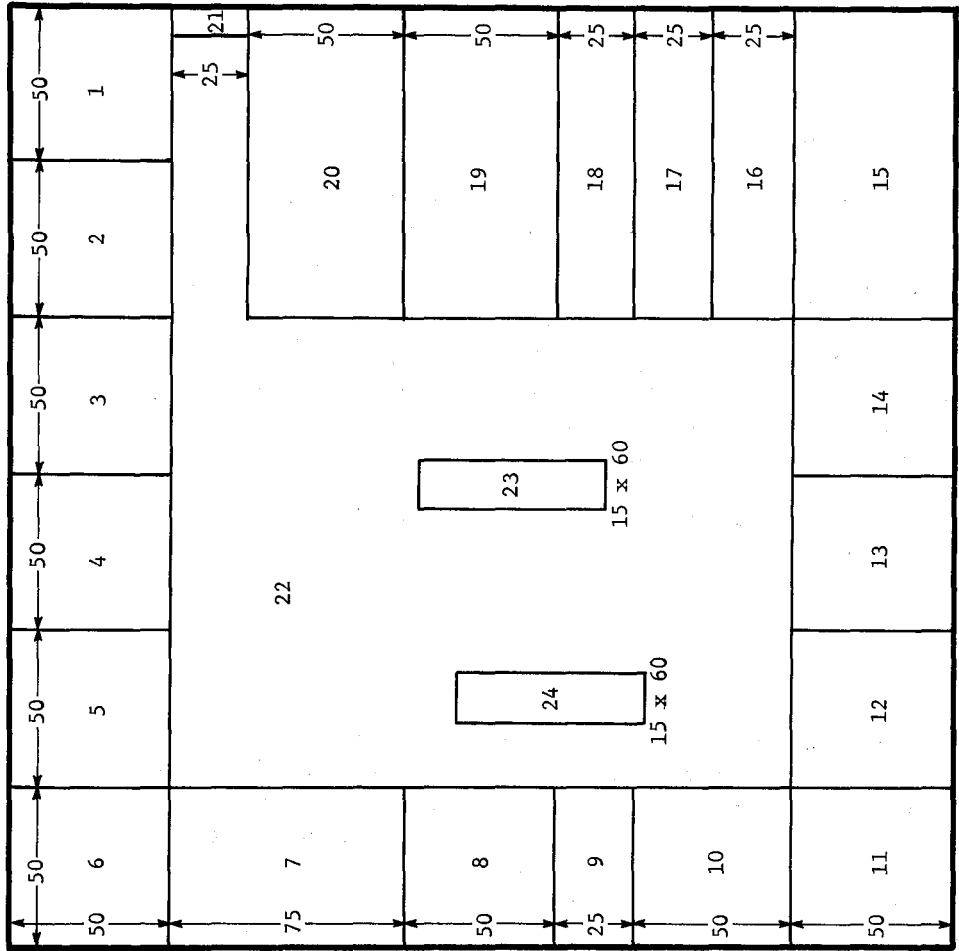


Fig. II-12 Preliminary Operations Concept



Legend:

1. Array Refurbishment Room
2. Array Refurbishment Room
3. Array Refurbishment Room
4. Array Refurbishment Room
5. X-Ray & γ-Ray Source Calibration Offices
6. Vacuum Chamber & Deposit Room
7. Simulator & Crew Training Precision Machine Shop
8. Computer Room
9. Offices
10. Telescope Refurbishment Room
11. Telescope Refurbishment Room
12. Telescope Refurbishment Room
13. Offices
14. Airlock Unloading
15. ECCU Storage & Servicing
16. Tool Storage & Issue
17. SL & Pallet MOD & Servicing
18. Optical Calibration Lab
19. Cryogenic Work Room
20. Payload Assembly Area
21. Payload Assembly Pad
22. Payload Assembly Pad

Bldg. is 300 x 300 x 50 ft and is 100,000 Class Cleanroom in all work areas. Access is interior to all work areas. 50-ton overhead crane in Payload Assembly Area.

Note: All dimensions in feet.

Fig. II-13 Payload Processing Facility at MSFC

2. Support Hardware Requirements

Table II-9 summarizes the payload support equipment required at each location for the operations phases. These requirements were taken from the Events Sequence and Resource Requirements data sheets included in Appendix A2, Volume III, Book 2.

In addition to the payload support equipment, support equipment is required at the Payload Integration Center (MSFC) for handling, refurbishing, integrating, and servicing the telescopes and arrays themselves. These requirements are summarized in Table II-10.

In both tables, the total quantities required were derived by considering the commonality, flight scheduling, and facility locations, and then estimating the number of items necessary to support the Astronomy Sortie program.

3. Personnel Requirements

Manpower and skill requirements were extracted from the Events Sequence and Resource Requirements data sheets in Appendix A2, Volume III, Book 2. The requirements were then summarized according to the facility at which they are necessary and are tabulated in Table II-11. These manpower requirements are based on the requirements for each payload and are direct labor only, and do not include any administrative, supervisory, or program management personnel.

A schedule of direct manpower use based on the Astronomy Sortie payload turnaround sequence of Chapter II.D.1 was prepared and is shown in Fig II-14.

The manpower indicated on this figure includes only that involved with the payloads, excluding the direct facility and laboratory personnel shown in Table II-11.

A schedule of direct manpower use was developed for the duration of the Astronomy Sortie program and is presented in Table II-12. This schedule is based on the manpower schedule of Fig. II-14 and the Baseline Flight Schedule presented in Table II-2. In the derivation of these manpower requirements, one Sortie Lab and pallet was used during the first year and one-half and two Sortie Labs and pallets thereafter. Each Sortie Lab and pallet payload had its own crew. The requirement for two Sortie Labs and pallets, each with its own crew, was based on the preliminary analyses reported in Volume II, Book 1. The analysis indicated that for five or more flights per year, two Sortie Labs and pallets, each having its own crew would be the most efficient way to satisfy the Astronomy Sortie program.

Table II-9 Payload Support Equipment

Equipment Description	Operations Phase						Total Quantity Required for Program
	I	II	III	IV	V	VI	
1 Payload Transfer Fixture	X	X		X	X	X	2
1 Environmental Cover and Control Unit	X	X		X	X	X	2
1 Payload Transfer Dolly	X	X		X	X	X	2
1 Tractor (Payload Transfer Dolly)	X	X		X	X		1 at Payload Integration Center (PIC) 1 at Launch Site 1 at Landing Site
1 Payload Lifting Sling Set	X	X			X		1 at PIC-MSFC 1 at Launch Site 1 at Landing Site
1 Lo-Boy and Tractor, with Tiedowns	X				X		1 at PIC-MSFC 1 at Launch Site 1 at Landing Site
2 Escort Vehicles	X	X		X	X		2 at PIC-MSFC 2 at Launch Site 2 at Landing Site
1 State Patrol Escort Car	X				X		1 at PIC-MSFC (on call) 1 at Launch Site (on call) 1 at Landing Site (on call)
2 13-Ton Portable Cranes	X				X		2 at MSFC Airport 2 at Launch Site Airport 2 at Landing Site Airport
1 Cargo Lift Trailer	X				X		1 at MSFC Airport 1 at Launch Site Airport 1 at Landing Site Airport
1 Tractor (Cargo Lift Trailer)	X				X		1 at MSFC Airport 1 at Launch Site Airport 1 at Landing Site Airport
1 Super Guppy Aircraft	X				X		1 (on call)
2 Ladders	X				X		2 at PIC-MSFC 2 at Launch Site
1 Cleaning Supplies Set	X	X		X	X		1 at PIC-MSFC 1 at Launch Site
4 Work Stands	X			X	X		4 at Launch Site 4 at Landing Site
6 Work Stands		X				X	6 at PIC-MSFC
1 Environmental Cover and Control Unit Lifting Sling Set		X		X		X	1 at Launch Site 1 at Landing Site 1 at PIC-MSFC
1 Cryogenics Servicing Unit		X					1 at Launch Site
1 Battery Handling Equipment		X		X			1 at Launch Site 1 at Landing Site
1 Checkout Console		X					1 at Launch Site

Table II-9 (concl)

Equipment Description	Operations Phase						Total Quantity Required for Program
	I	II	III	IV	V	VI	
1 Payload Environmental Support Unit		X		X			1 at Launch Site 1 at Landing Site
1 Guide Rail Set (for payload removal)				X			1 at Landing Site
10 Work Tables						X	10 at PIC-MSFC
2 Polaroid Cameras						X	2 at PIC-MSFC
1 Ground Cooling Set						X	1 at PIC-MSFC
4 Payload Mounting Locks						X	4 at PIC-MSFC
4 Cable Slings						X	4 at PIC-MSFC
1 Telescope Handling Dolly						X	1 at PIC-MSFC
1 Array Handling Dolly						X	1 at PIC-MSFC
1 Electric Tractor						X	1 at PIC-MSFC
2 Video Tape Recorders						X	2 at PIC-MSFC
2 Instrumentation Tape Recorders						X	2 at PIC-MSFC
2 Digital Processing Consoles						X	2 at PIC-MSFC
2 Electronic Test Sets						X	2 at PIC-MSFC
2 Optical Alignment Test Sets						X	2 at PIC-MSFC
1 Pallet Payload Simulator						X	1 at PIC-MSFC
1 Computer and Peripheral Equipment						X	1 at PIC-MSFC
1 Reproduction Equipment						X	1 at PIC-MSFC
4 Portable Hoists						X	4 at PIC-MSFC
4 Push-Cart Dollies						X	4 at PIC-MSFC
Telephone Voice and Facsimile Link between: SACF, PIC-MSFC, and Shuttle Launch Site	X						
SACF and Shuttle Launch Site		X					
SACF, Shuttle Mission Control, PIC-MSFC, Shuttle Launch Site, and World Wide Observatories			X				
SACF and Orbiter Landing Site				X	X		
Processing equipment for 95,000 frames of film per mission for solar payloads and for 8000 frames of film per mission for Stratoscope payloads.	X	X	X	X	X	X	All at Space Astronomy Control Facility (SACF)
Tape readers, computers, and printers to process 3 to 5 X 10 ⁹ bits per mission of electronic data	X	X	X	X	X	X	All at SACF
Desks, tables, viewers, projectors, typewriters, reproduction equipment for 6 personnel	X	X	X	X	X	X	All at SACF

Table II-10 Telescopes and Arrays Support Equipment

Equipment Description	Telescope Group				Array Group					Total Quantity Required for Program*
	1 PHG	2 XUV SHG; X-Ray & ICOC	3 SIII	4 IR	A Wide CVRG X-Ray	B Narrow Band	C Gamma Ray	D Large Mod Coll	E Large Area X-Ray & CPCS	
Work Stands	2	4	2	2						16
Telescope Handling Dolly	1	3	1	1	4	4	4	4	4	5
Array Handling Dolly					1	1	1	1	1	4
Telescope Package Handling Dolly		1								1
Cryogenic Handling and Movement cart							1			1
Gas Purge and Blanket unit								1	1	2
Instrument Handling Dolly									2	2
Cryogenics Supply, Helium and Neon				1						1
Cryogenic Supply Lines and Valves				1						1
Cryogenic Exhaust Lines and Valves						1	1	1	1	1
Facility Gas Supply Source						1	1	1	1	1
Gas Supply Line with Valve						1	1	1	1	4
Gas Exhaust Line with Valve										4
Polaroid Camera	1	1	1	1	1	1	1	1	1	4
Portable Hand Operated Hoists	2	6	2	2	2	2	2	2	2	12
Push cart Dollies	2	6	2	2	2	2	2	2	2	12
Cable Slings	4	6	4	4	4	4	4	4	4	24
Mirror Holding Fixture	2	1	2	2						5
Mirror Handling Dolly	2	1	2	2						5
5-Ton Overhead Crane	1	1	1	1					1	3
Electric Tractor	1	1	1	1	1	1	1	1	1	1
Laser Interferometer	1									1
Video Tape Recorder	1	3	1	1						4
Instrumentation Recorder	1	3	1	1	1	1	1	1	1	7
Monitoring and Control Console	1	3	1	1	1	1	1	1	1	7
Optical Test Set	1	3	1	1						6
Electronic Test Set	1	3	1	1	1	1	1	1	1	7
Digital Processing Equipment	1	3	1	1	1	1	1	1	1	7
Digital Tape Recorders	1	3	1	1	1	1	1	1	1	12
Protective Cover	1	1	1	1	1	1	1	1	1	9

*Total quantity assumes multiple usage of common equipment

Table II-11 Manpower Requirements

Payload Integration Center, (MSFC)	Pack, Ship, Transport Crew	Shuttle Launch and Landing Site
28 Two 14-man PIC-MSFC Transient Crew each having 1 PIE 2 Subsystem Specialists 1 ECCU Specialist 2 SL Pallet Engineers 2 SL Pallet Technicians 3 Scientists 3 Experiment Technicians	*(14) PIC-MSFC Transient Crew 3 PIC-MSFC Transient Guppy Support Crew 8 Handling Crew 3 PPF-MSFC Facility Crew 2 Tractor Operators (PT Dolly) 2 Escort Vehicle Drivers 2 General Mechanics 1 Guppy Cargomaster 1 Tractor Operator (CL Trailer) 3 Guppy Crew *(2) PPF-LS Facility Crew <hr/> 25 Total	2 Crane Operators 6 Payload Installation Technicians 4 Orbiter Electrical Technicians 4 Orbiter Mechanical Technicians 2 Cryogenics Servicemen 1 PESU Specialist 2 PPF-LS Facility Crew 8 Handling Crew 2 Tractor Operator (PT Dolly) - Tractor Operator (Lo-Boy) 2 PI 2 PPF-LS Facility Crew <hr/> 35 Total, plus 14 man PIC-MSFC Transient crew
18 Three 6-man Telescope Teams, each having 1 Telescope Engineer 5 Telescope Technicians	*14-man PIC-MSFC transient crew and 2-man PPF-LS facility crew are used but only when other personnel are not required. Hence, these 16 people are not included in total.	<hr/> 49 Total
10 Two 5-man SL Pallet Teams, each having 1 SL Pallet Engineer 4 SL Pallet Technicians	Space Astronomy Control Facility 4 Principal Investigators 9 Experiment Specialists 2 Film Processing Technicians 2 Computer Programmers Operators 4 Experiment Technicians <hr/> 21 Total	
12 Two 6-man Array Teams, each having 1 Array Engineer 5 Array Technicians		
10 Instruction and Planning Personnel, including 2 Telescope Operation Instructors 2 Array Operation Instructors 2 Simulator Operators 3 Mission Planning Specialists 1 Planning Supervisor		
39 PIC Ground Support Personnel, including 2 Crane Operators 6 Handling Crew 2 Facility Crew 2 Tractor Operator (PT Dolly) - Tractor Operator (Lo-Boy) - Electric Tractor Operators 3 Vacuum Deposit Equipment Operators 2 Optical Laboratory Technicians 2 X-Ray Room Technicians 20 Facility Technicians		
<hr/> 117 Total		

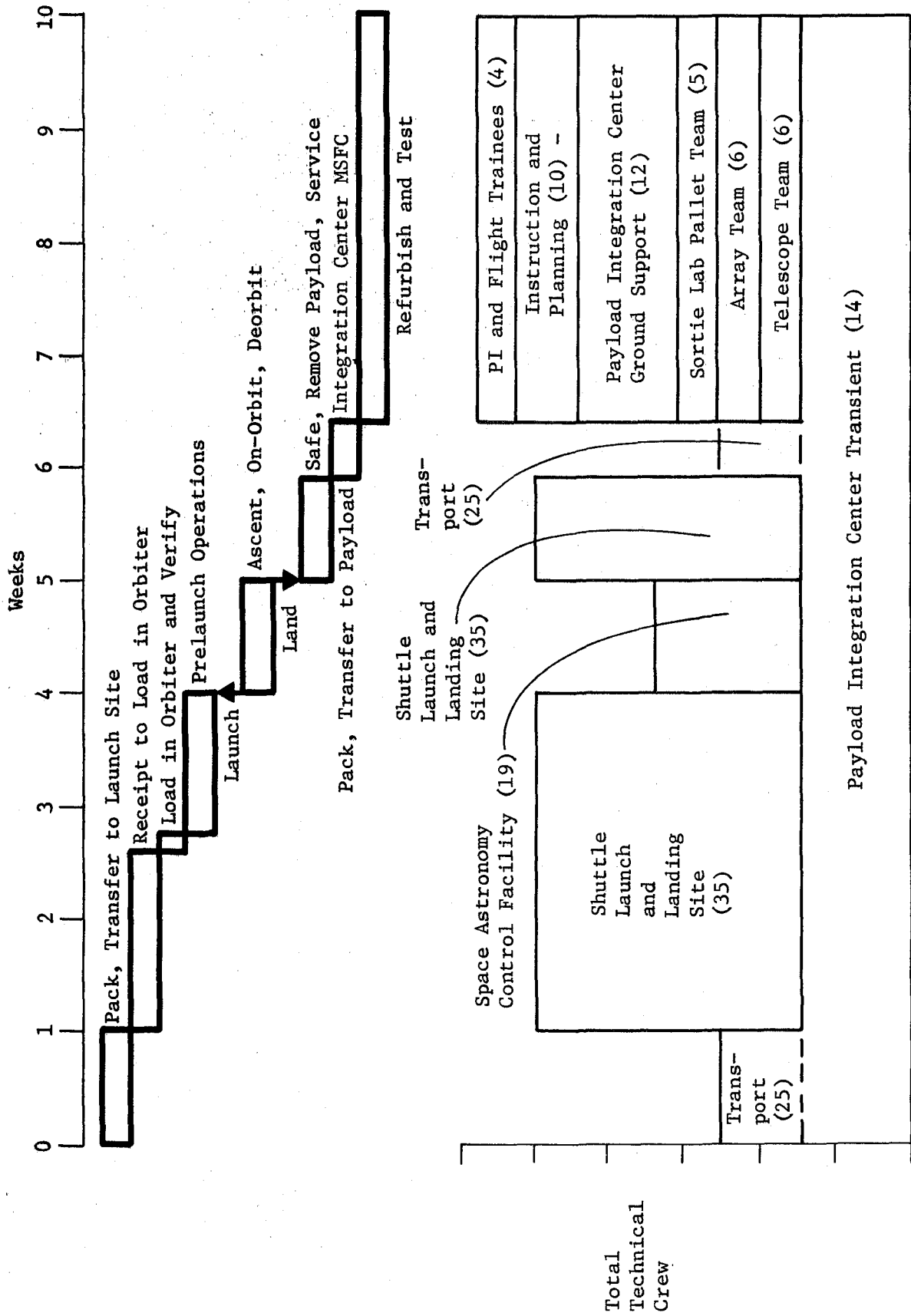


Fig. II-14 Manpower Requirements per Turnaround Cycle

Table II-12 Direct Labor Manpower for Astronomy Sortie Program

Manpower	Calendar Year											
	79	80	81	82	83	84	85	86	87	88	89	90
Transient	14	14	28	28	28	28	28	28	28	28	28	28
Launch	29	29	60	60	60	60	60	60	60	60	60	60
Mission	11	11	21	21	21	21	21	21	21	21	21	21
Support	11	11	22	22	22	22	22	22	22	22	22	22
Refurbish	0	17	62	67	67	67	67	67	67	67	67	67
Total	65	82	162	193	198	198	198	198	198	198	198	198

- Note:
1. Transient manpower includes the Payload Integration Center transient crews.
 2. Launch manpower includes the Shuttle launch and landing site personnel plus the pack, ship, and transport crew.
 3. Mission manpower are those personnel required at the Space Astronomy Control Facility to support the mission.
 4. Support manpower includes the Instruction and Planning personnel, two six-man telescope teams, and one six-man array team at the PIC.
 5. The refurbish manpower includes the remainder of the PIC personnel.

D. TIMELINES

Timelines were developed for the Astronomy Sortie mission turn-around schedule, payload refurbishment, and telescope and array refurbishment. These timelines were the basis for determining the quantity of facilities, personnel, and support hardware that would be required to support the Astronomy Sortie program over the life of the mission. The timelines were derived from the detailed analyses that were performed on the six operational phases. The worksheets for the detailed analyses are included in Appendix A2, Volume III, Book 2.

1. Turnaround Schedule

The overall sequences of events for all six program phases were integrated with the baseline Shuttle and Orbiter prelaunch sequence to derive the schedule shown in Fig. II-15. In this turnaround schedule a variable work week and multiple shifts were chosen for some functions to accomplish the work hours indicated in the week span times shown. In determining these span times, consideration was given to the necessity to maintain reasonable work weeks over the 12-year Astronomy Sortie program duration and to use the PIC transient crew with the launch site crew in providing multiple shift operations when necessary.

For this turnaround schedule, a 215-hr Shuttle processing schedule was used. This schedule requires that payload loading be started at launch minus 135 hr and allows 12 hr for installation and verification of the payload. Refurbishing the payload at the PIC requires 135 hr.

2. Payload Refurbishment

The sequence of events for payload refurbishment at the Payload Integration Center, Phase VI, requires a total of 135 work hours, including tests to establish flight readiness. This 135-hr period is shown as 3 weeks, 2 days in Fig. II-16, beginning at week four and is based on a 40-hr work week for one shift.

The merge point of telescopes and arrays with the Sortie Lab and pallet occurs on this schedule at week six. Detailed refurbishment schedules for each telescope and array are presented in Appendix A2, Volume III, Book 2 and are summarized in Fig. II-17. Mirror recoating should not be required after each flight, but a schedule for this function was estimated for each telescope. It is expected that the telescopes and arrays that are removed will not be flown

on the next flight. If "next flight" refurbishment is required, the experiments must be serviced in about 10 days so that they will be ready for installation when the Sortie Lab and pallet is prepared to receive them.

The shortest normal refurbishment cycle shown on Fig. II-16 is for the Stratoscope III telescope and either the narrow band spectrometer/polarimeter array group or the large modulation collimator array group. The longest normal refurbishment cycle is for any payload that has the large area X-ray detector and the collimated plane crystal spectrometer as the array group.

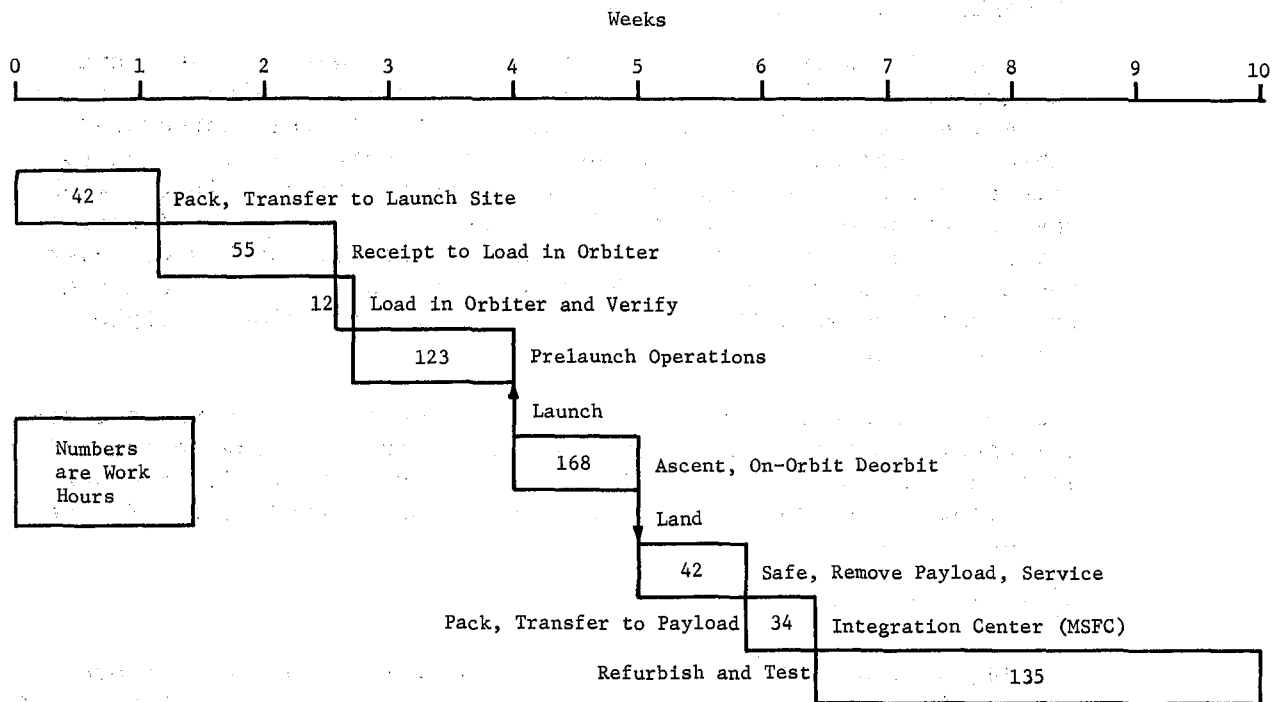


Fig. II-15 Turnaround Schedule

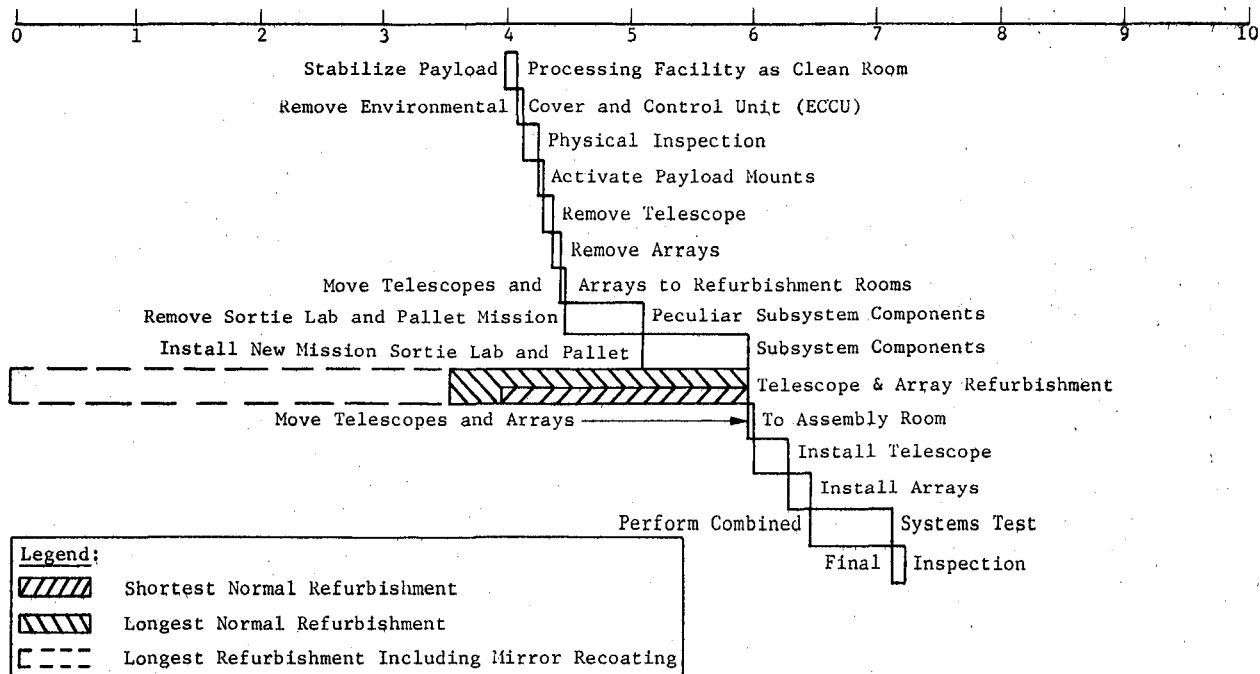


Fig. II-16 Payload Refurbishment Cycle

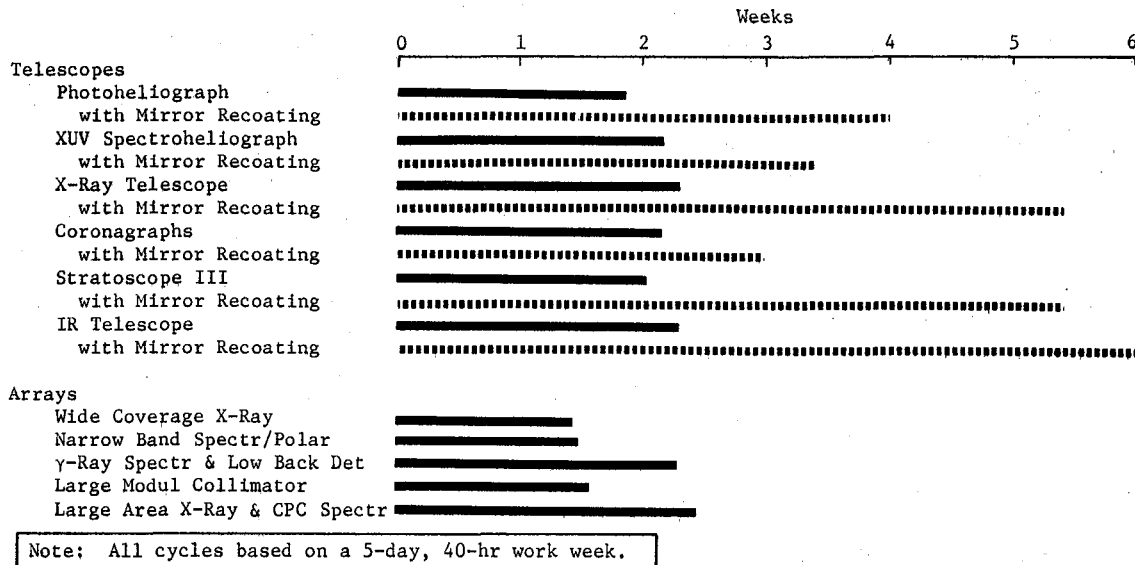


Fig. II-17 Telescope and Array Refurbishment Cycles

E. MISSION ANALYSES

Mission analyses were performed to determine the preferred orbital parameters for the astronomy telescopes and arrays. The results of the mission analyses indicate that the orbital parameters for the seven-day Sortie missions can be selected to maximize the experiment objectives.

1. Solar Astronomy Payloads

The basic requirements that solar payloads place on orbit selection are: (1) continuous sun viewing for the seven-day Sortie mission; (2) no viewing through the atmosphere of the earth; and (3) minimization of the doppler shift.

Ideally, for solar astronomy, it would be desirable to maintain the orbit plane perpendicular to the sun line (beta angle of 1.57 radians or 90 deg), because this orbit would satisfy all of the above solar requirements. Since this is not possible without altering the orbit, it is desirable to select orbits that satisfy the requirements although the beta angle does change.

a. Beta Angle - A three dimensional view of the orbit parameters that determine the beta angle is depicted in Fig. II-18.

A beta angle of 1.57 radians (90 deg) occurs when the following conditions are satisfied,

$$i = \frac{\pi}{2} - \delta_s \quad (\delta_s \geq 0 \text{ for this condition})$$

$$\Omega = \frac{\pi}{2} + \alpha_s$$

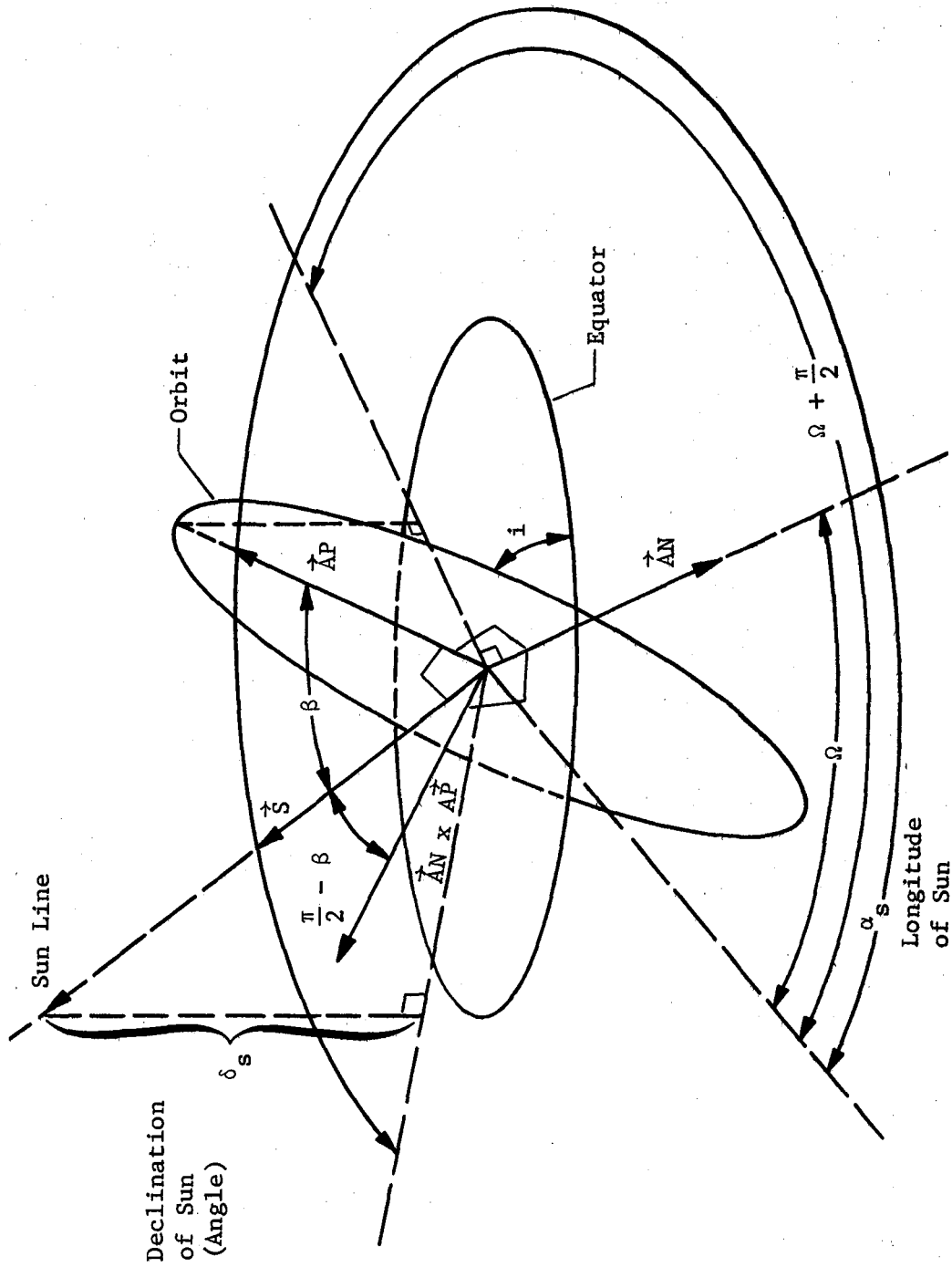
where

i = orbit inclination,

Ω = longitude of ascending node,

δ_s = sun declination (can vary from +23.5 to -23.5 deg),

α_s = sun right ascension (longitude) (varies from 0 to 360 deg).



$$\text{Beta Angle } (\beta) = \frac{\pi}{2} - \cos^{-1} [\vec{S} \cdot (\vec{AN} \times \vec{AP})]$$

Fig. II-18 Beta Angle Relationships

When $\delta_s \leq 0$ the following conditions must be satisfied

$$i = \frac{\pi}{2} + \delta_s$$

$$\Omega = \frac{3\pi}{2} + \alpha_s$$

This 90-deg beta angle occurs instantaneously. Movement of the sun with respect to the earth along with regression causes the beta angle to decrease. At any point in time the beta angle is given by

$$\beta = \frac{\pi}{2} - \cos^{-1} [\vec{S} \cdot (\overline{AN} \times \overline{AP})]$$

where the vectors \vec{S} , \overline{AN} , and \overline{AP} , all unit vectors in earth-centered inertial coordinates, are defined as follows:

The vector \vec{S} is a unit vector from the center of the earth toward the sun.

$$S_x = \cos(\alpha_s) \cos(\delta_s)$$

$$S_y = \cos(\delta_s) \sin(\alpha_s)$$

$$S_z = \sin(\delta_s)$$

The vector \overline{AN} is a unit vector from the center of the earth in the direction of the orbit ascending node.

$$AN_x = \cos(\Omega)$$

$$AN_y = \sin(\Omega)$$

$$AN_z = 0$$

The vector \overline{AP} is a unit vector from the center of the earth in the direction of a point on the orbit having a longitude of $\Omega + \pi/2$.

$$AP_x = \cos \Omega + \frac{\pi}{2} \cos(i)$$

$$AP_y = \cos(i) \sin \Omega + \frac{\pi}{2}$$

$$AP_z = \sin(i)$$

The vector $\vec{AN} \times \vec{AP}$ is a unit vector perpendicular to the orbit plane. By dotting this vector with the sun vector it is possible to compute the angle between them, that is $\pi/2 - \beta$.

Nodal regression for one revolution is approximated by

$$\delta\Omega \approx \frac{2\pi \left(\frac{3}{2} J_2\right) R_E^2}{R^2} \cos i$$

where

R_E = equatorial radius of earth,

R = orbital radius,

$J_2 = 1.082 \times 10^{-3}$.

After N days the total change in Ω will be

$$\Delta\Omega = \frac{N \delta \Omega}{P_N}$$

where

P_N = nodal period (days)

$$P_N = P_K \left[1 - \frac{3}{2} J_2 \left(\frac{R_E}{R}\right)^2 \left(\frac{3}{2} - \frac{7}{4} \sin^2 i\right) \right]$$

and P_K = Keplerian period (days)

$$P_K = \frac{2\pi R^{3/2}}{\sqrt{\mu}}$$

where

μ = the gravitational constant of the earth.

The orbit inclination required for a beta angle of 1.57 radians (90 deg) depends upon the declination of the sun and varies with launch date of the year from 1.16 radians (66.5 deg) to 1.57 radians (90 deg).

b. *Solar Payload Orbit Selection* - The approach that was used to select the preferred orbital parameters for the solar payloads was to first determine the launch inclination that would provide a beta angle of 1.57 radians (90 deg) and the orbital altitude that would provide continuous sun viewing without viewing through the earth's atmosphere. The next step was to investigate the doppler shift that would be realized as a result of the changes to the beta angle during the seven-day mission. The final step was to combine the results of these analyses to arrive at the preferred orbital parameters for the solar payloads.

Figure II-19 presents the orbital inclinations that would be necessary for a beta angle of 1.57 radians (90 deg) as a function of the launch date. The minimum orbital inclination that will provide a 90-deg beta angle is 1.16 radians (66.5 deg), and this occurs at the summer and winter solstices when the sun's declination is ± 0.41 radians (± 23.5 deg). The maximum inclination required is 1.57 radians (90 deg), which occurs when the sun's declination is zero. For the remainder of the year, inclinations will vary between these two extremes as a function of the launch date. The one constraint necessary to satisfy these conditions is that 24 hr a day launch capability exists. The 90-deg beta angle shown will occur instantaneously and will start to decrease, depending on the orbital inclination and altitude.

As the beta angle decreases, the solar instruments will have to view the sun through the earth's atmosphere unless the orbital altitude is high enough to account for the shift. Figure II-20 shows the minimum altitude that would be required to avoid viewing through a 185-km (100 n mi) atmosphere as a function of the initial orbit inclination. Two curves are shown, one for three and one-half days and the other for seven days. As can be seen, the minimum altitude for seven days becomes very high at the lower inclinations. The solar mission can be tailored to allow the beta angle to become 1.57 radians (90 deg) half way through the seven-day mission, and thus minimize the altitude required to provide continuous sun without viewing through the atmosphere. Since this mode of operation does minimize the energy required to satisfy the solar objectives, it was selected as the mission profile.

For the majority of the solar telescopes, a 185-km (100 n mi) atmosphere is sufficient. However, the XUV spectroheliograph does require a 400-km (216 n mi) atmosphere to satisfy the telescope objectives. Figure II-21 shows the minimum altitudes that would be required to provide continuous sun without viewing through the 400-km (216 n mi) atmosphere.

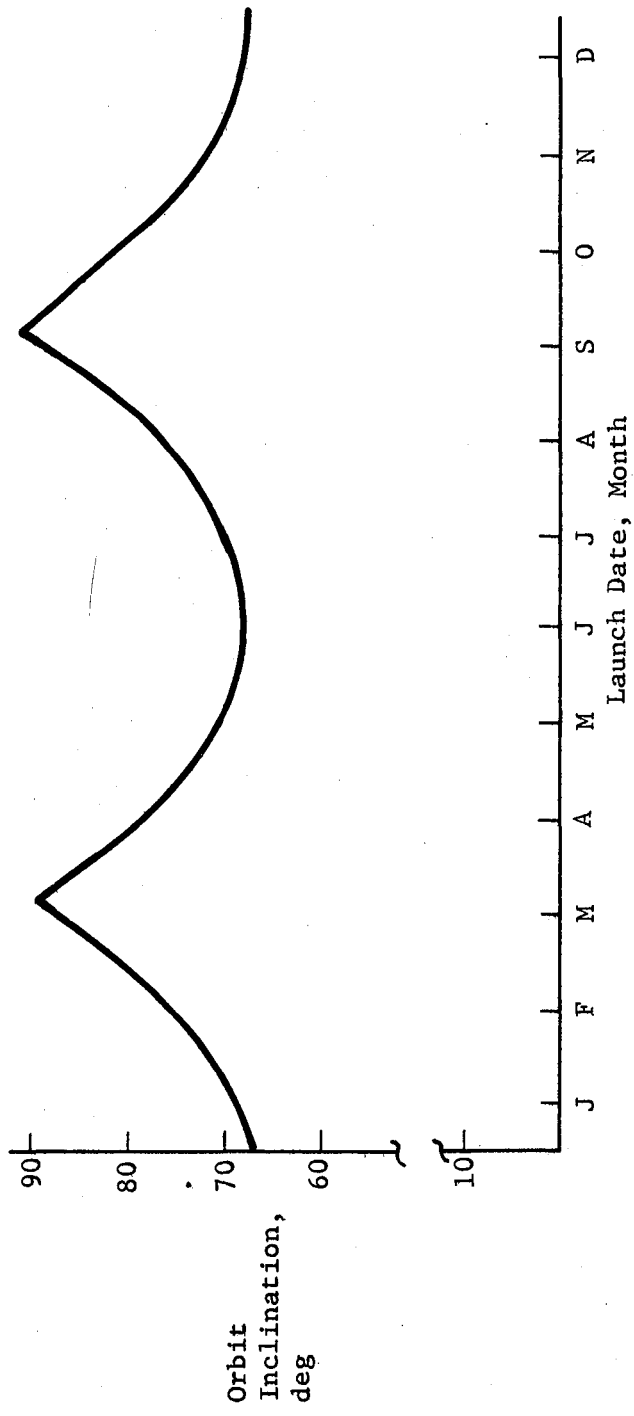


Fig. II-19 Inclination Required for 90-deg Beta Angle

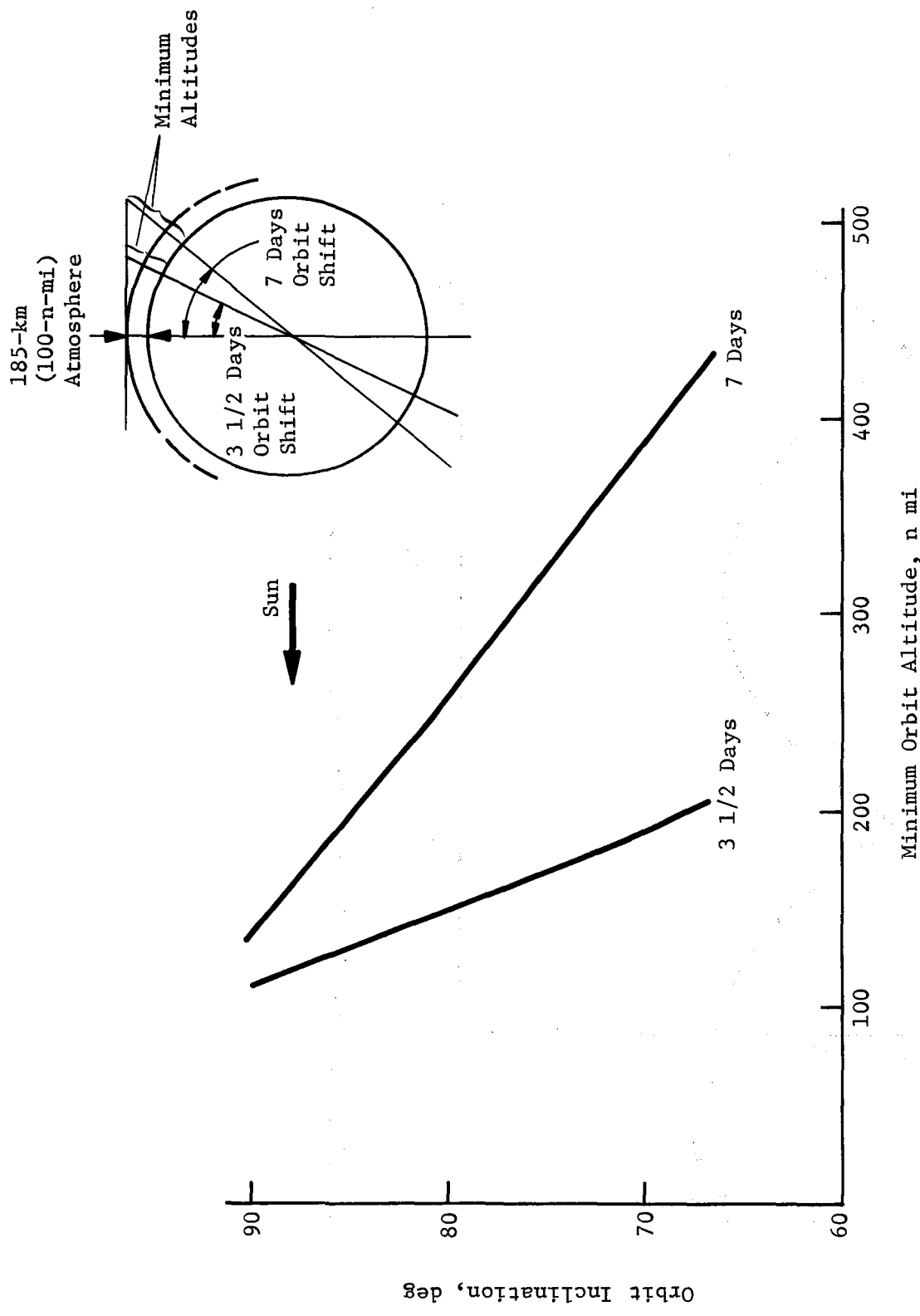


Fig. II-20 Altitude Required for Continuous Sun

Orbit regression varies from near zero to at 1.57 radians (90 deg) inclination, to approximately 0.1 radian (6 deg) per day at lower inclinations. Figure II-22 shows the variation in beta angle, at 3 1/2 days and at 7 days before or after beta angle of 1.57 radians (90 deg), for orbit inclinations suitable for the solar payloads and an altitude of 463 km (250 n mi). The change in beta angle shown includes both factors (sun position and orbit regression) that influence this shift.

The shift in beta angle results in a doppler shift that increases as the beta angle shifts further from 1.57 radians (90 deg). Shown in Figure II-23 is the maximum doppler shift at 7000 angstroms for various orbit inclinations suitable for solar telescopes and an altitude of 463 km (250 n mi).

The curves indicated as "3 1/2 days" and "7 days" will occur either before or after the zero maximum doppler shift point. For reference, the resolution capability of the photoheliograph spectrograph of 0.028 angstroms at 7000 angstroms is shown. It may be observed that the maximum doppler shift exceeds the resolution of the spectrograph at all orbit inclinations less than 1.38 radians (79 deg) for the 3 1/2-day curve and less than 1.54 radians (88 deg) for the 7-day curve.

The doppler shift presented is the result of the Orbiter having a delta velocity that is a function of the beta angle and the orbital altitude.

Doppler shift (A) = $\frac{\cos \beta V_{\text{orbital velocity}}}{V_{\text{speed of light}}} \lambda$ (A)

Sun ↑

The spectral range and spectral resolution for the solar experiments are listed in Table II-13. Also, the maximum doppler shift that would be seen by the instruments at an altitude of 463 km (250 n mi) and a beta angle of 1.35 radians (77 deg) is presented. Note from Fig. II-22 that a beta angle of 1.35 radians (77 deg) is the lowest expected for a 7-day mission, centered 3 1/2 days before and after a beta angle of 1.57 radians (90 deg).

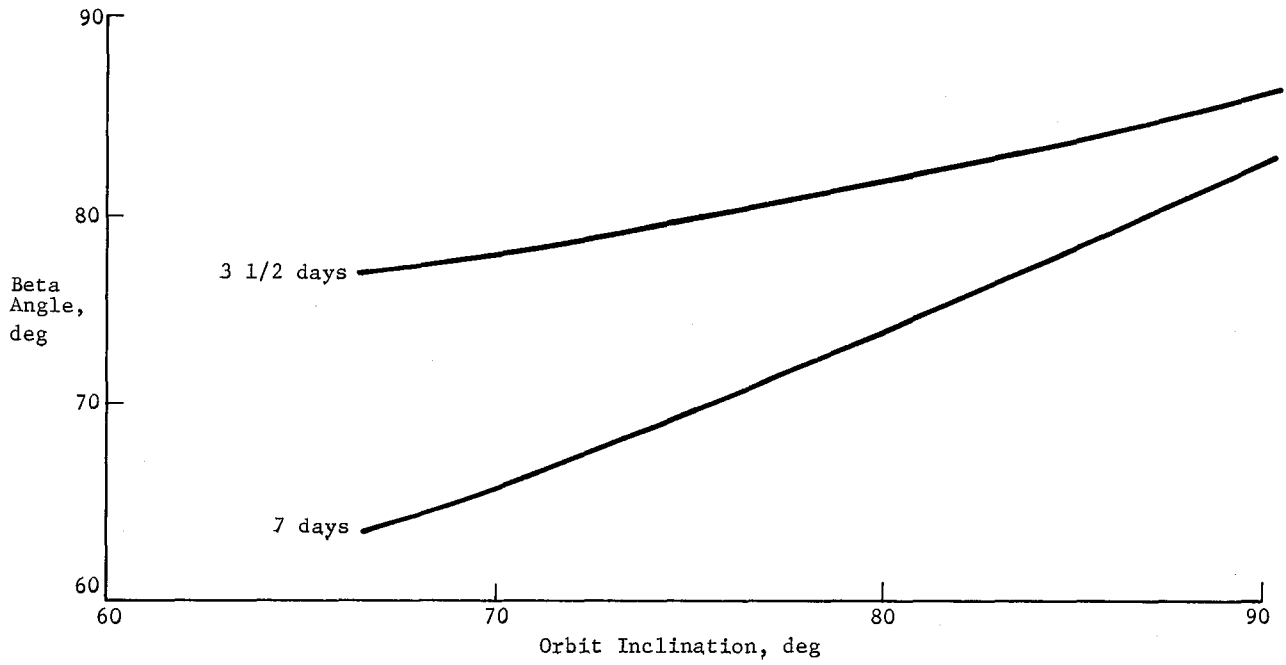
As can be seen from the table, the only instrument that would be sensitive to the maximum doppler shift would be the dual range spectrograph for the photoheliograph. The maximum doppler shift exceeds the resolution of the spectrograph at all wavelengths. In reality, the doppler shift would vary from zero to maximum value twice per orbit depending on the orbital location of the Shuttle.

Fig. II-23
 Altitude
 200
 300
 350
 Minimum
 Altitude
 of
 Orbit
 (km)
 (250
 nmi)
 Atmosphere

Orbit
 Inclination
 deg

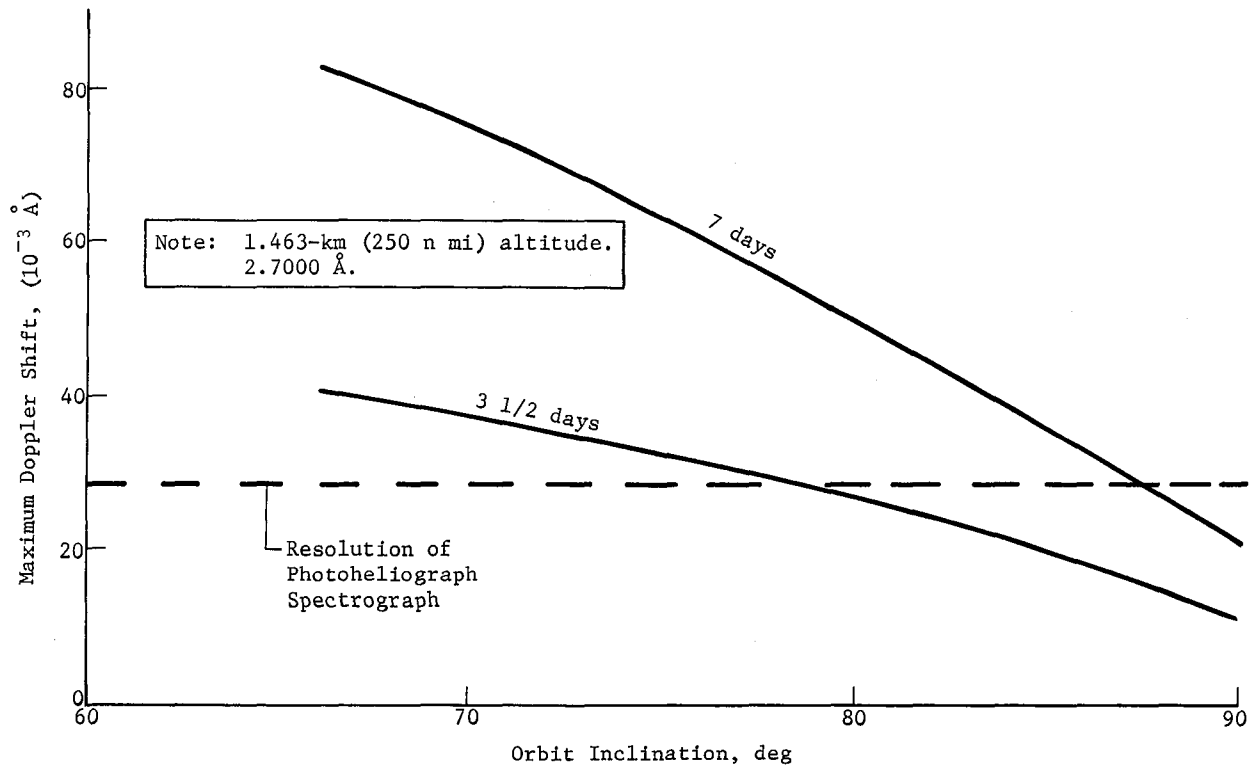
400 km (216 n mi)
 Atmosphere

Minimum
 Altitude
 of
 Shuttle
 Orbit



Note: 463-km (250 n mi) altitude.

Fig. II-22 Beta Angle Variations as a Function of Inclination



Note: 1.463-km (250 n mi) altitude.
2.7000 \AA .

Fig. II-23 Doppler Shift as a Function of Inclination

Table II-13 Effect of Doppler Shift on Solar Instruments

Telescope Instrument	Spectral Range, Å	Instrument Resolution, Å	Doppler Shift at 250 n mi; $\beta = 77^\circ$, Å
Photoheliograph	2000 to 7000		
Broadband Camera	2000 to 2500; 4000 to 7000	100 to 500	0.012 to 0.040
H-Alpha Camera	6563	0.250	0.038
Spectrograph, Dual Range	2000 to 3000 3000 to 7000	0.008 to 0.012 0.012 to 0.028	0.012 to 0.017 0.017 to 0.040
XUV Spectro- heliograph	170 to 650	0.015 to 0.058	0.001 to 0.004
X-Ray Telescope	2 to 100		
Crystal Spectrom- eter	2 to 20	0.001 to 0.010	0.00001 to 0.0006
Proportional Counter	10 to 100	5 to 50	0.00006 to 0.0006
Imaging System	2 to 100	1 to 50	0.00001 to 0.0006

The data indicate that to keep the maximum doppler shift less than the resolution of the spectrograph it would be necessary to limit the launch dates for the mission. Figure II-24 shows this limitation.

In the analysis of maximum doppler shift at 7000 angstroms in comparison with orbit inclination (Fig. II-23) it was shown that the resolution of the photoheliograph spectrograph (0.028 angstrom) is equal to the maximum doppler shift after $3\frac{1}{2}$ days for a circular orbit of 463 km (250 n mi) and an inclination of 1.38 radians (79 deg). From this observation, all orbit inclinations higher than 1.38 radians (79 deg) result in maximum doppler shifts that are less than the resolution of the spectrograph. The calendar dates for such missions are shown in Fig. II-24 as the 100 percent line on the bottom curve.

Further, a portion of the on-orbit period of $3\frac{1}{2}$ days for orbits at lower inclinations is within the resolution of the spectrograph. As shown, the portion of $3\frac{1}{2}$ days time within the limits is no less than 83.8% at the minimum inclination for solar telescopes of 1.16 radians (66.5 deg) on the summer and winter solsties.

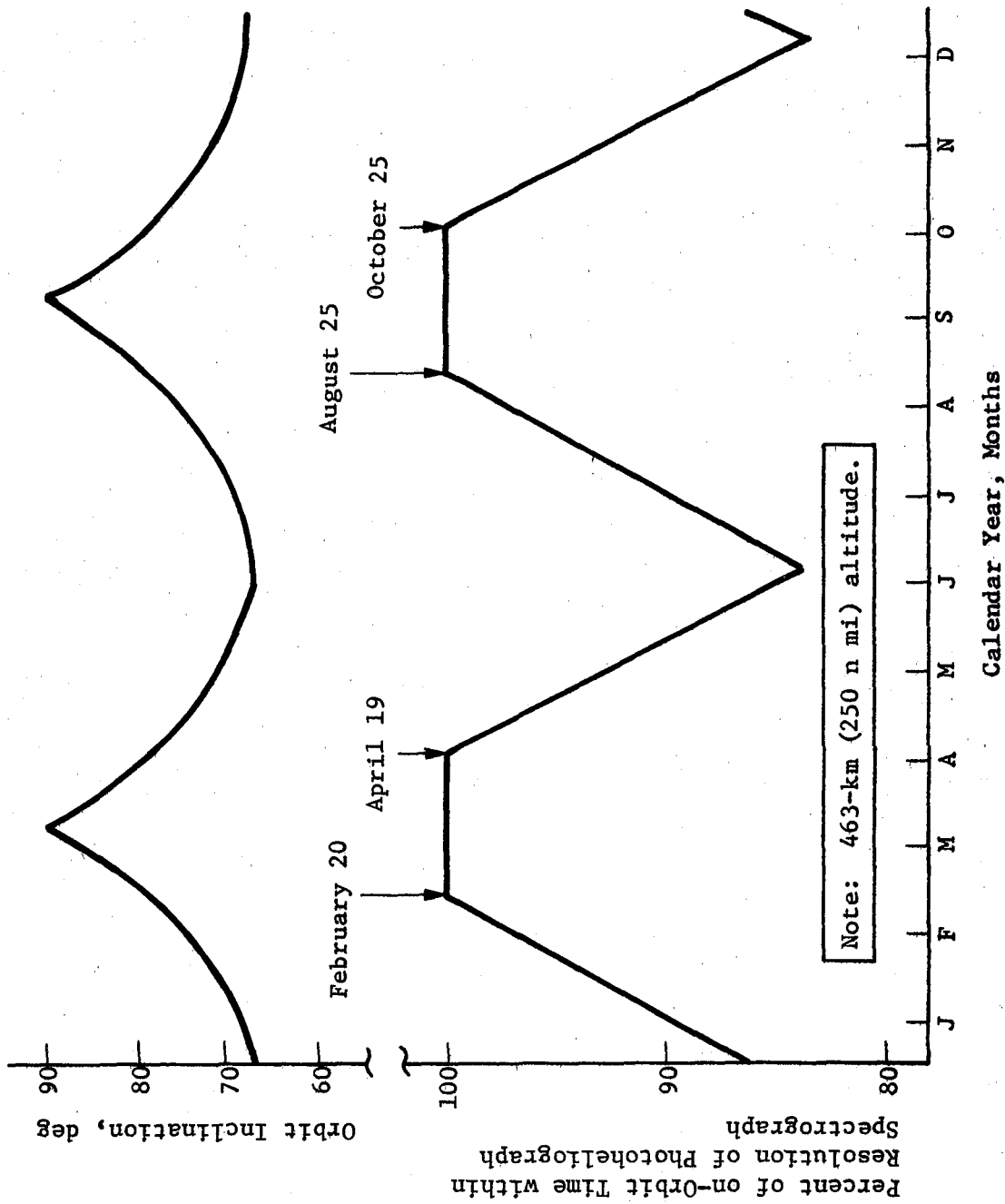


Fig. II-24 Photoheliograph Constraint on Inclination

Table II-14 summarizes the orbit parameters for the solar payload. For the baseline solar payload it will be necessary to restrict the launch dates as shown to maintain doppler shifts that are less than the resolution of the photoheliograph spectrograph. Also shown on the table are the orbit parameters that could be selected should the doppler shift not be important to a particular payload.

Table II-14 Solar Payload Orbit Parameters

Baseline Solar Payload	
Beta Angle:	Select Launch Time for beta equals 1.57 Radians (90 deg) at Midpoint of 7-day Mission
Inclination:	1.38 to 1.57 Radians (79 to 90 deg)
Altitude:	470 to 418 km (254 to 226 n mi)
Time of Year:	Feb 20 to Apr 19 and Aug 25 to Oct 25
Earth Atmosphere:	400 km (216 n mi)
Neglecting Doppler Shift	
Beta Angle:	Select Launch Time for beta Equals 1.57 Radians (90 deg) at Midpoint of 7-day Mission
Inclination:	1.16 to 1.57 Radians (66.5 to 90 deg)
Altitude:	574 to 418 km (310 to 226 n mi) for a 400 km (216 n mi) Atmosphere
	388 to 204 km (210 to 110 n mi) for a 185 km (100 n mi) Atmosphere
Time of Year:	Anytime

2. Stellar Astronomy Payloads

The basic requirements that stellar payloads place on orbit selection are: (1) maximize dark time; (2) maximize celestial sphere availability; (3) minimize sun, moon, and earth interference with viewing capabilities; (4) maximize angle for cone of continuous visibility; and (5) do not view through the atmosphere of the earth.

It is desirable to maximize the orbit dark time to enable more efficient operation of the telescopes and to maximize the amount of the celestial sphere that would be available for observations to enable flexibility in target selection.

It is also desirable to minimize the sun, moon, and earth interference with celestial viewing since these bodies will not be viewed with the stellar instruments because of the high flux levels that interfere with the stellar targets.

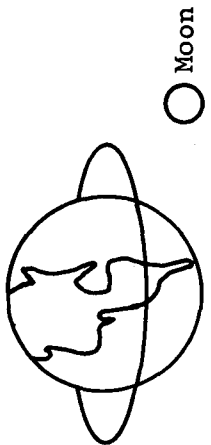
For long-duration observations on stellar targets it is desirable to place the targets in the cones of continuous visibility (North and South Poles of the orbit plane). The cones of continuous visibility are a function of the viewing constraints placed on the earth and the orbital altitude.

Finally, one major reason for going into space is to eliminate viewing through the earth's atmosphere.

a. Dark Time Analysis - An elliptical orbit was investigated to determine if there was a significant increase in dark time as compared to a more conventional circular orbit. The results of this analysis, included in Volume II, Book 1 of this report, indicated that a small increase in dark time (less than 3 minutes maximum) could be obtained with elliptical orbits. Because this is not a significant increase in dark time and elliptical orbits do have some operational disadvantages, it was recommended that only circular orbits be considered for the stellar payloads.

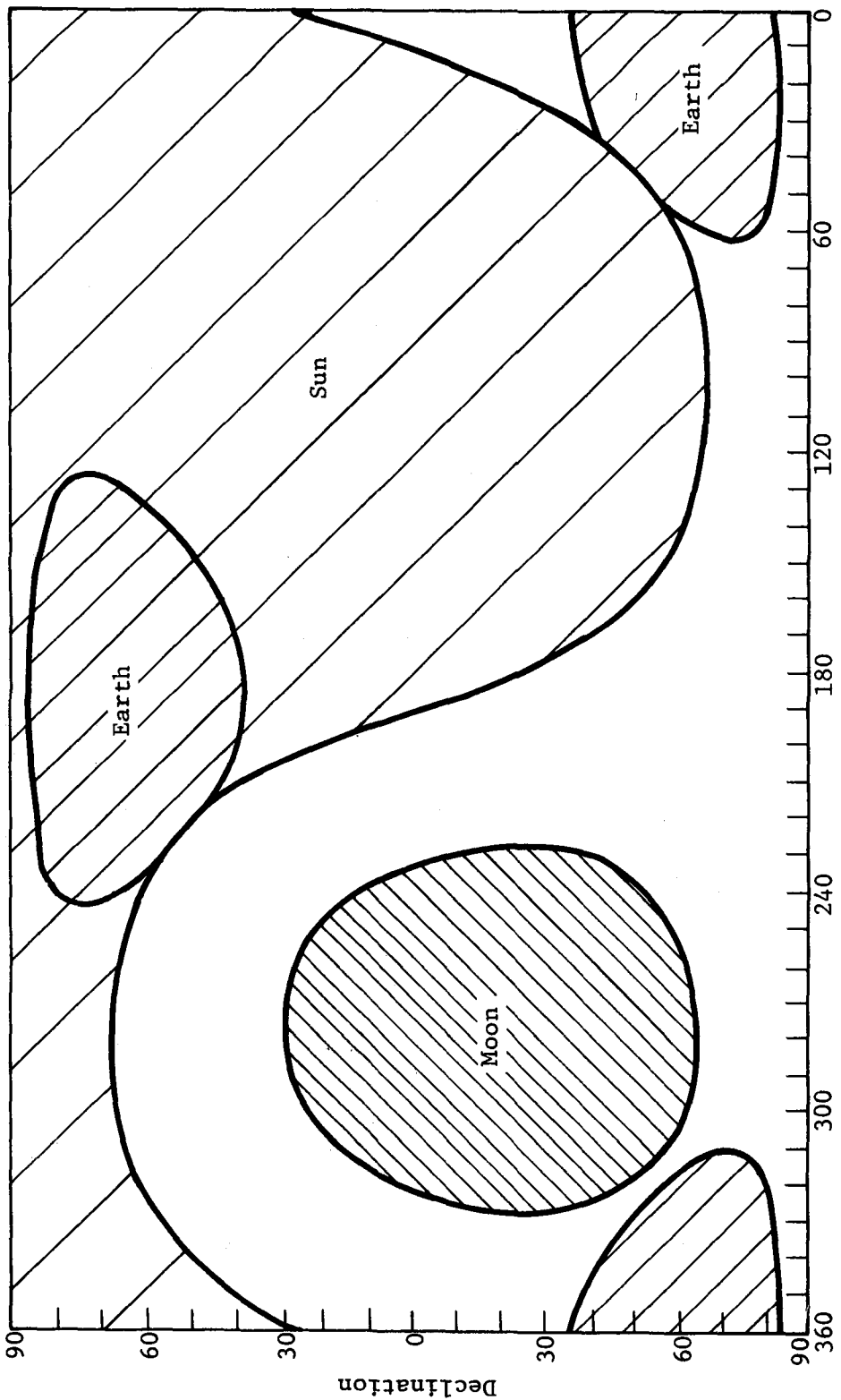
b. Celestial Sphere Availability - The percentage of the celestial sphere available for viewing depends on the experiment look angle constraints about the sun, earth, and moon. Figures II-25 and II-26 show the celestial sphere area (clear area) that would be available for viewing during a specific orbit for two sets of look angle constraints. Figure II-25 has the look angle constraints of no viewing within 1.57 radians (90 deg) of the sun and 0.79 radians (45 deg) of the limb of the earth or moon. Figure II-26 has the same constraint on the sun and earth, but only a 0.09 radian (5 deg) constraint on the moon. The figures shown are for a zero beta angle, an altitude of 463 km (250 n mi) and a date of July 1, 1977. The date shown is for a full moon because this date would minimize the amount of the celestial sphere available for viewing.

Figure II-27 shows the celestial sphere availability for a date of July 15, 1977. This is a new moon condition and the moon constraint is no longer important because the moon is located in the hemisphere of the sun.



Note: Cannot view within 90 deg of sun; 45 deg of earth and moon (July 1, 1977).

Sun



Right Ascension

Fig. II-25 Celestial Sphere Availability (45 deg Moon Constraint)



- Cannot View within 90° of Sun; 45° of Earth & 5° of Moon
- July 1, 1977
- Beta Angle of Zero

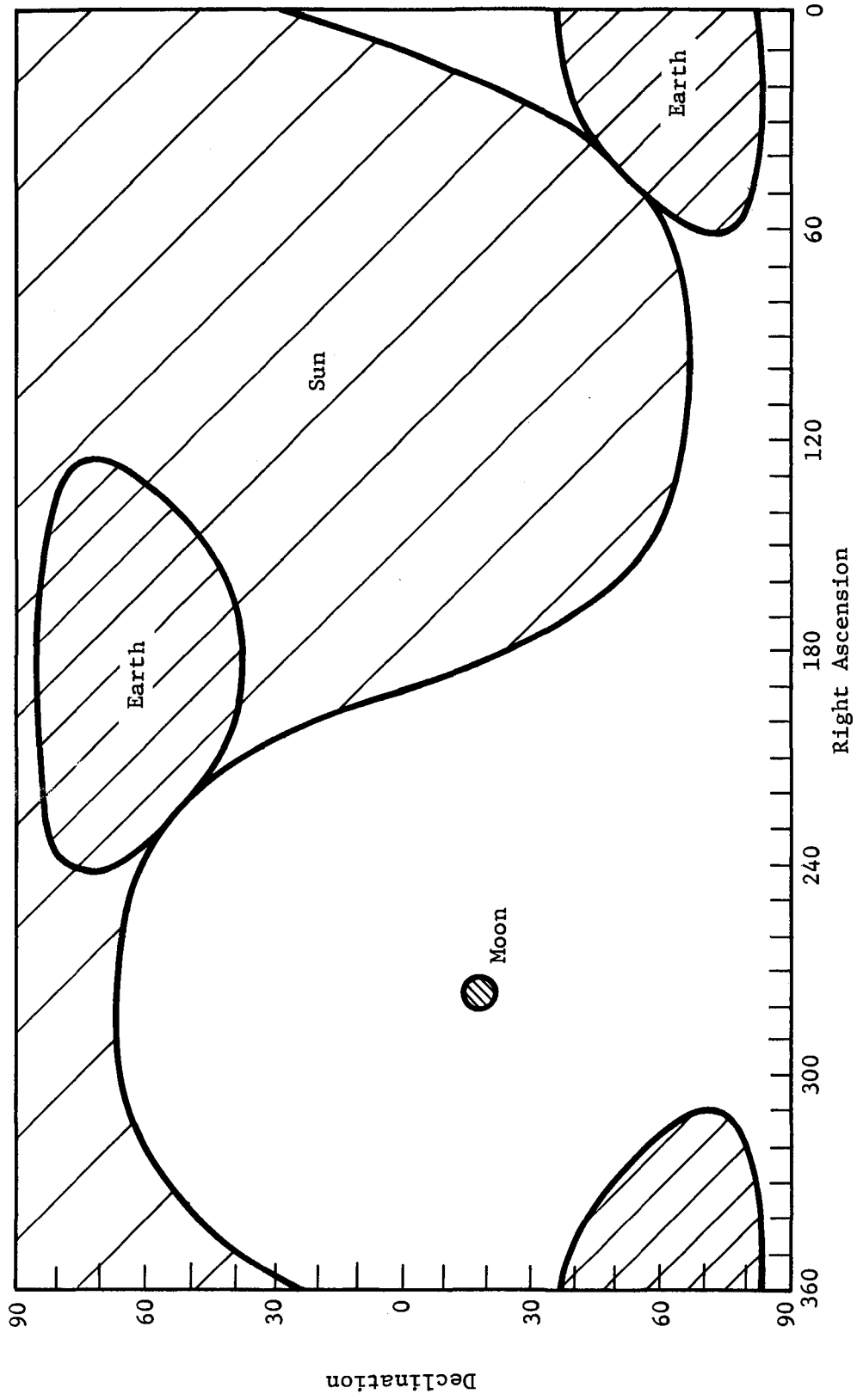
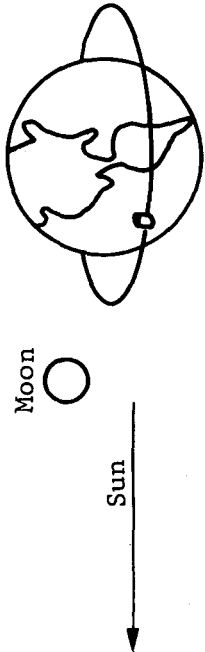


Fig. II-26 Celestial Sphere Availability (5 deg Moon Constraint)



Note: Cannot view within 90 deg of sun, 45 deg of earth and moon (July 15, 1977).

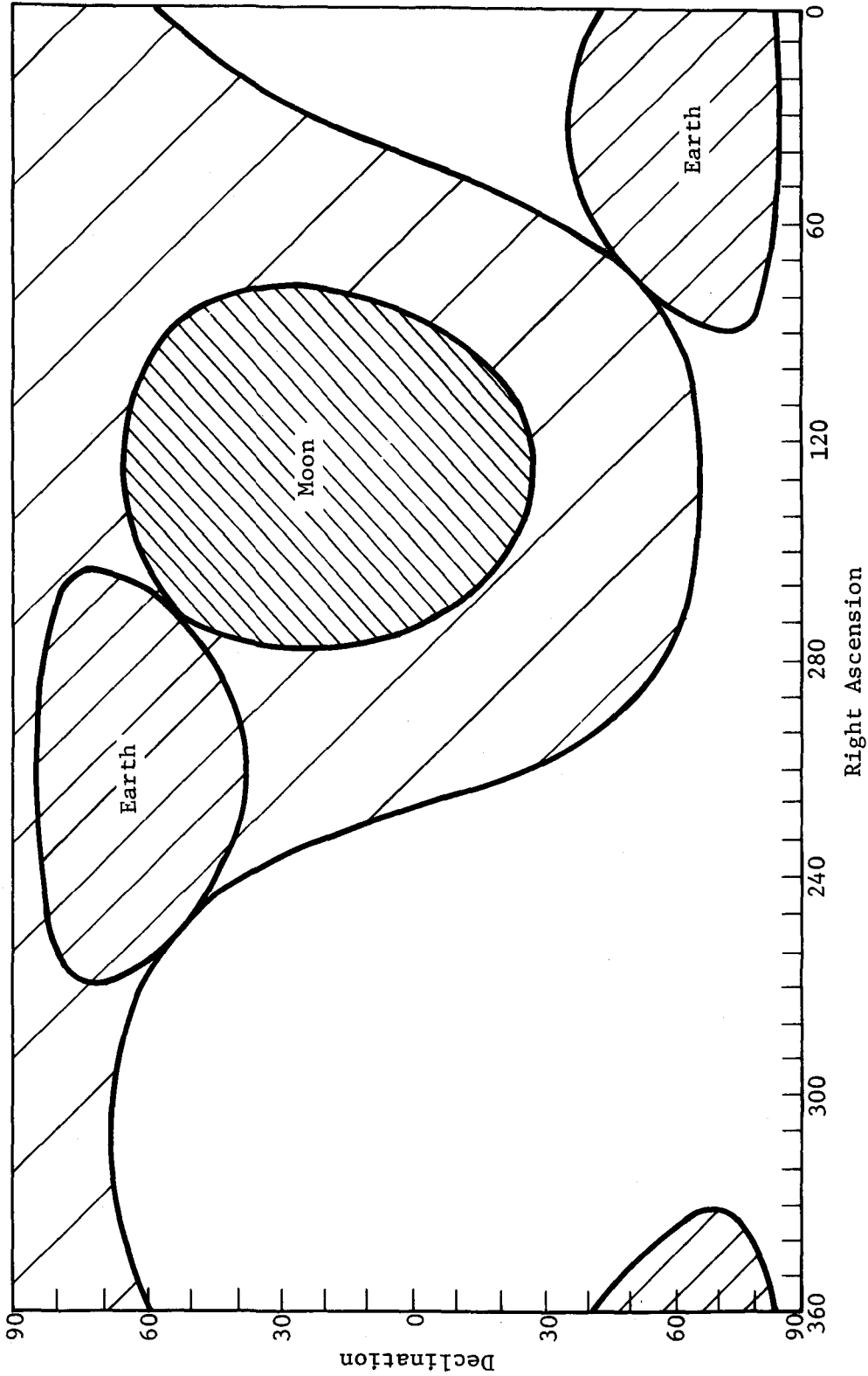


Fig. II-27 Celestial Sphere Availability (New Moon)

The minimum and maximum celestial sphere availability is a function of the lunar period, with the maximum viewing capability occurring when the area occulted by the moon lies entirely within the area occulted by the sun. Dates when this condition occurs may be determined by comparing the angle between the vectors from the earth to the sun and from the earth to the moon. The equation is:

$$\theta = \cos^{-1} (\vec{S} \cdot \vec{M}) \text{ in which:}$$

\vec{S} = unit sun vector, and

\vec{M} = unit moon vector.

In the above equation, the maximum viewing capability occurs when $\theta \leq \frac{\pi}{4}$. From these relationships, the variation during calendar year 1979 was derived for two pairs of look-angle limits as shown in Fig. II-28.

The top curve shown in Fig. II-28 is based upon the limits for Stratoscope III about the sun and moon only. Because of the earth's apparent motion about the Orbiter, the entire celestial sphere can be seen on a revolution-by-revolution basis with respect to the earth look-angle constraint of 0.262 radian (15 deg) for Stratoscope.

The bottom solid-line curve shows the change in percentage of the celestial sphere viewable for a different set of look-angle restrictions about the sun and moon. The dashed-line curve includes the viewing constraint imposed by the earth. It may also be observed that (in 1979) the duration of maximum percent regions varies from about 6.5 days to about 8.2 days. Thus, the seven-day Sortie mission viewing capability may be maximized by launching at the start of a maximum percent region. For small look angles about the moon, it would be possible to launch anytime since the amount of the celestial sphere occulted by the moon constraint would be very small.

Figure II-29 shows the percentage of the celestial sphere that is viewable for various look-angle constraints about the sun, earth, and moon. Flying these missions during the new-moon phase adds significantly to the viewable portion of the celestial sphere at the higher angles of constraint. This advantage decreases to near-zero at an angle of 0.524 radian (30 deg) about the sun and 0.262 radian (15 deg) about the earth and moon. At the constraint of 0.524 radian (30 deg) about the sun and 0.262 radian (15 deg)

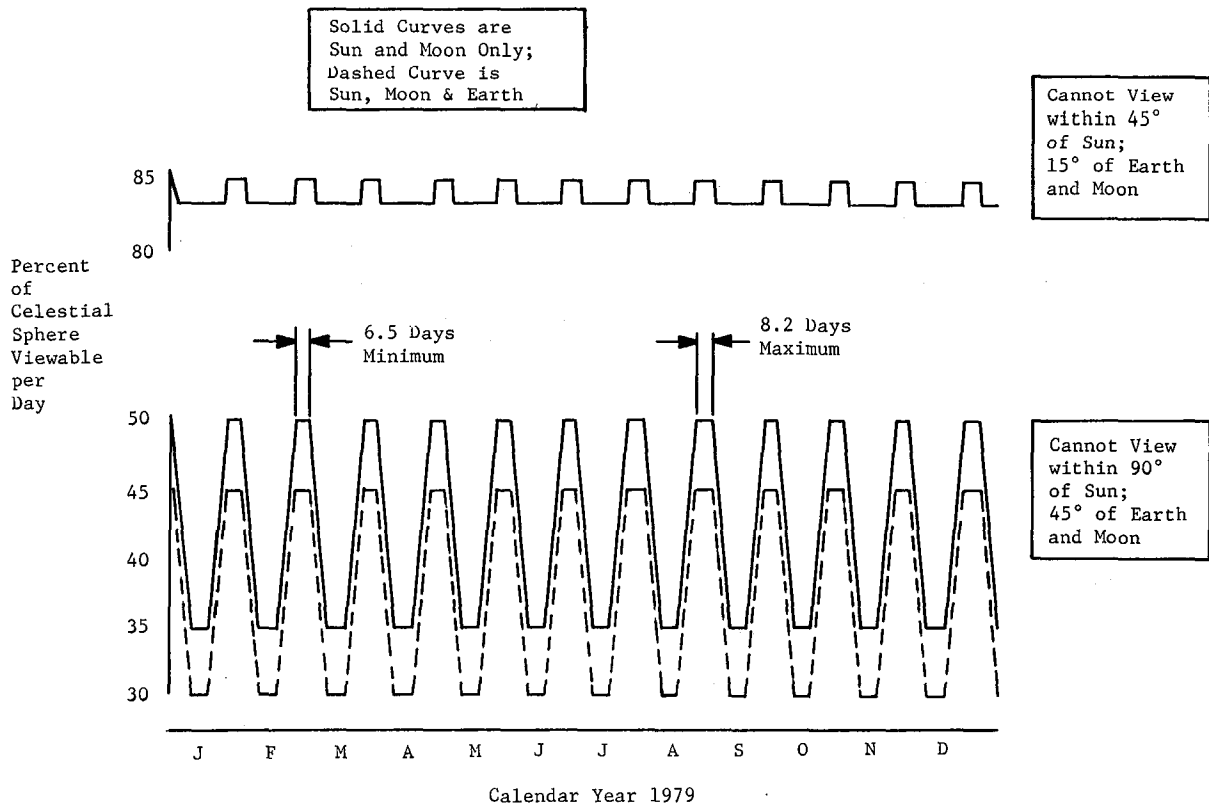


Fig. II-28 Stellar Viewing Variation with Sun and Moon Position

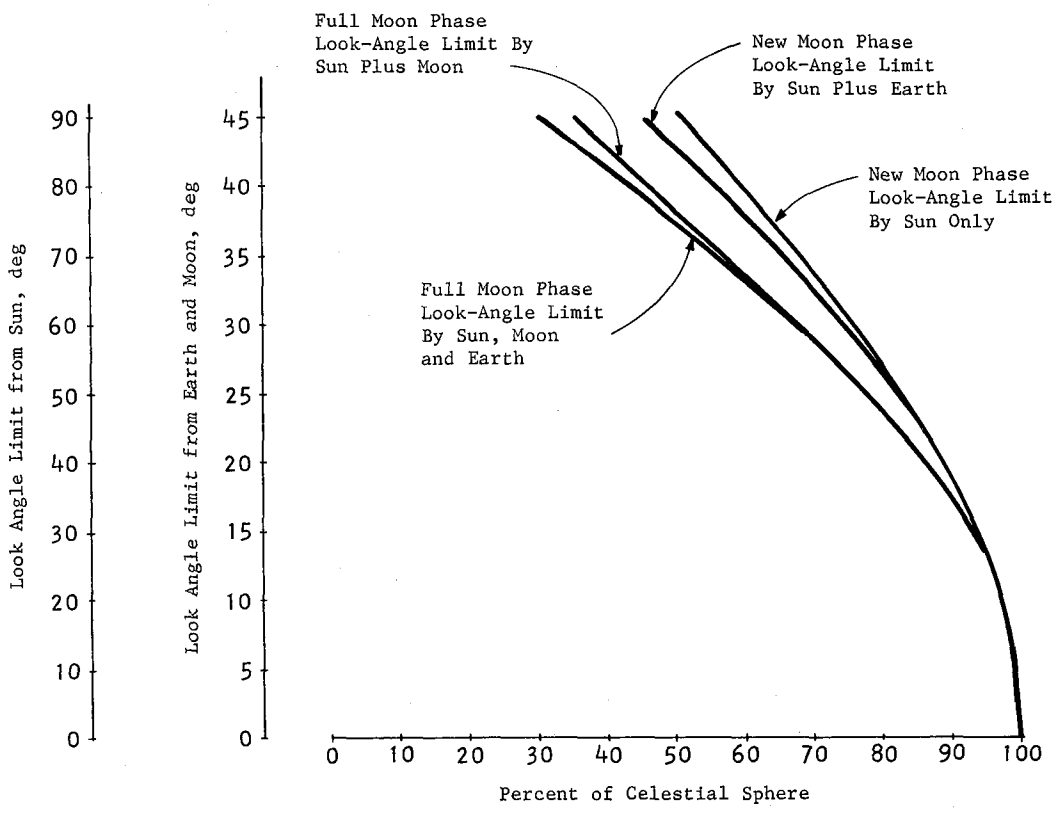


Fig. II-29 Look Angle Constraint Impact on Celestial Viewing

about the earth and moon, some 93% of the celestial sphere may be observed; thus little may be gained in reducing the look-angle constraints below this level unless a cone larger than 0.21 radian (12 deg) of continuous viewing is desired. For the larger cones of continuous viewing, as will be shown, constraints as low as 0.087 radian (5 deg) about the limb of the earth are desirable.

These constraints show the importance of including baffles in the design of the stellar telescope to permit look angles close to the sun, moon, and earth.

c. Cone of Continuous Visibility - The variation in the cone of continuous viewing for a circular orbit of 463 km (250 n mi) altitude is shown in Fig. II-30. For this altitude, the maximum full-angle cone viewable throughout the entire orbit is 0.558 radian (32 deg) at the limit imposed by the 185 km (100 n mi) atmosphere of the earth. The look angle constraint about the earth for this maximum cone of continuous viewing is 0.087 radian (5 deg).

The present look angle limits of 0.79 radian (45 deg) prescribed for the IR telescope lie 0.41 radian (24 deg) above the minimum angle for a continuous cone of viewing. Thus the present limits impose a 0.82 radian (48 deg) full-angle cone restricted to any viewing. This cone of no viewing was shown in Fig. II-25, II-26, and II-27 as the "earth" restriction.

d. Stellar Payload Orbit Selection - The selected orbits for the stellar payloads are shown in Table II-15. Two conditions are presented, one considers the preferred orbits for those telescopes that have view angle constraints greater than approximately 0.26 radian (15 deg) for the moon, while the other is for those telescopes that do not have constraints on the moon. In all cases, the operational aspects of the mission would be simpler if the moon was located in the new moon position.

Table II-15 Stellar Payload Orbit Parameters

	With Moon Constraint	Neglecting Moon
Inclination Radians (deg)	0.5 to 1.57 (28.5 to 90)	0.5 to 1.57 (28.5 to 90)
Altitude km (n mi)	463 to 370 (250 to 200)	463 to 370 (250 to 200)
Time of Year	Fly during New Moon	Anytime

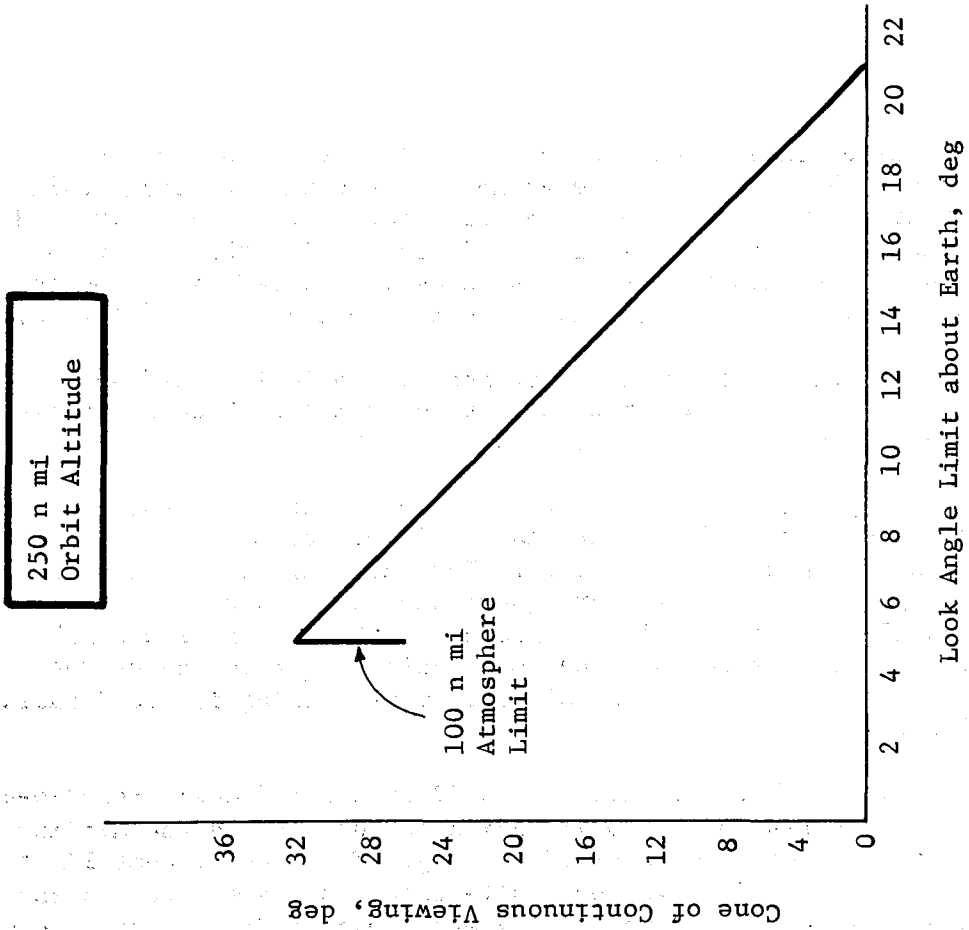
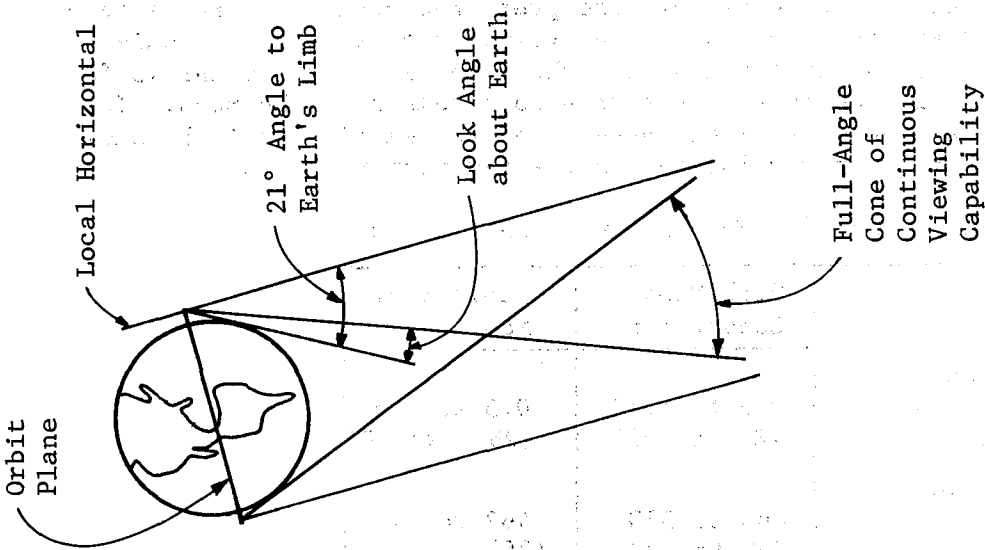


Fig. II-30 Cone of Continuous Visibility

For the IR telescope considered in this study, the viewing constraints were 1.57 radians (90 deg) about the sun, 0.79 radian (45 deg) about the earth, and 0.09 radian (5 deg) about the moon. For these constraints, a launch is possible anytime during the year, and the inclination can be selected to provide the area of the celestial sphere that wants to be observed.

The Stratoscope III telescope considered had viewing constraints of 0.79 radian (45 deg) about the sun and 0.26 radian (15 deg) about the earth and moon. As with the IR telescope, the Stratoscope III can be launched anytime and the orbit can be tailored to the telescope objectives.

3. Array Orbit Selection

The X-ray and gamma-ray arrays for the sortie payloads operate throughout the missions except during passage through the South Atlantic Anomaly. Thus the orbit altitude and inclination preference for the arrays is to minimize time spent in the anomaly area.

Figure II-31 shows the percent of time spent in the South Atlantic Anomaly for circular orbits from 370 to 741 km (200 to 400 n mi) altitudes and inclinations from 0.5 to 1.57 radians (28.5 to 90 deg). Although losses due to passage through the anomaly are lowest for low-altitude, high-inclination orbits, none of the losses exceed about 4.5%. Thus the orbit preferences of the telescopes as primary payloads may take precedence without seriously affecting results obtained with the arrays.

The South Atlantic Anomaly was represented by a cone having its apex on the earth's surface at -32° lat and 330° long., with a horizon angle of 8 deg. This model was based on $10^2/\text{cm}^2\text{-sec}$ flux contours for proton particles with energy levels greater than 15 Mev. The actual contour shape was approximated by a circle at each altitude.

Time spent in the South Atlantic Anomaly was then approximated by placing a pseudo tracking station at the point -32° lat, 330° long. and assigning it an 8 deg horizon angle. Existing computer program PD 267 (a tracking station simulation program) was used.

The horizon angle was determined by estimating the distance in nautical miles from the apex of the cone to the cone at the 400-n mi attitude. This distance was estimated to be 3130 n mi, then

h = horizon angle

$$= \sin^{-1} \frac{400}{3130} = 7.3^\circ$$

A value of 8 deg was used to allow some margin for error.

The percentage of time spent in the South Atlantic Anomaly area for various orbit attitudes and inclinations is shown in Fig. II-31.

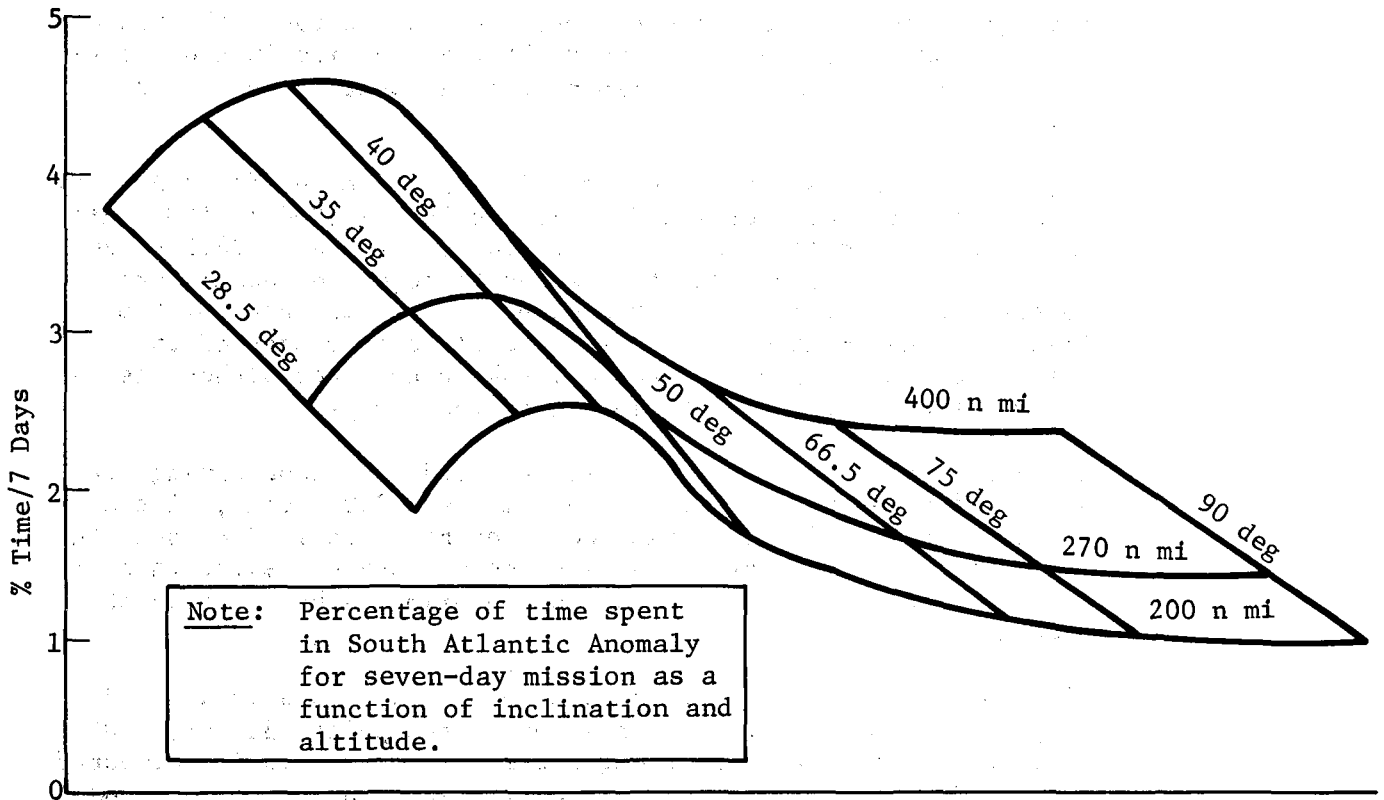


Fig. II-31 Array Time in South Atlantic Anomaly

F. MAINTAINABILITY AND RELIABILITY

The proposed ASM baseline payloads were evaluated to establish preliminary reliability requirements that could reasonably be achieved by using a combination of redundancy and limited in-flight maintenance. This evaluation included performance of component and assembly level failure mode and effects analyses (FMEA) to identify critical single failure points and to determine the effects of these failures on crew safety and mission success. Also, failure rates were estimated for the payloads to provide a means of evaluating the effects of adding selected redundancy to eliminate critical single failure points.

The primary ground rules and assumptions for this study are:

- 1) The astronomy telescopes are considered primary mission objectives and the arrays are secondary objectives;
- 2) There will be no planned EVA for the purpose of inflight maintenance.

1. Single Point Failure Analysis

FMEAs were performed on the subsystems and the experiments to the component and assembly level to identify all single failure points critical to crew safety and/or mission success for the baseline Astronomy Sortie missions. Each single failure point identified in the FMEA was categorized with respect to safety and mission criticality as follows:

- Category I - Failure that results in a potential crew safety hazard;
- Category II - Failure that results in total loss of experiment capability or inability to meet primary mission objectives;
- Category III - Failure that results in partial loss of primary objectives or loss of all secondary objectives;
- Category IV - Failure that results in only partial secondary data loss or has no significant effect.

The preliminary FMEAs are included in Appendix A4, Volume III, Book 2.

The critical single failure points as identified in the FMEAs are shown in Table II-16. Included in this table are the estimated failure rate for the critical component, the proposed method of elimination of the failure mode or reducing its effects, and the rationale for retention of those critical failure modes that are not eliminated.

The pointing and control subsystem has four critical single failure points as shown in Table II-16. These critical assemblies are all located in the unpressurized area and cannot be maintained inflight. Therefore, it is recommended that redundancy in the form of redundant gyros, redundant drive motors in the common mount assembly, and redundant drive assemblies in the telescope gimbal assembly be incorporated into the design to eliminate these single failure points.

The control and display subsystem has one critical single failure point, the keyboard assembly located in the pressurized area. It is recommended that a spare assembly be provided for inflight replacement to eliminate the effect of this single failure point.

The Stratoscope III contains five critical single failure points, all of which are considered a very low risk for the seven-day mission. It is recommended, however, that redundancy be incorporated in those areas where it can be accomplished easily for little additional cost. Suggested redundancies include drive motors and actuators for the light shield, the aperture door, and the beam directing assemblies.

The IR telescope has five critical single failure points, all of which have an extremely low risk of occurrence during the seven-day mission. As was the case in the Stratoscope III, redundant actuators and drive motors should be considered for the aperture door assembly, because there would be little additional cost and weight.

The solar astronomy telescopes did not contain any critical single failure points because there are four separate telescopes and no single failure was identified that would result in loss of all four telescopes.

Table II-16 Summary of Critical Single Failure Points from FMEA

Subsystem Component/Assembly	Effect of Failure on Mission	Estimated Failure Rate (Failure per 100 Flights)	Method of Elimination or Reduction of Effects	Rationale for Retention
<u>POINTING AND CONTROL</u>				
CMG IMU (Gyros)	Loss of Total Experiment Mission	1.33	Provide Redundant gyro or package	None
Telescope IMU (Gyros)	Loss of Astronomy Telescope	1.33	Provide redundant gyro or package	None
Telescope Common Mount Actuators	Loss of Astronomy Telescope	1.13	Provide redundant drive motors	None
Telescope Gimbal Actuators	Loss of Astronomy Telescope	1.13	Provide redundant drives	None
<u>CONTROL AND DISPLAY</u>				
Keyboard Assy	Loss of Experiment Mission	0.168	Provide an onboard spare assembly	None
<u>STRATOSCOPE III</u>				
Primary Mirror Assembly	Loss of Astronomy Experiment	0.0004	None	Risk of critical failure very low and redundancy not practiced
Secondary Mirror Assembly	Loss of Astronomy Experiment	0.0168	None	Risk of critical failure very low and redundancy not practiced
Beam Directing Assembly	Loss of Astronomy Experiment	0.02	Possible redundant actuator assemblies	Risk of critical failure very low for 7-day mission
Aperture Door Assembly	Loss of Astronomy Experiment	0.05	Incorporate redundant actuators and motors	Risk of critical failure very low for 7-day mission
Light Shield Assembly	Loss of Astronomy Experiments	0.0004	Incorporate redundant drive motors	Risk of critical failure very low and redundancy not practiced
<u>IR TELESCOPE</u>				
Primary Mirror Assembly	Loss of Astronomy Experiments	0.0004	None	Risk of critical failure extremely low in 7-day mission
Secondary Mirror Assembly	Loss of Astronomy Experiments	0.0002	None	Risk of critical failure extremely low in 7-day mission
Aperture Door Assembly	Loss of Astronomy Experiments	0.05	Incorporate redundant actuators	Risk of critical failure extremely low in 7-day mission
Optical Telescope Assembly	Loss of Astronomy Experiments	0.02	None	Risk of critical failure extremely low in 7-day mission
Optical References	Loss of Astronomy Experiments	0.084	None	Risk of critical failure extremely low in 7-day mission

The failure rates were estimated for the support subsystems and for the individual experiments as shown in Table II-17. These estimates were based on Martin Marietta and Bendix in-house studies. These failure rates provided the basis for determining the risk for the critical single failure points as discussed above. In addition, these estimates provide the basis for determining the maintenance spares requirements. Table II-18 shows the estimated failure rates for each of the baseline payload combinations. This table also lists the total failure rates for failure of all categories and the failure rate for critical failures for each payload combination per 100 flights.

Table II-17 Subsystem/Experiment Estimated Failure Rates

Subsystem/Experiment	Failure Rate _{10⁶ hr} Failure x 10 ⁶ hr
Support Subsystem	
Pointing and Control	319.13
Controls and Displays	75.46
Additional Telescope Gimbal Required for Solar Payload	67.00
Experiment	
Astronomy:	
Stratoscope III	304.325
Photoheliograph	100.29
XUV Spectroheliograph	30.71
X-Ray Focusing Telescope	100.70
Coronagraphs	53.72
IR Telescope	336.34
Arrays:	
Wide Coverage	30.0
γ-Ray Spectrometer	51.0
Low Background γ-Ray Detector	30.0
Large Modulation Collimator	11.0
Large Area X-Ray Detector	20.0
Collimated Plane Crystal Spectrometer	95.0
Narrow Band Spectrometer/Polarimeter	22.0

Table II-18 Estimated Failure Rates for Baseline Payload Groups

Payload Group	Subsystem/Experiment	Failure Rate, Failures X10 ⁻⁶ /hr	Total Failures per 100 Flights	Critical Failures per 100 Flights
<u>IR TELESCOPE</u>				
Payload 4AB	IR Telescope	336.34		
	Wide Coverage X-Ray Array	30.00		
	Narrow Band Spect/Polarimeter	22.00		
	Support Subsystems	394.59		
	Total	782.93	13.15	5.24
Payload 4AC	IR Telescope	336.34		
	Wide Coverage X-Ray Array	30.00		
	Gamma Ray Spectrometer	51.00		
	Low Background Detector	30.00		
	Support Subsystems	394.59		
Total	841.93	14.15	5.24	
Payload 4AD	IR Telescope	336.34		
	Wide Coverage X-Ray Array	30.00		
	Large Modulation Collimator	11.00		
	Support Subsystems	394.59		
	Total	771.93	12.95	5.24
Payload 4AE	IR Telescope	336.34		
	Wide Coverage X-Ray Array	30.00		
	Large Area X-Ray Detector	20.00		
	Collimated Plane Spect	95.00		
	Support Subsystems	394.59		
Total	875.93	14.70	5.24	
<u>STRATOSCOPE III</u>				
Payload 3AB	Stratoscope III	304.33		
	Wide Coverage X-Ray Array	30.00		
	Narrow Band Spect/Polar	22.00		
	Support Subsystems	394.59		
	Total	750.92	12.62	5.17
Payload 3AC	Stratoscope III	304.33		
	Wide Coverage X-Ray Array	30.00		
	Gamma Ray Spectrometer	51.00		
	Low Background Detector	30.00		
	Support Subsystems	394.59		
Total	809.92	13.57	5.17	

Table II-18 (concl)

Payload Group	Subsystem/Experiment	Failure Rate, Failures $\times 10^{-6}$ /hr	Total Failures per 100 Flights	Critical Failures per 100 Flights
<u>STRATOSCOPE III</u> (cont)				
Payload 3AD	Stratoscope III	304.33		
	Wide Coverage X-Ray Array	30.00		
	Large Modulation Col- limator	11.00		
	Support Subsystems	394.59		
	Total	739.92	12.41	5.17
Payload 3AE	Stratoscope III	304.33		
	Wide Coverage X-Ray Array	30.00		
	Large Area X-Ray De- tector	20.00		
	Collimated Plane Spect	95.00		
	Support Subsystems	394.59		
Total	843.92	14.17	5.17	
<u>SOLAR PAYLOAD</u>	Photoheliograph	100.29		
	XUV Spectroheliograph	30.71		
	X-Ray Telescope	100.70		
	Coronagraphs	107.14		
	Support Subsystems	461.59		
Total	800.43	13.50	5.09	

2. Trade Studies

The Stratoscope III payload groups are to be flown a total of 24 flights during the 12-year period. The estimated critical failures during this period for the baseline design without added redundancy are shown in Table II-19. The table shows that the critical failures during the 12-year period can be reduced from 1.24 to approximately 0.08 by incorporating the redundancy and inflight maintenance recommended in Table II-16. Assuming the cost of a Shuttle launch is between \$5 million and \$20 million, the savings on this payload group would be between \$5.78 million and \$23.12 million, (see Table II-20), which is greater than the cost of a launch.

The IR telescope payload groups are to be flown a total of 31 flights during the 12-year period. The estimate of critical failures for the baseline design without added redundancy during this period is shown in Table II-19 with the estimate of critical failures with the added redundancy and inflight maintenance. As can be seen in the table the number of estimated critical failures can be reduced from 1.62 to 0.118 per 31 flights. Using the same criteria for cost of Shuttle launches as was used above, the savings realized by incorporation of the redundancy would be between \$7.51 million and \$30.04 million, as can be seen in Table II-20.

Using the same criteria as above, critical failures estimated for the solar astronomy payload could be reduced from 1.32 to 0.073 per 26 flights at an estimated savings of approximately \$6.23 million to \$24.92 million. These values are also shown in Tables II-19 and II-20, respectively.

For all of the payload groups considered, the primary reduction in critical failures is a result of adding the redundancy recommended for the support subsystems. The redundancy recommended for the experiments reduces the total expected critical failures only slightly, but should also cost very little to incorporate in the design. Note that the cost savings shown above do not consider the cost of adding the redundancy to the subsystem or experiments, however, since the support subsystems are used for the total of 81 flights, these costs would probably be small compared to the total savings that are between \$19 million and \$78 million (see Table II-20). Therefore, it is assumed that the recommended redundancy and the one inflight maintenance item should be cost effective with the significant improvement in mission reliability that may be realized.

Table II-19 Estimated Critical Failures and Flight Reliability with and without Recommended Improvements

Payload (Including Support Subsystems)	Total Flights/12 yr	Critical Failures/12 yr		7-day Flight Reliability	
		Without Added Redundancy or Inflight Maintenance	With Added Redundancy or Inflight Maintenance	Without Added Redundancy or Inflight Maintenance	With Added Redundancy or Inflight Maintenance
Stratoscope III Group	24	1.24	0.084	0.945	0.9965
IR Telescope Groups	31	1.62	0.118	0.942	0.9962
Solar Astronomy Group	26	1.32	0.073	0.950	0.9972

Table II-20 Estimated Cost Savings by Incorporating Redundancy and Inflight Maintenance to Reduce Critical Failure Risk

Payload Group	Cost of Launches for 12 years, \$ Million		Cost of Critical Failure, \$ Million		Estimated Savings by Adding Redundancy and Inflight Maintenance, \$ Million	
	\$5 Mil- lion/ Launch	\$20 Mil- lion/ Launch	\$5 Mil- lion/ Launch	\$20 Mil- lion/ Launch	\$5 Mil- lion/ Launch	\$20 Mil- lion/ Launch
Stratoscope III (24 Flights)	120	480	6.2	24.8	5.78	23.12
IR Telescope (31 Flights)	155	620	8.1	32.4	7.51	30.04
Solar Astronomy (26 Flights)	130	520	6.6	26.4	6.23	24.92
Total (81 Flights)	405	1620	20.9	83.9	19.52	78.08

3. Maintainability and Reliability Requirements

The basic study ground rule that precludes any planned EVA, limits the potential inflight maintenance candidates to those items located in the pressurized area. In addition, the relatively short seven-day mission greatly reduces the requirements for inflight replacement or repair. Based on the analyses performed it was concluded that inflight replacement would be recommended only for the keyboard assembly in the control and display subsystem because this is a mission-critical item and can easily be made accessible for replacement inflight. All other critical items in the pressurized area are either redundant or very unlikely to need replacement during the short mission duration.

The requirements for ground maintainability for the experiments and support subsystems are shown in Table II-21, which includes the items that will need inspection, replacement, or refurbishment at the Payload Integration Center (MSFC) between flights. Included in this table are estimates of the intervals (hours and flights) between these maintenance actions required.

The reliability requirements are in the form of recommendations as to the redundancy that should be incorporated into the experiment and support subsystem designs. Based on the analyses performed, the critical single failure points could be significantly decreased in the support subsystems by the addition of a limited amount of redundancy. In the experiments the only redundancy recommended was that which could probably be incorporated with very little impact to the cost and weight of the design. Table II-22 shows the basic redundancy requirements for the support subsystems and experiments. This table also includes redundancy that already exists in the baseline conceptual design.

Table II-21 Maintainability Requirements

Subsystem Component/Assembly	Location (Pressurized or Unpressurized)	Inspection, Replacement, or Refurbishment Interval	Remarks
<u>POINTING & CONTROL:</u>			
CMGs	Unpressurized	9,000 hr (45 flts)	Refurbish
IMU Packages	Unpressurized	18,000 hr (90 flts)	Replace
Star Tracker	Unpressurized	18,000 hr (90 flts)	Replace
Common Mount Actuators	Unpressurized	4,500 hr (22 flts)	Inspect & repair or replace
Telescope Gimbal Actuation	Unpressurized	4,500 hr (22 flts)	Inspect & repair or replace
<u>CONTROL AND DISPLAY</u>			
Display CRT	Pressurized	1,000 hr (5 flts)	Replace
Keyboard Assembly	Pressurized	5,000 hr (25 flts)	Provide accessibility for inflight Replacement
Viewer	Pressurized	1,000 hr (5 flts)	Replace
Hand Controller	Pressurized	5,000 hr (25 flts)	Replace
Mission Time Display	Pressurized	2,000 hr (10 flts)	Replace
Event Timer	Pressurized	2,000 hr (10 flts)	Replace
Indicator Bank	Pressurized	2,000 hr (10 flts)	Replace
Strip Chart Recorder	Pressurized	200 hr (1 flt)	Inspect & repair or replace
<u>STRATOSCOPE III:</u>			
Primary Mirror Assembly	Unpressurized	2,400 hr (12 flts)	Inspect & clean or recoat as required
Secondary Mirror Assembly	Unpressurized	2,400 hr (12 flts)	Inspect & clean or recoat as required
Light Shield Assembly	Unpressurized	2,400 hr (12 flts)	Inspect & repair or replace as required
Aperture Door Assembly	Unpressurized	2,400 hr (12 flts)	Inspect & repair or replace as required
Beam Dir. Mirror Assembly	Unpressurized	2,400 hr (12 flts)	Inspect & repair or replace as required
F-12 Camera	Unpressurized	2,400 hr (12 flts)	Replace
Spectrograph	Unpressurized	2,400 hr (12 flts)	Replace cameras
<u>IR TELESCOPE:</u>			
Primary & Secondary Mirrors	Unpressurized	2,400 hr (18 flts)	Inspect & clean or recoat as required
Liquid Ne Cooling Assembly	Unpressurized	2,400 hr (18 flts)	Inspect & repair or replace as required
Liquid He Cooling Assembly	Unpressurized	2,400 hr (18 flts)	Inspect & repair or replace as required
Aperture Door Assembly	Unpressurized	2,400 hr (18 flts)	Inspect & repair or replace as required

Table II-21 (cont)

Subsystem Component/Assembly	Location (Pressurized or Unpressurized)	Inspection, Replacement, or Refurbishment Interval	Remarks
<u>IR TELESCOPE: (cont)</u>			
Interferometer Assembly	Unpressurized	2,400 hr (18 flts)	Inspect & repair or replace as required
Imaging System	Unpressurized	2,400 hr (18 flts)	Inspect & Repair or replace as required
Optical Telescope Assembly	Unpressurized	2,400 hr (18 flts)	Inspect & repair or replace as required
Detector Array	Unpressurized	2,400 hr (18 flts)	Inspect & repair or replace as required
<u>PHOTOHELIOGRAPH:</u>			
Mirror Assemblies	Unpressurized	3,000 hr (15 flts)	Inspect & clean or recoat as required
Aperture Door Assembly	Unpressurized	3,000 hr (15 flts)	Inspect & repair or replace as required
Alignment Detector	Unpressurized	3,000 hr (15 flts)	Inspect & repair or replace as required
Focus Control Assembly	Unpressurized	3,000 hr (15 flts)	Inspect & repair or replace as required
Folding Mirror Assembly	Unpressurized	3,000 hr (15 flts)	Inspect & repair or replace as required
H- α Camera	Unpressurized	800 hr (4 flts)	Replace
Broadband Spectrograph	Unpressurized	800 hr (4 flts)	Replace camera
<u>XUV SPECTROHELIOGRAPH:</u>			
Concave Grating Assembly	Unpressurized	3,000 hr (15 flts)	Inspect & repair or replace as required
Filter Assembly	Unpressurized	3,000 hr (15 flts)	Inspect & repair or replace as required
Aspect Sensor	Unpressurized	3,000 hr (15 flts)	Inspect & repair or replace as required
Film Camera	Unpressurized	800 hr (4 flts)	Replace
<u>X-RAY FOCUSING TELESCOPE:</u>			
Telescope Assembly	Unpressurized	3,000 hr (15 flts)	Inspect & repair or replace as required
Transmission Grating Assembly	Unpressurized	3,000 hr (15 flts)	Inspect & repair or replace as required
Filter Wheel Assembly	Unpressurized	3,000 hr (15 flts)	Inspect & repair or replace as required
Turret Assembly	Unpressurized	3,000 hr (15 flts)	Inspect & repair or replace as required
Image Intensifier Conv.	Unpressurized	3,000 hr (15 flts)	Inspect & repair or replace as required

Table II-21 (concl)

Subsystem Component/Assembly	Location (Pressurized or Unpressurized)	Inspection, Replacement, or Refurbishment Interval	Remarks
<u>X-RAY FOCUSING TELESCOPE:</u> (cont)			
Crystal Spectrometer	Unpressurized	3,000 hr (15 flts)	Inspect & repair or replace as required
PMT Detector	Unpressurized	3,000 hr (15 flts)	Replace
Film Camera	Unpressurized	800 hr (4 flts)	Replace
H- α Camera	Unpressurized	800 hr (4 flts)	Replace
<u>CORONAGRAPH (IC):</u>			
Occulting Disc Assembly	Unpressurized	3,000 hr (15 flts)	Inspect & repair or replace as required
Optical Assembly	Unpressurized	3,000 hr (15 flts)	Inspect & repair or replace as required
Thermal Mirror	Unpressurized	3,000 hr (15 flts)	Inspect & repair or replace as required
Aspect Sensor	Unpressurized	3,000 hr (15 flts)	Inspect & repair or replace as required
Film Camera	Unpressurized	800 hr (4 flts)	Replace
<u>CORONAGRAPH (OC):</u>			
Occulting Disc Assembly	Unpressurized	3,000 hr (15 flts)	Inspect & repair or replace as required
Optical Assembly	Unpressurized	3,000 hr (15 flts)	Inspect & repair or replace as required
Thermal Mirror	Unpressurized	3,000 hr (15 flts)	Inspect & repair or replace as required
Aspect Sensor	Unpressurized	3,000 hr (15 flts)	Inspect & repair or replace as required
Film Camera	Unpressurized	800 hr (4 flts)	Replace
<u>ARRAYS:</u>			
Wide Coverage X-Ray Det.	Unpressurized	2,000 hr (10 flts)	Inspect & repair or replace as required
γ -Ray Spectrometer	Unpressurized	2,000 hr (10 flts)	Inspect & repair or replace as required
γ -Ray Detector	Unpressurized	2,000 hr (10 flts)	Inspect & repair or replace as required
Large Modulation Coll.	Unpressurized	2,000 hr (10 flts)	Inspect & repair or replace as required
Large Area X-Ray Det.	Unpressurized	2,000 hr (10 flts)	Inspect & repair or replace as required
Coll. Plane Crystal Spect.	Unpressurized	2,000 hr (10 flts)	Inspect & repair or replace as required
Narrow Band Spect/Polar	Unpressurized	2,000 hr (10 flts)	Inspect & repair or replace as required

Table II-22 Redundancy Requirements

Subsystem: Component/Assembly	Type Redundancy Recommended	Remarks
<u>POINTING & CONTROL</u>		
CMGs	Function can be performed with two of three CMGs	This redundancy exists in baseline design
Star Trackers	Function can be performed with three of four star trackers	This redundancy exists in baseline design
IMU Packages	Provide redundant package	This applies to telescope and CMG IMU Packages
Common Mount Actuators	Provide redundant drive-motors and mechanism	This redundancy exists in baseline design
Telescope Gimbal Actuators	Provide redundant drive-motors and mechanism	This redundancy exists in baseline design
<u>STRATOSCOPE III</u>		
Aperture Door Assembly	Redundant drive motors and actuators	None
Beam Directing	Redundant drive motors and mechanism	None
Light Shield Assembly	Redundant drive motors and mechanism	None
<u>IR TELESCOPE</u>		
Aperture Door Assembly	Redundant actuators	None

G. LOGISTICS SUPPORT

The logistics support concepts have been developed for the ASM based on an evaluation of the individual requirements for servicing, maintenance, and refurbishment for each of the baseline payloads. As part of this evaluation the turnaround times were determined from the flight schedule and used as a basis to select the location for performing the logistics support function, as well as to determine the packaging, handling, and transportation requirements. The details of packaging, handling, transportation, and locations for these operations are included below.

1. Individual Payload Logistics Requirements

The logistics support concept will be essentially the same for all of the payloads considered except for the five payloads that require cryogenics. These are the four IR telescope payloads and the one Stratoscope payload that contains the gamma-ray array group. For these payloads the capability to supply cryogenics will be required at the launch site. A detailed description of the turnaround schedules, tasks, and support functions is included in Sections C. and D. of this chapter. The requirements for operational consumables and maintenance spares for the individual payloads are discussed in the following paragraphs.

a. Maintenance Spares Requirements - Maintenance spares requirements for the experiments and support subsystems will include replacement spares for both life-limited items and items that fail in flight. These estimates have been made at the component/assembly level because hardware definition has not been completed below this level, although it is understood that maintenance and refurbishment will be accomplished to the part/subassembly level in many cases. The estimates of maintenance spares required for the 12-year program are tabulated in Table II-23. These numbers are based on the expected number of flights for the hardware during the 12-year program, the estimated failure rates for the hardware, and the life-limited hardware included in the conceptual designs. These estimates are preliminary in nature and in some cases are based on limited hardware descriptions.

Table II-23 Maintenance Spares Estimate

Subsystem/Experiment: Component/Assembly	No. Spares Required, Maintenance and Refurbishment															12-Year Total
	Qty Used	Initial	79	80	81	82	83	84	85	86	87	88	89	90		
<u>IR Telescope:</u>																
Primary Mirror Assembly	1	0														0
Secondary Mirror Assembly	1	0														0
Liquid Neon Cooling Assembly	1	1								1						2
Liquid Helium Cooling Assembly	1	1								1						2
Aperture Door & Actuator Assembly	1	1								1						2
Interferometer	1	1														1
Detector Array	1	1														1
Optical Telescope Assembly	1	1														1
Imaging System	1	1								1						2
Optical Reference	1	1														1
<u>Stratoscope III:</u>																
Light Shield and Drive Assembly	1	1								1						2
Aperture Door and Actuator Assembly	1	1								1						2
Primary Mirror Assembly	1	0														0
Secondary Mirror Assembly	1	0														0
Beam Directing Mirror Assembly	1	1								1						2
F-12 Field Camera	1	1						1	1	1		1	1	1		7
Lo Resolution Spectrograph	3	1								3						4
<u>Photoheliograph:</u>																
Primary Mirror Assembly	1	0														0
Secondary Mirror Assembly	1	0														0
Aperture Door & Actuator Assembly	1	1							1							2
Internal Alignment Electronics	1	1														1
Laser Detector	1	1								1						2
Focus Control Assembly	1	1														1
Folding Mirror Assembly	1	1														1
Wavelength Control	1	1														1
H- α Camera	1	1			1	1	1	1		1		1		1		8
Broad Band Camera	1	1			1	1	1	1		1		1		1		8
Spectrograph	1	1				1		1		1		1		1		6
<u>X-Ray Focusing Telescope:</u>																
Telescope Assembly	1	1								1						2
Transmission Grating Assembly	1	1								1						2
Filter Wheel Assembly	1	1								1						2
Turret Assembly	1	1								1						2
Image Intensifier	1	1								1						2
Crystal Spectrometer	1	1								1						2
PMT Detector	1	1								1						2
Film Camera	1	1								1						2
H- α Camera	1	1			1	1	1	1		1		1		1		8
X-Ray Telescope Monitor	1	1								1						2
<u>XUV Spectroheliograph:</u>																
Aperture Door & Actuator Assembly	1	1								1						2
Concave Grating Assembly	1	1								1						2
Film Camera	1	1			1	1	1	1		1		1		1		8
Filter Assembly	1	1														1
Rejection Mirror	1	1														1
Aspect Sensor	1	1								1		1		1		3
<u>Coronagraph - IC:</u>																
Occulting Disc Assembly	1	1														1
Optical Assembly	1	1														1
Film Camera	1	1					1		1		1					4
Aspect Sensor	1	1							1			1				3
Thermal Mirror	1	1														1

Table II-23 (cont)

Subsystem/Experiment: Component/Assembly	No. Spares Required - Maintenance and Refurbishment														12-Year Total
	Qty Used	Initial	79	80	81	82	83	84	85	86	87	88	89	90	
<u>Coronagraph - OC:</u>															
Occulting Disc Assembly	1	1													1
Optical Assembly	1	1													1
Film Camera	1	1					1		1		1				4
Aspect Sensor	1	1							1		1				3
Thermal Mirror	1	1													1
Optical Bench (OC and IC)	1	0							1						1
<u>Arrays:</u>															
Large Area X-Ray Detector	1	1							1						2
Wide Coverage X-Ray	1	1							1						2
Large Modulation Collimator	1	1							1						2
Narrow Band Spectrometer/Polarimeter	1	1							1						2
Collimated Plane Crystal Spectrometer	1	1							1						2
γ-Ray Spectrometer	1	1							1						2
Low Background γ-Ray	1	1							1						2
Proton Flux Detector	1	1							1						2
<u>Pointing and Control System:</u>															
CMG Assembly															
Double Gimbal CMGs	3*	3							2						5
Inverters	3*	3													3
IMU	1*	1							1						2
Common Mount Actuators															
Azimuth Pointing	2*	2			1	1	1		1	1	1		1		9
Deployment	2*	2							1						3
Telescope Gimbal Actuators															
Elevation Pointing & Stability	2*	2			1	1	1		1	1	1		1		9
Azimuth Stability	2*	2			1	1	1		1	1	1		1		9
Roll	2*	2			1	1	1		1	1	1		1		9
Pitch & Yaw (Coronagraphs)	2*	2							1						3
Array Platform Actuator															
Elevation Pointing	2*	2			1	1	1		1	1	1		1		9
Reference Assembly															
Star Tracker - Strapdown (Solar)	8*	8							8						16
Star Tracker - Strapdown (Stellar)	4*	4							4						8
Telescope IMU (Solar)	2*	2							2						4
Telescope IMU (Stellar)	1*	1							1						2
Fine Sun Sensor (Coronagraph)	1*	1							1						2
Boresighted Star Tracker (Precision) (IR Only)	1*	1							1						2
Correlation Tracker (Solar)	1*	1							1						2
<u>Structures:</u>															
Common Mount Assembly															
Azimuth Table	2*	1													1
Azimuth Yoke	2*	1													1
Deployment Yoke	2*	1													1
Deployment Gerasmotors and Launch Locks	4*	4													4
Jettison Equipment	2*	2													2

*For one Sortie Lab and pallet.

Table II-23 (concl)

Subsystem/Experiment: Component/Assembly	No. Spares Required - Maintenance and Refurbishment														12-Year Total
	Qty Used	Initial	79	80	81	82	83	84	85	86	87	88	89	90	
Telescope Gimbal Assembly															
Outer Gimbal Rings (Solar)	2*	2							2						4
Outer Roll Ring (Solar)	2*	2							2						4
Inner Roll Ring (Solar)	2*	2							2						4
Roll Gear (Solar)	2*	2							2						4
Telescope P&C Platform (Solar)	2*	2							2						4
Gimbal Gearmotors and Launch Locks (Solar)	4*	4													
Outer Gimbal Ring (Stellar)	1*	1							1						2
Outer Roll Ring (Stellar)	1*	1							1						2
Inner Roll Ring (Stellar)	1*	1							1						2
Roll Gear (Stellar)	1*	1							1						2
Telescope P&C Platform (Stellar)	1*	1							1						2
Gimbal Gearmotors and Launch Locks (Stellar)	2*	2													2
Structures:															
Array Platform Assembly															
Array Mount	2*	2													2
Platform Gearmotors and Launch Locks	4*	4													4
Support Equipment Set															
CMG Support Structures	3*	1													1
WC X-Ray Detector Mount (Stellar Only)	1*	2													2
γ-Ray Spectrometer Housing and Extension Mechanism (Stellar Only)	1*	1							1						2
Solar Telescopes Housing Assembly															
Tubular Structure	1*	1													1
Bulkheads	2*	2													2
Sunshield-Fiberglass	1*	1													1
Aperture Doors	6*	6													6
Door Actuators	6*	6							6						12
Electronic:															
Control & Display															
C/B Distributor Panel	1*	1				1	1	1			1	1			6
Multipurpose CRT	2*	2				2	2	2			2	2			12
Symbol Generator	1*	1													1
Function Keyboard	1*	1							1						2
Alphanumeric Keyboard	1*	1							1						2
Keyboard Encoder	2*	2							1						3
Microfilm Viewer	1*	1		1	1	1	1	2	1	1	1	2			12
Event Timer	1*	1			1	1		1	1		1	1			7
Mission Timer	1*	1			1	1		1	1		1	1			7
Three-Axis Controller	1*	1				1					1				3
Annunciator Bank	2*	2		1	1	1	2	1	1	1	2	2			14
Recorder	1*	1		1	1	1	1	1	1	1	1	1			9
Electrical															
Load Center Switch	6*	6													6
Feeder Cables	1*	1													1
Junction Box	1*	1													1
Data															
Data Bus Interface Unit	4*	4													4
Coax Data Bus	1*	1													1
Pallet Instrumentation Box	1*	1													1
Data Processor	4*	4													4
Thermal Control:															
Thermal Coating	1*	0							1						1
Multilayer Insulation	1*	0							1						1

*For one Sortie Lab and pallet.

b. *Operational Consumables Requirements* - Operational consumables required for the ASM payloads will consist of cryogenics for five payloads and film, magnetic tape, and dry nitrogen gas for all nine of the payloads. Table II-24 shows the preliminary estimates of the type of operational consumables required for the 12-year period.

Table II-24 *Operational Consumables Requirements*

Consumable	Required for Subsystem/ Experiment	Location
Liquid Nitrogen (LN ₂)	γ-Ray Spectrometer	Launch Site PIC-MSFC
Liquid Helium (LHe)	IR Telescope	PIC-MSFC
Liquid Neon (LNe)	IR Telescope	PIC-MSFC
Dry Nitrogen Gas	Experiment Pallet	PIC-MSFC Launch Site
Film - 35 mm	Stratoscope III, XUV Spectroheliograph, X-Ray Telescope, Coronagraphs	PIC-MSFC
Magnetic Tape	Data Management	PIC-MSFC

2. Integrated Logistics Concept

The turnaround times necessary to meet the baseline flight schedule for the individual ASM payloads evaluated is sufficiently long to allow performance of all maintenance and refurbishment tasks at PIC (MSFC). The only exceptions are the requirement to supply some cryogenics and dry nitrogen gas at the launch site (MSFC) and the requirement for inflight replacement of the control and display keyboard assembly, which requires an onboard spare.

The integrated logistics requirements for the ASM support subsystems and payloads will be spread over the 12-year program as shown in Tables II-23 and II-24. All of the maintenance spares will be located at PIC (MSFC) except for the keyboard assembly in the control and display subsystem, which will be provided onboard.

The operational consumables will be required at the launch site (KSC) and at PIC (MSFC) as notes in Table II-24. All of these items will be required for the full 12-year program.

H. UTILIZATION OF MAN

Of great interest to the sortie concept is the role man should play in telescope operation. Several questions must be considered: What roles can he fill that improve performance? What roles do not affect performance but improve reliability or lower cost? What roles can he fill that add flexibility of schedule?

Effective use of man requires his application: (1) to tasks requiring the unique capabilities of human judgment and manual skills; (2) to nonrepetitive functions; and (3) to repeatable functions that are best performed by the crew. The Astronomy Sortie program relies upon man in two key areas: on-orbit and ground mission support.

1. On-Orbit

The two scientific-observer crewmen initiate, monitor, assess, verify, and terminate the tasks of checkout, setup, deployment, alignment, calibration, indexing, slewing, retracting, and stowing of the telescopes and arrays. The flight crewmen are essential to the decision processes for target selection, and initiate and control the slewing to acquire guide stars for stellar observations or features of interest on the sun. The crew will align and focus the larger telescopes (the smaller ones will require no adjustments), and will periodically calibrate these controls by overriding the servos in discrete steps and observing the resulting quality of the image.

The effect of the in-flight crew activities relative to data assures that the correct targets are observed and that data quality is acceptable. The crewmen decide (with voice consultation with ground-based scientists) when it is necessary to re-take data and when additional data are required. The crew will monitor the progress of each observation and terminate it if any unusual perturbation occurs. If, for instance, an out-of-specification vibration momentarily comes from the Shuttle, the crew could start the observation anew. The appearance of an unexpected bright contamination cloud would also terminate an observation. The crew will also judge when a new instrument calibration may be needed, and perform the calibration in some cases.

Of great importance will be the crew's ability to react to targets of opportunity, such as solar activity or a nova. Crew reaction time will probably be faster than that of the LST or

LSO, since no time is lost in writing and encoding commands. In general the crew will carry out the observation schedule so that the time and money normally allocated for computerized control will not be required.

The crew will coordinate with the Shuttle pilot to ensure that momentum dumps and waste ventings do not interfere with the scientific program. The crew will also coordinate with the principal investigator (PI) on earth or with ground observatories to make changes in the observing schedule or interpret unexpected data. This can greatly enhance the scientific output of the flight.

In the earlier phases of the Shuttle/sortie astronomy program, time should be allotted at the end of each flight for experimentation of contaminant brightness with time, effect on tube temperature, and limiting magnitude when the telescope is pointed closer to the sun than normal, etc. Such experiments should be performed under the control of the crew.

The philosophy that has been observed is that "if a crewman can do it effectively, don't automate the function." This crew-utilization philosophy imposes requirements for effective crew training and for onboard controls and displays equipment that provide the necessary data from which to make decisions and initiate action. It provides a mode of operations closely paralleling existing observatories in which the scientist is present at the data source to assure maximum results.

The selection of manual operation for the telescope function was based on the results of a trade study performed for each of the repetitive functions required by the telescopes. This trade study is documented in Appendix A3, Volume III, Book 2.

The trade study recommended that the manual mode of operation be the preliminary design choice for all repetitive functions, except those that must be automatic for technical reasons. The primary considerations for this recommendation were lower cost, flexibility, complexity, and mission success.

2. On-Ground

The scientific crewman's role in space is partly determined by activities on earth before and during the flight. There are three individuals, or groups of individuals, whose roles on the ground are of interest.

The astronomer, or PI, for each flight will set the scientific objectives, select the targets and guide stars, and specify the choice of instruments and operating conditions. He will brief the scientific crewman and train him to react to the observations and conditions expected. He will coordinate with the crew during the flight, and will be responsible for data reduction after the flight. The degree to which the astronomer is able to brief the crew will determine how well the crew can monitor the observations as they progress and make adjustments to maximize the scientific output.

The engineering and ground support that precedes each flight also affects the role of the crew in orbit. A perfectly programmed and preconditioned telescope should make few technical demands on the crew. However, a tradeoff exists between the time and money spent for total scientific mission reliability and reliance on the crew to react to the unexpected, or his ability to do so.

Finally, there is the scientific crewman himself and his ability to assimilate the scientific briefings, or his background experience with image analysis and telescope adjustment. The scientific crewman should have thorough scientific and technical training, and it would be preferable for the scientific crewman to be an associate or colleague of the astronomer based on the ground.

I. SYSTEM PERFORMANCE

The baseline flight schedule identifies 26 solar missions through the 12-year Astronomy Sortie program. The mission requirements and the mission and systems plan for satisfying these requirements are summarized in Table II-25.

Table II-25 Solar Payloads

Mission Requirement	Recommended Mission and Systems Plan
Continuous Sun for 7-Day Period	Select inclination according to date and time of flight with adequate minimum altitude.
Minimize Doppler Shift	Requires beta angle of 1.57 radians (90 deg). Select inclination according to date so that beta angle of 1.57 radians (90 deg) occurs midway (3½ days) through mission.
Do Not View Through Earth's Atmosphere	400 km (216 n mi) atmosphere imposes a higher minimum altitude to allow for orbit regression. Range of altitudes selected exceed these minimums corresponding to inclinations.

The main driver to maximize scientific data return from solar experiments is to provide continuous sun throughout the seven-day sortie mission. This requirement is met by selecting the appropriate orbit inclination according to the date and time of each flight with an adequate altitude.

The baseline flight schedule identifies 24 Stratoscope III missions and 31 IR telescope missions in the Astronomy Sortie program. The mission requirements and the mission and systems plan for satisfying these requirements for the stellar experiments are summarized in Table II-26.

The main constraints to increasing scientific data return are the viewing limits on the IR telescope. Under present limitations, no more than half of the celestial sphere may be viewed because of the restriction about the sun, and further reduction is imposed by the earth even when the moon is in the new-moon position.

Table II-26 Stellar Payloads

Mission Requirement	Stratoscope III Mission and Systems Plan	IR Telescope Mission and Systems Plan
Minimize Sun, Moon, and Earth Interference with Viewing	Cannot view within 0.785 radian (45 deg) of sun and 0.262 radian (15 deg) of earth and moon. Not a driving constraint.	Cannot view within 1.57 radians (90 deg) of sun and 0.785 radian (45 deg) of earth. Fly during new-moon condition so moon is within constraint of sun. Reduce viewing restrictions by using baffles or other design innovations.
Maximize Cone of Continuous Visibility	12 deg full-angle cone, available about orbit plane poles with present viewing limits.	Cone of continuous visibility is not possible with IR constraint on earth viewing.
Maximize Dark Time	Cannot be significantly increased; can be reduced. Select time of launch and inclination to provide sky coverage desired.	
Maximize Celestial Sphere Availability	Fly missions during near new-moon conditions so moon is within constraint of sun.	
Do Not View Through Earth's Atmosphere	185 km (100 n mi) atmosphere imposes absolute viewing limit about earth. Constraint is reduced at higher altitudes.	

Efficiencies of the baseline missions were derived by analyzing the mission profiles included in Appendix A3, Volume III, Book 2. Summaries of these efficiencies are presented in the following subsections.

1. Solar Payload 1-2

The use of time from liftoff until initiation of deorbit for Solar Payload 1-2 is summarized as follows:

<u>Function</u>	<u>Time (hr:min)</u>
Boost, insert, transfer, attitude stabilization	2:30
Sortie Lab checkout and crew ingress	1:00
Payload inspection, deployment and checkout	7:02
Experimentation time	151:00
Payload shutdown and retract	3:26
Secure Sortie Lab and pallet	:32
Check out Orbiter	<u>1:00</u>
Total	166:30

During the 151-hr of experimentation time, the photoheliograph repeatable on-orbit operations sequence will be performed 24 complete times, plus a partial cycle, achieving 113 hr 44 min of operations time. The resulting mission efficiency for the photoheliograph is

$$\frac{113 \text{ hr } 44 \text{ min}}{166 \text{ hr } 30 \text{ min}} = 68\%$$

For the X-ray focusing telescope, the repeatable on-orbit operations sequence will be performed 40 times, plus a partial cycle, achieving 110 hr 22 min of operations time. The mission efficiency for this telescope is thus

$$\frac{110 \text{ hr } 22 \text{ min}}{166 \text{ hr } 30 \text{ min}} = 66\%$$

Both the XUV spectroheliograph and the coronagraphs (inner and outer) will be operated continuously during the 151 hr of experimentation time. The efficiency of this mission for these instruments is thus

$$\frac{151 \text{ hr}}{166 \text{ hr } 30 \text{ min}} = 91\%$$

2. Stratoscope III Payloads

The use of time from liftoff until initiation of deorbit for Stratoscope III payloads is summarized as follows:

<u>Function</u>	<u>Time (hr:min)</u>
Boost, insert, transfer, attitude stabilization	2:30
Sortie Lab checkout and crew ingress	1:14
Payload inspection, deployment and checkout	2:14
Experimentation time	155:27
Payload shutdown and retract	3:14
Secure Sortie Lab and pallet	:32
Check out Orbiter	<u>1:00</u>
Total	165:57

During the 155 hr 27 min of experimentation time, the Stratoscope will be operated through 102 complete cycles, plus a partial cycle, for a total of 119 hr 29 min of operations time. The resulting mission efficiency is

$$\frac{119 \text{ hr } 29 \text{ min}}{165 \text{ hr } 57 \text{ min}} = 72\%$$

3. IR Telescope Payloads

The use of time from liftoff until initiation of deorbit for IR telescope payloads is summarized as follows:

<u>Function</u>	<u>Time (hr: min)</u>
Boost, insert, transfer, attitude stabilization	2:30
Sortie Lab checkout and crew ingress	1:00
Array inspection, deployment and checkout	2:14
Telescope inspection, deployment, and checkout (in addition to array time)	4:16
Telescope experimentation time (array experimen- tation time equals 151:35 plus 4:16 = 155:51)	151:35
Payload shutdown and retract	2:50
Secure Sortie Lab and pallet	:32
Check out orbiter	<u>:60</u>
Total	165:57

During the 151 hr 35 min of experimentation time, the IR telescope will be operated for 97 cycles for 88 hr 26 min of operations time. The resulting mission efficiency is

$$\frac{88 \text{ hr } 26 \text{ min}}{165 \text{ hr } 57 \text{ min}} = 53\%$$

The arrays for the IR payloads will have the same efficiency as the Stratoscope III payloads of 91%.

III. SUBSYSTEM ANALYSIS

The analysis, selection, and definition of the subsystems for the selected ASM concept involved the thermal control, structure, stabilization and control, and electronics disciplines. An extremely useful thermal math model was developed for the ASM payloads, incorporating the complex influences of the Shuttle Orbiter on the thermal environment of the orbiting payload. The structural subsystem that was defined, provides rigid, lightweight platforms for the experiments and maximizes commonality of hardware usage. The conceptual design and analysis of the IR telescope was accomplished as a special emphasis task, involving thermal control and structures disciplines. The stabilization and control subsystem was designed to satisfy the pointing and stabilization requirements of the experiments, consistent with Shuttle capabilities. The electronics subsystem designs make maximum use of the capabilities of the Sortie Lab and require the addition of a minimum of equipment to augment these capabilities.

A. THERMAL CONTROL SYSTEM ANALYSIS

The objective of the thermal study of the Astronomy Sortie mission is the development of preliminary thermal control system designs that are compatible with the other vehicle subsystems, the Orbiter thermal environment, and the mission requirements. In this study methods of thermal control for the 100-cm photoheliograph, 25-cm XUV spectroheliograph, 32-cm X-ray telescope 2.45- and 4.0-cm coronagraphs, 120-cm stratoscope III, and the IR telescope are developed and the thermal characteristics of the designs investigated.

The IR telescope was selected for the analysis of the effects of thermal transients resulting from the orbital environment. A heat rate model from an in-house study was used to analyze the radiative interactions and orbital heating rates in the complex geometrical configuration represented by the Orbiter vehicle with the astronomy payload deployed. Transient heat rate calculations were made using the Martin Marietta Thermal Radiation Analyzer Program (MTRAP) and are presented in subsection 1, of this section. The analysis of the thermal performance of the IR telescope thermal control system involved the development of a 102-node thermal math model of the telescope for input to the Martin Marietta Interactive Thermal Analyzer System (MITAS). The analyses and results are presented in subsection 2 of this section.

The thermal study of the other five telescopes (photoheliograph, spectroheliograph, X-ray, coronagraphs, and stratoscope III) involved simplified calculations to evaluate configuration concepts, establish preliminary thermal design concepts, and establish preliminary thermal control system requirements. This task is presented in subsection 3 of this section.

1. Shuttle Thermal Environment Model

The emphasis of the initial thermal design of the astronomy payloads is placed on the orbital operational mission phase with the attendant range of deployed modes and orbital and environmental conditions. A heat rate model developed in a Martin Marietta study (Ref III-1) was used to analyze the radiative interactions and orbital heating rates in the complex geometrical configuration represented by the Orbiter vehicle with astronomy payload deployed. This model consists of 131 external surface nodes including 33 that define the telescope. Figure III-1 is a three-dimensional view of the configuration used in the heat rate model. The figure shows the astronomy payload deployed out of the Orbiter cargo bay.

Figure III-2 illustrates in detail the nodal breakdown of the pallet/astronomy payload portion of this model and features the Sortie Lab, IR telescope, and the arrays. These figures are illustrative of the plotting capabilities of MTRAP (Ref III-2) used in this study to determine orbital environment heating rates and grey body radiation factors (ϵ). This MTRAP optional overlay permits the surface description input data to be visually checked using views from any desired observer position. Preparation of these data is the most difficult part of the program input because of a requirement to define surface data relative to several orthogonal coordinate systems. The plotter option, therefore, is almost indispensable in the accurate preparation of surface description input.

Transient calculations were made using MTRAP to calculate grey-body radiation factors, and absorbed orbital heat fluxes for the hot condition with the telescope solar oriented and broadside to the sun. Examples of absorbed fluxes from the three sources--solar, albedo, and earth--as plotted by MTRAP for two surface nodes on the IR telescope are shown in Fig. III-3 and III-4. The fluxes include the effects of multiple reflections of the orbital environment from the Orbiter/payload, and are based on the orbital and environmental conditions listed in the following tabulation.

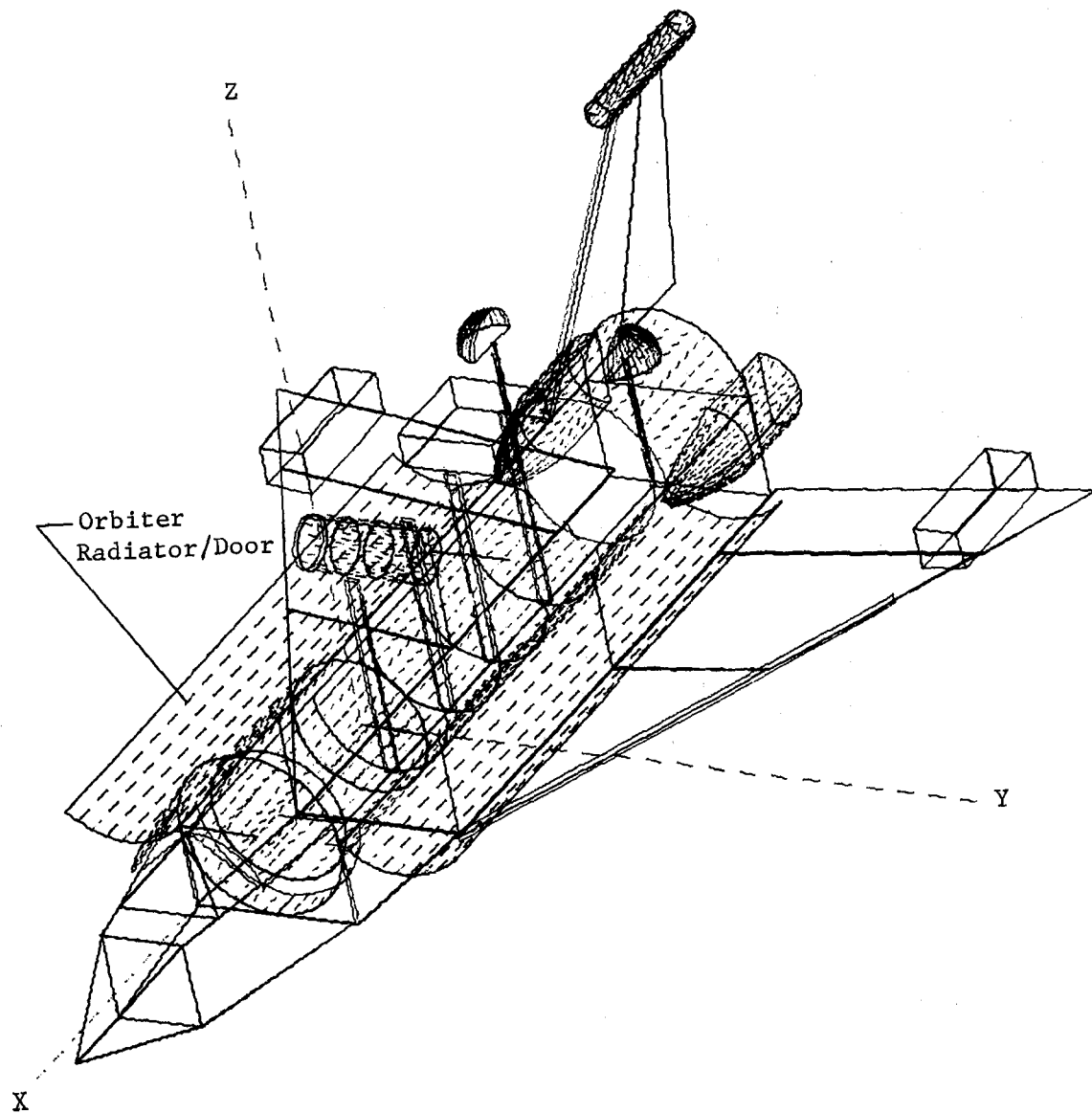


Fig. III-1 Orbiter/Payload Configuration

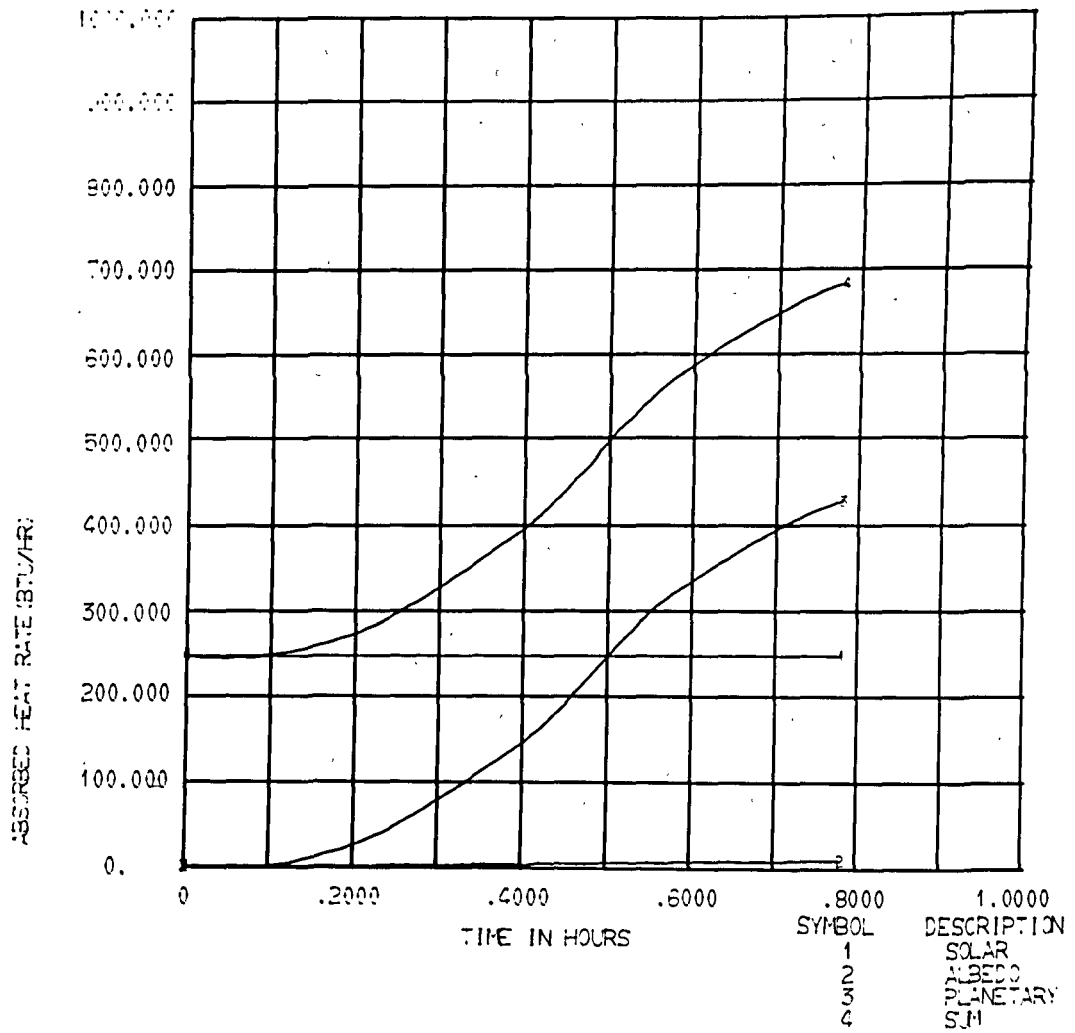


Fig. III-3 Node 1661; Transient Heating, Polar Orbit, IR Telescope Payload

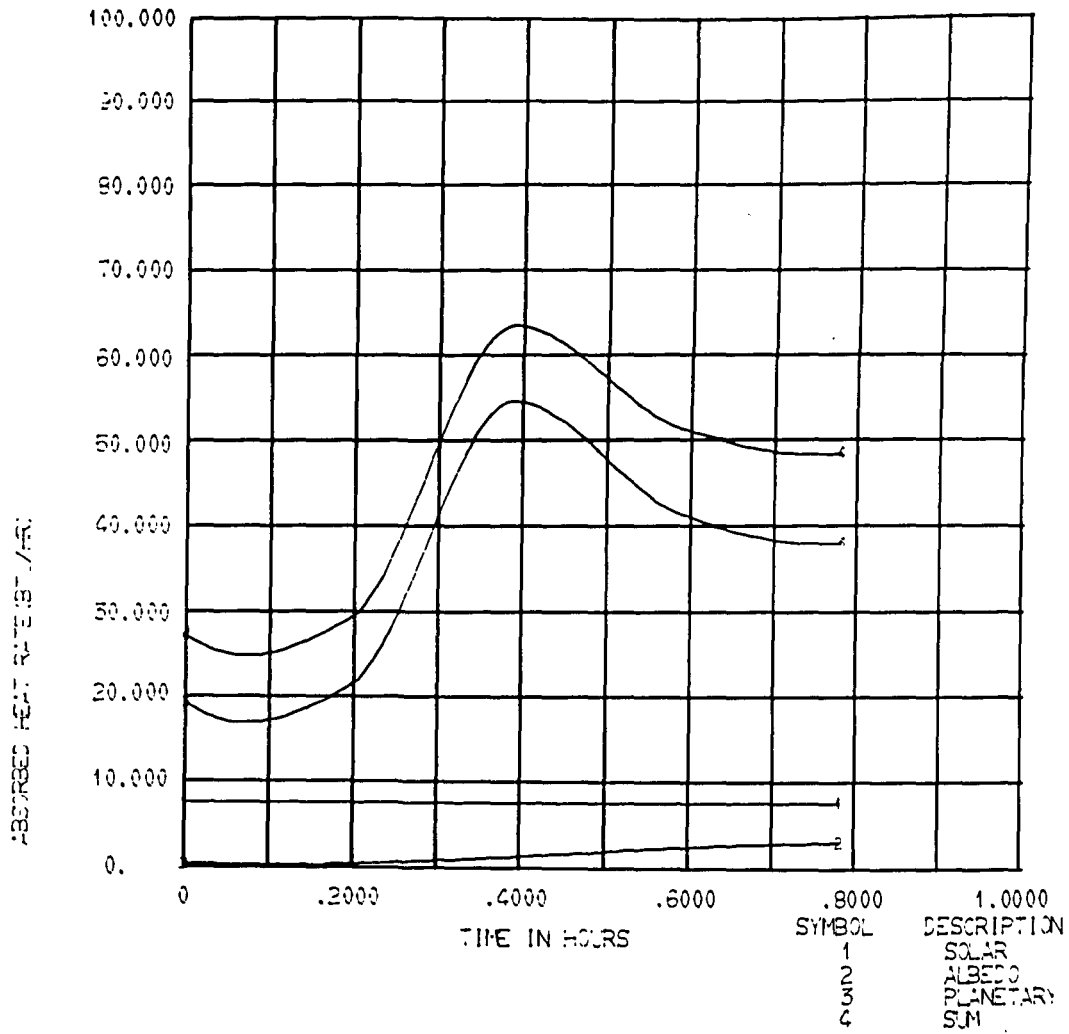


Fig. III-4 Node 1665; Transient Heating, Polar Orbit, IR Telescope Payload

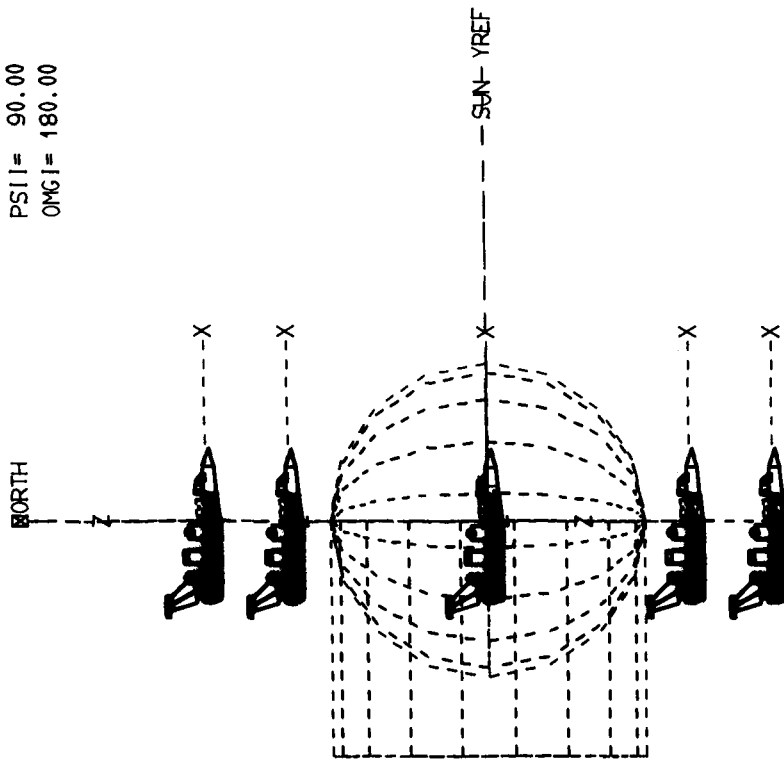
Orbital Conditions	
Orbit Altitude	235 n mi
Beta Angle	90 deg
Orientation	Solar Oriented
Environmental Conditions	
Solar Constant	458 Btu/hr-ft ²
Albedo	0.4
Planetary Emission	78 Btu/hr-ft ²
Surface Coating Properties, α/ϵ	
Orbiter	0.9/0.9
Orbiter Radiator	0.1/0.9
Pallet/Payload	0.2/0.9

Figure III-5 shows the orientation of the Orbiter, in the earth orbit investigated, with the IR telescope deployed broadside to the sun and pointing parallel to the Orbiter -Y axis during the half-orbit illustrated. For the remainder of the orbit the elevation drive is assumed to point the telescope parallel to the orbiter +Y axis. The resulting orbital symmetry has been used to save computer time by calculating fluxes for a half-orbit only and completing the remainder considering the mirror image nature of the flux data. The transient absorbed fluxes for the telescope, combined from the three sources--solar, albedo and earth--are shown in Fig. III-6 at eight locations around the circumference.

Figure III-5 was plotted by an MTRAP optional overlay and used for visual checkout of the orbit input data and the orientation of the surface data in orbit. Other computation options employed in the MTRAP calculations to define the telescope environment are summarized in Fig. III-7 together with the input parameter groups and output options. A significant feature of the card and tape output is that the format permits direct input to the MITAS thermal analyzer program.

MITAS (Ref III-3) is used to analyze thermal analog models represented by a resistance-capacitance network. It has been used here to compute the environment for the IR telescope in the form of equivalent space sink temperatures. This approach permits the complex environment resulting from the numerous Orbiter/payload IR radiative interactions to be reduced to that of an isothermal

PHII= 0.
 PSII= 90.00
 OMC1= 180.00



DPHIDT= 0.
 DPSIDT= 0.
 DOMGDT= 0.

SUN ORIENTED
 SOL DECL= 0.
 BETA= -90.0
 ORBIT INCL= 90.0
 ALPH= 90.0
 OMEGA= 90.0

VIEW 3-D

VIEW FRONT

SCALE= .00070

3-D VIEW

Fig. III-5 Orbiter Orientation and Earth Orbit Views

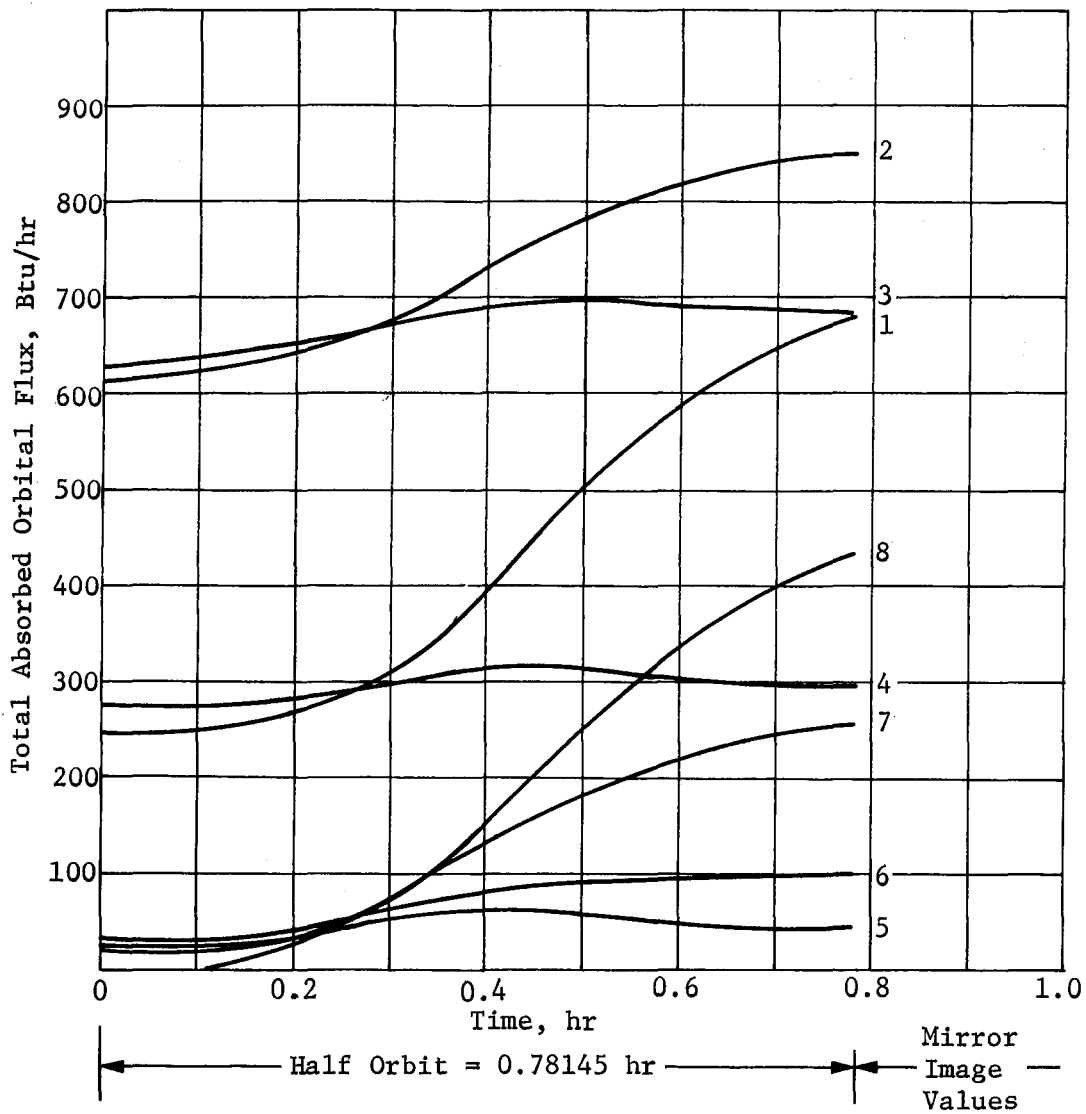
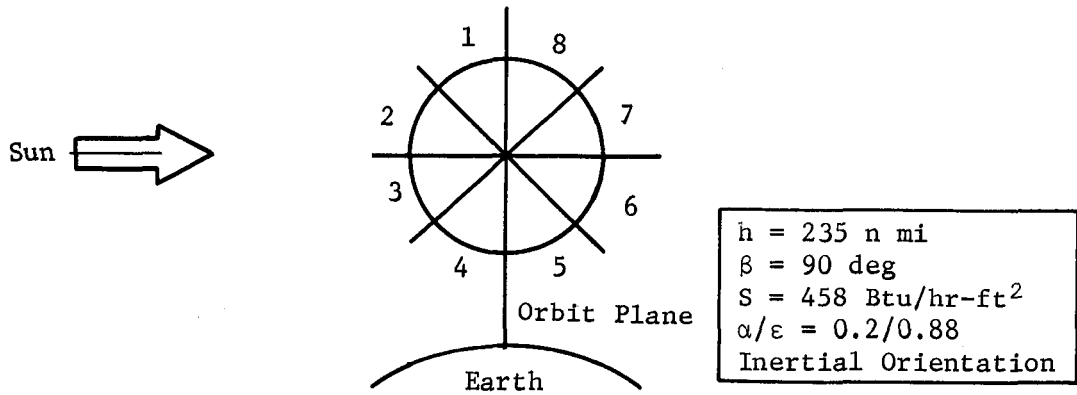


Fig. III-6 IR Telescope Transient Heat Flux Distribution

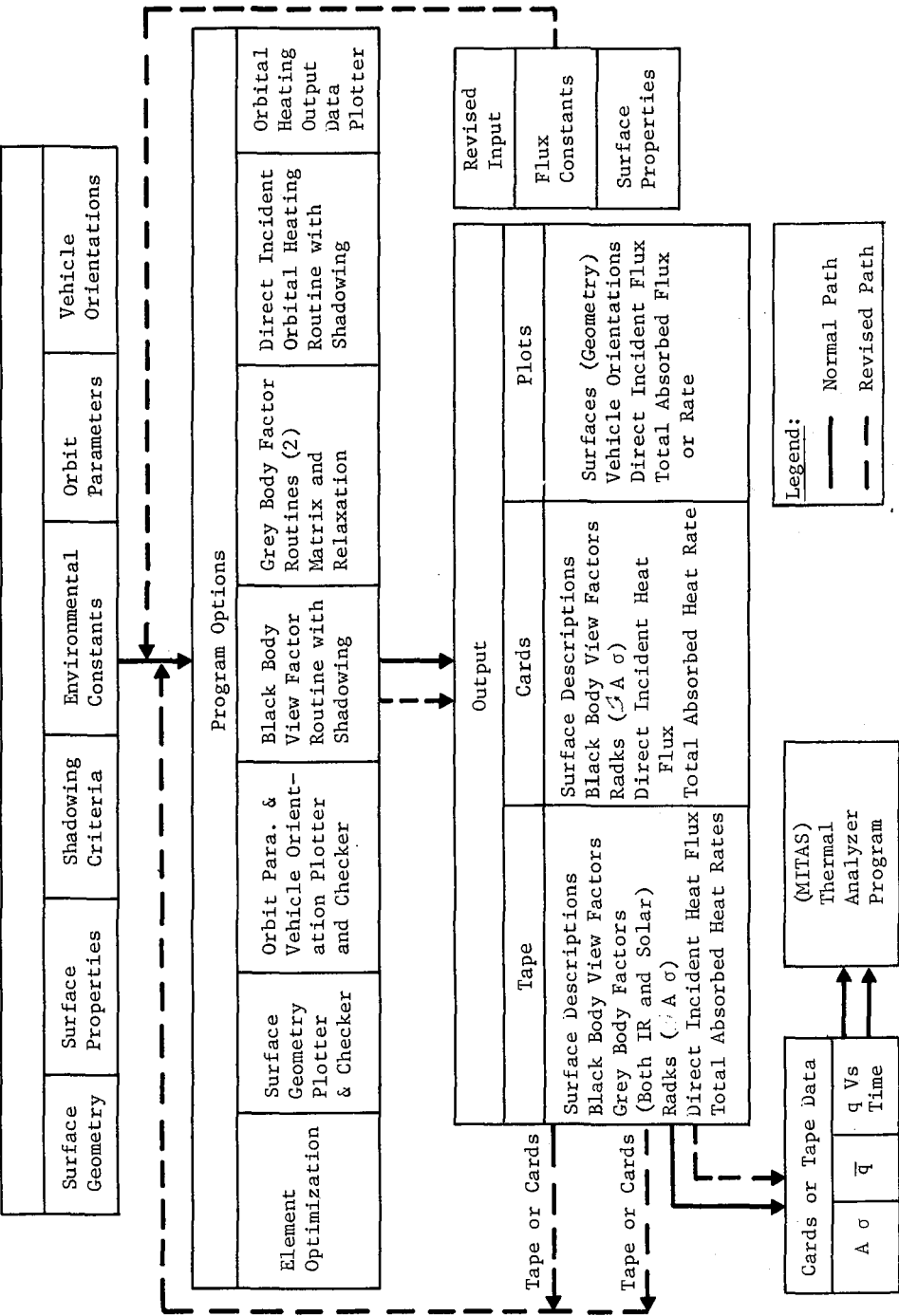
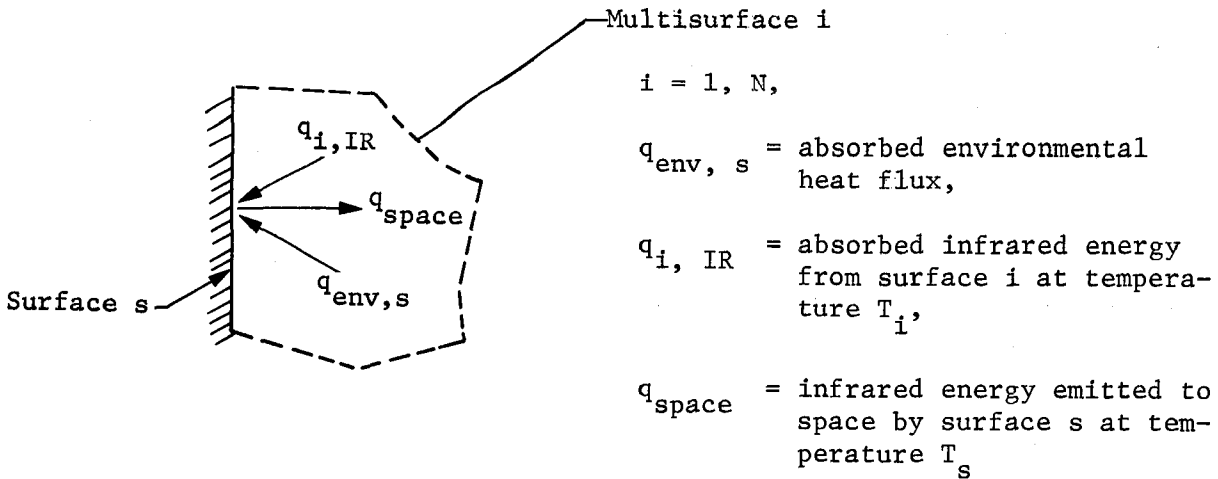


Fig. III-7 MTRAP Options

envelope or sink that completely surrounds each telescope nodal surface and exchanges energy with it. This concept is commonly applied to the thermal analysis of spacecraft and is presented in the following paragraphs.

A simple thermal network was formed representing the Orbiter/payload with adiabatic nodal surfaces, and the Orbiter radiator with boundary nodes at 90°F. Thus performing a heat balance at a nodal surface, s,



$$q_{env, s} + \sum_{i=1}^N q_{i, IR} = q_{space} \quad [III-1]$$

$q_{i, IR}$ is expressed in the thermal network by

$$q_{i, IR} = B \mathcal{J}_{s, i} A_s (T_i^4 - T_s^4) \quad [III-2]$$

and q_{space} by

$$q_{space} = B \mathcal{J}_{s, space} (A_s T_s^4) \quad [III-3]$$

where B = Stefan-Boltzmann constant,
 A = Area of Surface, s.

The time variant temperature T_s calculated by MITAS, using the q_{env} and $\mathcal{J}_{s, i}$ input data previously determined by the MTRAP analysis, is defined as the equivalent space sink temperature $T_{sink, s}$ for node S.

Combine Eq [III-1,-2,-3] and rearranging terms, the following expression for $T_{\text{sink},s}$ results,

$$T_{\text{sink},s} = \left[\left(q_{\text{env},s} + B \sum_{i=1}^N \mathcal{J}_{s,i} A_s T_i^4 \right) / BA_s \epsilon_s \right]^{1/4} \quad [\text{III-4}]$$

$$\left(\text{where } \epsilon_s = \mathcal{J}_{s,\text{space}} + \sum_{i=1}^N \mathcal{J}_{s,i} \right)$$

The environmental parameter T_{sink} is a function only of the absorbed heat fluxes on surface, s , which include solar, albedo, planetary fluxes, and multiple reflections of these lumped into $q_{\text{env},s}$, the nearby infrared heat sources, and the total $\mathcal{J}_{s,i}$ of the surface s . Hence, the sink temperature is calculated separately for each node and then used as a simplified boundary condition in the design evaluation of the telescope. Thus a heat balance at a surface s on the meteoroid shield expressed as

$$q_{\text{env},s} + \sum_{i=1}^N \dots - q_{\text{internal}} - q_{\text{stored}} - q_{\text{space}} = 0$$

is simplified by Eq [III-4] to

$$BA_s \epsilon_s \left(T_{\text{sink},s}^4 - T_s^4 \right) - q_{\text{internal}} - q_{\text{stored}} = 0$$

where, q_{internal} = energy transferred to internal locations,

and, q_{stored} = energy stored in surface s .

Several of the time variant sink temperatures computed by MITAS for the IR telescope payload are plotted in Fig. III-8 thru III-11. These represent the effective thermal environment surrounding the telescope (Fig. III-8), the experiment mounts (Fig. III-9), the arrays (Fig. III-10), and the pallet and Sortie Lab (Fig. III-11).

Table III-1 presents a summary of the IR telescope environment in terms of fluxes averaged around the cylindrical surface and averaged over a one-orbit period. Also shown is the impact of the proximity of Orbiter/payload on the thermal environment of the telescope as indicated by comparison with a free-flying telescope.

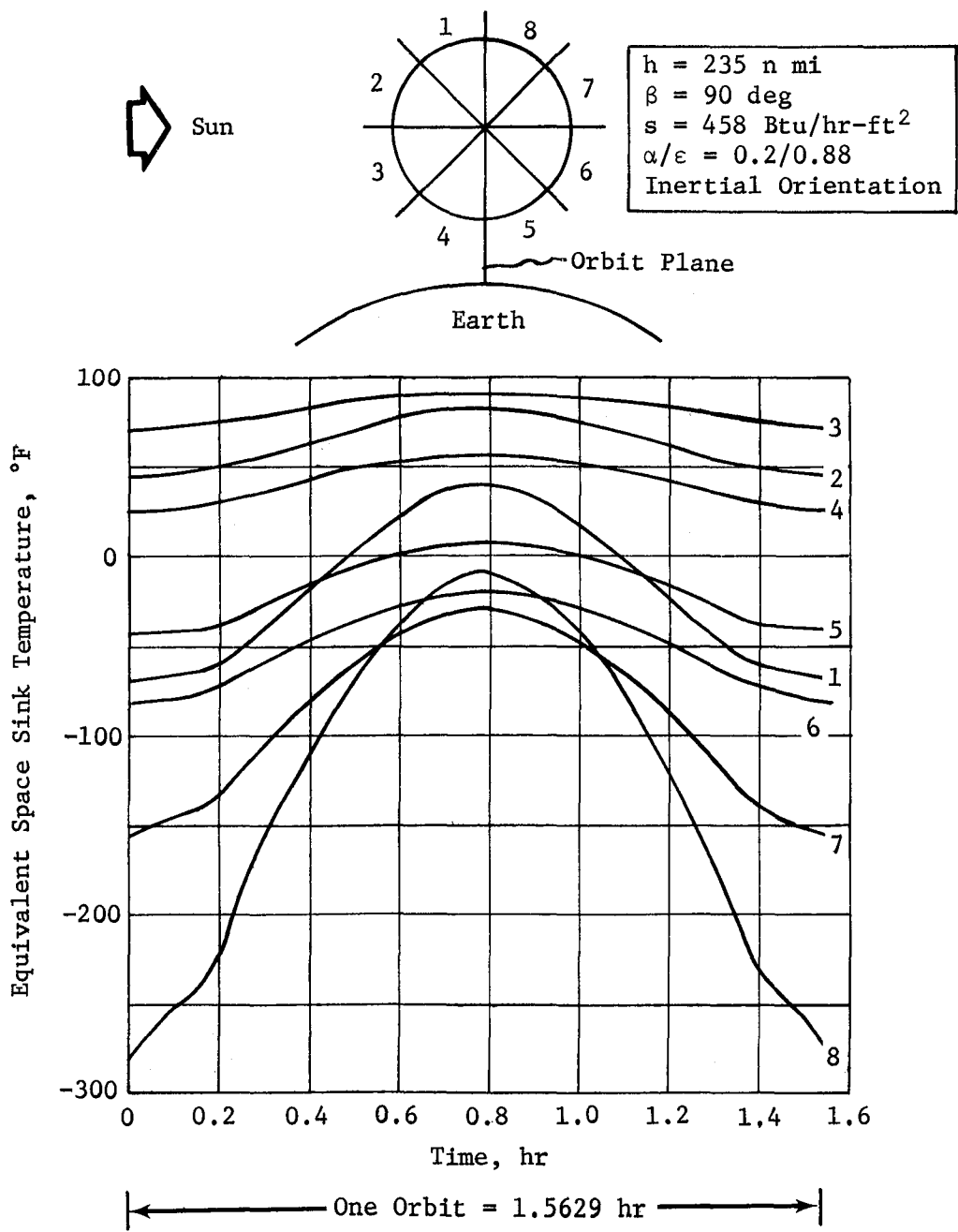


Fig. III-8 IR Telescope Transient Equivalent Space Sink Temperatures

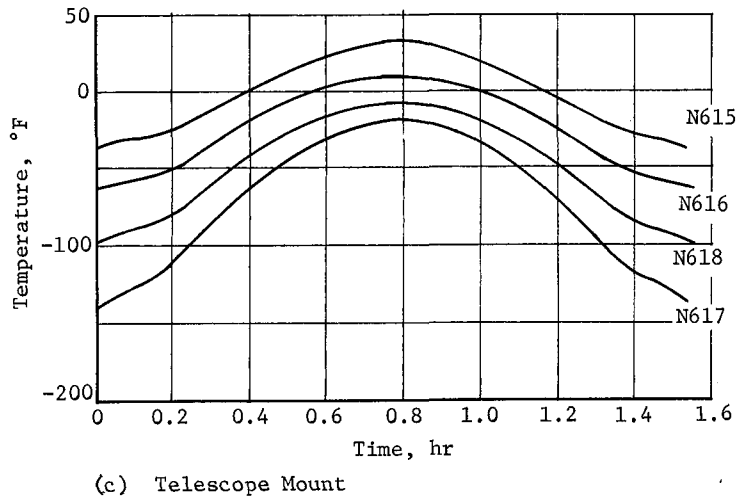
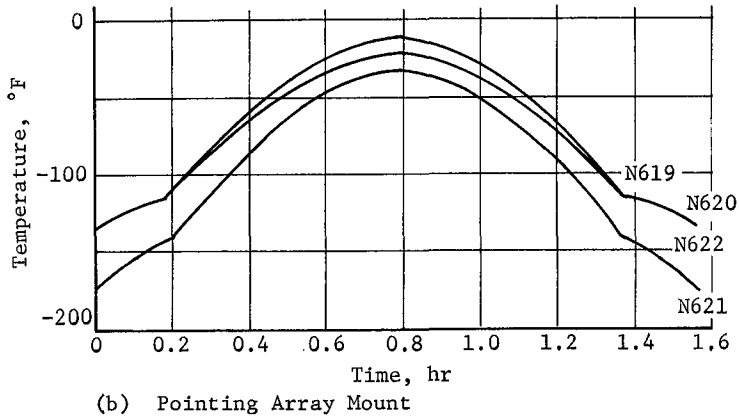
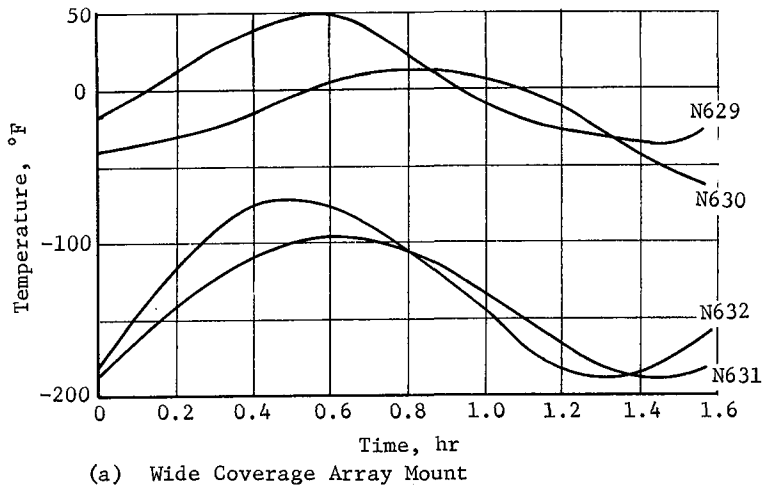


Fig. III-9 Pallet Experiment Mounts Equivalent Space Sink Temperatures

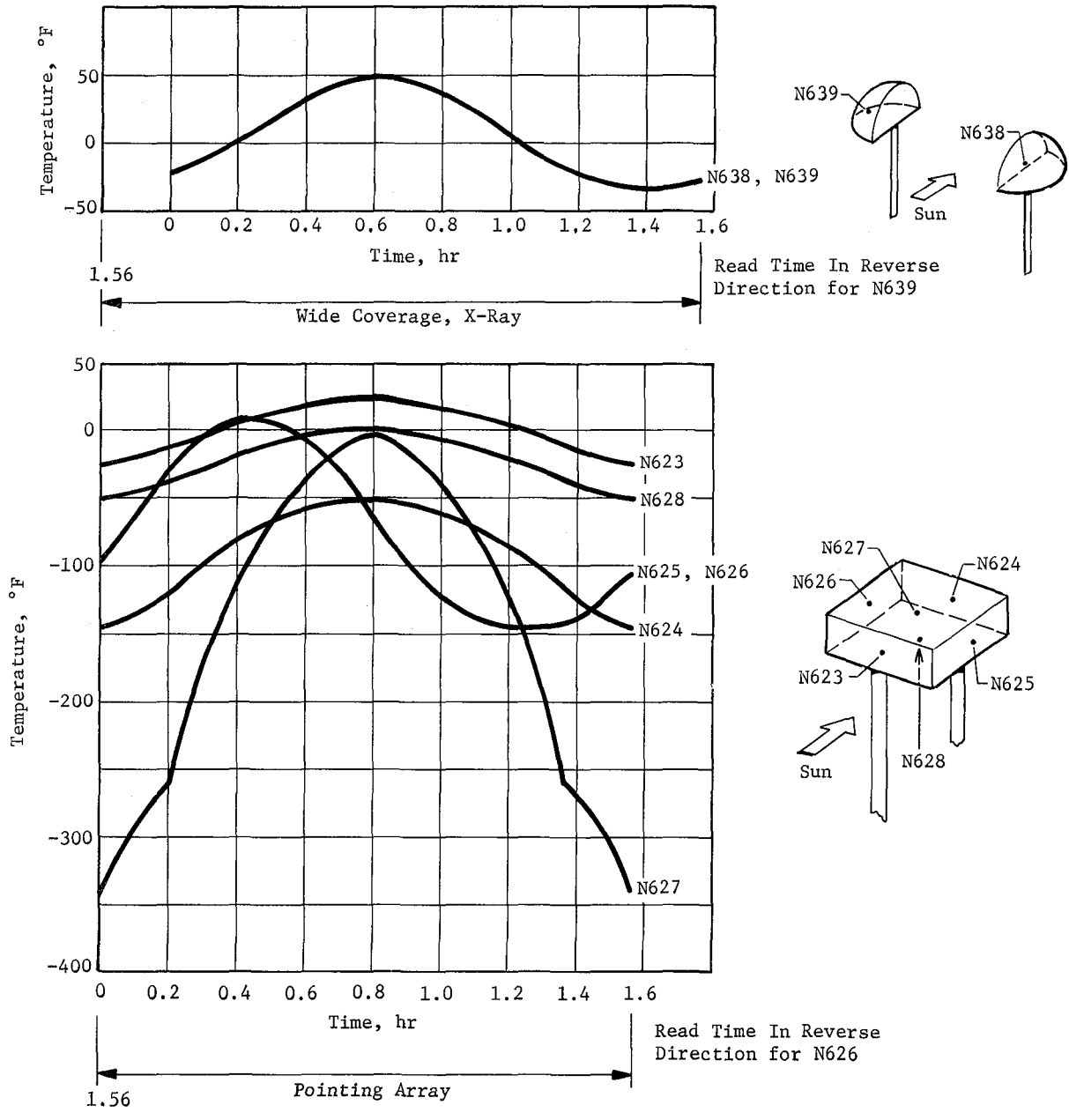


Fig. III-10 Array Equivalent Space Sink Temperatures

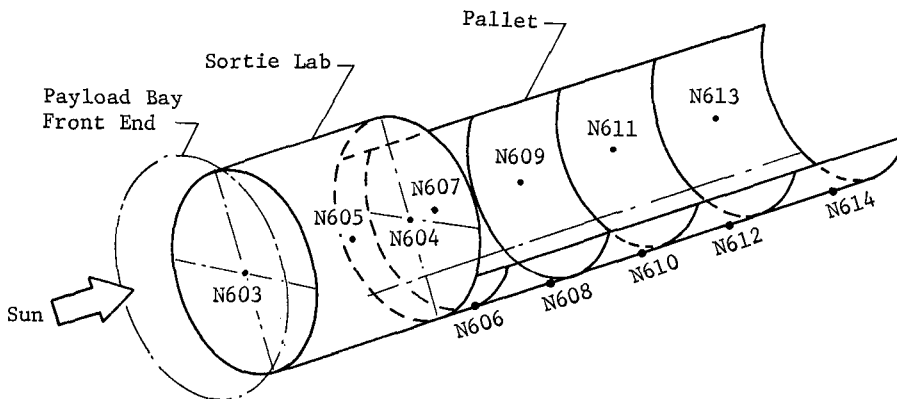
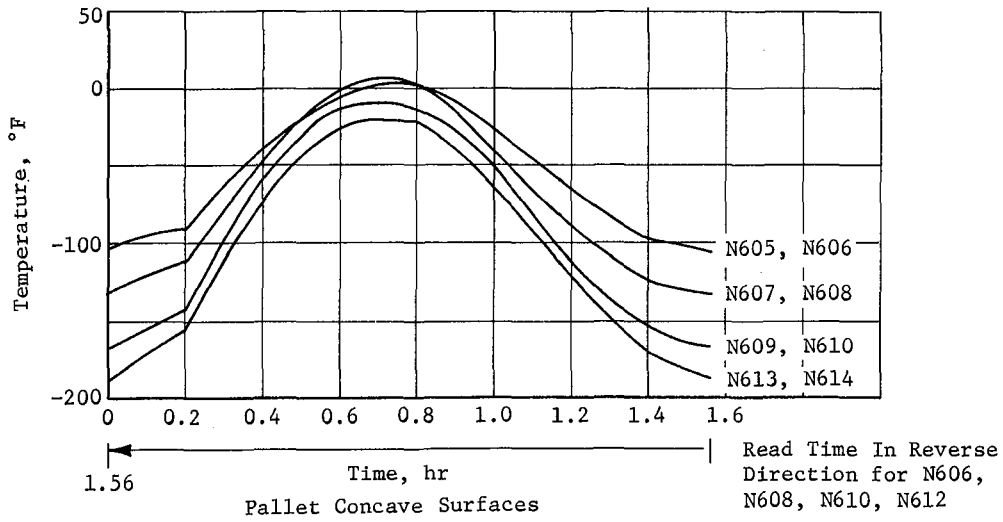
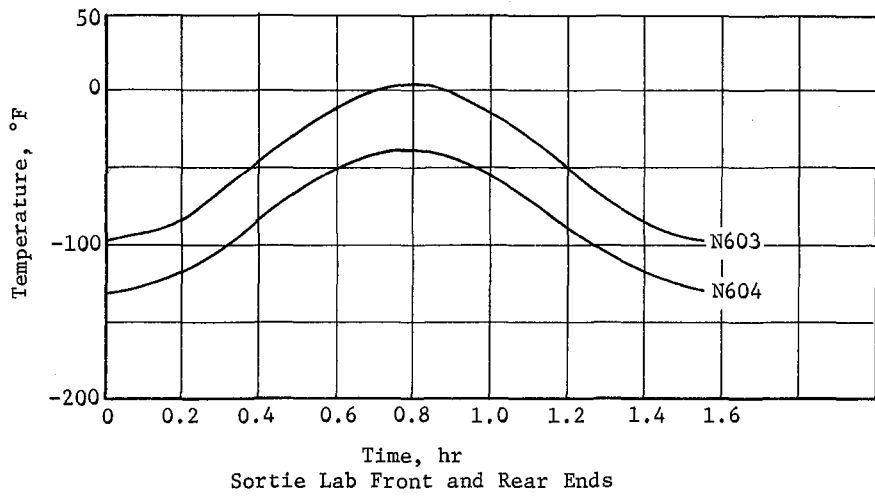


Fig. III-11 Pallet and Sortie Lab Equivalent Space Sink Temperatures

Table III-1 IR Telescope Thermal Environment Summary

Heat Source	Absorbed Flux, Btu/ft ² -hr	
	Orbiter Deployed	Free Flying
Solar	29.2	29.4
Albedo	0.234	0.95
Earth IR	13.3	22.3
Reflected	1.9	0
Orbiter/Payload IR	-1.9	0
Total	42.74	52.6
↳ to space	0.55	0.88
Equivalent Space Sink Temperature	1°F	-28°F

2. IR Telescope Thermal Analysis

The analysis of the thermal design was performed in two stages. The first (Ref III-4) involved simplified calculations to evaluate configuration concepts, establish preliminary thermal control system cryogen requirements. The second stage, described here, involved a comprehensive thermal analysis to establish the thermal performance in greater detail. A 102-node thermal math model of the IR telescope was constructed and used to calculate total cryogen vented, the contribution to this total from individual heat leaks, and the temperature transients during nonvent periods.

a. Thermal Design - The requirements, assumptions, and description of the IR telescope thermal design are discussed in the following paragraphs.

Requirements - The general requirements imply a design that is capable of maintaining the telescope at or below 30°K and the signal sensors of the instruments at 2°K for a seven-day mission period.

Assumptions - The following assumptions were made:

- 1) The IR telescope configuration used in this analysis is as shown in Fig. III-29 in Section B of this chapter;
- 2) Optics and other internal structures will be precooled on the ground;
- 3) Initial ullage volume is 20% at deployment;
- 4) Programmed nonventing periods of 3 hr will be required during observation periods;

- 5) Electrical heat dissipation rates for the instruments and components are as provided in Table III-2;
- 6) Thermophysical property data necessary for the analysis are given in Table III-3;
- 7) Grey diffuse radiative surface properties were used in the analysis.

Table III-2 Electrical Heat Loads

Components	Average Heat Dissipation, W
Four Gimbal Actuators	75 Each
Detector Instrument	25

Table III-3 Thermophysical Properties

Material	Density lb/in ³	Specific Heat, Btu/lb-°F	Thermal Conductivity, Btu/hr-in.-°F
Aluminum	0.0975	0.23	8.5
Invar	0.291	0.123	0.503
Cervit (Fused Silica)	0.08	0.02 (At -410°F)	0.07
Fiberglass	0.0635	0.3	0.0125
Multilayer Insulation	--	--	4.16 x 10 ⁻⁶
Neon	0.0434	0.485	
Latent Heat = 36.6 Btu/lb			
Contact Conductances		Btu/hr-°F	
Bolted Construction		1.33	
Flexible Coupling		0.3	
Roller Contact		0.004	

Description - To achieve the objective of an upper temperature limit of 30°K for the optics and telescope barrel, the entire telescope is enclosed within a jacket in which liquid neon is maintained at a pressure near one atmosphere. The optics and other internal structures will be precooled by a ground supply of liquid neon. Condensate formation is prevented by providing a slight positive pressure of helium within the telescope barrel on the ground and

during ascent. In addition the presence of the helium provides a heat transfer medium that assists cooling of the optics. Once orbit is achieved, the front cover will be removed and the telescope pressure allowed to approach the near-zero ambient pressure. The following thermal control techniques are employed to attain the desired thermal control performance:

- 1) Use of the constant temperature control, high heat transfer rates, and high heat absorption characteristics of the boiling process. Thus the boiling neon can maintain the telescope within 24.5°K and 27.2°K by controlling its pressure between 0.4257 atm and 1 atm.
- 2) Use of thermal coatings and insulation as a means of controlling heat transfer rates. Thus the neon boiloff rate, and telescope temperature rise during nonboiling periods (programmed venting hold) can be minimized.
- 3) Use of relatively low conductance structural materials to reduce heat leaks to the neon jacket.

The heat loads on the IR telescope can be subdivided into four areas: the one-dimensional heat transfer through the large insulation area, the insulation edge effects, the heat transfer resulting from a temperature gradient in the telescope supports, and the internal heat load.

Two inches of multilayer insulation and a low α/ϵ (0.2/0.9) coating on the meteoroid shield external surface are the primary means of limiting the heat input to the liquid neon in space. During the ground hold period the multilayer will either be gas filled or compressed within a flexible vacuum jacket and will therefore be a relatively poor insulator. To limit the ground hold heating, a foam layer is interposed between the multilayer and tank wall. The foam must be sealed to the tank and must be sealed at its outer surface with an impermeable vapor barrier. The need for an impermeable seal is reduced if helium is used as the purge gas since it will not condense at the temperature of liquid neon. Nitrogen gas, however, offers advantages from the standpoint of cost and lower thermal conductivity. The ratio of thermal conductivities of helium and nitrogen is nearly six.

To avoid serious edge effects where the eight support tubes penetrate the insulation and at the rear access cover, careful attention must be applied to the details of the insulation assembly. The recommended approach is detailed in Fig. III-12 thru III-14.

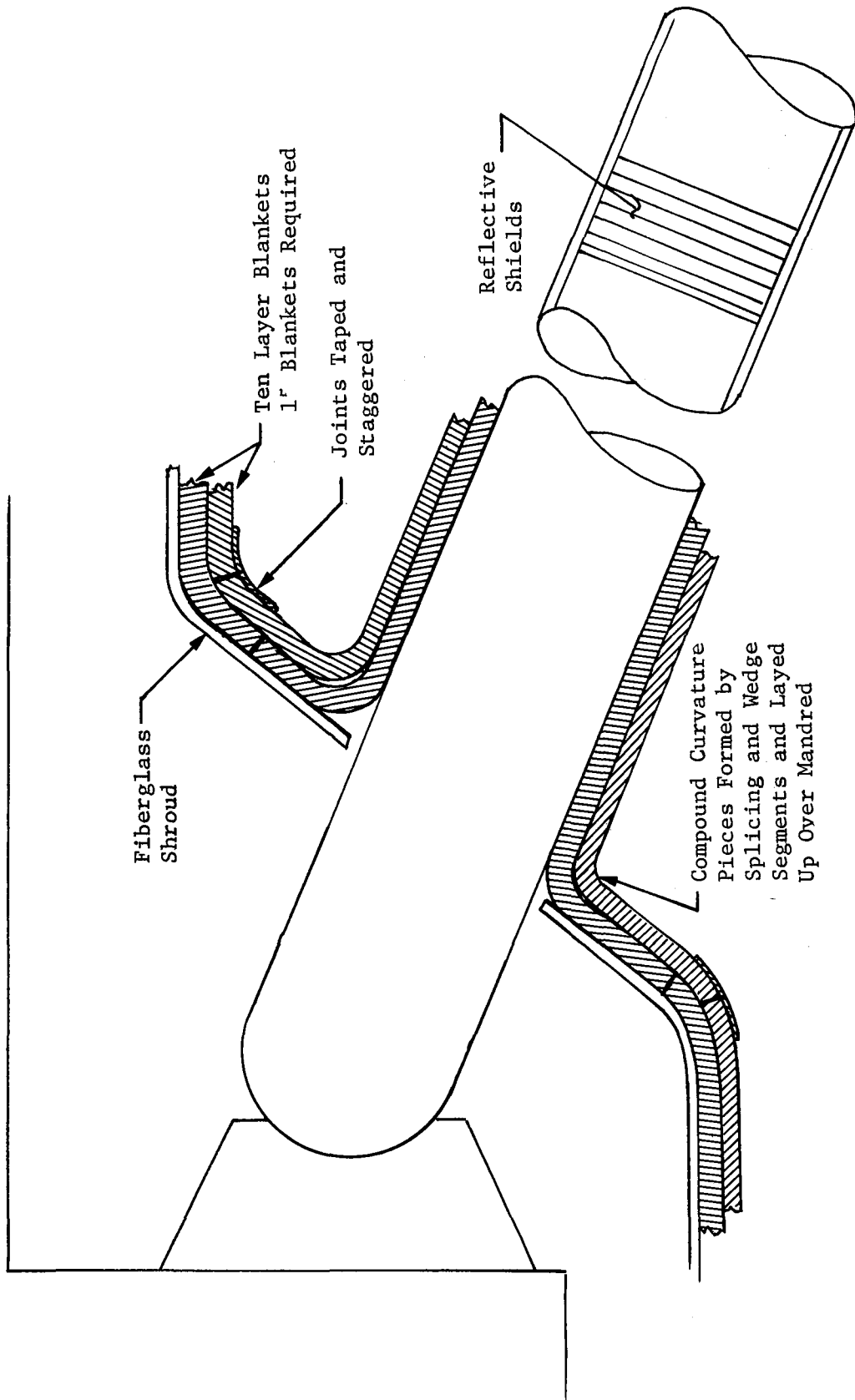


Fig. III-12 Insulation Detail at Tubular Supports

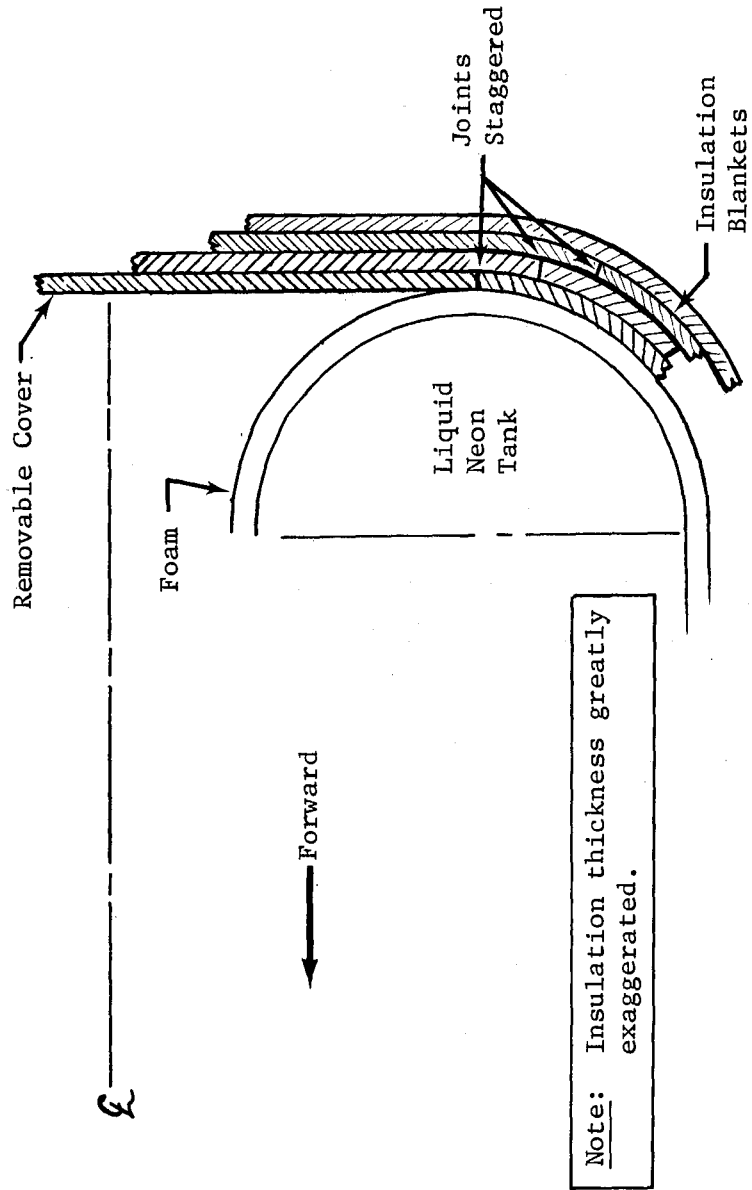


Fig. III-13 Insulation Detail At Rear Access Cover

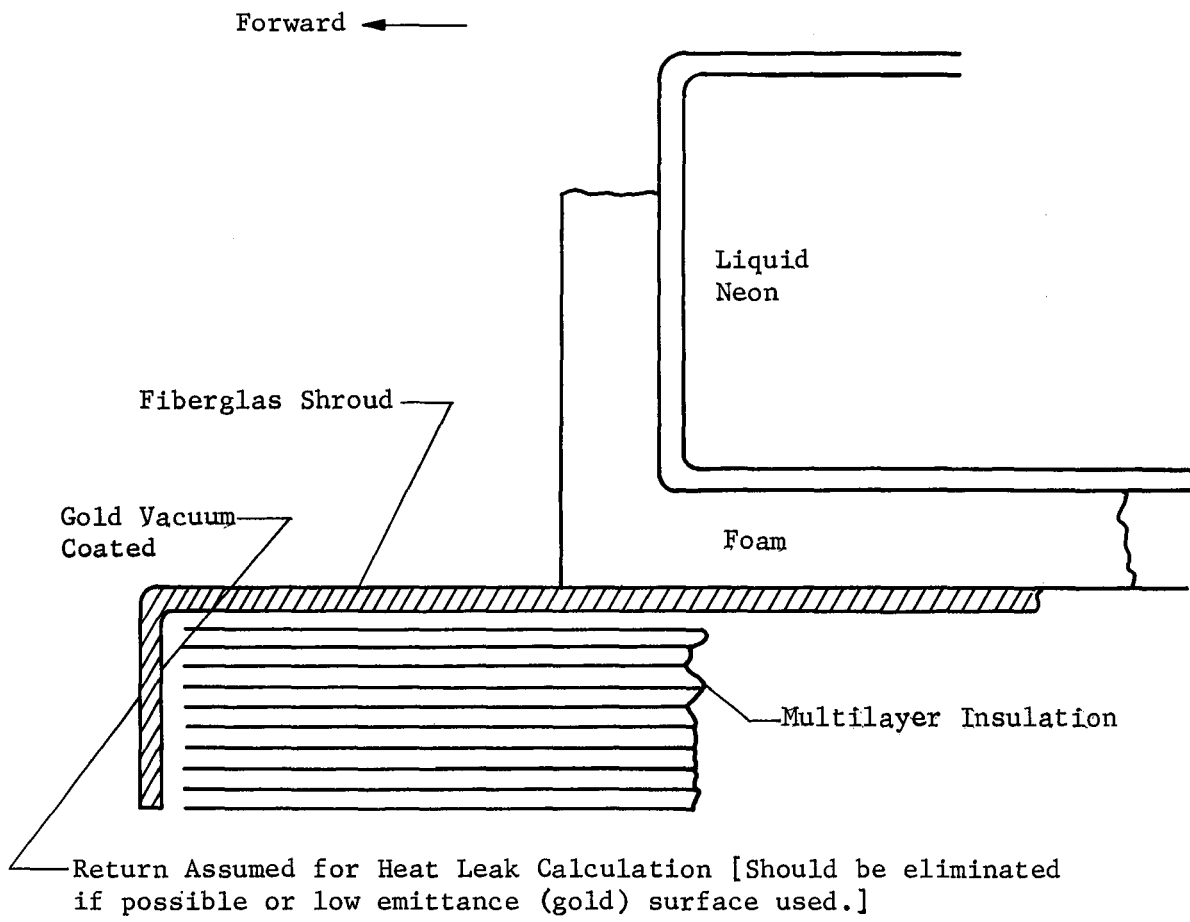


Fig. III-14 Forward Termination of Multilayer Insulation

The insulation is made up in ten layer blankets. Joints in each blanket layer are staggered. Where the cut edges of the insulation are exposed to a relatively conductive penetration, such as the lateral support rods, there will be a heat transfer from the insulation to the penetration. An analysis of this effect is presented in Ref III-4.

The conduction heat load in the supports is predicated on eight 2.0-in. O.D. longitudinal invar support tubes with an 0.080-in. wall thickness and eight 5/16-in.-diameter lateral invar support rods. Effective lengths for heat transfer were assumed to be 50 in. for the longitudinal tubes and 12 in. for the lateral rods.

A liquid orientation and vent system must be provided that will allow venting of liquid-free gas in the zero-g environment in an efficient manner. It is recommended that a screen liner be used to trap a thin layer of liquid against the interior walls of the annular tanks with communication provided between the inner and outer walls. As a result of ring or longitudinal stiffeners it may be necessary to divide the space into compartments. The recommended vent system consist of an open-loop refrigeration process in which liquid neon is extracted from the wall bound layer and throttled isenthalpically to a lower pressure and temperature in a wall mounted heat exchanger. The process is shown on thermodynamic coordinates in Fig. III-15. To avoid solid formation in the heat exchanger the lower pressure must be maintained above the triple point; which is 0.4257 atm for neon. The enthalpy gain in the process described is nearly identical to the latent heat of vaporization at the storage pressure if the storage pressure is in the range of one to two atmospheres and the heat exchanger pressure is 0.6 atm. The temperature difference available when expanding from 1 atm storage pressure to 0.6 atm is small, i.e., 1.6°K but probably adequate. At 2 atm storage pressure the temperature difference increases to 4.1°K.

By locating the heat exchanger tubes on the inner tank wall the tank contents will tend to circulate as in a heat pipe. Evaporation will occur at the screen on the outer wall with condensation at the inner wall with capillary pumping of liquid from the inner to outer wall. This is shown schematically in Fig. III-16. The circulation is beneficial since it will tend to eliminate temperature gradients in the stored fluid, which result in a decrease in the energy storage capability.

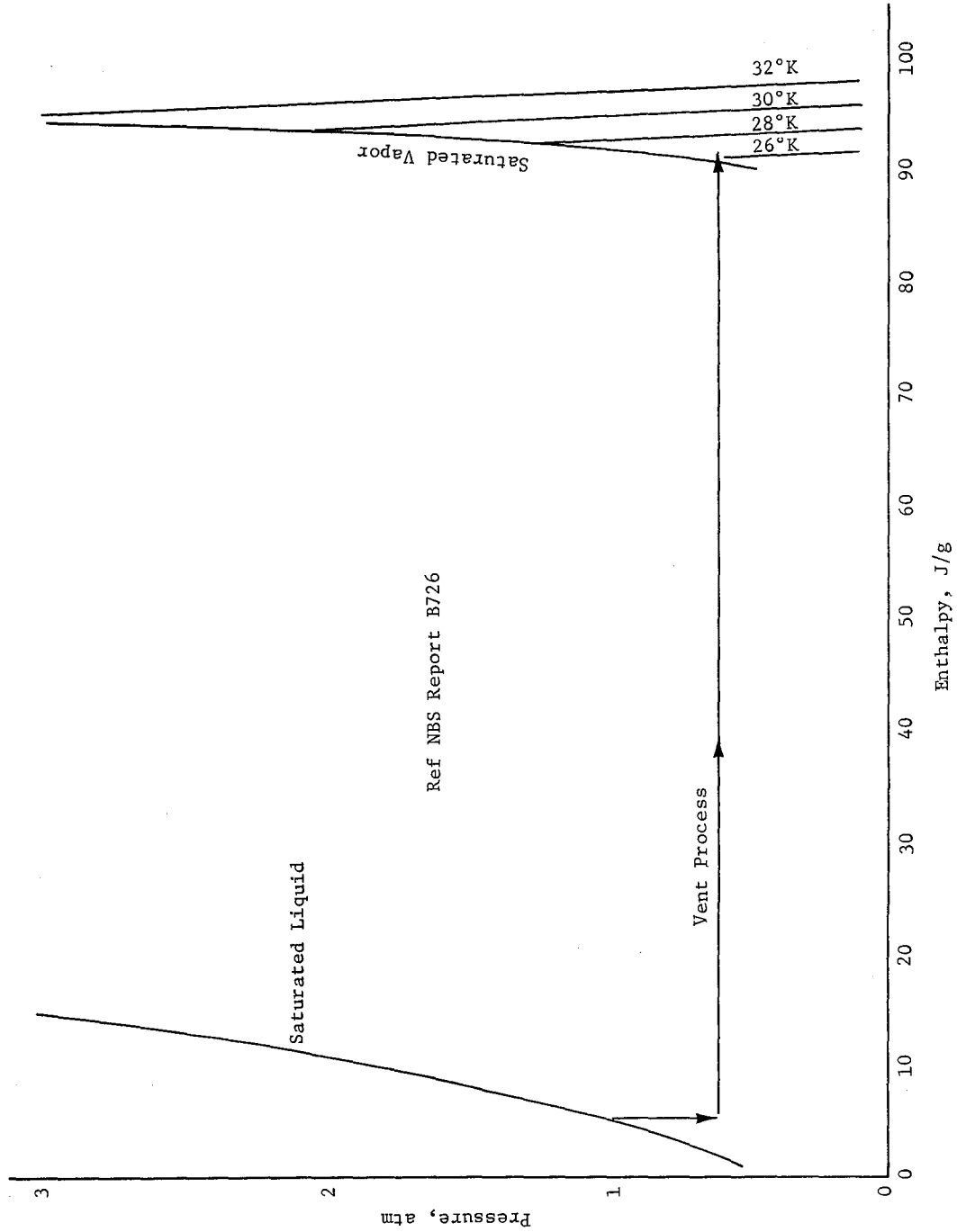


Fig. III-15 Pressure-Enthalpy Vent Process Diagram for Neon

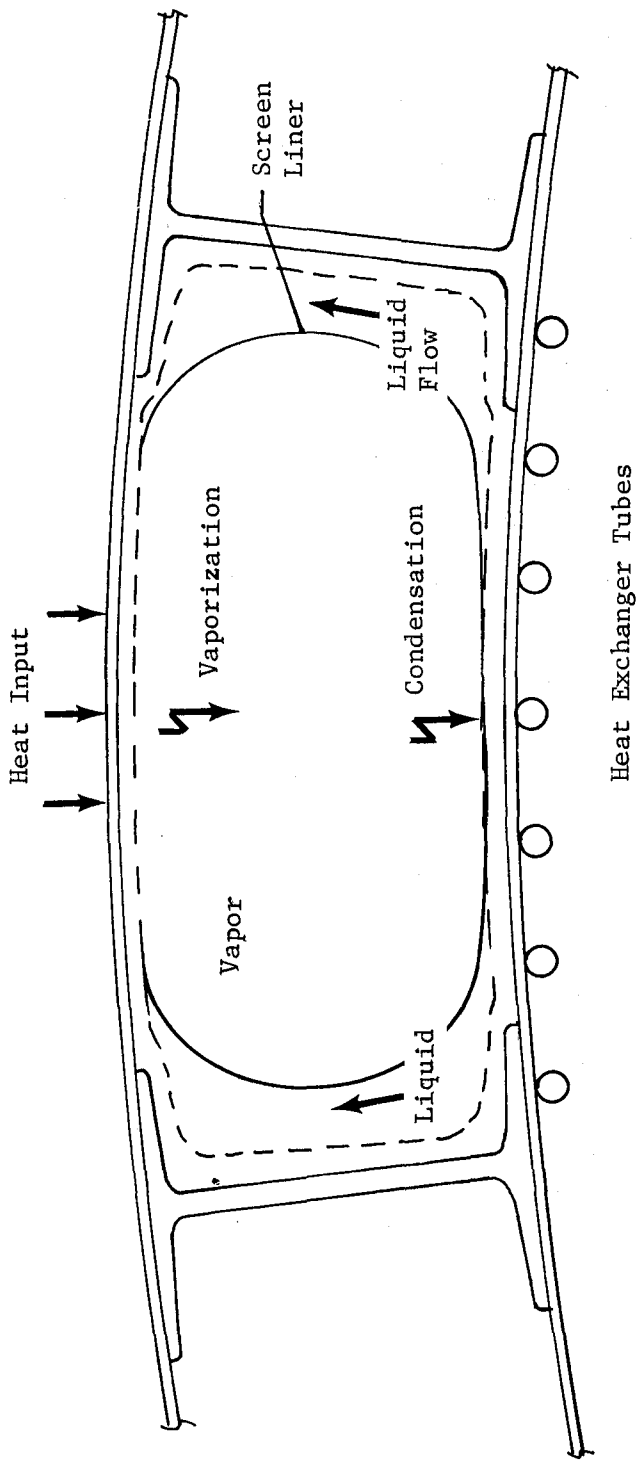


Fig. III-16 Liquid Orientation and Vent System

The 2°K temperature requirement for the instrument sensors dictates the use of liquid helium as the cooling medium. The precise temperature requirement should be examined in some detail since the 2°K requirement presents major complications relative to say, 2.5°K. The 2°K requirement implies the use of superfluid helium II for which a zero-g dewar is currently beyond the state of the art. Below the superfluid transition temperature of 2.2°K, helium exists in the superfluid form with properties that vary radically from the normal fluid helium I. The thermal conductivity of helium II becomes very large and the viscosity approaches zero. Helium II, as a result of its low viscosity, will flow through otherwise impermeable materials. Further, a very thin film of liquid forms over all containing surfaces.

For the seven-day mission a closed-loop cooling system is not warranted and cooling is best accomplished by boiling helium II at a pressure of approximately 20 mm Hg or less. The production of temperature down to about 1°K by this method is fairly simple in a gravitational environment (Ref III-5). Below this temperature the superfluid helium II film, which is absorbed on the interior dewar surfaces penetrates up the vent tube where it vaporizes and recondenses. It is presumed that this lower limit will be raised somewhat in the near zero-g environment.

The optimum design may consist of a supply dewar of normal helium I with expansion cooling to form helium II in a dewar in contact with the detector. The detector dewar would not be filled until after orbit is achieved and the telescope evacuated. The thermal protection system on the supply dewar would thus need to be designed for the one atmosphere ambient while the detector dewar would have to contend only with the less severe vacuum environment. The requirements for the containment of superfluid helium II in low gravity are not well understood. The liquid phase must somehow be restrained from flowing out of the vent via the superfluid film. At a minimum, the presence of the film represents a greatly increased heat load on the dewar. The Jet Propulsion Laboratory is currently studying the containment problem (Ref III-6) and has outlined a rather ambitious experimental program that will lead to the development of a suitable low-gravity dewar design.

A system for controlling the liquid level in the helium II dewar could possibly be adapted from the one-gravity system described by Elsner (Ref III-7). In this system when the liquid level falls below the set point in the Helium II working volume, Helium I is fed from a supply dewar to an expansion volume in which the temperature is reduced by pumping away vapor. The expansion volume is separated from the working volume by a porous plug, superfilter, which

is impermeable to Helium I. The superfilter is in contact on one side with the expansion volume liquid and on the other side with vapor in the working volume. When the temperature of the Helium II in the expansion volume is reduced a very small amount below that in the working volume, the lower temperature liquid flows through the plug. This phenomenon is explained in terms of a two fluid model in which Helium II is composed of a temperature-dependent mixture of a normal component and a superfluid component. The lower the temperature, the higher the concentration of the superfluid component. The superfluid component flows across the plug in an attempt to balance out the concentration difference of the superfluid component. To operate in zero g, fluid orientation devices must be developed that would ensure that the expansion chamber liquid were in contact with the superfilter on one side and working volume vapor on the other side

b. Method of Analysis - This subsection describes the thermal math model and the analytical approach used in its construction.

Analytical Approach - A flow diagram showing each of the steps in the construction of the thermal math model is presented in Fig. III-17. Steps 1 thru 3 are concerned with the generation of the model's radiation interchange couplings and external environment fluxes. Step 4 is the calculation of node thermal capacitances and the conductive couplings between them in the network.

Step 1 involves analyzing two groups of surface configurations to derive a nodal breakdown that satisfies the subsequent performance analysis.

The first group is concerned with the deployed mode of the telescope in order to compute hot case orbital conditions. The configuration shown in Fig. III-1 was selected considering: (1) the constraint that observation is limited to no closer than 90 deg to the limb of the sun and no closer than 45 deg to the limb of the earth and moon; and (2) the pointing technique recommended for the Astronomy Sortie mission, viz, a deployed wide angle gimbal with a Shuttle inertial attitude of X-POP. This surface group was developed in an in-house study (Ref III-1), and consists of a 131 nodes including 33 nodes describing the telescope external surface.

The second group is concerned with the internal layout of the telescope involving the optics assembly and instrument chamber. The configuration is shown in Fig. III-18 as plotted by MITRAP and was represented by 80 nodal surfaces.

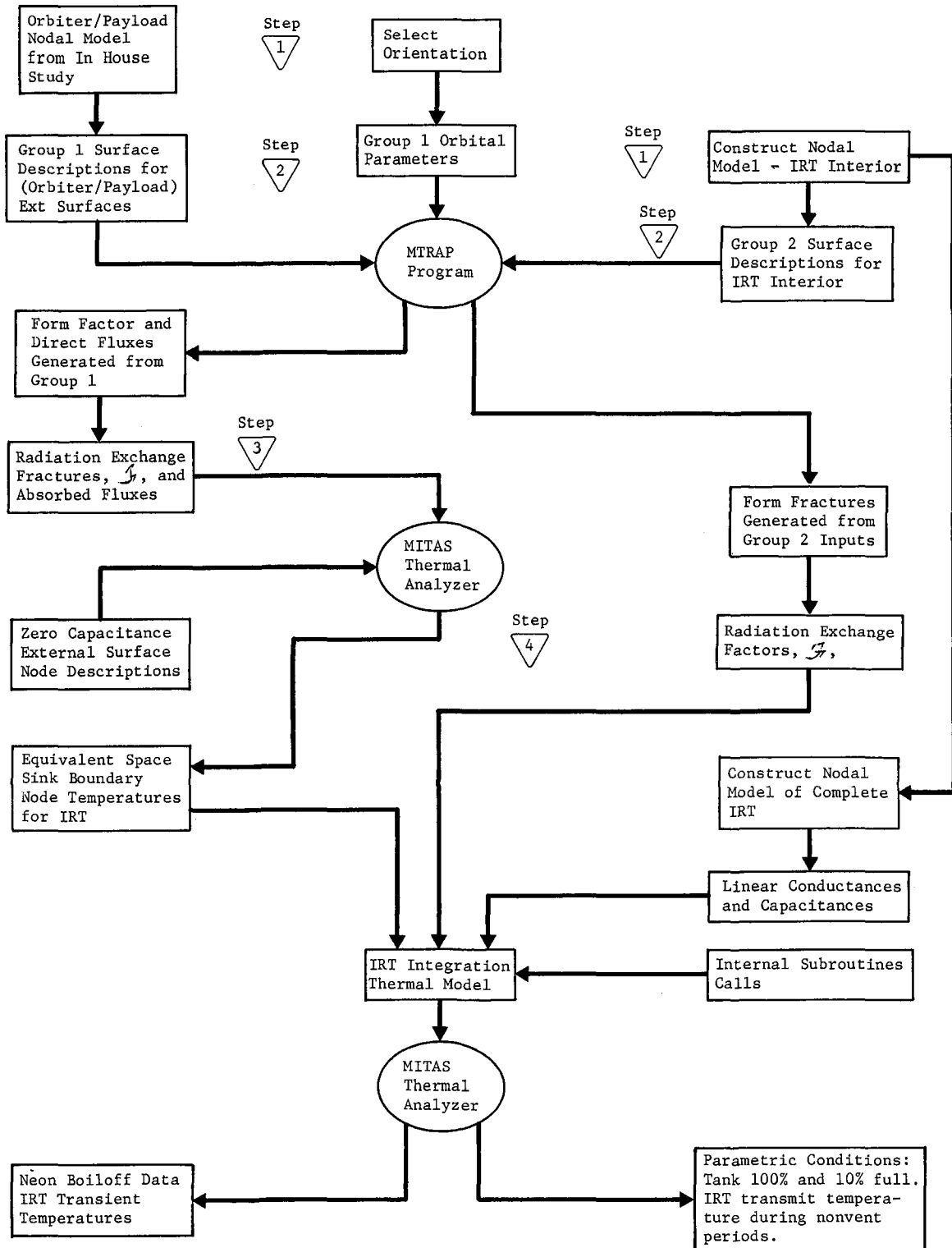


Fig. III-17 Flow Diagram for Construction of IRT Thermal Model

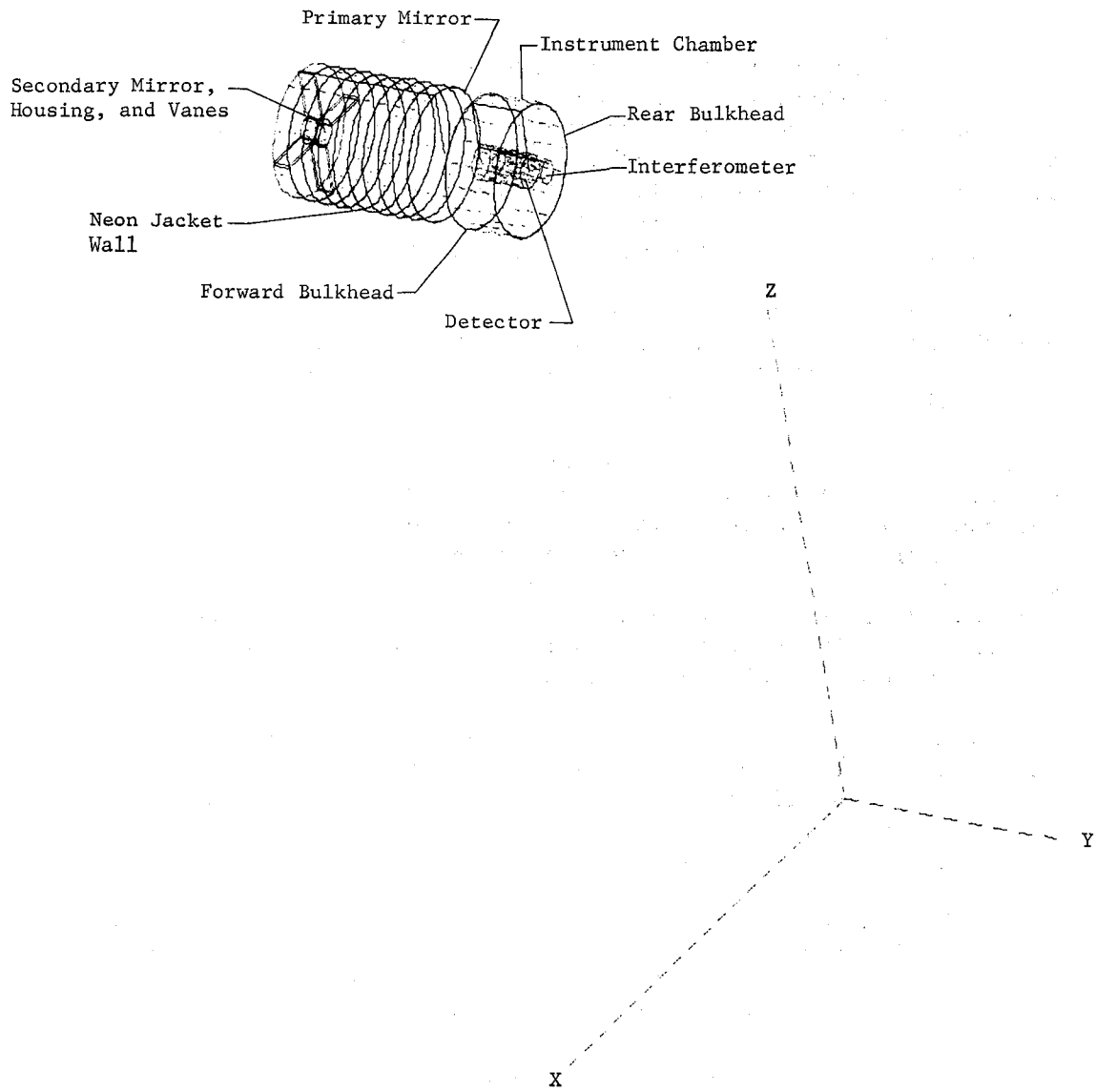


Fig. III-18 Optics Assembly and Instrument Chamber

Step 2 consists of describing the two groups of surface inputs and the orbital conditions to MTRAP. The program has a storage limit of 140 nodes; therefore the group 2 surface data were run separately to generate the necessary form factors and radiation exchange factors. A 90-deg beta angle orbital inclination with the telescope solar oriented and broadside to the sun provides the 100% time in sunlight hot extreme orbital conditions used in this investigation to generate the external environment fluxes.

Step 3 uses the radiation exchange factors (f) and absorbed fluxes calculated by MTRAP from the group 1 surface data, and zero capacitance nodal descriptions to generate equivalent space sink boundary nodes using the MITAS thermal network analyzer.

Step 4 consists of constructing the conductance/capacitance network of the total telescope based on drawing and weight documents for subsequent input to the MITAS program. The conductances describe either radiation, f , or conduction couplings between nodes. The conductive couplings were calculated by hand and the f values calculated by MTRAP from the group 2 surface data. In addition, calls to certain MITAS internal subroutines were input to compute neon boiloff rates and integrate the same.

Thermal Model Description - The IRT model is quite comprehensive, consisting of 102 nodes, 1143 radiation connections, 152 conduction connections, and 17 time variant boundary node temperatures. The purpose of the detailed model is to provide thermal performance verification of the preliminary IRT design.

Generally, the overall model is subdivided externally at the meteoroid shield into four axial rings and eight circumferential sectors, and internally into the optics assembly and instrument chamber. Figure III-19 shows the nodal location, and the nodal information is in Table III-4. The structural interface with the Orbiter is taken at the gimbal ring assembly. Each of the three rings were subdivided into four circumferential sectors and values assigned to the flexible couplings and bearing conductances as indicated in Table III-3. The average heat load used in the simulation for each of the four gimbal actuators is 70 W. The telescope assembly is supported by the gimbal assembly by means of an adapter. The eight tubular truss members of the adapter are invar, 50 in. long, 2 in. in diameter with a 0.08-in. wall thickness, and thermally isolated from the external environment by multilayer insulation blankets. This truss conduction heat leak to the neon together with that of the eight 5/16-in.-diameter invar tension tie members of the adapter was simulated in the model. Bolted joint

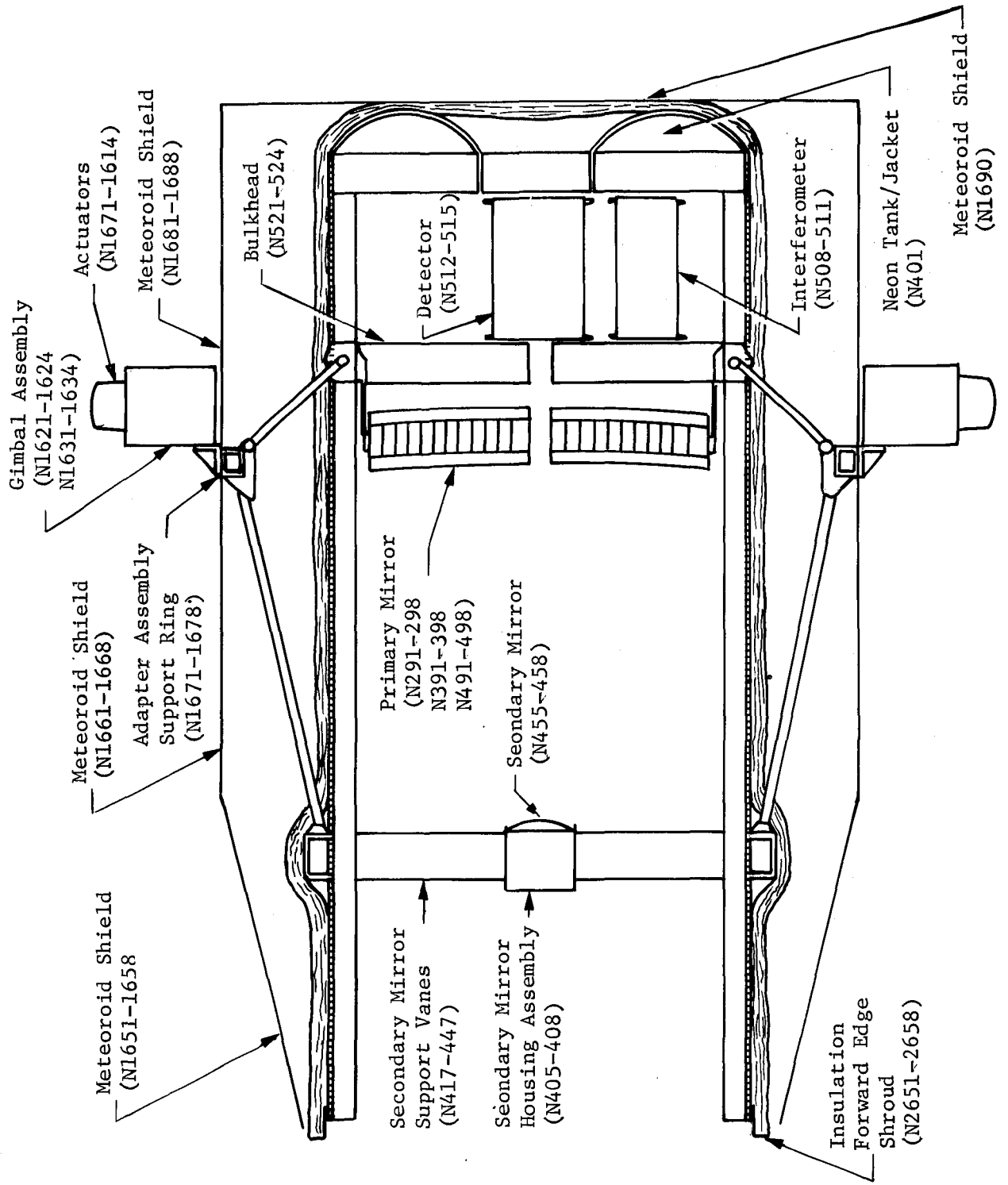


Fig. III-19 IR Telescope Nodal Layout

Table III-4 Thermal Model Nodal Information

Assembly	Material	Surface Emittance	Number of Nodes and Breakdown
Gimbal	Aluminum	$\alpha/\epsilon = 0.2/0.9$	8 (4 circumferential by 2 radial)
Actuators	--	$\alpha/\epsilon = 0.2/0.9$	4 (1 each actuator)
Support Ring (Meteoroid Shield/Gimbal)	Invar	$\alpha/\epsilon = 0.2/0.9$	8 (8 circumferential)
Meteoroid Shield	Aluminum	$\alpha/\epsilon = 0.2/0.9$	25 (3 axial by 8 circumferential plus 1 at base)
Primary Mirror	Cervit	0.1	24 (3 axial by 2 radial by 4 circumferential)
Secondary Mirror	Cervit	0.1	4 (4 circumferential)
Secondary Mirror Housing	Invar	0.1	4 (4 circumferential)
Secondary Mirror Vanes	Invar	0.1	4 (1 each vane)
Telescope Neon Jacket	Invar/Neon	0.1	1 (condensed from 32)
Forward Bulkhead	Invar	Optics side: 0.04 Instruments side: 0.1	4 (4 circumferential)
Detector	--	0.1	4 (4 circumferential)
Interferometer	--	0.1	4 (4 circumferential)
Insulation Forward Edge Shroud	Fiberglas	Outside: $\alpha/\epsilon = 0.2/0.9$ Inside: $\alpha/\epsilon = 0.04$	8 (8 circumferential)
Deep Space	--	--	1
Equivalent Space Sink	--	--	17 (2 axial by 8 circumferential plus 1 at base)

conductance values were included as indicated in Table III-3. It was concluded from the results of the initial analysis stage (Ref III-4), that the influence of the insulation edge rejection at penetrations and particularly at the termination of the insulation at the forward end is significant. Accordingly, this heat leak to the neon was simulated in the model, but with the addition of intermediary insulation between the multilayer insulation and the edge included in the form of a gold deposited film.

The primary mirror that was analyzed is a cored monolith having the dimensions and nodal breakdown shown in Fig. III-20. Heat transfer within the mirror core considers radiation interchange as well as conduction. The mirror is mounted to the telescope oplice frame by three supports. The secondary mirror area model includes the mirror, its mount, and the four support vanes. The tube between the primary and secondary mirrors includes the neon tank or jacket and this area was condensed from the 36 nodes previously used to determine β factors to one node in order to simplify the analysis of the total heat leak effect on the neon boiloff rate.

The instrument chamber is largely enclosed by the neon jacket to which the detector and interferometer partially radiate, and partially conduct via the front and rear bulkheads. Because of its larger power dissipation of 25 W the detector was assumed to be the active instrument in the simulation.

c. Thermal Performance Analysis - Transient analyses of the preliminary thermal design indicate the capability of the system to meet the thermal design objective of controlling the optical assembly to 30°K or less. Further, the required neon quantity for a seven-day mission is well within the available tank volume by a factor of two. The minimum tank volume of 26.7-cu ft is dictated by structural considerations for an annular tank. Hence, the thermal system has an inherent growth capability to accommodate changes during the design cycle to internal heat dissipation, materials, mission duration, etc.

The results of these analyses are presented in Table III-5 and III-6. From Table III-5 the detrimental effect on insulation performance of edge rejection is shown to be reduced to negligible proportions through the use of an intermediary gold shield. The most significant influence on the quantity of neon lost to boiloff results from the internal heat dissipation of the detector instrument (25 W). The total rate of neon boiloff computed is 3.59 lb/hr out of which 2.33 lb/hr results from the internal heat load. Hence, a great care must be exercised in the specification of this interface. For a seven-day mission the quantity of neon lost to boiloff

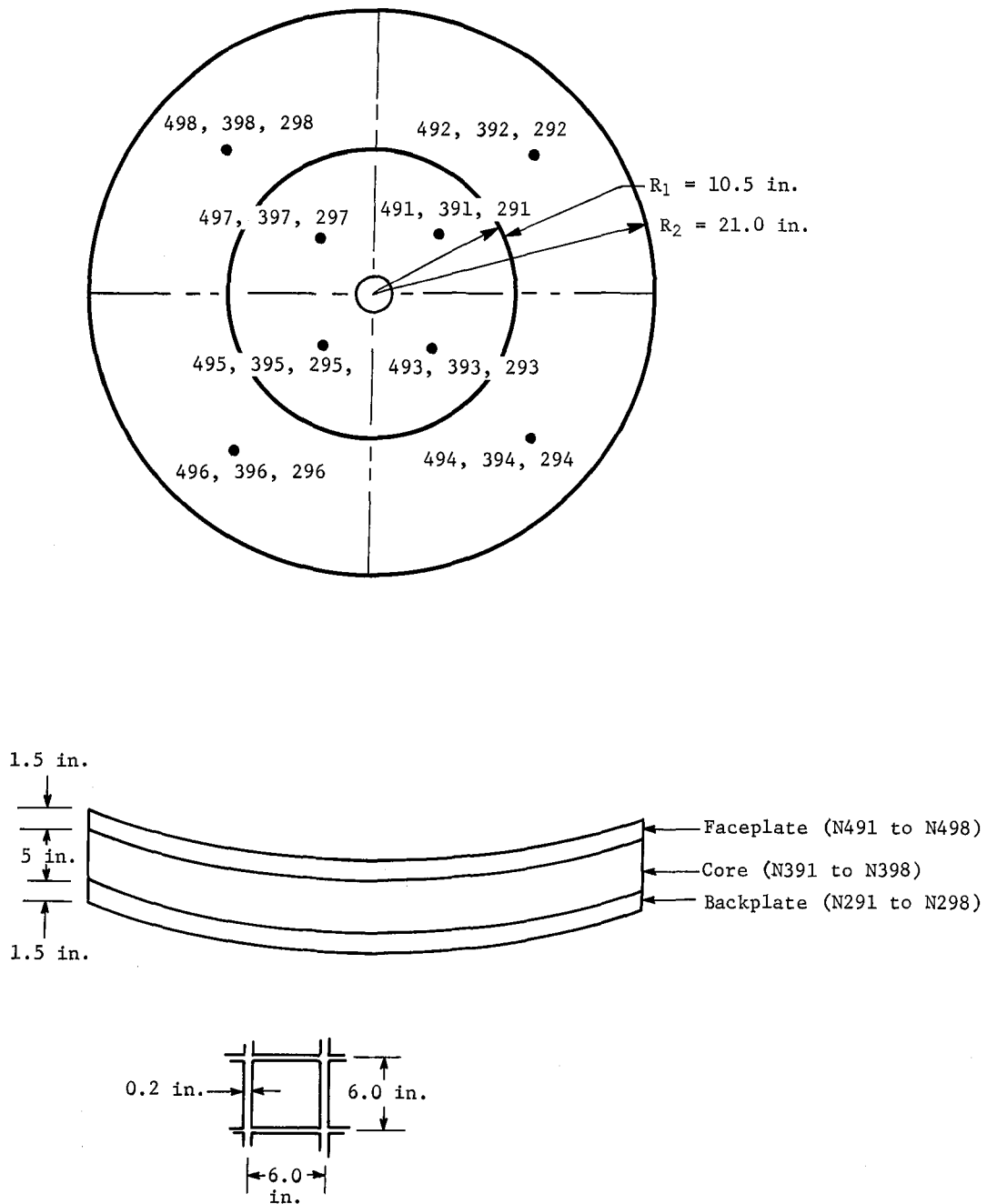


Fig. III-20 Nodal Model of Primary Mirror

is 605 lb if the broadside-to-sun telescope orientation is sustained, which is unlikely. However, this configuration provides an extreme worst design case for the purposes of sizing the total quantity of neon required. Further, as mentioned earlier, the analysis shows that the internal heat generation load (25 W) has a greater impact on neon boiloff than heat transferred through the structure from the external environment influences. The individual contributions to neon boiloff by the primary heat leaks--tank insulation, trusses, and ties--computed by MITAS for the initial 2 hr of the mission are plotted in Fig. III-21. The loaded quantity of neon should be at least 30% greater than the computed boiloff to ensure an adequate heat capacity during the no-vent periods near the end of the mission and to allow for uncertainties in the analysis. The loaded quantity is then 785 lb. The tank volume required, assuming an initial ullage volume of 20% due to the ground hold heat flux and ascent heat flux is 12.5 cu ft.

The temperature effects for the optical assembly and instrument chamber are summarized in Table III-6. The conditions analyzed considered: (1) the neon boiling at near one atmosphere (27.6°K); (2) no boiling during a 3-hr nonvent period and tank 100% full (785 lb neon); and (3) no boiling during a 3-hr nonvent period and tank 10% full (78.5 lb neon). In general the temperature level of the optics assembly is stable at 27.6°K with negligible gradients and negligible excursions during the 3-hr nonvent period although the external structure experiences large temperature excursions, as shown in Fig. III-22. The heat dissipating instruments will require direct neon cooling; otherwise the heat load on the 2°K sensor helium cooling system will be excessive. With mainly radiative cooling to the neon jacket enclosure, the average temperature level increases, initially at a rate of 4°F/hr, to 234°K (-38°F). Detailed consideration is recommended in this area.

Table III-5 Neon Boiloff Summary

Item	lb hr
One-dimensional heat transfer through insulation	0.677
½-in.-diameter holes in insulation at lateral supports and other penetrations, 14 places	0.000
Edge effect at termination of insulation at front of telescope	0.001
Conduction through eight longitudinal invar support tubes, 2 in. diameter x 50 in. with 0.08 in. wall thickness	0.350
Lateral invar support rods, 5/16 in. diameter x 12 in. long	0.233
Internal power	2.328
Total	3.589

Table III-6 Temperature Effects Summary, °F

Item	Venting	3 hr of Nonvent Operations	
		Tank 100% Full	Tank 10% Full
<u>Primary Mirror</u>			
Average Temperature	-410.3	-410.3	-410.3
Orbital Excursions	0	0	0
Axial Gradient	0	0	0
Radial Gradient	0	0	0
Circumferential Gradient	0	0	0
<u>Secondary Mirror Assembly</u>			
Average Temperature	-410.3	-410.3	-410.3
Orbital Excursions	0	0	0
<u>Telescope Tube</u>	-410.3	-410.0	-409.7
<u>Instruments</u>			
Detector	-37.8	-37.8	-37.8
Interferometer	-410.3	-410.3	-410.3

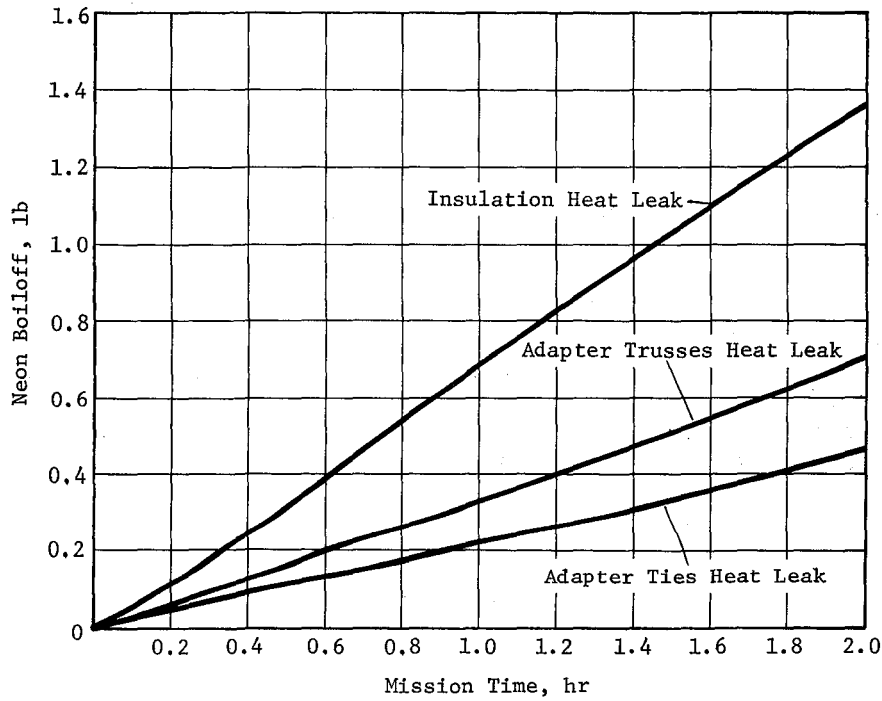


Fig. III-21 Heat Leak Imposed Neon Boiloff

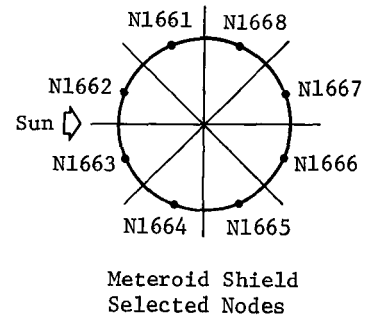
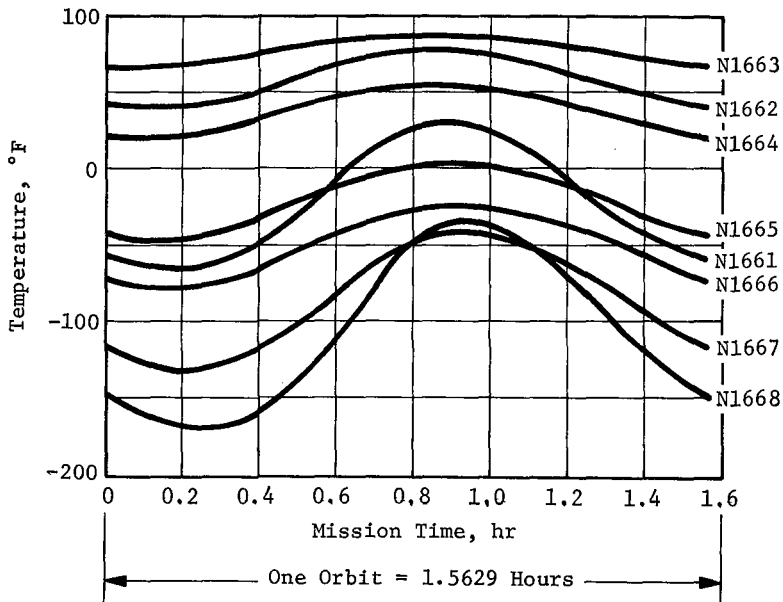


Fig. III-22 IR Telescope Transient Temperatures

3. Recommended Thermal Control Systems

The thermal control system for the 100-cm IR telescope has been defined in the previous subsection. This subsection discusses the thermal study of the other five telescopes (120-cm Stratoscope III, 100-cm photoheliograph, 25-cm XUV spectroheliograph, 32-cm X-ray telescope, and 2.45- and 4.0-cm coronagraphs). The thermal designs of the telescopes use passive methods as the primary means to regulate the heat flow across the telescope's boundaries to obtain the desired temperatures. These methods involve the use of surface finishes and insulations. Active or semi-active methods are used only if passive methods will not provide the required temperature control. Thermal decoupling of the telescope tube from the fluctuations of the external environment is a thermal design approach common to all the telescope types. However, the thermal control methods depend on the nature of the experiment. Solar astronomy telescopes view the sun directly and suitable methods of dissipating the solar heat load must be provided. In the case of the stellar astronomy telescope, Stratoscope III, the thermal control method must reduce and compensate for the radiation heat loss to space through the optics viewing aperture. Further, the thermal design effort for any of the telescopes is concerned mainly with the preservation of critical optical tolerances of the telescopes.

a. 120-cm Stratoscope III - The thermal requirements, as extrapolated from the LST study, are presented here along with a discussion of preliminary thermal design concepts and analysis of the recommended thermal control system.

Requirements - The thermo-optical requirements are derived from optical wavefront error budgeting and are the best estimate at present.

Primary Mirror

Temperature level	70 ± 22.5°F
Axial gradient	28°F
Axial gradient variation	4.7°F
Radial gradient	16°F

Secondary Mirror

Temperature	70 ± 19°F
Axial gradient	22.4°F
Axial gradient variation	8.4°F
Radial gradient	15°F

The cameras and spectographs have been identified as having the temperature requirements of $9 \pm 2^\circ\text{F}$.

This instrumentation dissipates a total of 80 W during warmup, standby, and observation periods, and 120 W during the readout period. The requirements are to reject the power dissipations, maintain camera temperatures, and minimize heat inputs to the mounting structure.

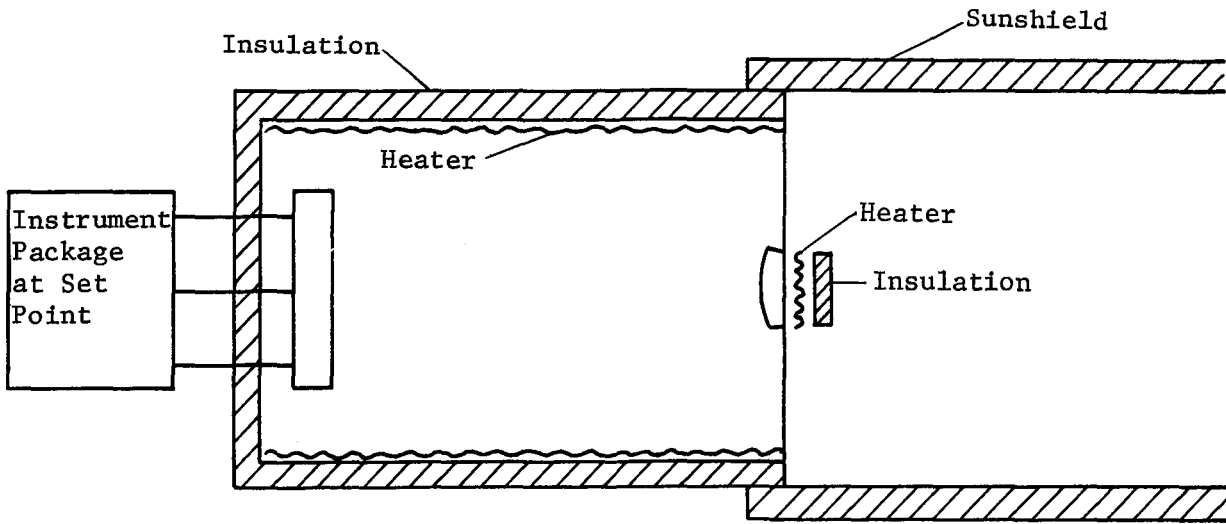
Assumptions - The following assumptions were made:

- 1) The Stratoscope III configuration used in this study is as shown in Figure IV-24 in Chapter IV;
- 2) The spectograph detectors will be preconditioned on the ground;
- 3) Overall effective emittance of the insulation blanket is 0.01;
- 4) The instrument compartment interface is adiabatic.

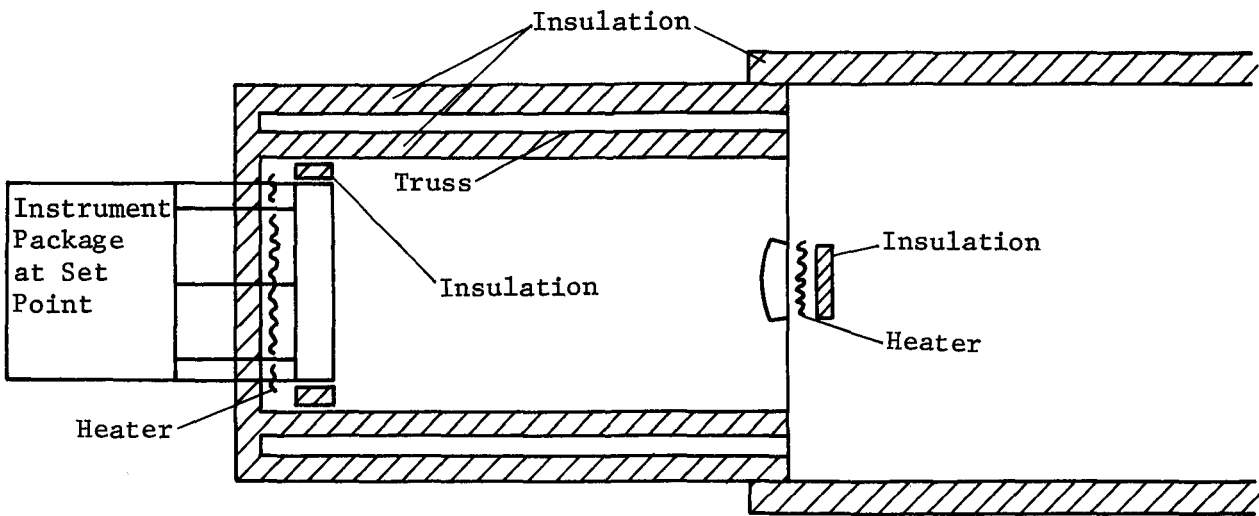
Conceptual Design Description - A tradeoff was performed (Ref III-8) between two thermal control concepts for amaintaining the optics system of the LST near room temperature and within the allowable gradient limits:

- 1) Tube heating - maximum power, minimum gradients [Fig. III-23 (a)].
- 2) Mirror heating - minimum power, maximum gradients [Fig. III-23 (b)].

The results of this conceptual analysis indicated that mirror heating would not only minimize thermal control power but it would meet the design requirements. Consequently this concept was selected as the preferred approach for the Stratoscope III, which has less stringent requirements than the LST. The parts of the telescope system that are passively controlled, and the techniques employed are described in the following paragraphs.



(a) Tube Heating



(b) Mirror Heating

Fig. III-23 Thermal Control Concepts

Sunshield - The main purpose of the sunshield is to provide stray light protection. However, it also acts as a thermal attenuator. That is, it dampens transient temperature effects by moving the aperture farther from the interior of the telescope and reduces heat losses to deep space from the interior. The sunshield temperatures will run comparatively cold and it is, therefore, thermally isolated from the telescope proper at its attachment points.

Secondary Back Housing and Secondary Mounting Spiders - The housing that encloses the secondary mirror and alignment assembly is directly exposed to the telescope aperture and will require insulation. The same is true of the secondary spiders. The spiders must be carefully insulated so that optical obscuration will not be increased. Exterior surfaces will be optically black for stray light considerations.

Secondary Light Baffle - The light baffle attaches in the peripheral area of the secondary mirror. Since the secondary mirror is controlled to approximately 70°F and the baffle will run considerably colder, care must be exercised in thermally isolating the baffle and secondary structure at the attachment points. A low thermal conductor such as fiberglass is recommended for the baffle material.

Main Truss, Meteoroid Shield, and Internal Light Baffle - The main ring beam (primary mirror mount) is actively controlled, while temperature control for the remainder of the truss is passive. The overall temperature level is allowed to stabilize at a relatively cold level. The design approach is to isolate the truss from temperature transients. Multilayer insulation blankets (effective emittance of 0.01) are installed on the meteoroid shield and the outside of the internal light baffle. The truss is thermally protected between the two blankets. In addition, the surfaces would be designed to have a low emissivity of 0.05. Therefore, a thermally isolated truss is recommended for baseline design consideration.

The exterior of the meteoroid shield will employ a low α/ϵ thermal coating to provide low sensitivity to the orbital thermal environment fluctuations. The drawback to this type of surface is that its temperature level is relatively low and it requires more thermal power for the system than for a surface having a higher α/ϵ ratio. As temperature requirements become better defined, higher α/ϵ surfaces will be considered. Presently a surface finish having a α/ϵ ratio of 0.2/0.9 is recommended.

Thermal Design Approach, Instrument Truss - The instrument truss is to be thermally isolated from the external thermal environment to provide dimensional stability for the instrument complement. It is intended to maintain this temperature passively. The truss members are to be insulated by low emittance coatings and possibly with multilayer insulation blankets. The supporting electronics that are mounted in the instrument compartment and "view" the instrument truss are to be insulated from the truss by insulating blankets.

Instrument Thermal Control Concept - The detectors of the cameras and some of the spectrographs have to be maintained at 9°F as noted previously. The baseline approach to maintain this temperature level is to use thermo-electric (Peltier) coolers. The detectors are small and are located at the end of the camera tube, and Peltier heat pumps show good application for meeting this temperature requirement. The heat losses off the detector can be minimized to approximately 1 W, which is in the range of Peltier heat pumps.

Design Analysis - The analysis involves simplified calculations to establish maximum orbital average power requirements for the mirror heating system. The pertinent orbital and boundary condition parameters chosen for this task and detailed below consider the telescope axis parallel to the solar vector to produce minimum solar loading and maximum power requirements.

Orbital Conditions	
Orbit altitude	250 n mi
Beta Angle	90 deg
Orientation	Solar Oriented
Environmental Conditions	
Surface coating properties, α/ϵ	
Orbiter	0.9/0.9
Pallet Payload	0.2/0.9
Orbiter Radiator	0.1/0.9
Net Environmental Heat Load (BTU/hr-ft ²)	13.5
\mathcal{A} to space	0.55
Equivalent Space Sink Temperature	-114°F

In Fig. III-24 the equivalent networks for radiation in the telescope tube enclosure are shown. Conduction losses along the telescope and sunshield tube axis are neglected. Thus the heat balance at the telescope tube interior surface give the wall temperature, T_2 , from

$$BA_1 \mathcal{F}_{1-2} (530^4 - T_2^4) + BA_2 \mathcal{F}_{2-5} (346^4 - T_2^4) + BA_4 \mathcal{F}_{4-2} (T_4^4 - T_2^4) - BA_2 \mathcal{F}_{2-6} T_2^4 = 0$$

which on substituting for the \mathcal{F} and area, A, values reduces to

$$90.1 - 12.84 BT_2^4 + 10.5 BT_4^4 = 0 \quad \text{[III-5]}$$

The heat balance at the sun shield interior surface gives the wall temperature, T_4 , from

$$BA_1 \mathcal{F}_{1-4} (530^4 - T_4^4) + BA_4 \mathcal{F}_{4-5} (346^4 - T_4^4) + BA_4 \mathcal{F}_{4-2} (T_2^4 - T_4^4) - BA_4 \mathcal{F}_{4-6} T_4^4 = 0$$

which on substituting for the \mathcal{F} and area values reduces to

$$1539 - 83.2 BT_4^4 + 10.5 BT_2^4 = 0 \quad \text{[III-6]}$$

Solving Eq [III-5] and [III-6] yields

$$BT_2^4 = 24.7$$

and hence $T_2 = -113^\circ\text{F}$

and, $BT_4^4 = 21.6$

and hence $T_4 = -125^\circ\text{F}$

The primary mirror radiant heat dissipation at the set point temperature of 70°F can now be evaluated from

$$Q_{\text{mirror}} = BA_1 \mathcal{F}_{1-2} (530^4 - T_2^4) + BA_1 \mathcal{F}_{1-4} (530^4 - T_4^4) + BA_1 \mathcal{F}_{1-6} 530^4$$

which yields,

$$Q_{\text{mirror}} = 106 \text{ Btu hr} = 31 \text{ W}$$

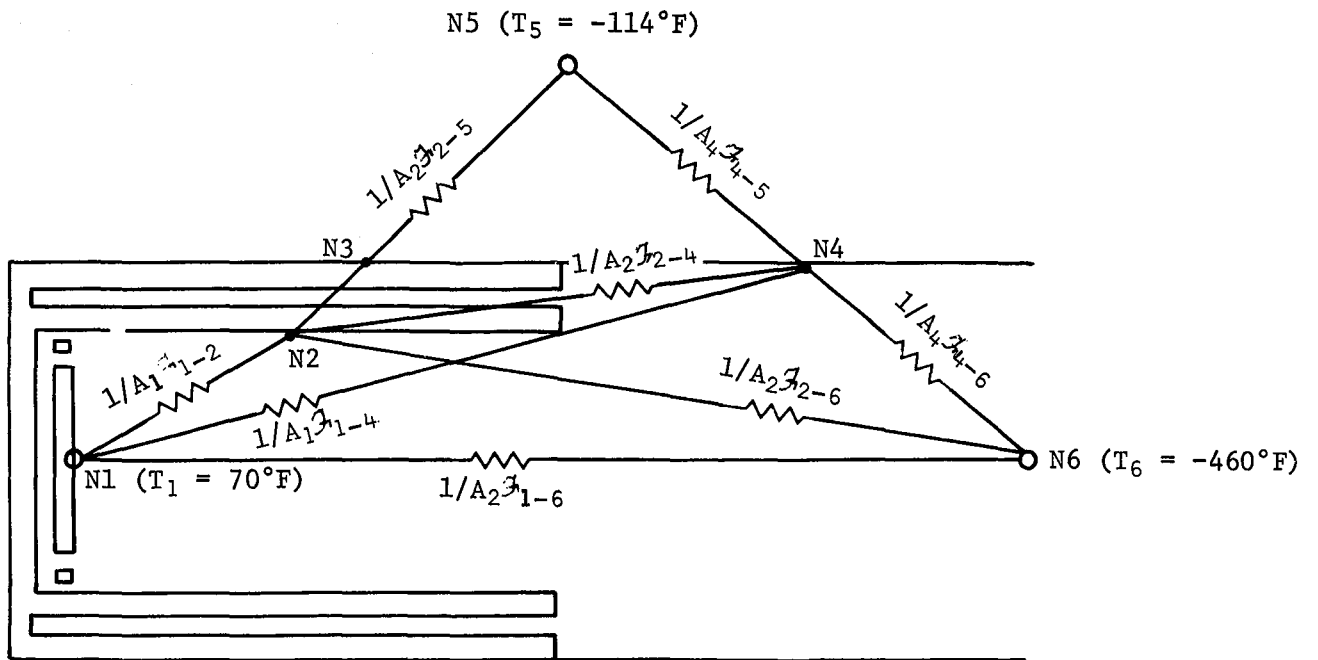


Fig. III-24 Stratoscope III Equivalent Network for Radiation

A comparison can be made with the free-flying LST analysis (Ref III-8) based on a 182-node thermal math model, which gave a LST primary mirror heat power requirement of 180 W.

Since the two telescopes are approximately in proportion, then for the primary mirrors,

$$Q_{1.2 \text{ m}} = \left(\frac{1.2 \text{ m dia}}{3.0 \text{ m dia}} \right)^2 \times Q_{3.0 \text{ m}}$$
$$= \left(\frac{1.2}{3.0} \right)^2 \times 180 = 29 \text{ W}$$

which is in close agreement with the calculated value of 31 W.

Furthermore, since the LST analysis indicates that approximately 50% of the total telescope heater power is required by the primary mirror, then for the Stratoscope III, the telescope heater capacity is

$$Q_{\text{total}} = 2 \times 31 \text{ W} + 25\% \text{ Safety Factor}$$

Hence, the telescope thermal control power consumption, including heaters for the primary mirror, primary mount, and secondary mount, is approximately 78 watts.

b. Solar Telescopes - These telescopes (100-cm photoheliograph, 25-cm XUV spectroheliograph, 32-cm X-ray telescope, and 2.45 and 4.0-cm coronagraphs) are discussed collectively because the design problems are similar. Any differences in the baseline configurations of the telescopes that result in differences in the thermal control approach are identified. The principal considerations, however, are those of removing the solar heat load that enters the telescope aperture, and minimizing the temperature gradients.

Requirements - Table III-7 lists the soak temperatures required for each of the four solar telescopes. These are nominally room temperature levels. Allowable thermal deformations are now unknown, but it appears the tightest thermal specifications will be in the allowable transverse gradients in the structure. To a first approximation the allowable gradient across the telescope tubes is $\leq 3^\circ\text{F}$, which is quite a tight tolerance for a structure that will be exposed to a space environment. In the case of the spectroheliograph, however, the gradient is a problem only if it changes during an exposure. Such rapid temperature changes are not likely to occur.

Table III-7 Solar Telescope Allowable Temperature Limits

Telescope	Operational Temperature Range, °F
100-cm Photoheliograph	64 to 75
25-cm XUV Spectroheliograph	63 to 70
2.45- and 4.0-cm Coronagraphs	64 to 75
32-cm X-Ray	63 to 70

Assumptions - The following assumptions were made:

- 1) The telescope configurations used in this study are as shown in Fig IV-19 for the X-ray telescope, Fig. IV-20 for the coronagraphs, Fig IV-21 for the Spectroheliograph (SHG), and Fig IV-23 for the photoheliograph (PHG);
- 2) All mirror solar absorptances are 0.14;
- 3) One percent of the solar energy is transmitted through the heat shield mirror aperture of the PHG;
- 4) Overall effective emittance of insulation blanket is 0.01;
- 5) The instrument compartment interface is adiabatic.

Conceptual Design Description - Thermal design concepts for the baseline configurations of the four solar telescopes are discussed in the following paragraphs. For purposes of clarity the telescope systems have been categorized into optical, structural, and instrument assemblies.

Optical Assemblies - To develop conceptual designs for optical component thermal control, it is necessary to consider the magnitude of the solar heat loads. Table III-8 presents the results of these calculations. The spectroheliograph and X-ray telescope have a negligible solar heat load entering the telescope since the apertures are covered by metallic films. Hence the thermal environment for the optical components in these instruments is not very severe. Simple conduction and radiation thermal control techniques are expected to be sufficient to accommodate the thermal requirements of their optical components.

The principal consideration for the photoheliograph is one of removing the 1100 W of solar power that enters the 100-cm aperture. This is significantly reduced by a heat shield mirror that folds most of the solar image out of the side of the telescope as shown in Fig. III-25. Preliminary calculations show that the absorbed solar energy in the primary and secondary mirrors cannot be dissipated by direct radiation to space only. A heat pipe system is recommended to transport the energy absorbed by the primary and secondary mirror assemblies to radiators that emit to space. The heat rejection aperture and the two thermal radiators are situated to be unaffected by either the Orbiter or other experiments. Doors are provided at the telescope and heat rejection aperture. These would be closed to conserve heat should observation of the sun cease for several orbits at a time. (They would also be closed to protect against contamination).

The two coronagraph lens assemblies and optical assemblies are small and shielded from the incident solar energy so that no significant problems are presented. The shielding results from the presence of an occulting disc assembly that blocks any solar energy from entering the lens system, as shown in Figure III-26. In addition, a heat rejection mirror mounted around the periphery of the primary objective lens reflects the unwanted solar energy streaming past the occulting disc assembly back into space, protecting the instrument from undue heating. The major thermal problem, then, associated with the coronagraph optics is the dissipation of the solar heat load absorbed by this heat shield mirror. Preliminary calculations show that in the two coronagraphs these mirrors would attain temperatures between 500 and 600°F if cooled only by radiation to deep space through the front aperture. Direct radiation to space from the rear of the mirror is precluded by the presently configured baseline design. As an alternative a heat pipe system is recommended to transport the absorbed solar energy to a radiator that emits to space. The heat rejection mirror is not an image forming optical component and precise thermal control is not required. However, the mirror should be thermally isolated from the primary objective lens that it surrounds.

Structural Assemblies - The major thermal problem associated with the structure is to minimize temperature gradients so that alignment can be maintained between the optical components. The design approach is to isolate the structure from the external environment fluctuations. This is accomplished by multilayer insulation blankets that envelope the internal structure. Low conductance mounts support the meteoroid shield that employs thermal control coatings to provide low sensitivity to the orbital environment fluctuations.

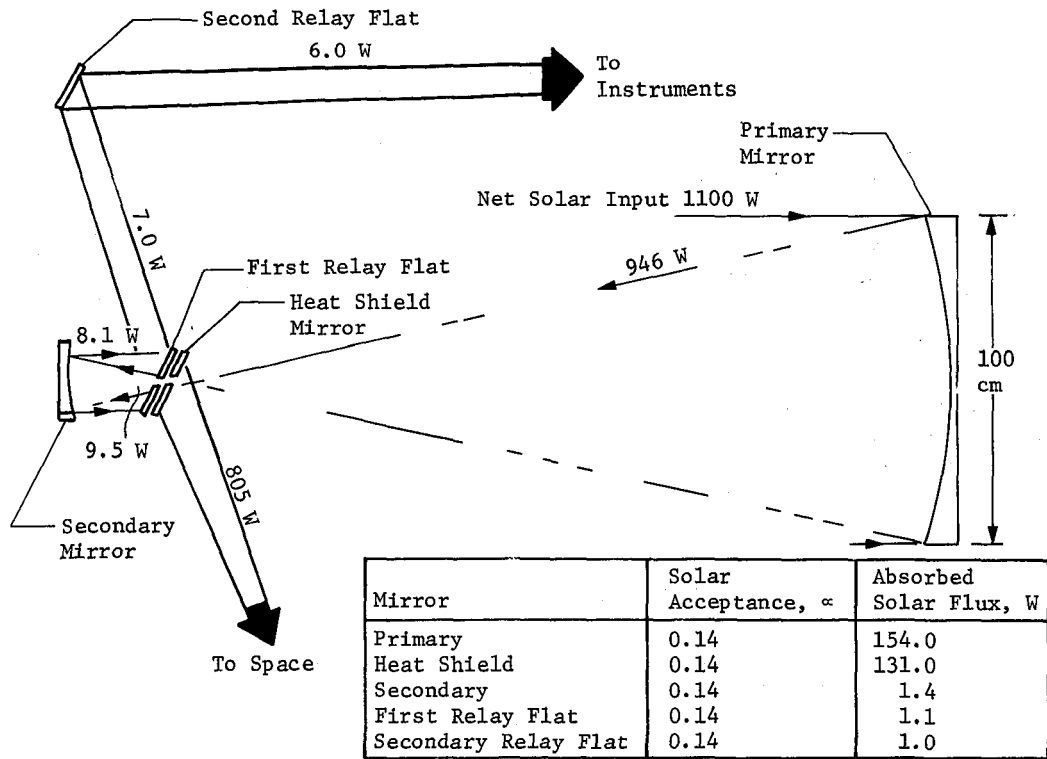


Fig. III-25 100-cm Photoheliograph Heat Flow

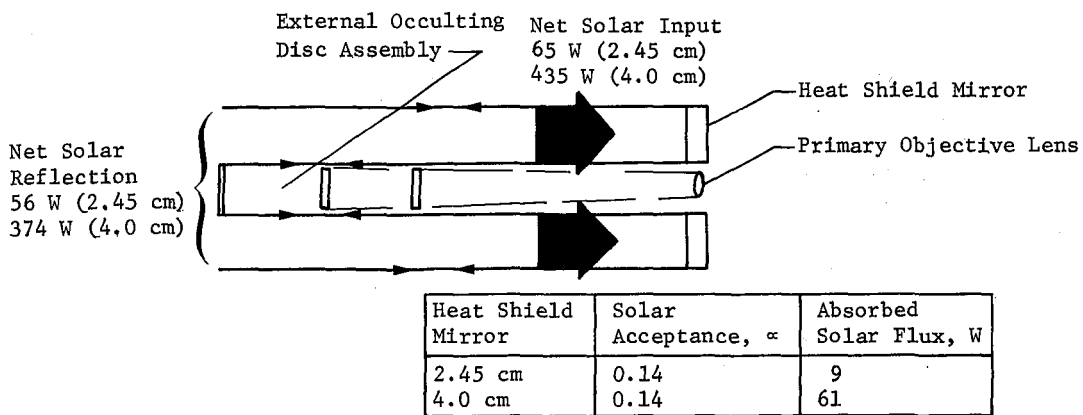


Fig. III-26 2.45- and 4.0-cm Coronagraph Heat Flow

It will be necessary to supply some heat to the interior structure to make up heat losses through the cylindrical walls (zero direct solar incidence) and through open apertures to maintain the "room temperature" levels. For simplicity it is recommended that this heat be introduced with zoned and thermostatically controlled electrical heaters to minimize gradients. Alternatively the thermal design of the meteoroid shield could use circumferential heat pipes to control gradients by providing an external telescope boundary temperature that is relatively uniform.

The heater power required for each telescope is presented in Table III-8. The indications are that for the photoheliograph a heat pipe system that redistributes the unwanted solar energy from the optics to the structure would be an attractive alternative approach in a power-limited mission.

Instrument Assemblies - The support instruments do not present a major thermal control problem because of the low electrical power output. The instruments can be cold biased and use instrument power dissipation to maintain thermal control during operational conditions. Heaters, louvers, or thermal switches can be used to provide thermal control for nonoperational conditions.

Design Analysis - The analysis involves simplified calculations to establish mirror heat rejection requirements and orbital average power requirements for the interior structure heaters. The pertinent orbital and boundary condition parameters chosen for this task are as described for Stratoscope III in Section A.3 a of this chapter. The solar flux level entering the apertures of the telescopes used in this analysis was 444 Btu/hr-ft² (0.14 W/cm²).

Mirror Heat Rejection - The solar flux entering the apertures of the telescopes can be divided into three categories: (1) the flux reflected back into space; (2) the flux absorbed by the telescope components; and (3) the flux reradiated back into space. The remaining portion of the absorbed flux that is not radiated back to space is retained within the telescope to elevate its temperature to the steady-state condition. This is estimated from the relationship

$$Q_{\text{solar}} = \mathcal{F}_{\text{space}} BT^4$$

$$\text{Thus } T = \left(\frac{0.14 \times 444}{B \mathcal{F}_{\text{space}}} \right)^{\frac{1}{4}}$$

$$\text{where } \mathcal{F}_{\text{space}} = 1 / \left(1/\epsilon - 1 + 1/\bar{F}_{\text{space}} \right)$$

Table III-8 Solar Telescope Heat Balance Summary

Telescope	Mirror Heat Balance				Equilibrium Temperature, °F	Cooling Load at 75°F	Internal Structure Heater Power, W
	Mirror	Absorbed Solar Flux, W					
100-cm Photoheliograph	Primary	154			552	142	184
2.45-cm Coronagraphs	Heat Shield	9			566	8	6
		61			520	56	27
32-cm X-Ray	Grazing	~ 1			70	N/A	28
25-cm Spectroheliograph	N/A	N/A			N/A	N/A	65

and, \bar{F}_{space} is the view factor to space of the mirror (emittance, $\epsilon = 0.004$) enclosed by black reradiating walls. Temperatures determined for the photoheliograph and the coronagraph, the only telescopes with a significant solar flux entering the aperture, are shown in Table III-8. These temperatures are excessive and the unwanted absorbed solar energy must be rejected by other means. The remaining absorbed solar flux not reradiated to space at the mirror allowable set point temperature establishes the heat load to be rejected by the thermal control system. These values are shown in Table III-8.

Structure Heater Power - The heat loss from the structure to the environment is derived from heat transferred through the cylindrical walls to the equivalent space sink temperature (-114°F). In addition the heat radiated from the structure to deep space through the telescope aperture is considered for the photoheliograph and coronagraph. To minimize this loss the exposed structure interior is wrapped with multilayer insulation blankets. The heater power is estimated from the relationship

$$Q_{\text{heater}} = A \epsilon_{\text{MLI}} B \left(T_{\text{struct}}^4 - T_{\text{sink}}^4 \right) + A \mathcal{F}_{\text{space}} B T_{\text{struct}}^4$$

where $\mathcal{F}_{\text{space}} = 0$ for the SHG and XRT,

and for the PHG and CG,

$$\mathcal{F}_{\text{space}} = 1 / \left(1 / \epsilon_{\text{MLI}} - 1 + 1 / \bar{F}_{\text{space}} \right)$$

where \bar{F}_{space} is the view factor to space of tube interior with black reradiating walls.

The thermal control average heater power consumption for the four solar telescopes is shown in Table III-8 and includes a 25% safety factor.

B. STRUCTURAL ANALYSIS

Design and analysis of the structures and mechanisms to support the various experiments included in the ASM baseline payload combinations were carried to the level necessary to establish the feasibility of the concepts, and to provide a realistic design approach to be used as a basis for future design activities. Mass properties data were then developed based on these concepts and the actual mass characteristics of similar, existing hardware. Detailed design information on the structure of the Sortie Lab and pallet was not available at this time, thus certain assumptions were required in the design of structural interfaces. However, the pallet structure assumed for purposes of interface design imposes no unusual requirements on this structure.

The cooled IR telescope design, reflecting the thermal control approach developed in Section A of this chapter, was also carried to the level where feasibility of the basic design approach was established, and mass properties were generated.

1. Structural Design Criteria

The structural design criteria established for analysis of the Orbiter payload retention and erection hardware and for the IR telescope, were extracted from in-house activities in response to the Space Shuttle RFP. The loads cases considered are as follows:

- 1) Steady state liftoff with slow release - no wind;
- 2) Steady state liftoff with slow release - wind on Orbiter;
- 3) Steady state liftoff with slow release - side wind;
- 4) $(1-\cos)$ gust shape load;
- 5) Thrust termination loads - step cutoff;
- 6) Thrust termination loads - 0.10-sec ramp tailoff;
- 7) Thrust termination loads - 0.20-sec ramp tailoff.

The above cases resulted in load reactions at the forward and rear attachment points between the Orbiter and liquid propellants drop tank. It was determined that the most severe loads were a function of Case 5, which is considered to be an unrealistic condition for

thrust termination. Therefore, load cases 2 and 6 result in the most severe, realistic loads at the Orbiter/tank interface. These loads with appropriate coordinate definition are presented in Table III-9. These interface loads were used in conjunction with the Orbiter weight to determine acceleration load factors, which are also presented in Table III-9. Figure III-27 is a diagram illustrating the local coordinate system used for identification of the applicable loads and load factors. These load factors are transferred directly to the Orbiter center of gravity, in a rigid body sense, for application to the payload hardware structural analysis.

Table III-9 Orbiter Loads

Load Coordinate	Fy, kips	Fz, kips	Ax, kips	Ay, kips	Az, kips	Maximum Load Factors		
						Nx	Ny	Nz
+	149	196	14	151	184	--	--	--
-	117	532	1377	192	269	1.53	0.90	3.96
Orbiter Weight	347.5 kips							

All load factors extracted from the Space Shuttle analyses include factors of 1.2 to 1.4 applied to power, normal aerodynamic data, drag, and weight to account for uncertainties in estimating these parameters. These Shuttle loads are used to determine the limit load factors used in structural analyses of Orbiter payloads with an additional factor of 1.5 applied to determine design loads (i.e., 1.5 x limit load = design load).

Three basic materials are proposed for use in construction of payload items and supporting structure. These are 22.9 aluminum, invar, and 4130 steel. Aluminum is used in primary and secondary structural support elements where stiffness and light weight are more important than strength. Invar is used where minimum thermal growth is desired, as in the IR telescope structure. This is necessary to ensure a minimum distortion of critical optical parameters associated with telescope mission requirements. The launch locks will be made of 4130 steel.

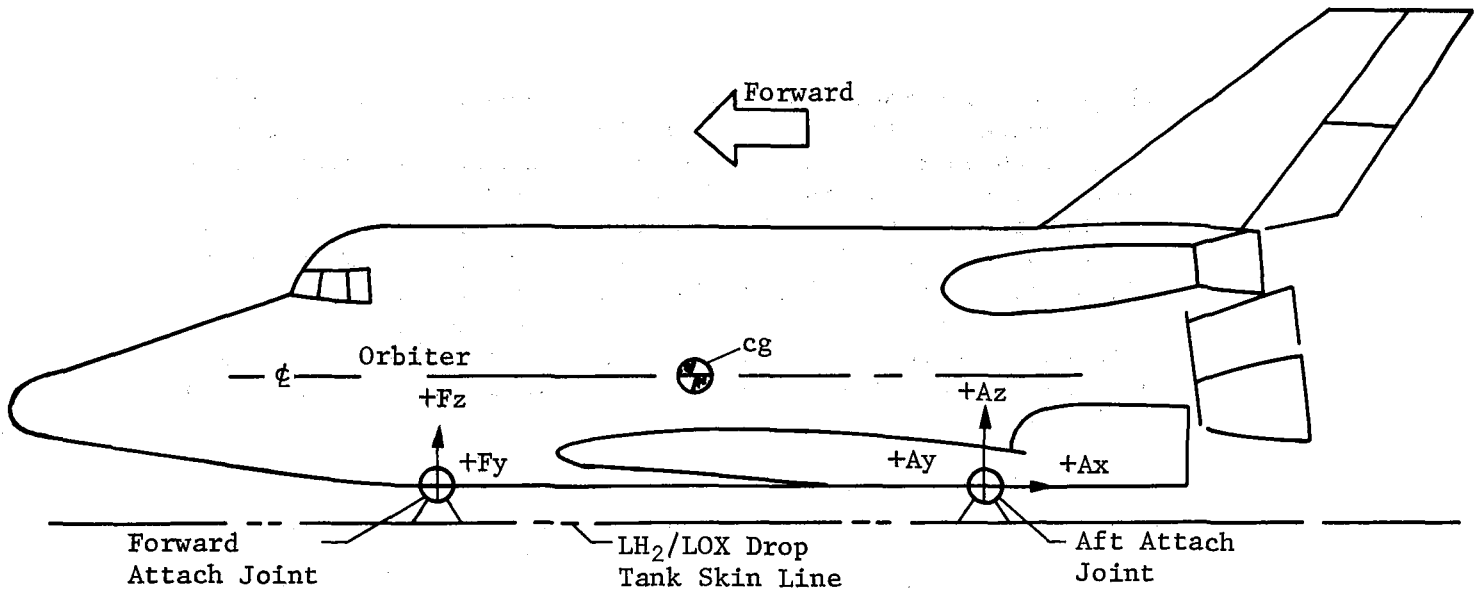


Fig. III-27 Coordinate System

The material strength properties used in all structural analyses are shown in Table III-10.

Table III-10 Material Properties

Material	F_t (ultimate), psi	F_t (yield), psi	F (crippling), psi
2219 Aluminum	57,000	40,000	29,000
Invar Steel	104,000	98,500	--
4130 Steel	95,000	75,000	--

The design criterion to be used for onboard pressure vessels within the Orbiter vehicle is to design all vessels for a factor of 2.0 applied to actual storage vessel pressures. The storage vessel pressure is taken as a limit value, and when multiplied by 2.0, it becomes the ultimate pressure value for design of the vessel structure.

2. IR Telescope Structural Analysis

The primary influences on the design of the telescope are the requirements to maintain an operating temperature of approximately 28°K on the entire telescope and to provide a stable structure for the telescope optics. To conserve cryogenic fluids, a high degree

of thermal isolation of the telescope from the pointing and stabilization hardware is necessary. This complicates the telescope support structure and adds considerable weight because long heat paths with small cross sectional areas are required to achieve the desired thermal isolation. The thermal design of the telescope is discussed in Section A of this chapter. The concept shown in Fig. III-28 represents a promising approach to the design of a cooled IR telescope and should prove feasible with additional development effort.

a. *IR Telescope Configuration*

Major Issues - Two major issues were resolved before layout of the telescope structure could proceed. These were: (1) prelaunch vs on-orbit chilldown; and (2) active cryogenic system vs integral cryogenic tank approach.

Prelaunch chilldown makes the cold optical elements of the telescope more susceptible to contamination than when the cooling is accomplished in the relatively contamination-free environment of space. However, some form of protection is required, even if on-orbit chilldown is performed. The major deterrent to on-orbit chilldown is the weight penalty involved in carrying a large volume of cryogenic fluid to orbit.

The decision to baseline prelaunch chilldown resulted from the following calculation for the weight of liquid neon required to precool a telescope to the desired operating temperature of 28°K (50.4°R).

Where:

$$W_{Ne} = \frac{C_p \Delta T}{L} W_{dt}$$

$$= \frac{.123 \times 267}{20.3}$$

$$W_{Ne} = 1.615 W_{dt}$$

W_{Ne} = weight of liquid neon, kg,

W_{dt} = Dry weight of telescope, kg,

C_p = mean specific heat of telescope, (cal/gm-°C)

ΔT = temperature change, °C

L = latent heat of liquid neon, (cal/gm).

or 1.615 kg (3.55 lb) of Ne per 1.0 kg (2.2 lb) of telescope.

Final dry weight of the concept shown in Fig. III-28 is approximately 1565 kg (3450 lb) which requires more than 2500 kg (5500 lb) of liquid Ne for chilldown, making on-orbit chilldown impractical.

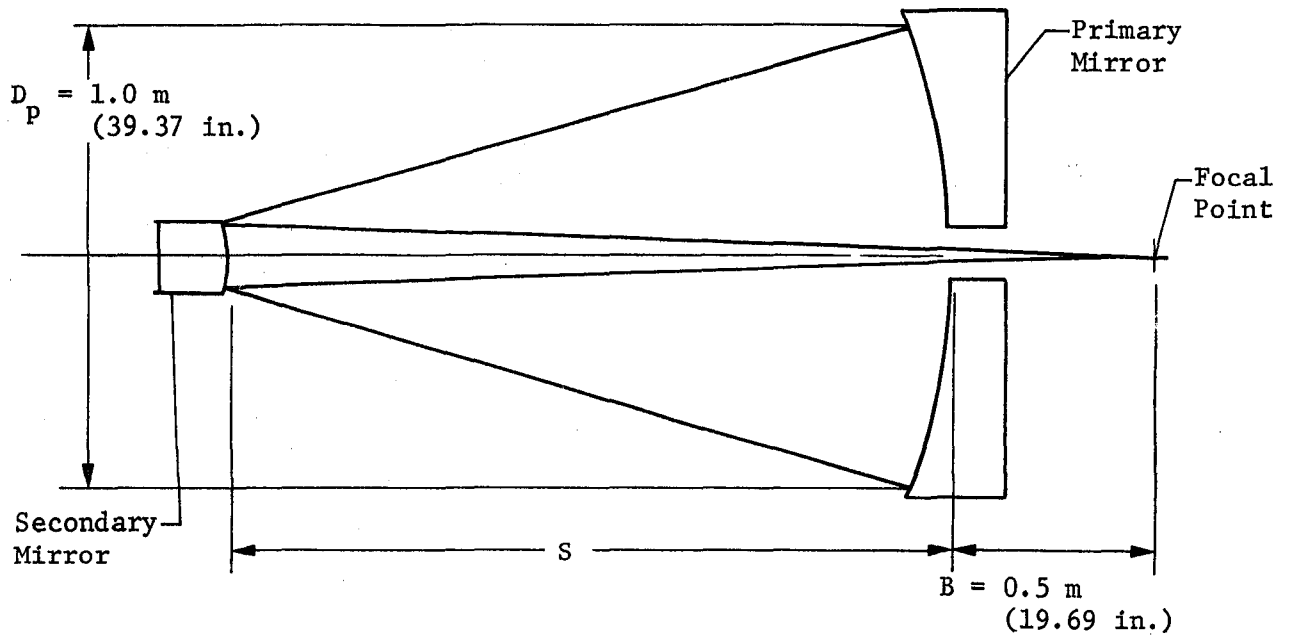
The problem of contamination of the telescope optics due to pre-launch chilldown appears to be easier to solve than the problems and penalties associated with on-orbit chilldown.

When evaluating the active cryogenic system, two system locations were considered. A pallet-mounted system isolates the telescope from vibration sources such as pumps and valves. However, the problem associated with routing of cryogenic transfer lines between elements that move with respect to each other, the effects of the disturbing torques on the telescope pointing and stabilization system, and additional heat loads due to long transfer lines favor the telescope-mounted system.

When comparing the telescope-mounted active system to an integral cryogenic tank approach, the integral approach is more promising for the following reasons:

- 1) Requires no active distribution system because capillary forces can be used for circulation to wet the telescope walls;
- 2) Simplifies construction because complex manifolded distribution system is eliminated;
- 3) Minimizes disturbance of the telescope stabilization system by eliminating rotating machinery and complex fluid flow control components;
- 4) Better thermal design because the telescope inner wall is also the wall of the cryogenic storage tank. This eliminates thermal losses and possible distortion-producing thermal gradients that could be a problem inherent in a distribution system using tubes.

Optical Arrangement - The spacing of the major optical elements of the telescope was determined by the following method:



$$\begin{aligned}
 S &= \frac{F_p (F \times D_p - B)}{F_p + F} \\
 &= \frac{1.5 (10 \times 1 - 0.5)}{1.5 + 10} \\
 &= \frac{1.5 (9.5)}{11.5} \quad 1.239 \text{ M (48.78 in.)}
 \end{aligned}$$

where: F = system ratio = 10,

F_p = primary ratio = 1.5,

$B \approx 0.5 \text{ m}$ (19.69 in.),

D_p = aperture = 1.0 m (39.37 in.).

Telescope Design - The concept pictured in Fig. III-28 reflects the decision to baseline an annular tank structure with prelaunch chilldown, and the optical arrangement calculations discussed above.

The design approach involves compartmenting of the telescope into two sections, the optical section and the instrument section, both jacketed by the cryogenic tank. The two instruments defined for use in the telescope may be alternately rotated into operating position by remotely controlled actuators. The secondary mirror and its supporting spider, the aperture doors, and the Cer-Vit primary mirror are cooled by conduction paths and radiation to the cold inner wall of the cryogenic tank. Light baffles are attached directly to the inner wall of the tank and are cooled by conduction.

To prevent contamination of the telescope optics starting at pre-launch chilldown until reaching orbit, an insulated cover is installed over the open end of the telescope. Helium purge gas is introduced into the interior of the telescope before chilldown and flow continues until liftoff. A small positive pressure is maintained by leakage past the cover seals. This cover is removed when orbit is reached and is not replaced while on orbit. To close the aperture while on-orbit, four butterfly doors are located forward of the secondary mirror. These doors are closed to minimize contamination during Shuttle dumps and when the telescope is not being operated. Metallic labyrinth seals exclude contamination under the free molecular motion conditions encountered in space. A housing on the secondary mirror mount encloses an actuator and mechanism for rotating the doors.

An insulated access door in the aft bulkhead of the telescope allows ground removal and replacement of the scientific instruments.

The adapter structure that mounts the telescope to the inner roll ring of the gimbal assembly is carefully designed to provide a maximum of thermal isolation of the cold telescope from the warm gimbal structure. Eight tubes, intersecting at four hard points on the secondary mirror support frame, tie to the adapter ring, also at four points. Eight pretensioned rods tie the telescope main frame to the same adapter ring. The combination of the adapter ring, eight tubes capable of taking tension or compression, the eight pretensioned rods, and the heavy telescope tank structure work together to provide a rigid structure. The adapter ring is supported on the inner roll ring of the gimbal assembly by four support lugs.

The total volume of the tank is approximately 0.75 m^3 (26.7 ft^3), while the required volume is less than half of this, based on the thermal analysis in Section A of this chapter. Preliminary investigations of the feasibility of manufacturing the tanks indicated that the minimum spacing between the tank walls was 5.08 cm

(2.0 in.). This spacing established the volume of the tanks. A beneficial result of having this large volume is that the tanks can be operated for longer periods of time between ventings and maximum design pressure may be reduced.

The very low coefficient of thermal expansion, coupled with good weldability and relative ease of fabrication, led to the selection of Invar for the basic structure of the telescope and adapter.

The body of the IR telescope consists of two welded tank sections bolted together just aft of the main mirror. This manufacturing splice is necessary to facilitate assembly and is designed to serve as the telescope main frame. This frame supports the primary mirror mounts, the instrument section forward bulkhead, and is the attachment structure for the eight pretensioned rods of the adapter structure. These tank sections are completely welded of Invar sheets and machined elements. The tanks are interconnected to form, in effect, a single tank. The tanks are designed to withstand pressurization levels that allow containing the Ne gas for several orbits before venting is required. This requires a thick inner tank wall to withstand collapsing pressures. The annular tank structures include four longerons running the full length of each tank section. These longerons are located in line with the four attachment points of the adapter tubes to the secondary mirror support frame, to transmit longitudinal loads to the adapter ring. Capillary screens are attached to the inner surfaces of the tank walls before closure welding the tanks, to facilitate the wetting of the walls by the liquid portion of the Ne liquid-gas mixture in the tanks.

The entire outer surface of the telescope body is covered with foam and multilayer insulation and the adapter tubes and rods are covered with multilayer insulation. An aluminum shell meteoroid cover shields the sides and aft end of the telescope assembly. This shield is covered with thermal control paint and is attached to the adapter ring to maximize thermal isolation from the cold telescope.

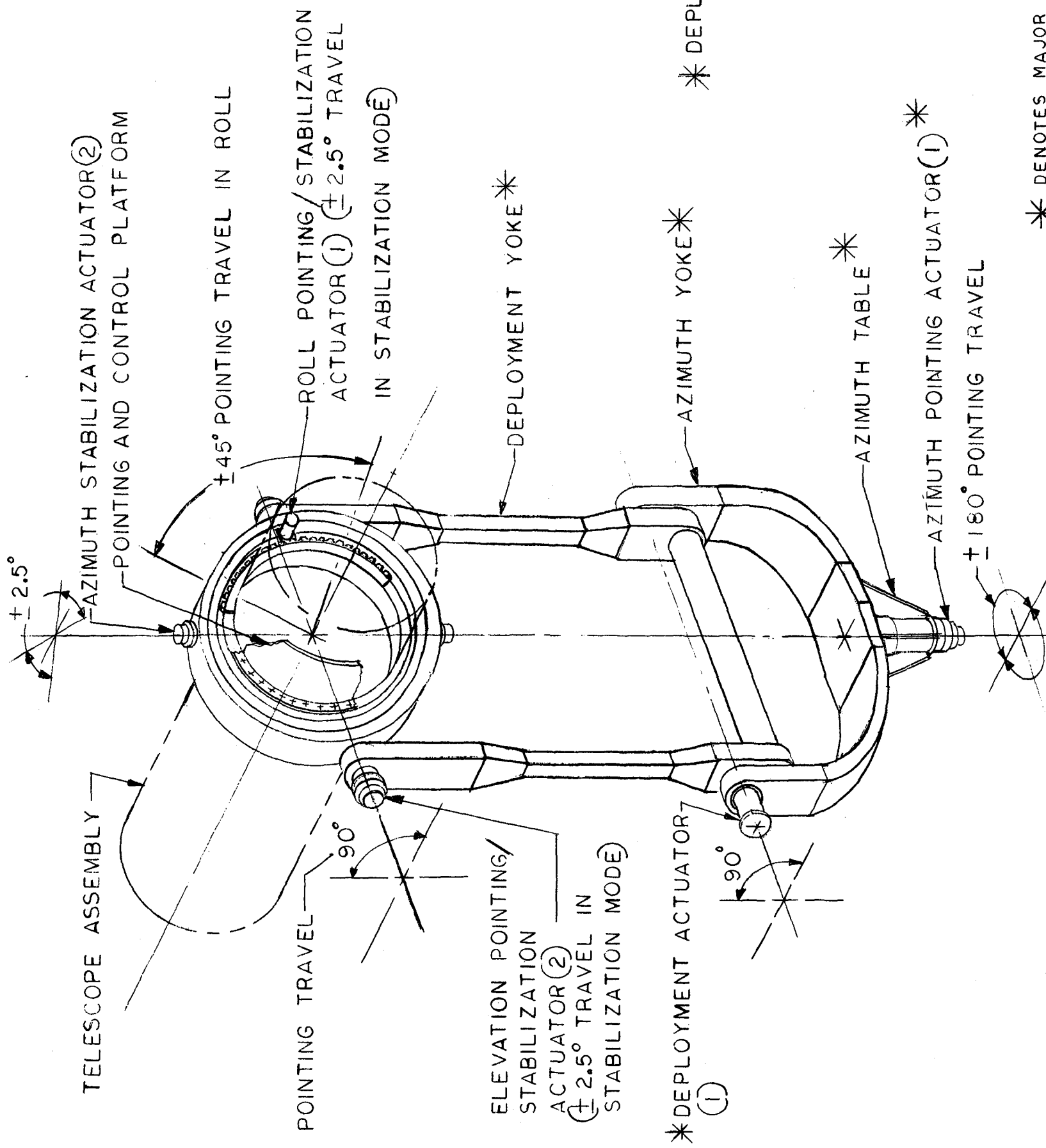
b. Stress Analysis - The IR telescope was analyzed as a circular cylinder with an annular liquid neon chamber between concentric cylinder walls. Basic diameter of the IR telescope cylinder is 1.219 m (48 in.) with 5.08 cm (2 in.) annular chamber, resulting in an outside cylinder diameter of 1.321 m (52 in.). The internal pressure of liquid neon chamber was taken to be a limit value of two atmospheres (30 psi) with a design factor of 2.0. The material proposed for the cylinder body and primary telescope structure

is invar steel. This is desirable because invar has the property of dimensional stability under variable temperatures. Analyzing the barrel section as an internal cylinder subjected to a compressive load and the outer cylinder to a tensile load, the minimum skin gages required are 6.35 mm (0.250) and 38 mm (0.015 in.) respectively. The telescope adapter structures, which is a truss and ring configuration, was analyzed for basic Shuttle vehicle load factors that resulted in the most severe conditions. The highest set of tri-axial load factors was found to result from launch-ground winds and thrust termination conditions. These loads were used to analyze the truss-strut structure that attaches the IR telescope to the adapter ring. The adapter ring in turn will transfer loads to the inner wall ring of the gimbal assembly. The telescope adapter structure is made of invar steel for dimensional growth compatibility with the telescope barrel. Volume III, Book 2, Appendix B2-1 contains the results of these analyses.

c. Mass Properties - Mass properties calculations for the IR telescope were based on the design shown in Fig. III-28, and the stress analyses and thermal analysis described in Section A of this chapter. Preliminary center of gravity calculations were conducted to locate the adapter ring. Weight was optimized by resizing the Ne tanks in conjunction with revised Ne volume requirements. Materials other than invar were not considered at this time because of the absence of suitable substitutes for this application. Table III-11 is a detailed weight estimate of the IR telescope.

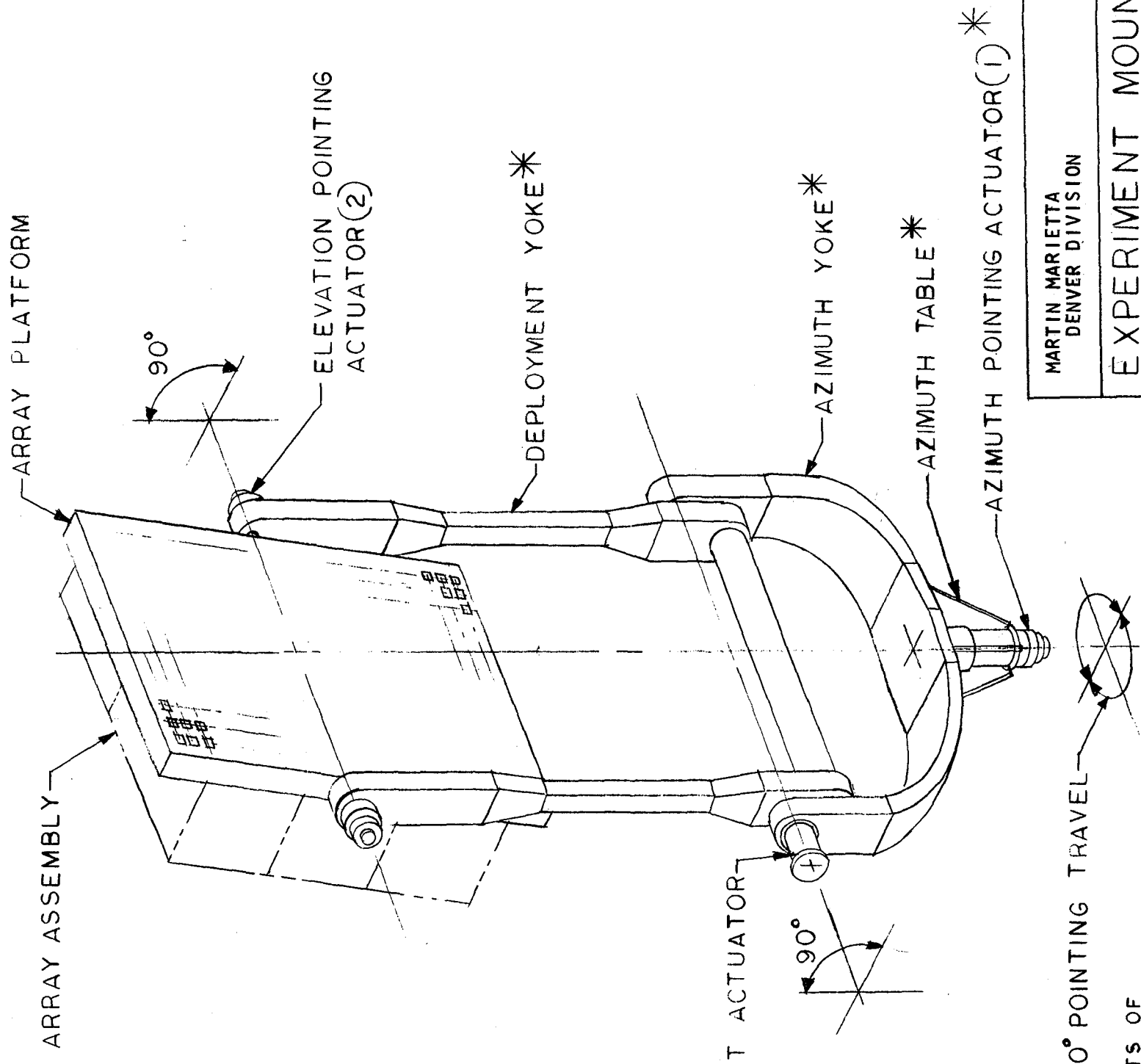
3. Experiment Mount Structural Analyses

The advantages of the deployed, wide-angle gimbal mounting concept, which provides hemispherical viewing capability for telescopes and arrays, led to its adoption earlier in this study. Application of the common-mount philosophy, also adopted earlier in this study, resulted in configurations that emphasize maximum commonality and simplicity of hardware. This is illustrated in the designs of the telescope and array mounts in deployed position, shown in simplified form in Fig. III-29. Both mounts use the common mount assembly consisting of the azimuth table, azimuth pointing actuator, azimuth yoke, deployment yoke, deployment actuator, and jettisoning equipment. The pallet-mounted deployment launch locks are also identical for the two mounts. Addition of the telescope gimbal assembly and the elevation pointing/stabilization actuators to the common mount, yields a complete telescope mount. To convert the telescope mount to the array mount configuration, the gimbal assembly and elevation pointing/stabilization actuators are removed and replaced with an array platform and the simpler, elevation pointing actuators.



TELESCOPE MOUNT ASSY

* DENOTES MAJOR ELEMENTS OF THE COMMON MOUNT, USED IN THE TELESCOPE MOUNT ASSY AND THE ARRAY MOUNT ASSY.



ARRAY MOUNT ASSY

MARTIN MARIETTA DENVER DIVISION
EXPERIMENT MOUNTS
FIG. NO. III-29

Table III-11 IR Telescope Weight, kg (lb)

Structure		919.4 (2027)
Aft Tank	11.8 (26)	
Aft Bulkhead	37.6 (83)	
Forward Bulkhead	45.4 (100)	
Inner Shell	480.8 (1060)	
Outer Shell	131.5 (290)	
Aft Ring Frame	8.6 (19)	
Splice Frame	19.5 (43)	
Secondary Mirror Support Frame	10.0 (22)	
Nose Frame	11.3 (25)	
Longerons	6.4 (14)	
Forward Attach Ring	36.3 (80)	
Adapter Ring	66.2 (146)	
Adapter Tie Rods	1.8 (4)	
Adapter Tubes	9.1 (20)	
Aperture Cover	12.3 (27)	
Baffles	3.6 (8)	
Secondary Mirror Housing	3.6 (8)	
Secondary Mirror Spider	5.4 (12)	
Aperture Doors and Mechanisms	18.2 (40)	
Meteoroid Protection		79.4 (175)
Thermal Portion		118.8 (262)
Fiberglass Insulation Supports	20.4 (45)	
Foam Insulation	41.2 (91)	
Multilayer Insulation	43.1 (95)	
Heat Exchanger Tubes	14.1 (31)	
Tank Capillary Screens		13.6 (30)
Primary Mirror		281.2 (620)
Primary Mirror Supports		20.4 (45)
Secondary Mirror		3.6 (8)
Secondary Mirror Mechanisms		4.5 (10)
Instruments		103.9 (229)
Interferometer	59.4 (131)	
Interferometer Control	2.3 (5)	
Detector	42.2 (93)	
Instrument Supports and Drives		22.8 (50)
Instrument Cooling		61.2 (135)
Liquid Neon		349.3 (770)
Liquid Helium (for Instrument Cooling)		10.0 (22)
Total		1988.1 (4383)

The support and deployment assemblies for the wide coverage X-ray detector array and the gamma-ray spectrometer array are necessarily designed for their specific purposes and commonality could not be achieved, beyond the use of identical assemblies for the two halves of the X-ray detector array.

a. Operation of Telescope and Array Mounts - The operation of these mounts can best be visualized by referring to Fig. III-29 and IV-2 in Chapter IV. More details of these mounts are pictured and described in the following sections of this report.

The telescope mount was designed to provide hemispherical viewing for the telescopes supported by it. This is accomplished in the following manner. After releasing the launch locks, the telescope is moved out of the pallet by using the deployment actuators to rotate the deployment yoke 90 deg with respect to the azimuth yoke. A brake located in the deployment actuator locks the yoke in this position. The telescope longitudinal axis is kept parallel to the floor of the pallet during deployment by driving the pointing section of the elevation pointing/stabilization actuator at the same rate as the deployment actuator. This feature was incorporated to preserve commonality of the telescope mount with the array mount, since it allows greater deployment clearances for the array mount and future growth of experiment lengths on both mounts. The telescope is then coarse-pointed in azimuth and elevation by using the azimuth pointing actuator to pivot the azimuth yoke and the pointing section of the elevation pointing/stabilization actuator to pivot the gimbal assembly into the desired position. These actuators are held in position by internal brakes while fine pointing is accomplished.

The entire gimbal assembly is supported on the deployment yoke arms by flex pivots incorporated into the output shafts of the elevation pointing/stabilization actuators. Elevation fine pointing and stabilization are accomplished by energizing the stabilization sections of the actuators that torque against the flex pivots, thereby positioning and holding the gimbal assembly at the precise elevation desired. The roll ring assembly is supported on the outer gimbal ring by flex pivots incorporated into the output shafts of the azimuth stabilization actuators. These actuators are energized to torque against the flex pivots to position and hold the roll ring assembly, and the telescope at the desired azimuth angle. One telescope, the photoheliograph, needs to be rotated 90 deg about its longitudinal axis during polarization measurements. Therefore, the inner roll ring is designed to accomplish the rotation by actuating the pointing section of the roll pointing/stabilization actuator. This actuator operates in the stabilization mode at all other times and for all other payloads.

The entire mount with telescope installed, may be operated in the upright attitude at one g, with the exception of the deployment actuators. To deploy the heaviest telescope package requires a maximum actuator torque of 725,000 in.-lb. This would require an extremely large rotary actuator and heavy deployment yoke, or discarding the simple system shown and adopting a heavier, more complex deployment mechanism. The decision was made to rely on ground equipment for deployment rather than to penalize the entire telescope mount. All elements of the mount are capable of supporting and moving the telescope after it is deployed.

The telescope mount requires mechanical locks called launch locks, to assure firm support of the telescopes during the high accelerations and vibration levels experienced during Shuttle Orbiter launch, staging, atmosphere reentry, aerodynamic flight, and landing. These locks are placed in locations where they reduce, to acceptable levels, the loads on the flex pivots of the gimbal assembly, the actuators, and the structures that comprise the mount. Two sets of locks are used. The deployment locks are mounted to the structure of the pallet. These locks restrain the arms of the deployment yoke just forward of the elevation pointing/stabilization actuators. They are designed to take loads acting in a plane normal to the longitudinal centerline of the orbiter. The gimbal locks are attached to the inner roll ring and engage lugs attached to the upper and lower surfaces of the deployment yoke arms, thereby preventing excessive loads on the gimbal assembly flex pivots and actuators. As described above, the deployment yoke arms are restrained in this area by the deployment locks. This results in high tension loads, but relatively small bending loads on the arms, allowing the deployment yoke to be relative light structure.

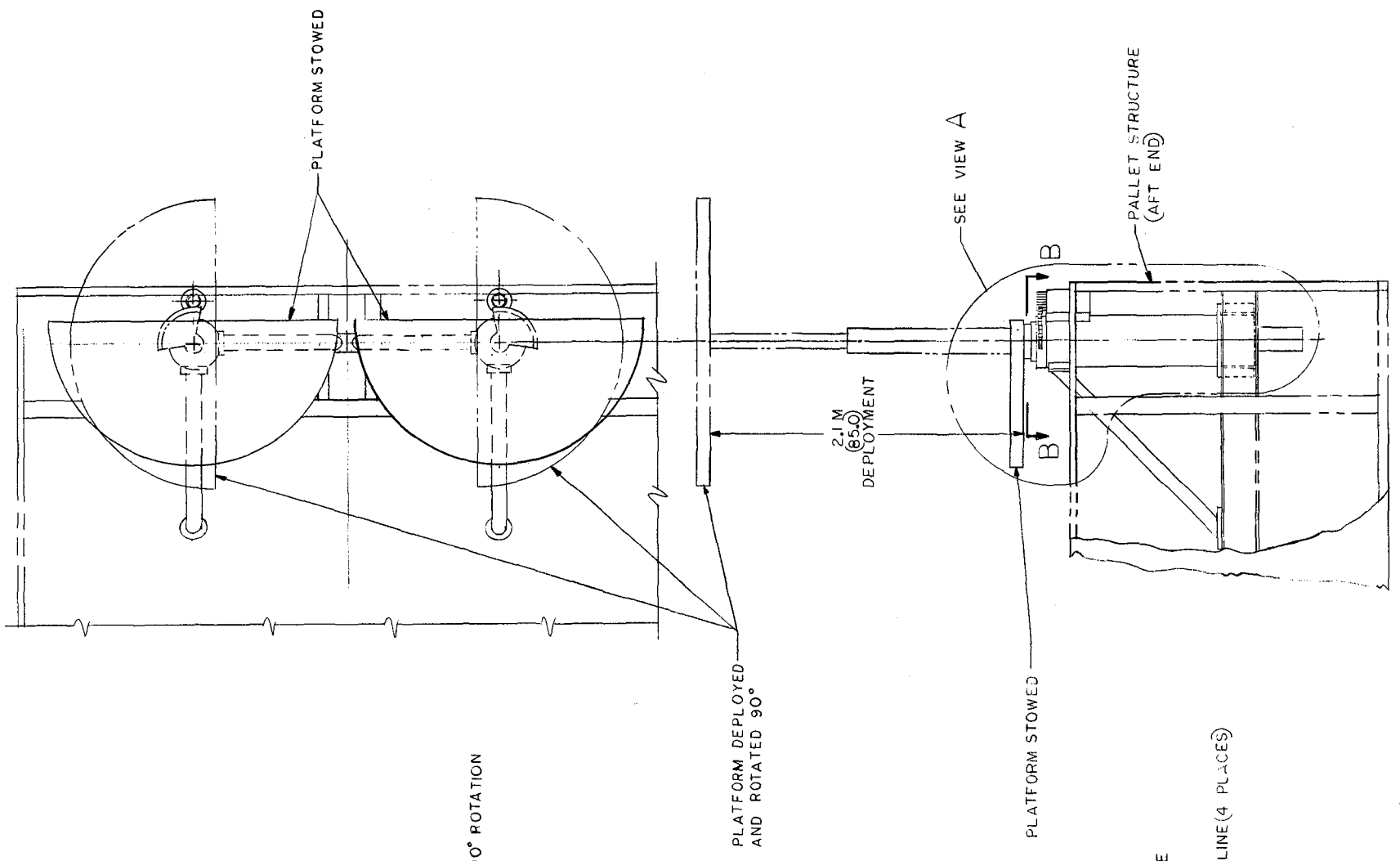
Operation of the array mount is identical to that of the telescope mount up to the point of fine pointing and stabilization. The arrays' pointing and stability requirements are generous enough to be accomplished without use of the gimbal assembly. A simple platform driven by elevation pointing actuators is substituted for the gimbal assembly. Substitution of the array platform for the gimbal assembly requires only the replacement of launch lock lugs on the deployment yoke arms and installation of the elevation pointing actuator in place of the more complex elevation pointing/stabilization actuator. The lugs are replaced because of the modified geometry of the platform launch locks compared to the gimbal locks.

b. *Operation of Specialized Array Mounts* - The wide coverage X-ray detector array mount is shown in Fig. III-30 and IV-2 (in Chapter IV). Two mounts are required because the array was divided into two packages due to the large size of the complete array. The mounts are rigidly attached to the aft area of the pallet, and the drives are locked during launch and reentry. After attaining orbit, the telescoping tubes are extended to deploy the array package for viewing. After extension, the packages are rotated 90 deg to provide hemispherical viewing for the complete array.

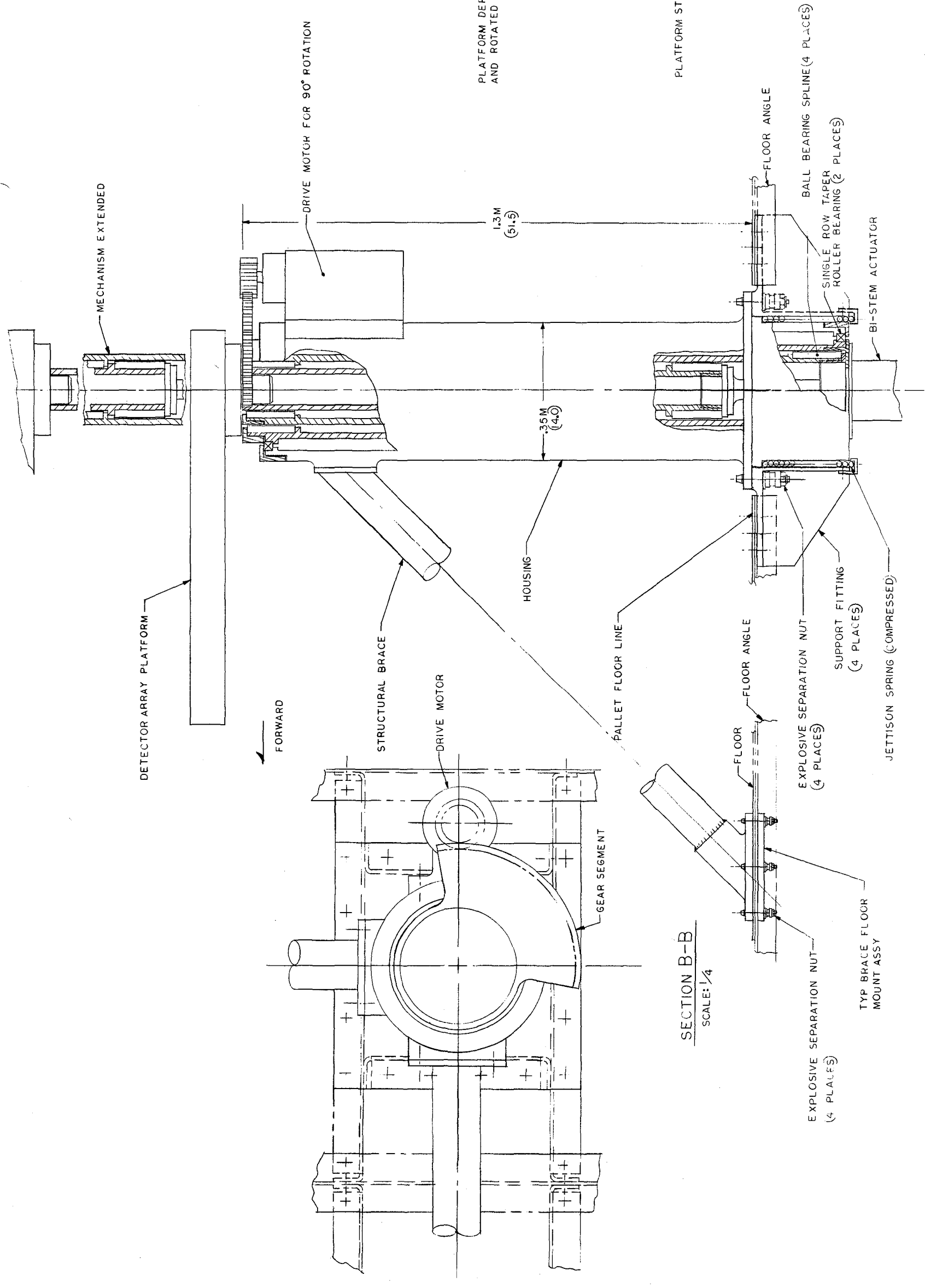
The gamma-ray spectrometer imposes unique requirements for housing and deployment. First, the array is mounted on the array platform with the low background gamma-ray detector, as shown in Fig. IV-4 (in Chapter IV). A tentative requirement is that the entire platform must slowly oscillate about the elevation axis. Second, the array must be protected from radiation during passages through the South Atlantic anomaly. Protection is provided by a paraffin-filled housing. Third, the array includes a cryogenic refrigerator. Referring to Fig. III-31, the approach to satisfying these requirements takes on the appearance of a jack-in-the-box. To operate, the paraffin-filled cover on the housing is opened and the array is extended out sufficiently far to operate.

c. *Structural Design Approach* - The primary requirements imposed on the structures of the mounts are to provide a rigid, stable, but lightweight platform to support the telescopes and arrays and enable them to be accurately pointed and stabilized. Aluminum was selected as the basic material to be used since most of the elements are designed for stiffness and are considerably overstrength. Minimum feasible manufacturing gages of machined sections dictated the design in many areas, rather than strength requirements. Extensive welding is used in the structures to reduce weight penalties associated with the use of fasteners. Actuator mounting surfaces and other areas requiring close control are machined after welding. Numerous ribs and webs are incorporated to stabilize the large thin sections involved in this type of structure. Steel is used in the launch locks where loads are very high.

d. *Common Mount* - The common mount is used as the basic building block for the telescope and array mounts. It consists of the azimuth table, azimuth pointing actuator, azimuth yoke, deployment yoke, and deployment actuators. Figure III-32 shows the common mount and its interfaces with the pallet. The telescope gimbal and array platform are shown for reference.

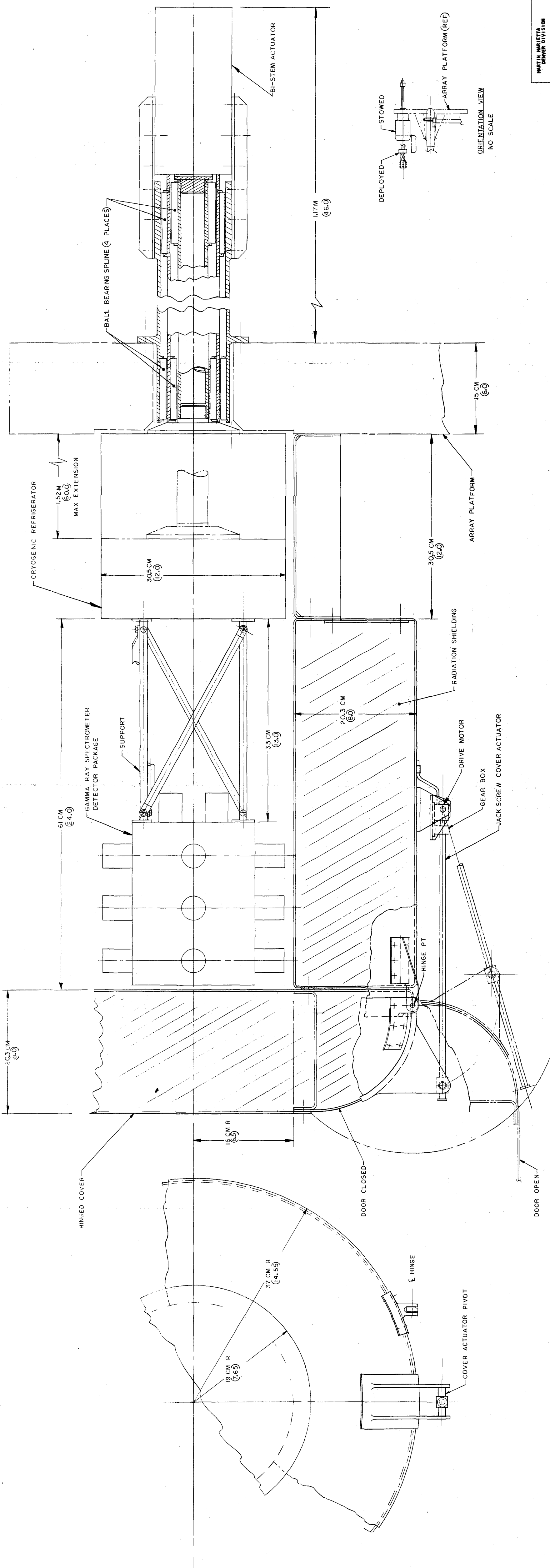


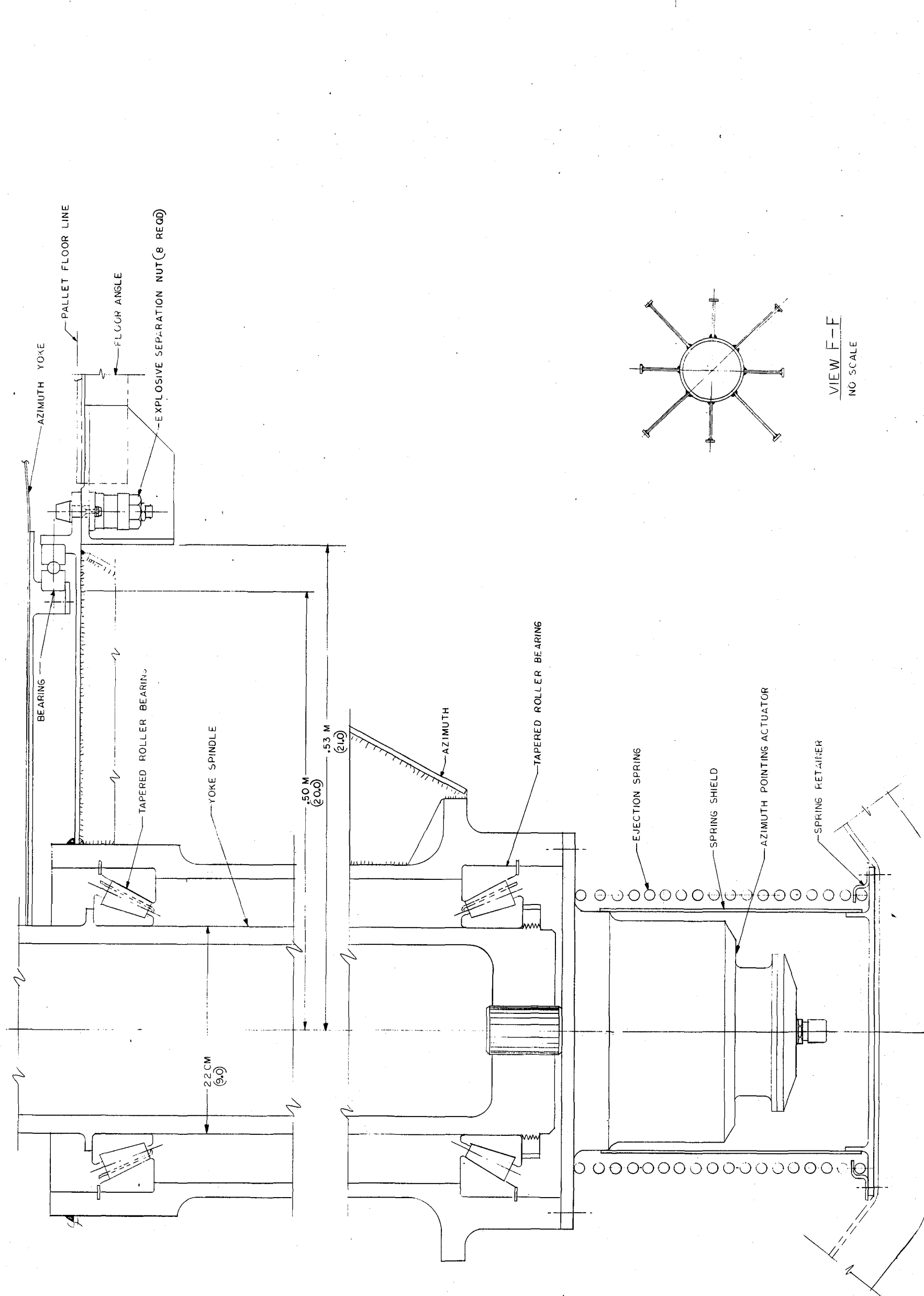
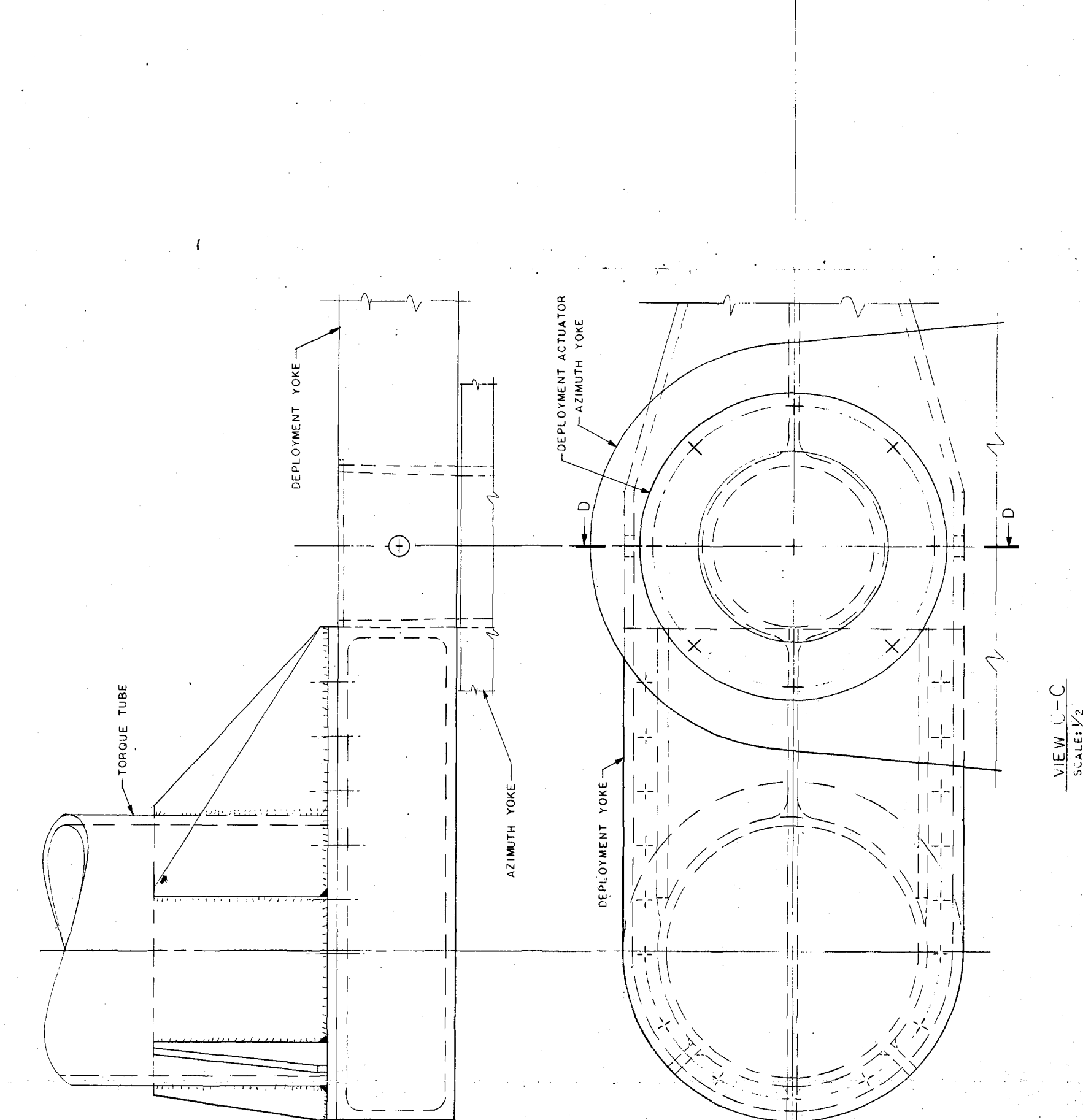
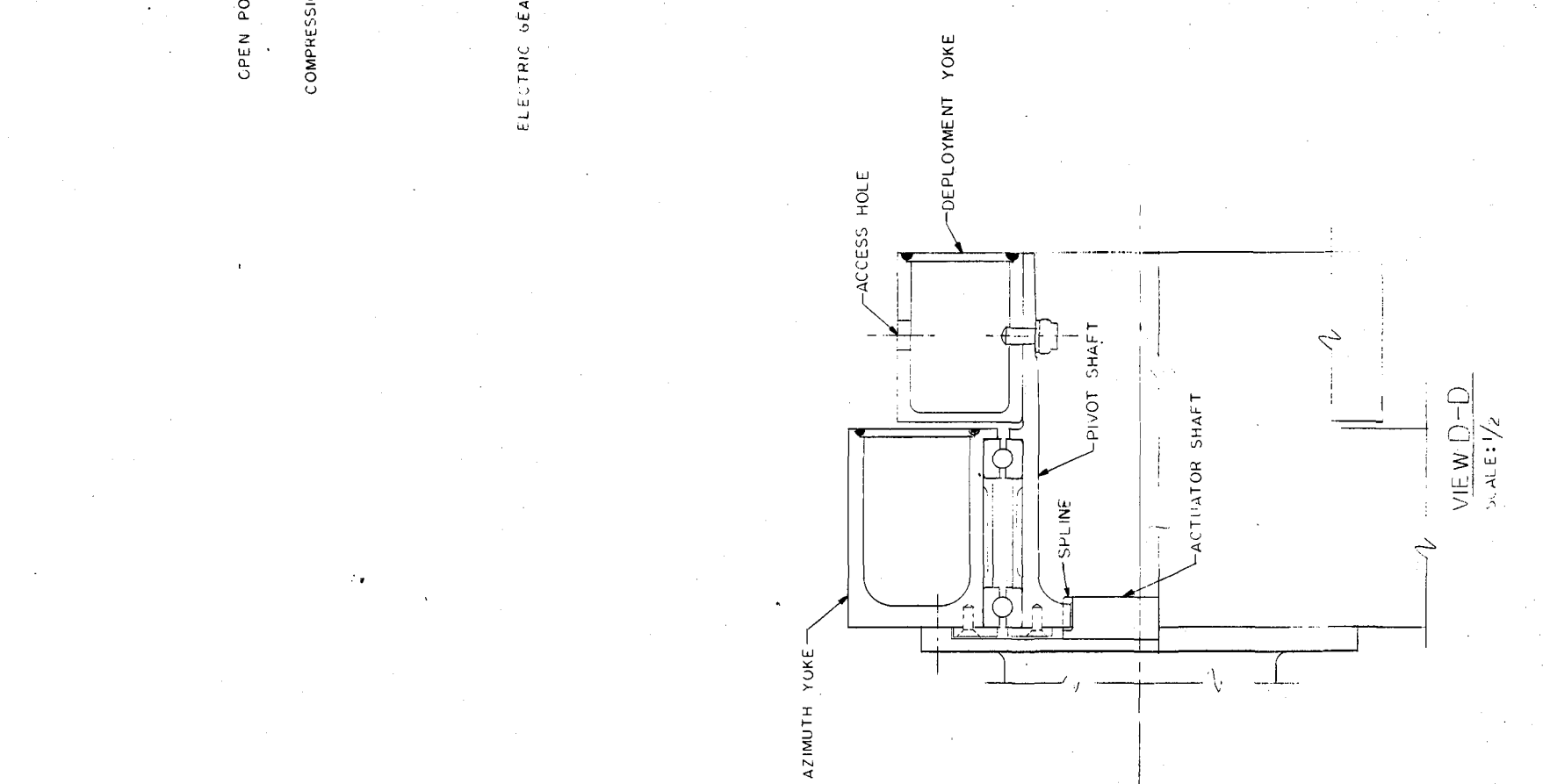
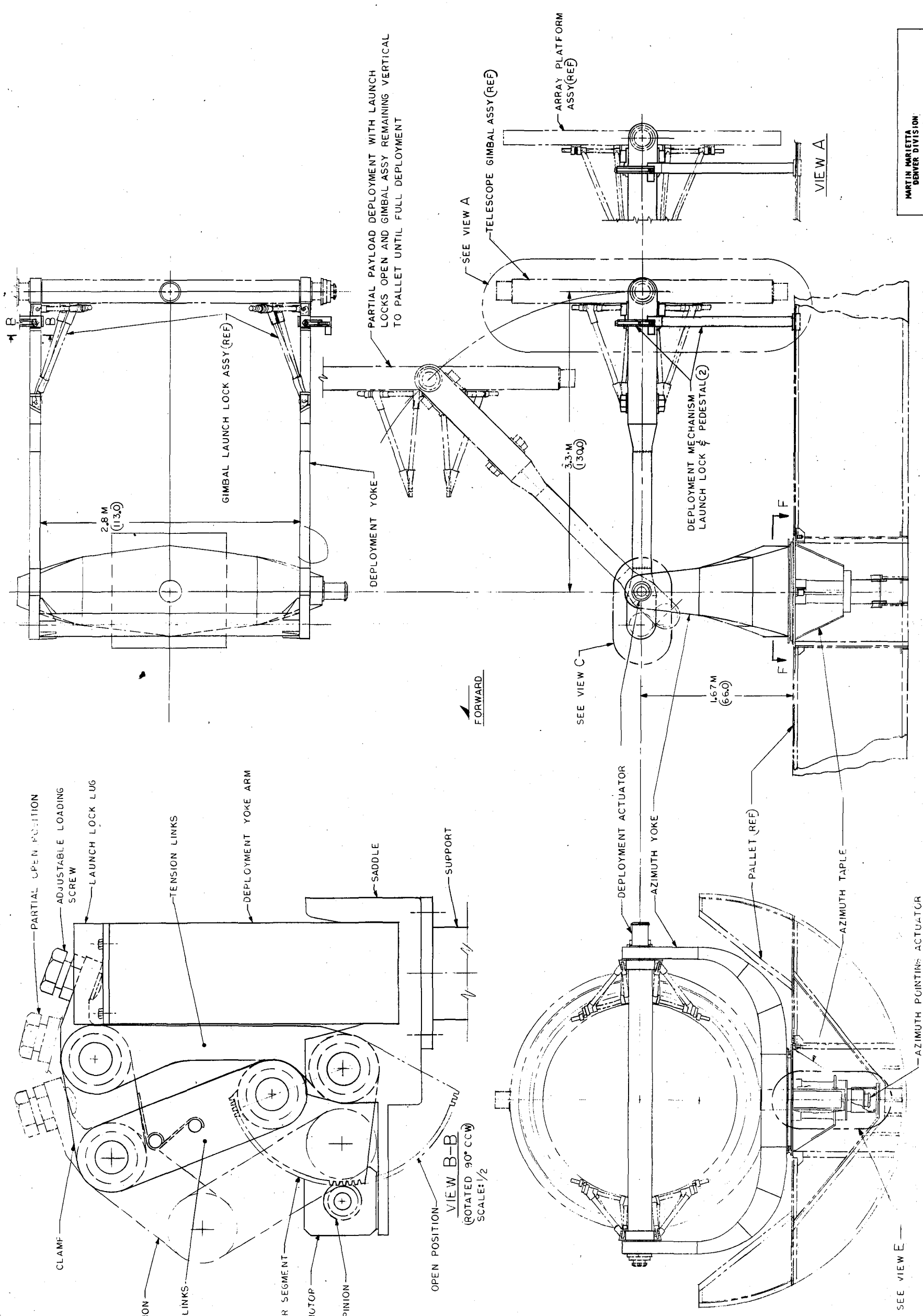
SCALE: 1/20



VIEW A
SCALE: 1/5
(PALLET DETAIL DELETED
FOR CLARITY)

SECTION B-B
SCALE: 1/4





The azimuth table supports the entire telescope or array mount on the Shuttle pallet, assisted by the pallet-mounted deployment locks, which are used during launch and return of the Orbiter to earth. A Shuttle requirement imposed on all payloads requires jettisoning of any device if its failure would prevent closing of the Shuttle doors. The interface between the table and pallet was selected as the simplest jettisoning interface for the entire mount. Six explosive bolts, similar to the Titan stage separation bolts tie the table to the major structure on the pallet. A compression spring, based on the pallet, is used to push the entire mount out of the payload bay after the electrical cables have been cut. If the failure occurs with the experiment package fully deployed, the center of gravity of the jettisoned equipment will be close to the spring thrust line, making jettisoning easy. If the experiment is partially deployed, the offset cg of the mount and experiment will cause tipping as the spring strokes. Guides may be needed to prevent tipping. This problem requires further study. Another promising technique involves translating the Orbiter away from the released mount, eliminating the need for guides and for the spring. This also requires further study because this technique may be applied to payloads of other types than those carried on the Astronomy Sortie missions.

The azimuth table is a welded and machined aluminum structure containing three azimuth yoke support bearings. The table mounts the azimuth pointing actuator used to pivot the azimuth yoke. The angular contact roller bearings take loads acting along the centerline of the azimuth yoke shaft as well as moments on the shaft, while the large diameter ball bearing is mounted in such a way that its primary purpose is to react loads due to moments imposed on the yoke by tension and compression loads in the deployment arms during launch and reentry. The azimuth yoke is also a welded and machined aluminum structure that supports the deployment yoke arms to provide support for the pivot tubes of the deployment yoke. The pivot tubes are pressed into heavy hubs in the deployment yoke and are then held in place with tapered pins.

The deployment yoke consists of two arms and a torque tube that ties the arms together into one assembly. The torque tube location was dictated by the clearance required for the longest telescope package while stowed in the payload bay and during deployment.

The yoke arms are designed to accommodate either the elevation pointing/stabilization actuators used with the telescope gimbal assembly or the elevation pointing actuators used with the array platform assembly. Just forward of the actuator mounting pads,

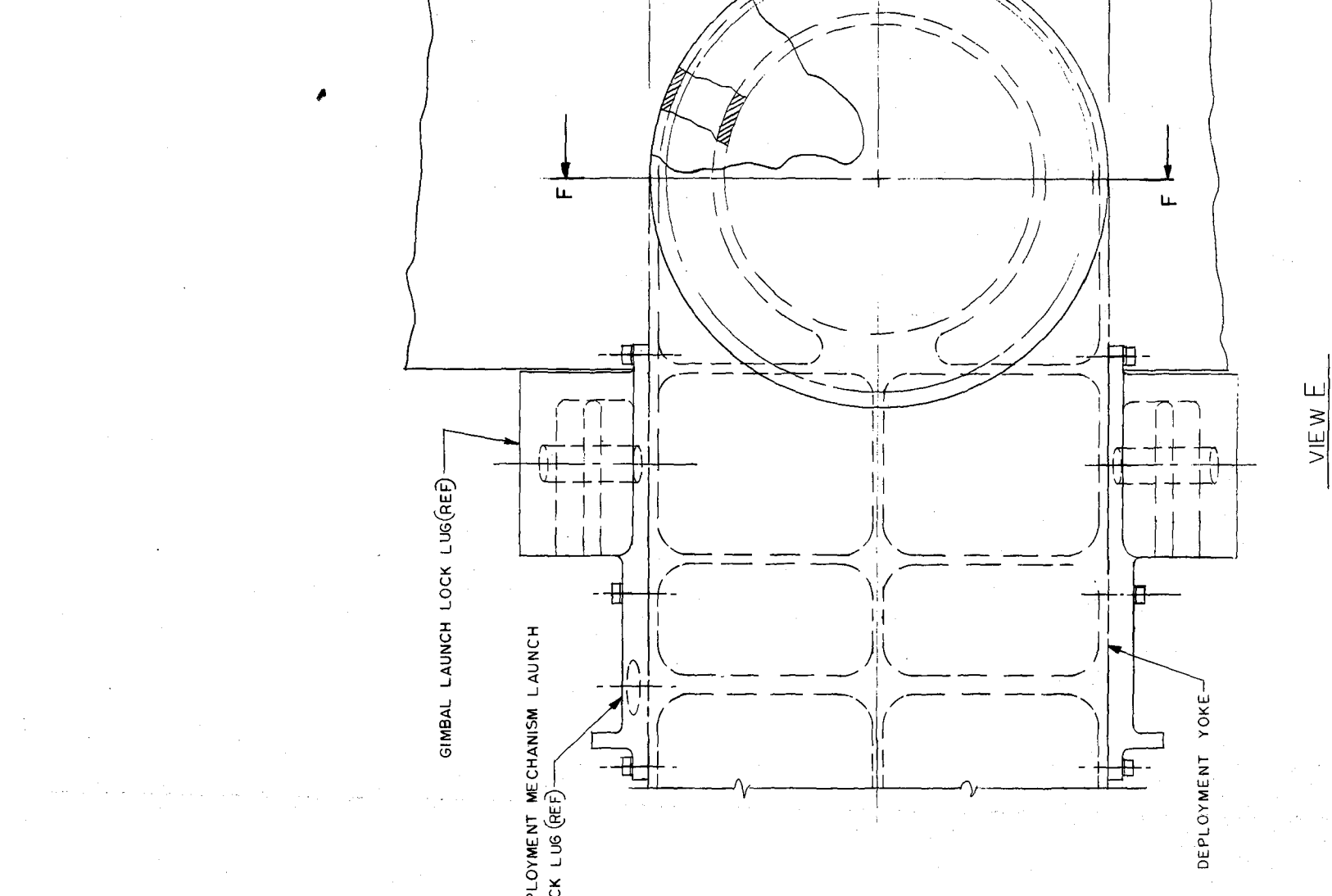
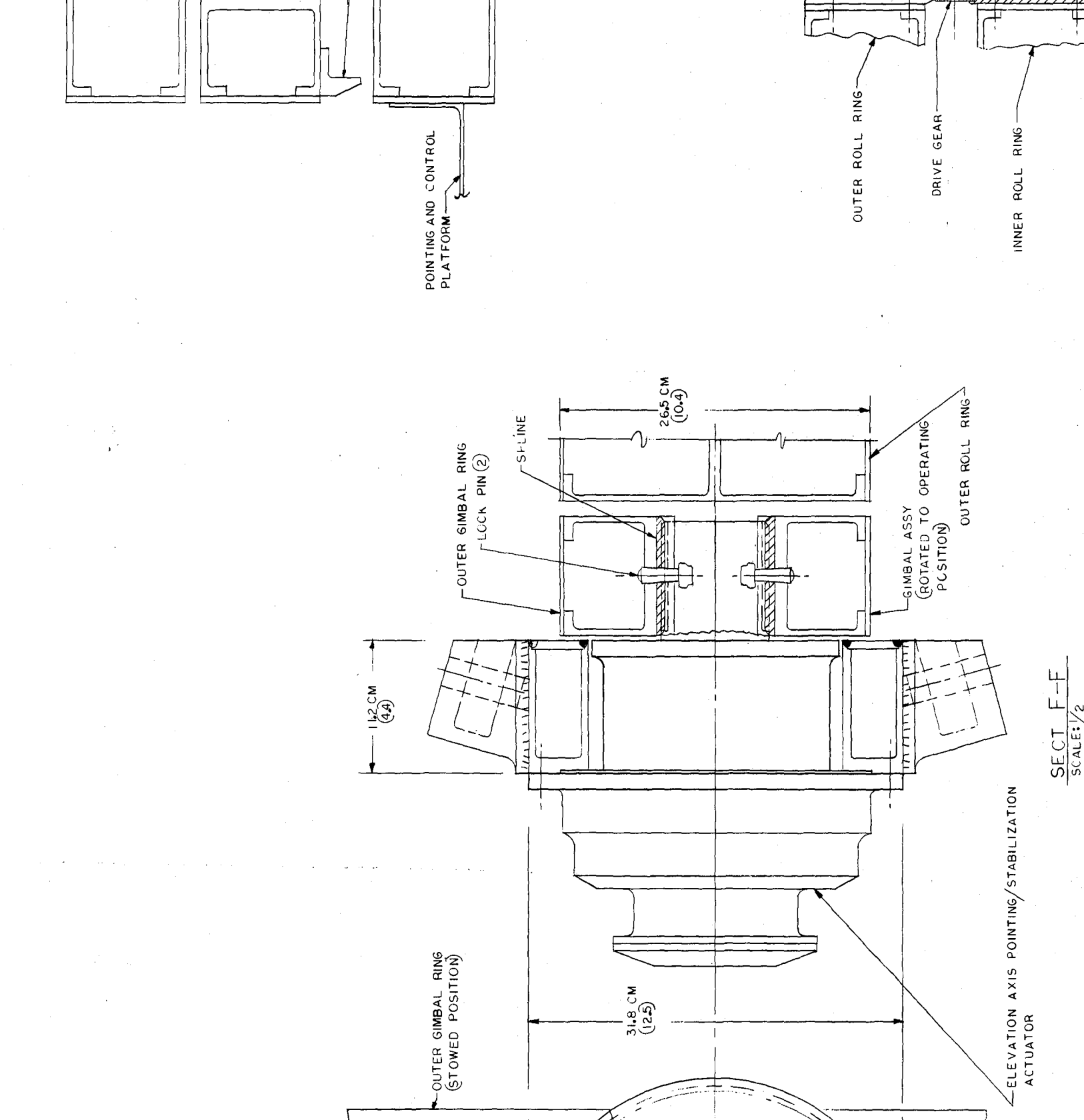
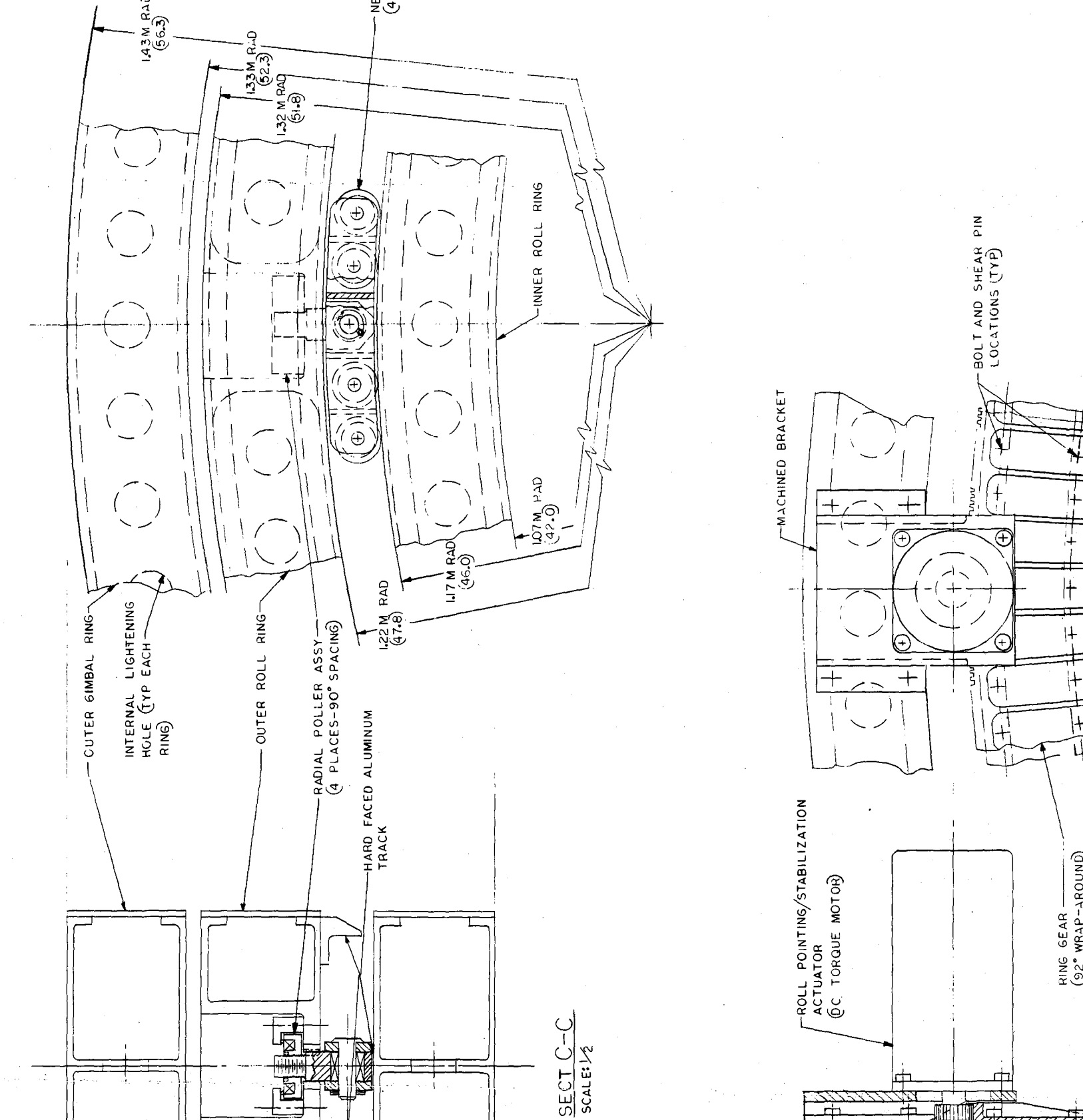
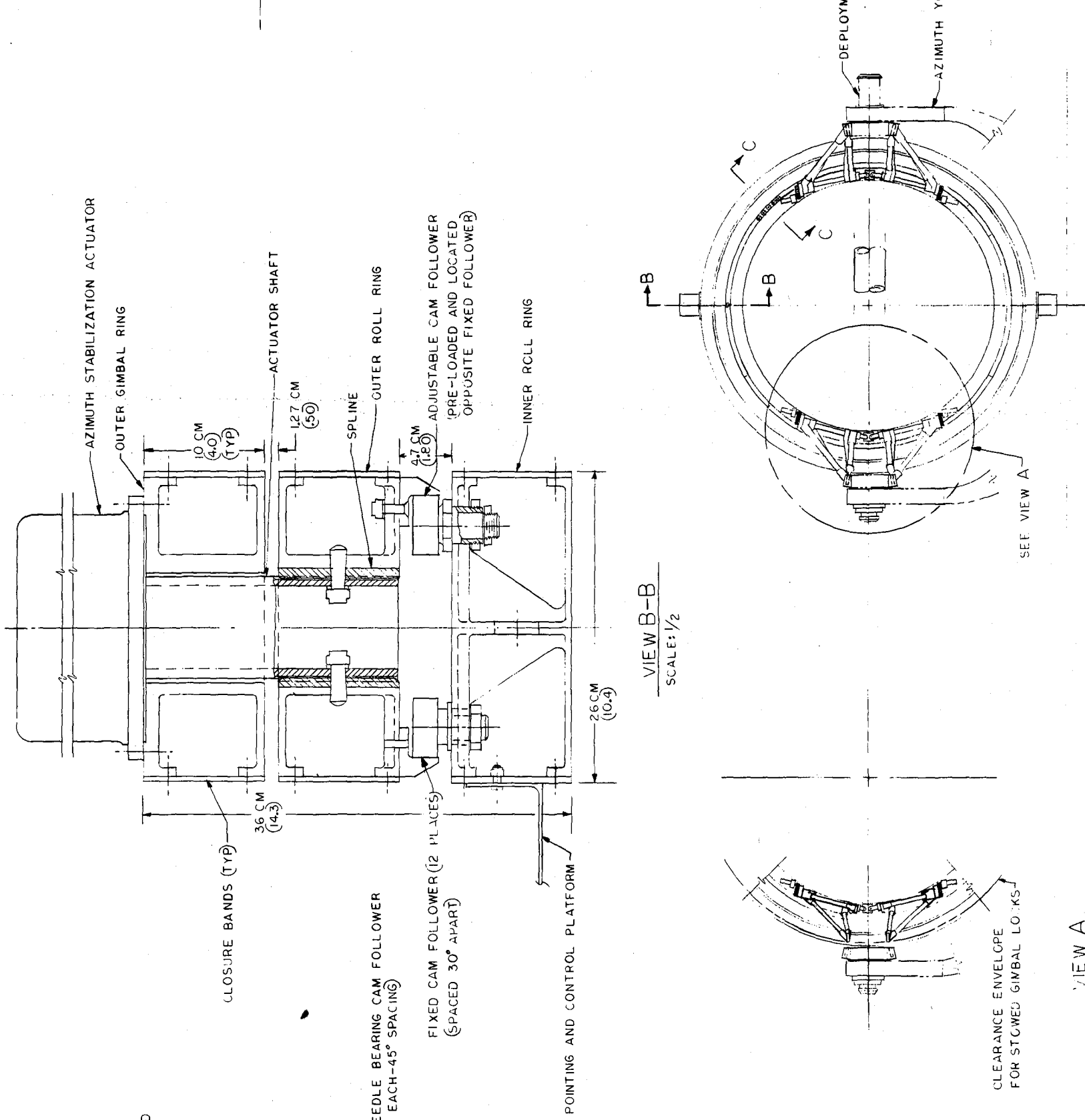
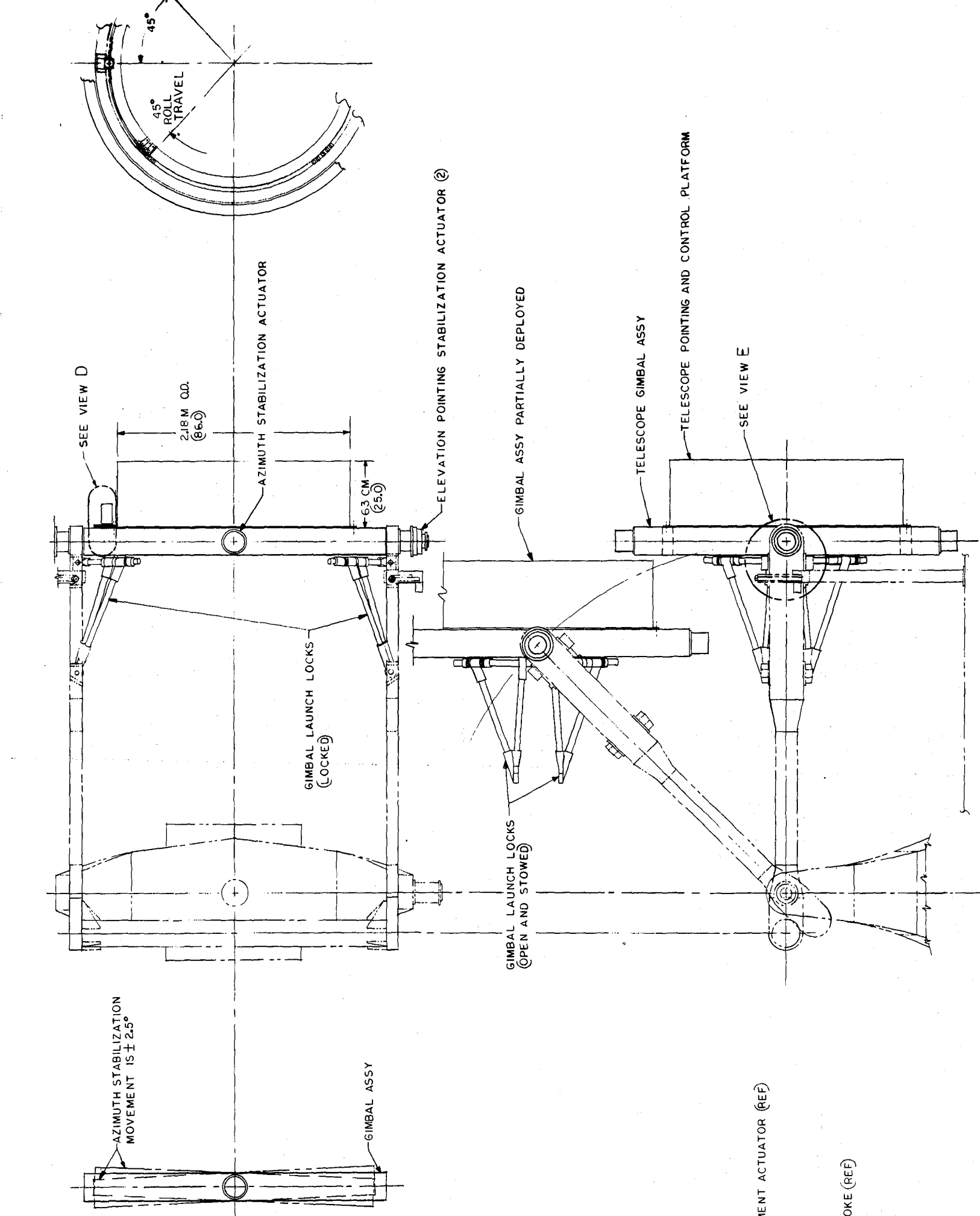
replaceable launch lock lugs are bolted to the upper and lower faces of the arms. Two sets of lugs are required, one for use with the telescope gimbal assembly, another for use with the array platform assembly.

e. Telescope Gimbal - Three gimbal rings are used in the gimbal assembly, which is capable of supporting any of the baselined telescope groups. Figure III-33 shows the gimbal assembly and its interfaces with the deployment yoke. The gimbal ring is supported on the deployment yoke by two flex pivots that are a part of the output shafts of the elevation pointing/stabilization actuators. The roll ring assembly, and the telescope, which is hard mounted to the inner roll ring, are supported on the gimbal ring by two flex pivots that are a part of the output shafts of the azimuth stabilization actuator. All three rings are machined from aluminum ring forging, with cover plates bolted and pinned in place to create rigid torque boxes.

The roll ring assembly is designed to allow the inner ring to rotate 90 deg with respect to the outer ring. To accomplish this, the roll pointing/stabilization actuator is mounted on the outer ring. A pinion gear mounted on the actuator output shaft drives a 94 deg ring gear attached to the aft face of the inner roll ring. A system of steel rollers and hard-faced aluminum tracks accurately maintain the co-alignment of the two rings. The radial track surface is machined on the body of the outer roll ring. Thrust tracks are located on the inner face of the outer ring. These tracks are accurately machined in place on the ring. The forward track is removed to allow assembly of the inner roll ring with its rollers, and then replaced. Adjustments are provided on the radial roller assemblies and on the forward set of thrust rollers to assure proper alignment between the rings and smooth rolling of the inner ring.

The gimbal locks are attached to the forward face of the inner roll ring. Each lock consists of two strut assemblies, which are driven by redundant electric gearmotors. In the locked position, the strut assemblies engage steel pins in the lugs on the deployment yoke arms. To unlock, the strut assemblies are rotated and stowed in a position that clears the deployment yoke arms to allow the gimbal assembly to be free to rotate about the elevation axis.

Attached to the aft side of the inner roll ring is a short cylindrical structure, the telescope pointing and control platform. This structure is used to rigidly support the star trackers and rate gyros required for telescope orientation.



TORQUE TUBE SELECTED FOR CLAMITY

VIEW A

VIEW B-B
 SCALE: 1/2

SECT C-C
 SCALE: 1/2

SECT F-F
 SCALE: 1/2

VIEW E
 SCALE: 1/2

VIEW D
 SCALE: 1/2

f. *Array Platform* - The array platform, shown in Fig. III-34 is a rectangular structure, machined from a single piece of aluminum. The design approach shown provides great rigidity with low weight. Multiple attachment points are available to secure the various array goups that must be accommodated. The platform is supported on the deployment yoke by the output shafts of the elevation pointing actuators. Platform launch locks, which use the same drive motors as the gimbal launch locks, are mounted to the sides of the platform and function in the same manner as the gimbal launch locks.

g. *Wide Coverage X-Ray Detector Mount* - Figure III-30 depicts the mount assembly and details. The mount is designed to provide a rigid platform for the array and accurate orientation for viewing. This is accomplished by providing a sturdy base for the mount and tying it to major structure on the pallet. The telescoping tube assembly uses ball splines to guide the tubes relative to each other and to the base. The ball splines are capable of transmitting torque for rotation of the array package after deployment. Rotation is accomplished by using a gearmotor, mounted on the base to drive a gear located at the upper end of the bearing-mounted outer tube. The telescoping tubes are extended and retracted by mounting a Bi-Stem-type actuator on the rotatable outer tube and attaching the extendable tube to the bottom of the center tube. This mount must be jettisonable since inability to fully retract the array would preclude closing the Orbiter payload bay doors.

h. *Gamma-Ray Spectrometer Housing and Mount* - Figure III-31 shows the housing and mount for the gamma-ray spectrometer. The housing is required to contain the paraffin used to shield the sensitive array from high radiation levels in space. The mount is similar to the wide coverage X-ray detector mount except that the base is designed to mount to the array platform and the telescoping tube assembly does not need to be rotated 90 deg after deployment. Rigidity under bending loads will be an important consideration influencing the telescoping tube assembly weight, if platform oscillation is established as a firm requirement.

i. *Stress Analysis* - Preliminary stress analyses were conducted on major elements of the experiment mounts to facilitate the development of realistic mass properties. These analyses are included in Appendix B2-2, Volume III, Book 2.

j. Mass Properties - Weight estimates of the telescope mount, array mount, wide coverage X-ray detector mount, and gamma-ray spectrometer housing and mount are shown in detail in Table III-12, and summarized by payload in Table III-13. These estimates were based on layout drawings and preliminary stress analyses.

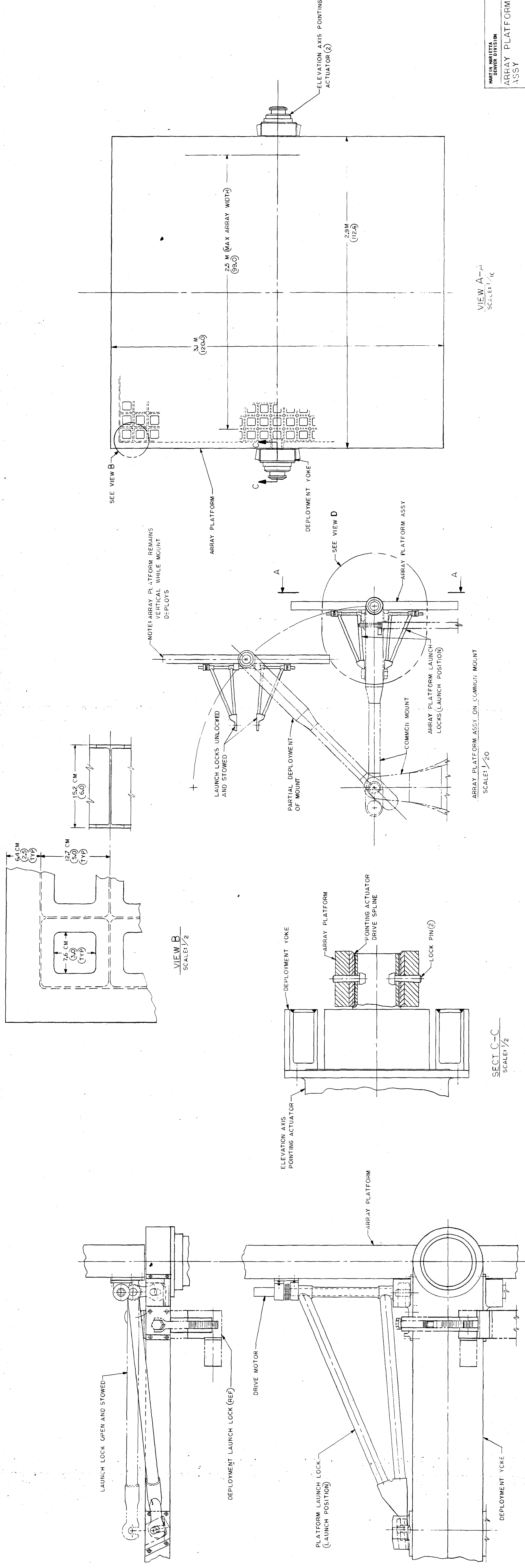


Table III-12 Experiment Mount Weights, kg (lb)

Azimuth Table		147.0 (324)
Floor Plate	31.8 (70)	
Hub	22.7 (50)	
Bearings	38.1 (84)	
Gussets	18.1 (40)	
Explosive Bolts	3.6 (8)	
Cable Cutter	3.2 (7)	
Ejection Spring	13.6 (30)	
Actuator	15.9 (35)	
Azimuth Yoke		179.6 (396)
Yoke	102.5 (226)	
Bearing Plate	10.0 (22)	
Shaft	26.8 (59)	
Trunnions (Including Bearings)	19.0 (42)	
40" Base Bearing	14.1 (31)	
Cabling	7.2 (16)	
Deployment Yoke and Actuators		111.5 (254)
Torque Tube	20.0 (44)	
Arms	59.9 (132)	
Actuators (2 at 30)	27.2 (60)	
Cabling	5.4 (12)	
Thermal Coating	2.7 (6)	
Gimbal Assembly		437.3 (964)
Inner Roll Ring	95.3 (210)	
Outer Roll Ring	138.8 (306)	
Gimbal Ring	106.6 (235)	
Elevation Stabilization/Pointing Actuator (2 at 62)	56.2 (124)	
Azimuth Stabilization/Pointing Actuator (2 at 35)	31.8 (70)	
Roll Stabilization/Pointing Actuator	8.6 (19)	
Array Platform		190.5 (420)
Wide Coverage X-Ray Detector Mount (2 at 170)		154.2 (340)
Gamma-Ray Spectrometer Housing and Mount		476.3 (1050)
Paraffin and Housing	388.3 (856)	
Base	15.9 (35)	
Mechanisms	68.0 (150)	
Spacer Cryogenic Refrigerator to Detector	4.1 (9)	
Launch Locks (Gimbal)		88.9 (196)
Gimbal Locks (2 at 38)	34.5 (76)	
Deployment Locks and Supports (2 at 44)	39.9 (88)	
Lock Fittings on Deployment Yoke	14.5 (32)	
Launch Locks (Array)		88.0 (194)
Array Locks (2 at 37)	33.6 (74)	
Deployment Locks and Supports	39.9 (88)	
Lick Fittings on Deployment Yoke	14.5 (32)	
Telescope Pointing and Control Platform		30.4 (67)

Table III-13 Summary of Experiment Mount Weights for Payload Combinations

Item	Weight, kg (lb)		Total
	Fwd	Aft	
Common Mount Items			
Azimuth Table	147.0 (324)	147.0 (324)	
Azimuth Yoke	179.6 (396)	179.6 (396)	
Deployment Yoke	115.2 (254)	115.2 (254)	
Deployment Locks	39.9 (88)	39.9 (88)	
Total Common Mount	481.7 (1062)	481.7 (1062)	963.4 (2120)
Mount Installation Payload 1-2			
Common Mount Items	481.7 (1062)	481.7 (1062)	
Gimbal Assembly	437.3 (964)	473.3 (964)	
Launch Locks (Gimbal)	34.5 (76)	34.5 (76)	
Lock Fittings on Deployment Yoke	14.5 (32)	14.5 (32)	
Telescope Pointing & Control Platform	30.4 (67)	30.4 (67)	
Total Mount Payload 1-2	998.4 (2201)	998.4 (2201)	1996.8 (4402)
Mount Installation Payloads 3AB,3AD,3AE,4AB,4AD,4AE			
Common Mount Items	481.7 (1062)	481.7 (1062)	
Gimbal Assembly	437.3 (964)		
Telescope Pointing & Control Platform	30.4 (67)		
Array Platform		190.5 (420)	
Azimuth Stabilization Actuators		31.8 (70)	
Launch Lock (Gimbal)	34.5 (76)		
Launch Lock (Array)		33.6 (74)	
Lock Fittings on Deployment Yoke (Gimbal)	14.5 (32)		
Lock Fittings on Deployment Yoke (Array)		14.5 (32)	
Wide Coverage X-Ray Detector Mount		154.2* (340)	
Total Mount Payloads 3AB,3AD,3AE,4AB,4AD,4AE	998.4 (2201)	906.3 (1998)	1904.7 (4199)
Mount Installation Payloads 3AC and 4AC			
Gamma Ray Spectrometer Mount (Add to above)		476.3 (1050)	
Total Mount Payloads 3AC and 4AC	998.4 (2201)	1382.6 (3048)	2381.0 (5249)
* Separate location on extreme end of pallet.			

C. STABILIZATION AND CONTROL SUBSYSTEM ANALYSIS

The function of the ASM stabilization and control subsystem is to provide the ASM experiment pointing and stabilization required by the experiments. The baseline ASM experiment payload mounted in the bay of Shuttle Orbiter consists of three principal elements: a telescope complement, a set of high-energy arrays, and a wide coverage X-ray detector. These three experiment elements have varying pointing and stabilization requirements.

The pointing and stabilization requirements of the six baseline telescopes are listed in Table III-14. The telescope roll stabilization requirements not listed in the table range from 0.025 to 0.3 mrad (5 to 60 sec). The ASM stabilization and control subsystem design goals for pointing and stabilizing the entire telescope complement as one unit are

Pointing: 10 μ rad (2 sec)

Stabilization: 0.5 μ rad (0.1 sec) in azimuth and elevation and
0.025 mrad (5 sec) in roll.

Note that for Stratoscope III and the photoheliograph the design goals for external telescope pointing and stabilization in azimuth and elevation are not sufficient. These two telescopes require an additional internal Image Motion Compensation (IMC) pointing and stabilization system to meet their final pointing and stabilization requirements.

The high-energy arrays have a pointing requirement of 0.3 mrad (1 min) in azimuth and elevation and none in roll. Their stability requirements range from 0.3 to 3 mrad (1 to 10 min) in azimuth and elevation and are approximately 0.1 radian (6 deg) in roll. These stability requirements can be furnished by the baseline CMG stabilized Shuttle Orbiter described in Chapter II, Section B since its projected stability is 0.3 mrad (1 min). For the high-energy arrays, the ASM stabilization and control system must only furnish the 0.3 mrad (1 min) pointing required in azimuth and elevation.

For the wide-coverage X-ray detector, its orientation is not critical as long as any convenient orientation that it selected is maintained within a three-axis stability of 9 mrad (30 min). Just as in the case of the high-energy arrays, these stability requirements are compatible with those of the baseline Shuttle Orbiter stabilization system selected in Section II.B and therefore, the

wide-coverage X-ray detector needs no additional stabilization. Because the Shuttle Orbiter is stabilized in an inertial attitude (X-POP), the wide-coverage X-ray detector can be hardmounted to the ASM pallet with the Orbiter supplying the pointing and stability requirements.

Table III-14 Baseline ASM Telescope Pointing and Stabilization (Azimuth and Elevation) Requirements

Telescopes	Pointing, μrad ($\overline{\text{sec}}$)	Stability, μrad ($\overline{\text{sec}}$)
Photoheliograph	1.5 (0.3)	0.25 (0.05)
XUV Spectroheliograph	75 (15)	0.5 (0.1)
X-Ray	50 (10)	0.5 (0.1)
Coronagraph		
Inner	10 (2)	5 (1)
Outer	25 (5)	10 (2)
Stratoscope III	1.0 (0.2)	0.1 (0.02)
IR	20 (4)	2.5 (0.5)

1. Telescope Pointing and Stabilization System

To accurately point the telescope complement, a telescope inertial measuring unit (IMU) is needed to determine precisely its attitude with respect to some inertial reference frame. The appropriate telescope closed-loop pointing commands are derived from this IMU. A quaternion strapdown IMU was selected. This system consists of three rate gyros, one mounted along each telescope axis and four strapdown star trackers for initializing and updating the strapdown IMU. Appendix B3-1, Volume III, Book 2, contains a derivation of the four quaternions, and their associated IMU strapdown equations including an initialization and update procedure. The accuracy of this strapdown IMU and therefore, the telescope pointing system is limited by the accuracy of the four star trackers. To meet the pointing accuracy goal of $10 \mu\text{rad}$ ($2 \overline{\text{sec}}$), the star trackers should have an accuracy in the neighborhood of $5 \mu\text{rad}$ ($1 \overline{\text{sec}}$).

The telescope fine stabilization system contains two key elements, its fine attitude sensor and its mechanical actuation system. The actuation system stabilizes the telescope complement using input signals derived from the outputs of the fine attitude error sensor and the rate gyros mounted to the telescope complement. The telescope fine attitude error sensor is also used to drive the image motion compensation systems required by Stratoscope III and the photoheliograph. The following two subsections describe the candidate fine attitude error sensors and actuation systems considered in this study.

a. Telescope Fine Attitude Error Sensor - The two candidate telescope fine attitude error sensors considered in this study are: (1) a boresighted sensor mounted within the structural envelope of the telescope complement; and (2) using the scientific telescopes to derive their own attitude signals. The fine error sensor must be capable of providing three-axis attitude error information. For a stellar telescope, two guide stars are needed to provide sufficient information for determining the required three axis--azimuth, elevation, and roll-attitude error signals.

The advantages of a boresighted fine attitude error sensor are that it does not place design requirements on the ASM telescopes, and since it is a single-purpose instrument with no requirements for collecting scientific data, it has the potential of large field of view (FOV). Depending on the magnitude of the stars that this sensor can accurately detect and locate, a large FOV may be necessary to ensure that at least two guide stars are present in the FOV. For Stratoscope III and photoheliograph, a boresighted sensor would make the problem of driving the required image motion compensation (IMC) systems very difficult, if not infeasible. Since the boresighted sensor is not in the main optical path of the telescope, any correction made by the IMC system would go undetected by the boresighted sensor. The IMC system would operate open loop because it would be unable to monitor the results of any corrective action taken by the IMC. This system could under correct or over correct and not be aware of it. Another problem with a boresighted sensor is that its accuracy is limited by the errors associated with its alignment with the telescope and the structural motion between the two instruments due to their bending modes and thermal flexures. The size and location of this boresighted sensor mounted in the telescope complement may also be a problem.

Using the main optics of the primary scientific telescope for deriving its own attitude errors does not have the alignment, bending modes, and thermal problems associated with a boresighted sensor. Unlike a boresighted sensor, the telescope does sense attitude due to structural deflections caused by bending modes and thermal gradients and therefore, can attempt to command corrective actions. In an attempt to ensure that the final pointing requirements of Stratoscope III and the photoheliograph and that the stability requirements of all the telescopes can be achieved, the telescopes should be used as their own fine attitude error sensor where feasible and where it does not unduly limit the objectives of the mission by imposing undesirable constraints on telescope design.

After a preliminary analysis of the six baseline ASM telescopes, it appears that only Stratoscope III and the photoheliograph can feasibly be used as their own fine attitude error sensor. This ability to provide their own attitude error signals is important because both instruments require IMC. The remaining four baseline ASM telescopes appear to require a boresighted sensor.

The six baseline ASM telescopes have been grouped into the following four baseline telescope complements:

Complement 1: Photoheliograph;

Complement 2: XUV spectroheliograph, X-ray telescope, and the inner and outer coronagraphs;

Complement 3: Stratoscope III;

Complement 4: IR telescope.

Complements 1 and 2 are solar payloads. The required three-axis attitude error information for these two payloads is obtained from tracking the sun. For complement 1, the attitude error information is derived using solar energy collected from the main optical path of the photoheliograph. For complement 2, none of the scientific instruments can be used for collecting attitude error information therefore, a boresighted sun sensor has been added for this purpose. The appropriate three-axis attitude error signals for these two payloads are derived using a Bendix Solar Area Correlation Tracker attached to both the photoheliograph and the boresighted sun sensor. This Solar Area Correlation Tracker is being developed for MSFC under NASA Contract NAS8-29037 by Bendix Aerospace Systems Division/Mishawaka Operations. This tracker has the capability of deriving three-axis attitude information although the one that will be delivered to MSFC has only a two-axis capability.

Complements 3 and 4 are stellar payloads. As previously mentioned complement 3, can be used to derive its own attitude error information. Unlike Stratoscope III, the IR telescope, complement 4, cannot be used to derive its own attitude error signals, therefore, a boresighted star tracker is added to the IR telescope as a fine attitude error sensor. To generate the three-axis attitude error information necessary to stabilize a stellar payload in all three axes, two guide stars must lie within the field of view of the fine attitude error sensor. For Stratoscope III, these two guide stars must lie within its total field of view, but outside its scientific FOV since energy from the target cannot be diverted for deriving these attitude error signals. The required FOV of the fine attitude error sensor as a function of detectable star magnitudes can be determined using star population charts such as those contained in C.W. Allen's book, *Astrophysical Quantities*, 1955. Figure III-35 shows the number of stars equal to or brighter than photographic magnitude M_p (in one square mrad) at the galactic equator (0°), the galactic pole (90°), and averaged over the entire sky. The probability of finding just n stars of magnitude M_p or brighter in a given field of view with a density of m stars of magnitude M_p or brighter is given by the following Poisson probability density function.

$$P_n = \frac{m^n}{n!} e^{-m}$$

m can be computed using Fig. III-35. For example, if there are on the average two stars of magnitude M_p or brighter in one square mrad and the field of view is 2 by 2 mrad,

$$m = (2 \text{ stars/mrad}^2) (4 \text{ mrad}^2/\text{FOV}) = 8 \text{ stars/FOV}$$

If the field of view is increased to a 4 by 4 mrad, its cross sectional area is increased to 16 mrad² and

$$m = (2 \text{ stars/mrad}^2) (16 \text{ mrad}^2/\text{FOV}) = 32 \text{ stars/FOV}$$

The probability P of finding at least two stars of magnitude M_p or brighter in a given field of view

$$P = 1 - \sum_{n=0}^1 P_n = 1 - P_0 - P_1 = 1 - (1+m)e^{-m}$$

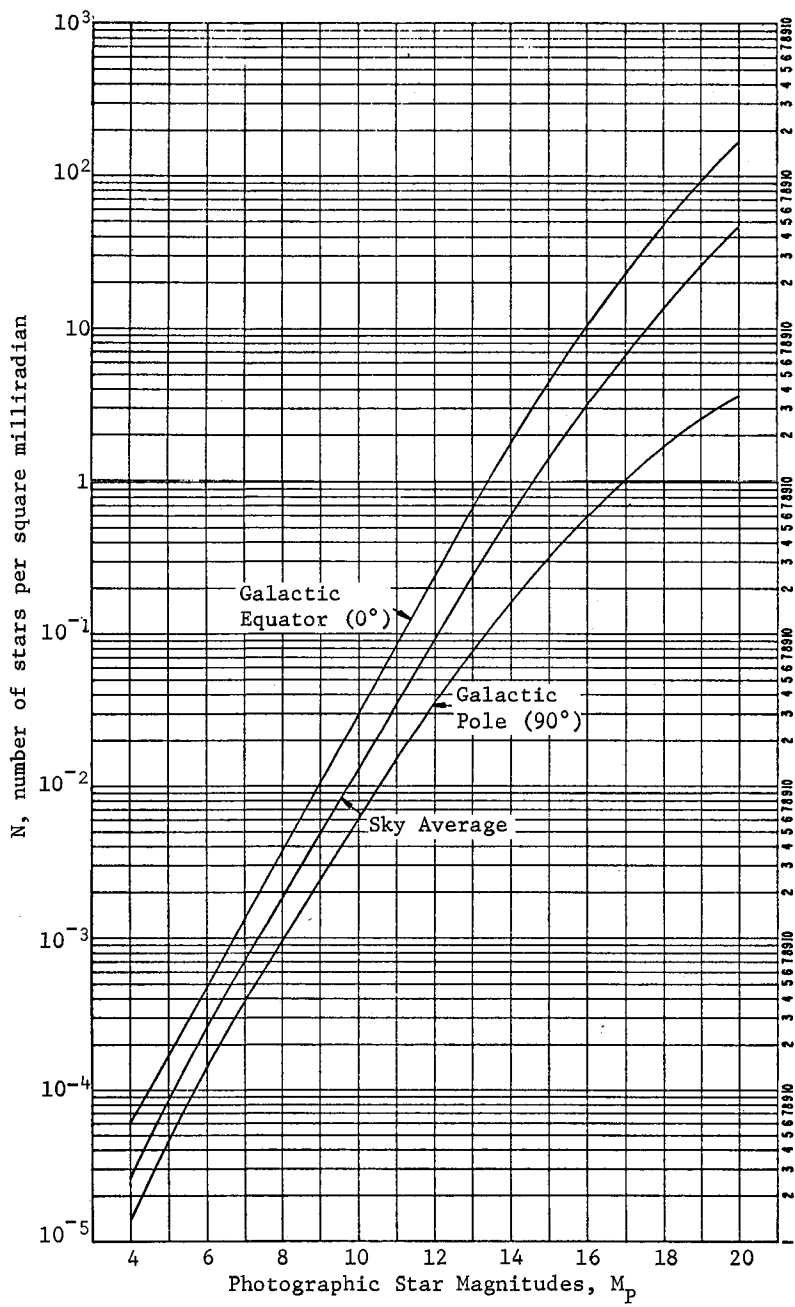


Fig. III-35 Number of Stars per Square Milliradian As A Function of Photographic Star Magnitude, M_p , or Brighter

Figures III-36 thru III-41 show the probabilities P of finding at least two guide stars of photographic magnitude M_p of 8, 10, 12, 14, 16, and 18 or brighter, respectively as a function of sensor field of view. These probability curves are based on the averaged star densities shown in Fig. III-35. Figure III-42 shows the required telescope fine attitude error sensor FOV as a function of minimum star magnitude M_p and probabilities P of 0.8, 0.9, and 0.95. Note that for a probability P of 0.95, a 20 by 20 mrad field of view must be able to detect and measure the location of tenth magnitude stars.

Normally as the required detectable star magnitude M_p decreases, the uncertainty of locating a star of magnitude M_p in the sensor field of view is increased due to the reduced sensor signal-to-noise ratio associated with decreasing star magnitudes. In the selection of a fine attitude error sensor, its field of view and its signal-to-noise ratio as a function of M_p should be optimized.

Described in Appendix B3-2, Volume III, Book 2, is a method for extracting three-axis attitude error information from the relative locations of two guide stars.

b. Telescope Pointing and Fine Stabilization Actuation Systems - In search for an optimal experiment pointing and stabilization system, several gimbal concepts were investigated. Each of these is briefly discussed below, and described more completely in Appendix B3-3, Volume III, Book 2.

- I. A system with separate outer gimbals for wide-angle pointing and inner gimbals for isolation and fine stabilization, and
- II. A dual-purpose system of gimbals for both wide-angle pointing and fine stabilization.

Various mechanizations of each of these concepts are discussed below and summarized in Table III-15.

- I. Separate Pointing and Fine Stabilization
 - A. Deployable wide angle gimbal with roll ring and flexible suspension bearings - The deployable wide-angle gimbals provide the viewing freedom required, while the flex pivots provide the azimuth and elevation stabilization required. A servoed roll ring is used to provide telescope pointing and stabilization

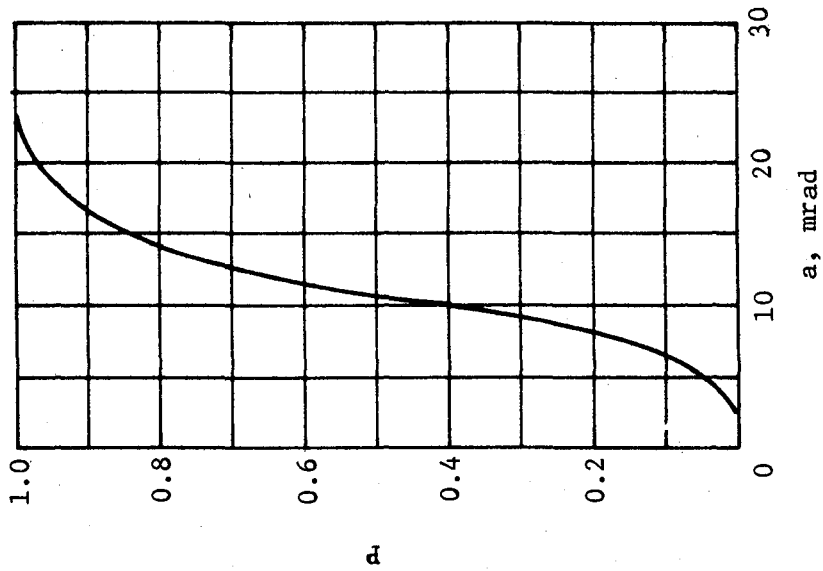


Fig. III-37 Probability P of Two Stars of Magnitude $M_p = 10$ or Brighter Lying in an $a \times a$ FOV

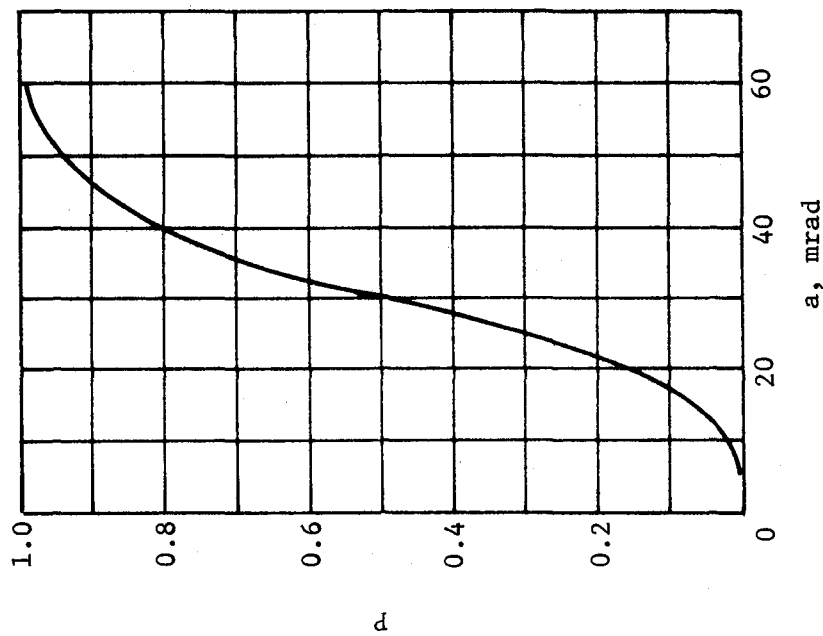


Fig. III-36 Probability P of Two Stars of Magnitude $M_p = 8$ or Brighter Lying in an $a \times a$ FOV

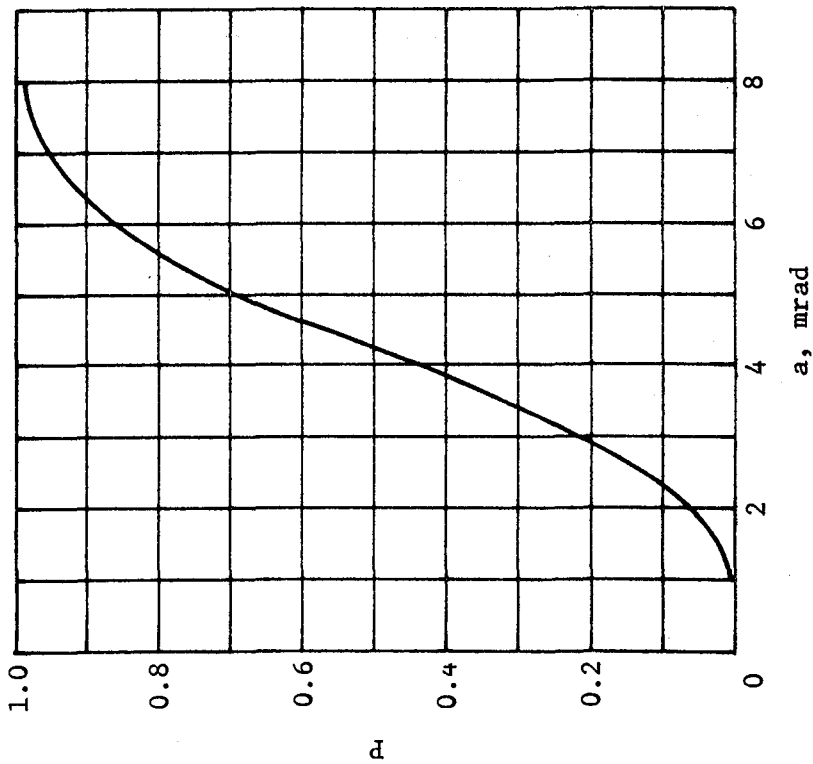


Fig. III-38 Probability P of Two Stars of Magnitude $M_p = 12$ or Brighter Lying in an $a \times a$ FOV

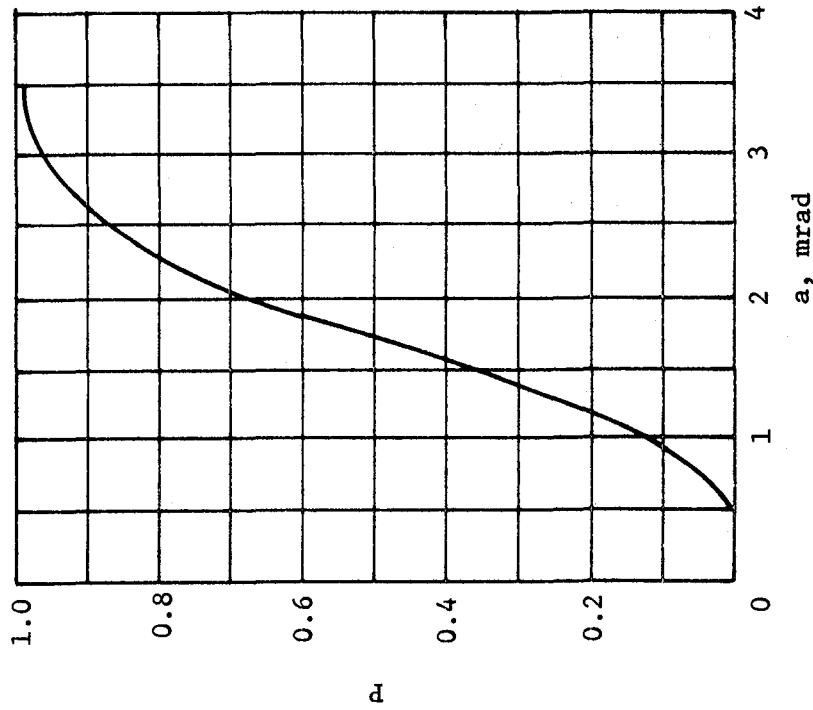


Fig. III-39 Probability P of Two Stars of Magnitude $M_p = 14$ or Brighter Lying in an $a \times a$ FOV

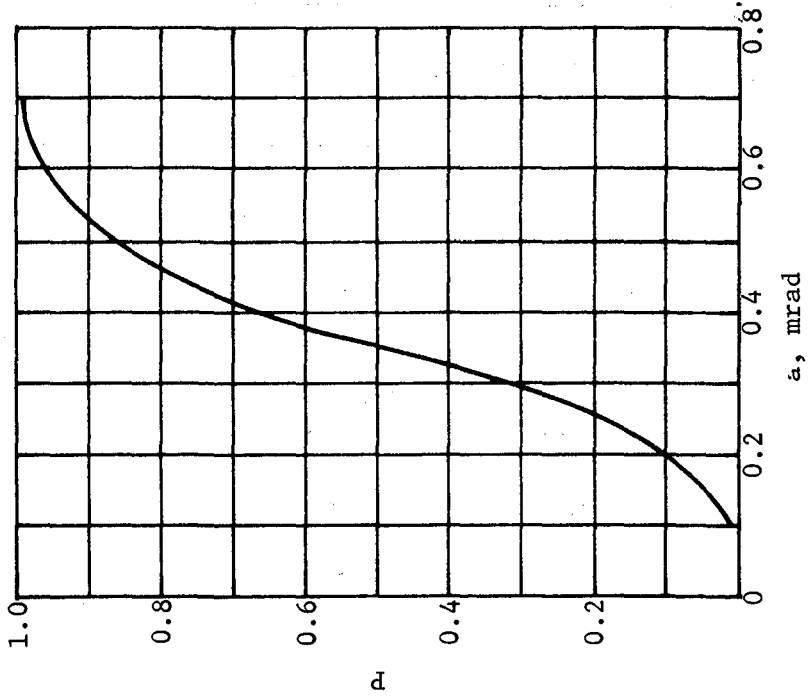


Fig. III-41 Probability of Two Stars of Magnitude $M_P = 18$ or Brighter Lying in an $\alpha \times \alpha$ FOV

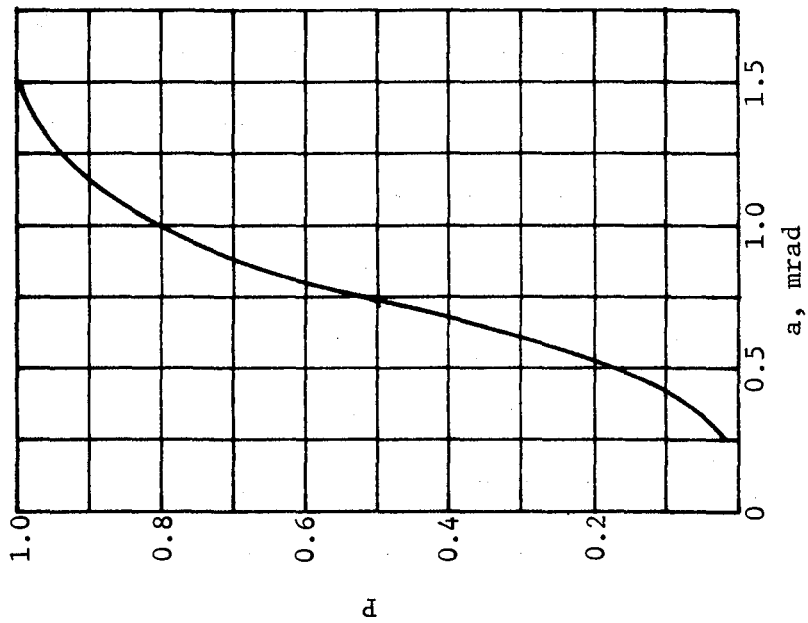


Fig. III-40 Probability of Two Stars of Magnitude $M_P = 16$ or Brighter Lying in an $\alpha \times \alpha$ FOV

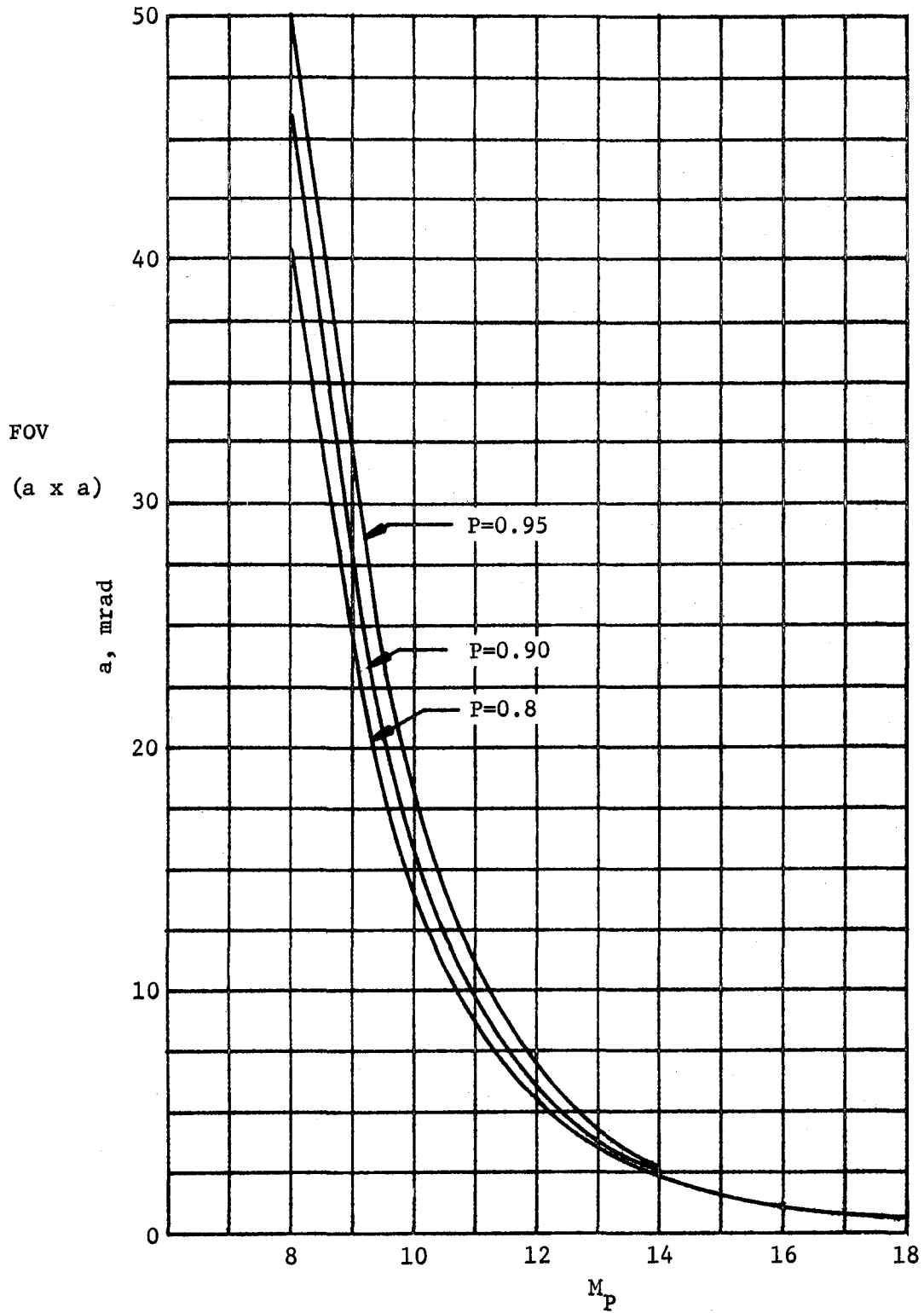


Fig. III-42 Required Fine Attitude Error Sensor Field of View as a Function Star Magnitude, M_P

in roll. This flex-pivot concept is similar to one used for Skylab's Apollo Telescope Mount (ATM). Although the stabilization requirements for ASM are more stringent than those for Skylab it is believed that this concept can provide adequate performance in the 1978 time frame with state-of-the-art sensors and with carefully designed mechanical and electro-optical mechanization. It appears that this concept can be developed with a reasonable cost and relatively low technical risk. Figure III-43 is a sketch of this system, Concept IA.

- B. Deployable wide-angle gimbal with spherical gas bearings - there are three mechanization subsets conceived: (1) a small spherical bearing located within the telescope tube at the center of mass of the instrument group (Concept IB-1); (2) a small spherical bearing at the "bottom" end of the tube with a counterweight (Concept IB-2); and (3) an "equivalent" section of a sphere surrounding the tube at the center of mass of the instrument group (Concept IB-3). These three gas bearing systems are shown in Fig. III-44. As discussed in Appendix B3-3, only the large girded concept (IB-3) is recommended for further analysis. Even though there are some penalties, as summarized in Table III-15, the gas bearing concept has potential performance advantages that warrants its retention as a candidate.
- C. Deployable wide-angle gimbal with roll ring and gas bearings (Concept IC) - This system is the same as Concept IA (Fig. III-43), except that the flexible suspensions are replaced with gas-support bearings as shown in Fig. III-45. This concept has no particular advantages. It was therefore dropped from further consideration.

II. Dual Pointing and Stabilization

- A. Deployable wide-angle gimbal plus roll ring with image motion compensation internal to each telescope - This concept (II A), simplifies the common telescope gimbal as shown in Fig. III-46, but greatly increases the program costs over other alternatives. It is questionable that IMC can be accomplished on some instruments, e.g., X-ray Telescope. This approach is therefore not recommended.

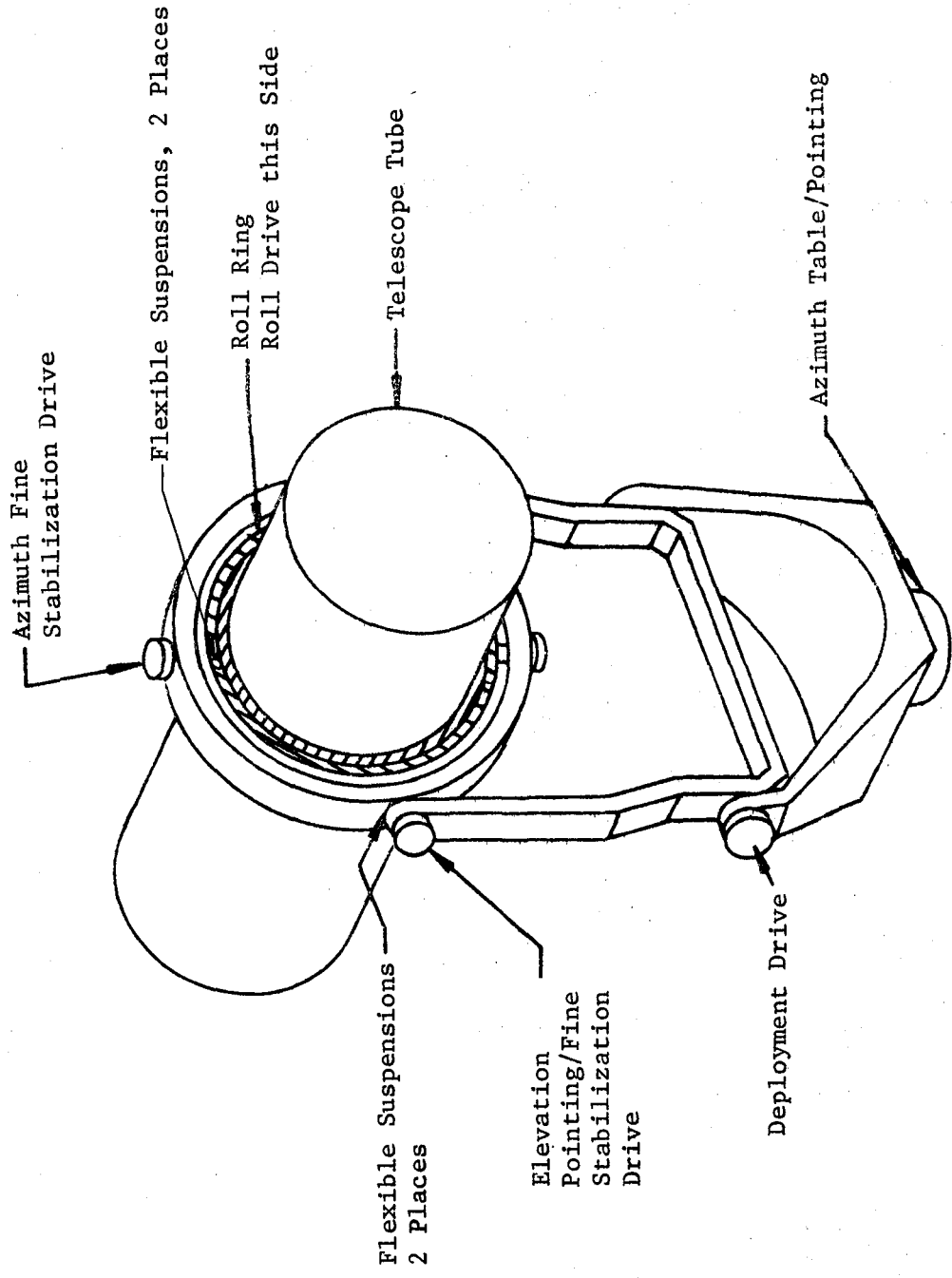


Fig. III-43 Flexible Suspension Gimbal System (Concept IA)

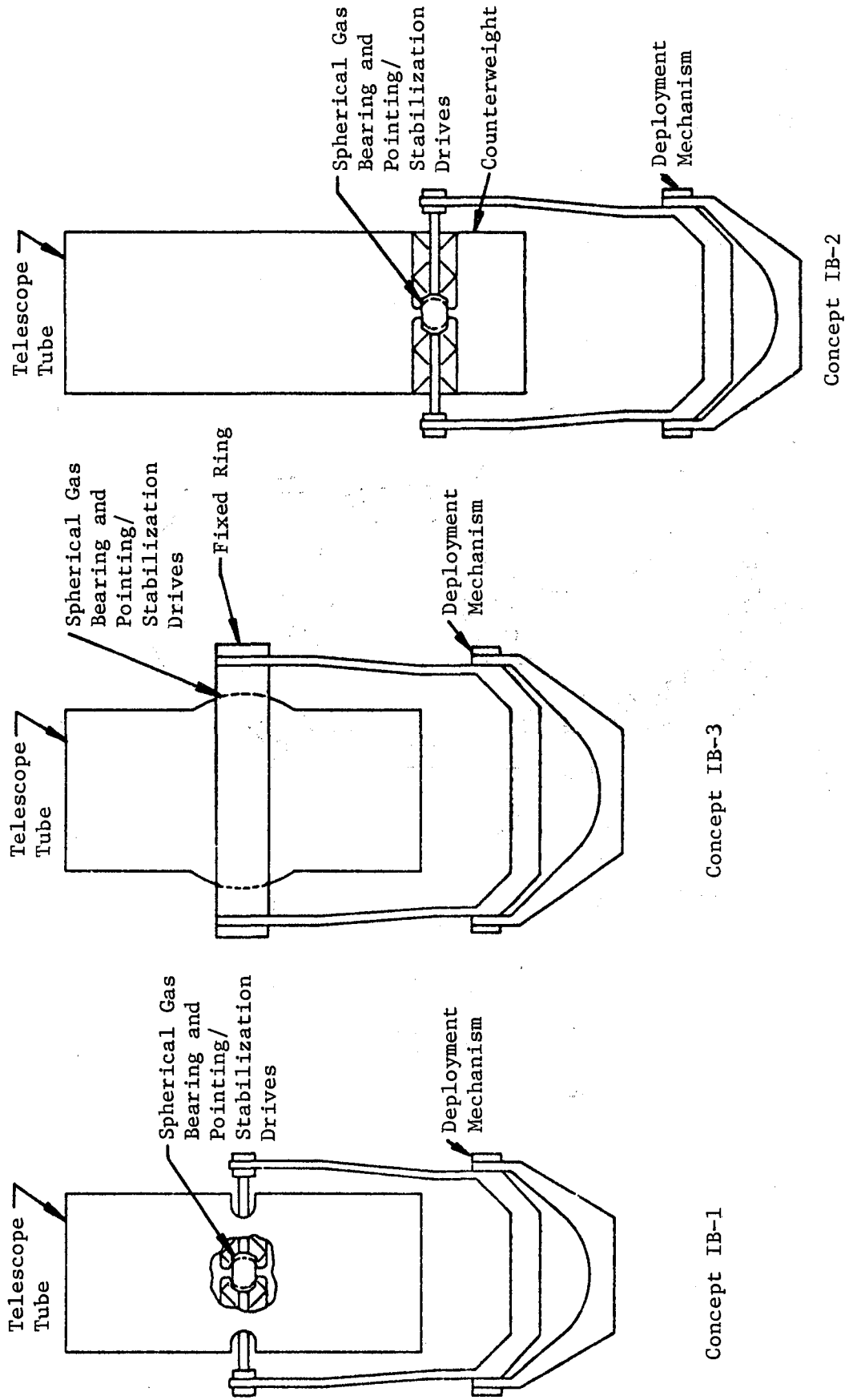


Fig. III-44 Wide-Angle Spherical Gas Bearing Configurations
(Concepts IB-1, IB-2, IB-3)

Table III-15 Experiment Pointing and Stabilization Concepts

Telescope Pointing and Stabilization Concept	Remarks
<p>I. Pointing and Fine Stabilization ($\pm 0.1 \text{ sec}$)</p> <p>A. DWAG* + Roll Rings + Flexible Suspensions</p> <p>B. DWAG + Spherical Gas Bearing</p> <p>(1) Small, internal at instrument cg</p> <p>(2) Small, external with counterweight</p> <p>(3) Girded, external at instrumentation cg</p> <p>C. DWAG + Roll Ring + Gas Gimbal Bearings</p> <p>II. Dual Pointing and Stabilization</p> <p>A. DWAG + Roll Ring</p> <p>B. Wide Angle Gas Bearing (External at Instrument cg)</p>	<p>Probably adequate, least technical risk, probably lowest weight and cost</p> <p>Weight penalty, integration problem, potential contamination</p> <p>Serious weight and volume penalty, integration problem, potential contamination</p> <p>Weight and volume penalty, requires development, potential contamination</p> <p>Complex, weight penalty, potential contamination</p> <p>Requires internal IMC[†] on each instrument, total cost high, performance questionable</p> <p>Weight and volume penalty, requires development, potential contamination</p>
<p>*DWAG - Deployable Wide Angle Gimbal</p> <p>†IMC - Image Motion Compensation</p>	

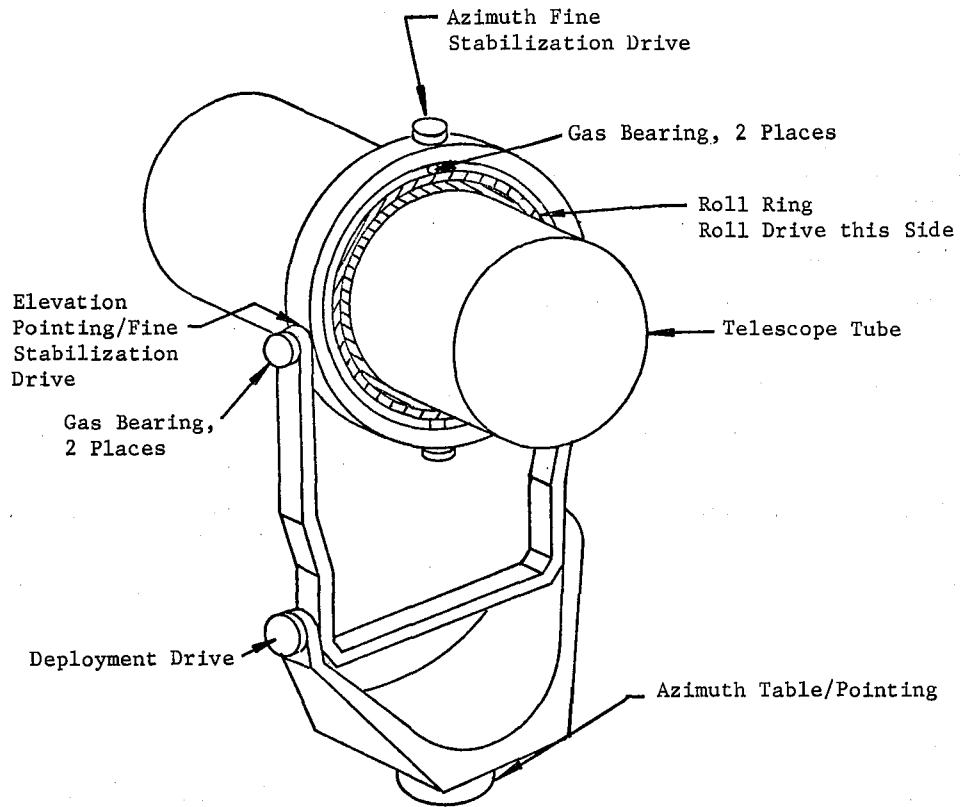


Fig. III-45 Gas Bearing Gimbal System (Concept IC)

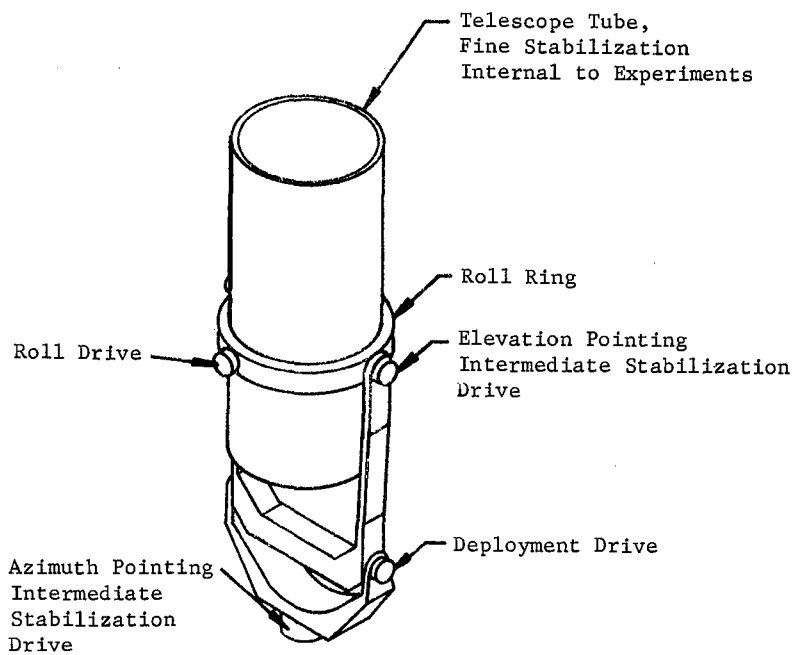


Fig. III-46 Coarse External - Internal IMC System (Concept IIA)

- B. External wide angle gas bearing at the instrument center of mass (Concept II B) - This concept is similar to the girded concept (IB-3 of Fig. III-44) except that this "stator" configuration consists of two large pads on a frame that allows the telescope tube to rotate 1/2 revolution or more in elevation. This concept is shown in Fig. III-47. This system is retained as a candidate because of its potential high performance capabilities.

Tradeoff data were generated for the four systems selected for further evaluation, Concepts IA, IB-3, IIA, and IIB. The results of this trade study are contained in Table III-16. In nearly all categories the DWAG with flexible suspensions appear to be the best choice.

Because of the projected high cost and the questionable mechanization of image motion compensation on some of the telescopes, concept IIA is not recommended for the Astronomy Sortie mission payloads.

The two gas bearing concepts, IB-3 and IIB appear to have the inherent high-performance capability required by the ASM telescopes. The drawbacks of these systems appear to be a high estimated cost, weight, volume, and technical risk and a possibility of contaminating the ASM experiments. Because of these disadvantages, neither of these two systems were selected as the baseline system, but further study of those systems is recommended due to their high inherent performance capability.

The DWAG plus flexible suspension gimbal/roll ring system, Concept IA, is the selected baseline ASM telescope pointing and stabilization system. Hardware commonality between the telescopes and high-energy array pointing systems is possible with this system.

c. Performance Analysis of Selected Telescope Fine Stabilization System - A linear dynamic model of the telescope baseline flex-pivot, roll ring stabilization system is presented in Appendix B3-4, Volume III, Book 2. The telescope complement and Shuttle Orbiter are assumed to be attached as shown in Fig. III-48 by a hinge point defined by the geometric center of rotation of this stabilization system. The resultant linear block diagram of this system is shown in Fig. III-49. $H_x(s)$, $H_y(s)$, and $H_z(s)$ are the transfer functions for the X, Y, and Z axis fine stabilization actuators, respectively. For a detailed discussion of this model, see Appendix B3-4, Volume III, Book 2.

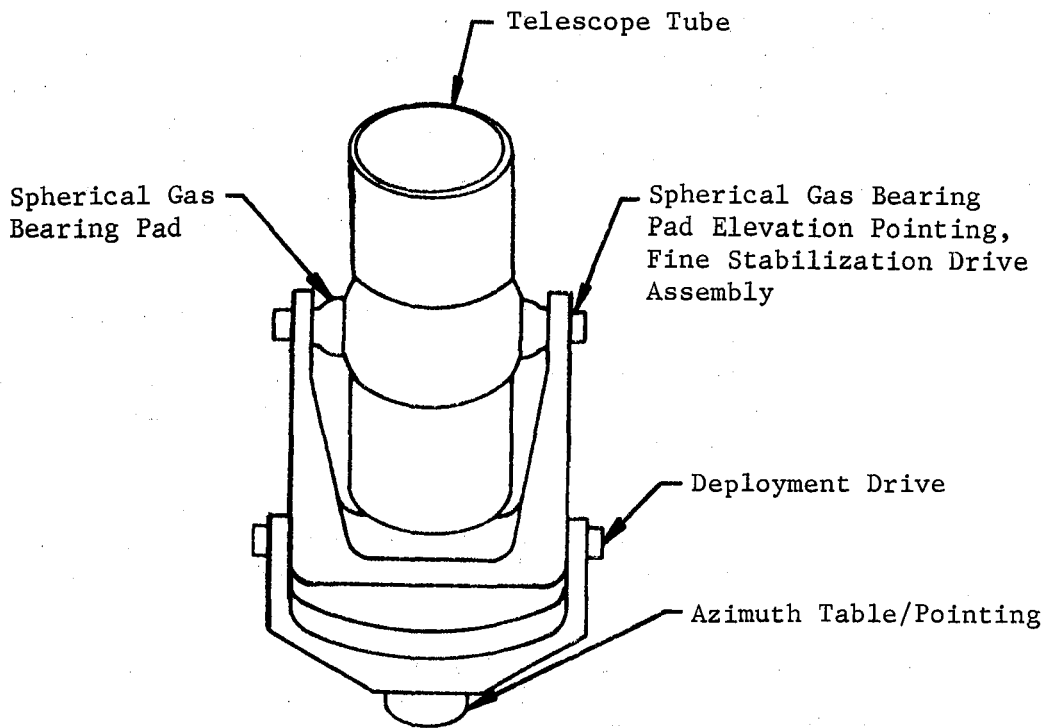


Fig. III-47 Wide Angle Spherical Gas Bearing, Two-Pad Configuration (Concept IIB)

Table III-16 Experiment Pointing and Stabilization Concept Tradeoffs

	Cost \$1000	Weight, Kg (lb)	Volume, m ³ (ft ³)	Power, W	Relative Complexity & I/F Problems	Contami- nation	Total Technical Risk	Remarks
<p>Concept IA</p> <p>Deployable Wide Angle Gimbal Pointing Plus Roll Ring and Flexible Suspension Fine Stabilization</p>	600	1400 (3000)	2.5 (90)	1500 Peak 500 Av	Low	None	Moderate	Selected configuration
<p>Concept IB-3</p> <p>Deployable Wide Angle Gimbal Pointing plus Girded Spherical Gas Bearing External to Tube at cg for Fine Stabilization</p>	3100	3000 (6500)	4.8 (170)	1500 Peak 400 Av	Low	Some	High	Recommend continued study
<p>Concept IIA</p> <p>Deployable Wide Angle Gimbal for Pointing and Intermediate Stability plus Roll Ring and Image Motion Compensation Internal to Telescopes</p>	6680	1400 (3000)	1.8 (65)	1500 Peak 500 Av	High	None	Very High	Not Recommended
<p>Concept IIB</p> <p>Wide Angle Gas Bearing Operating in Conjunction with Azimuth Table</p>	3100	3100 (6700)	4.8 (170)	1500 Peak 400 Av	Low	Some	High	Recommend continued study

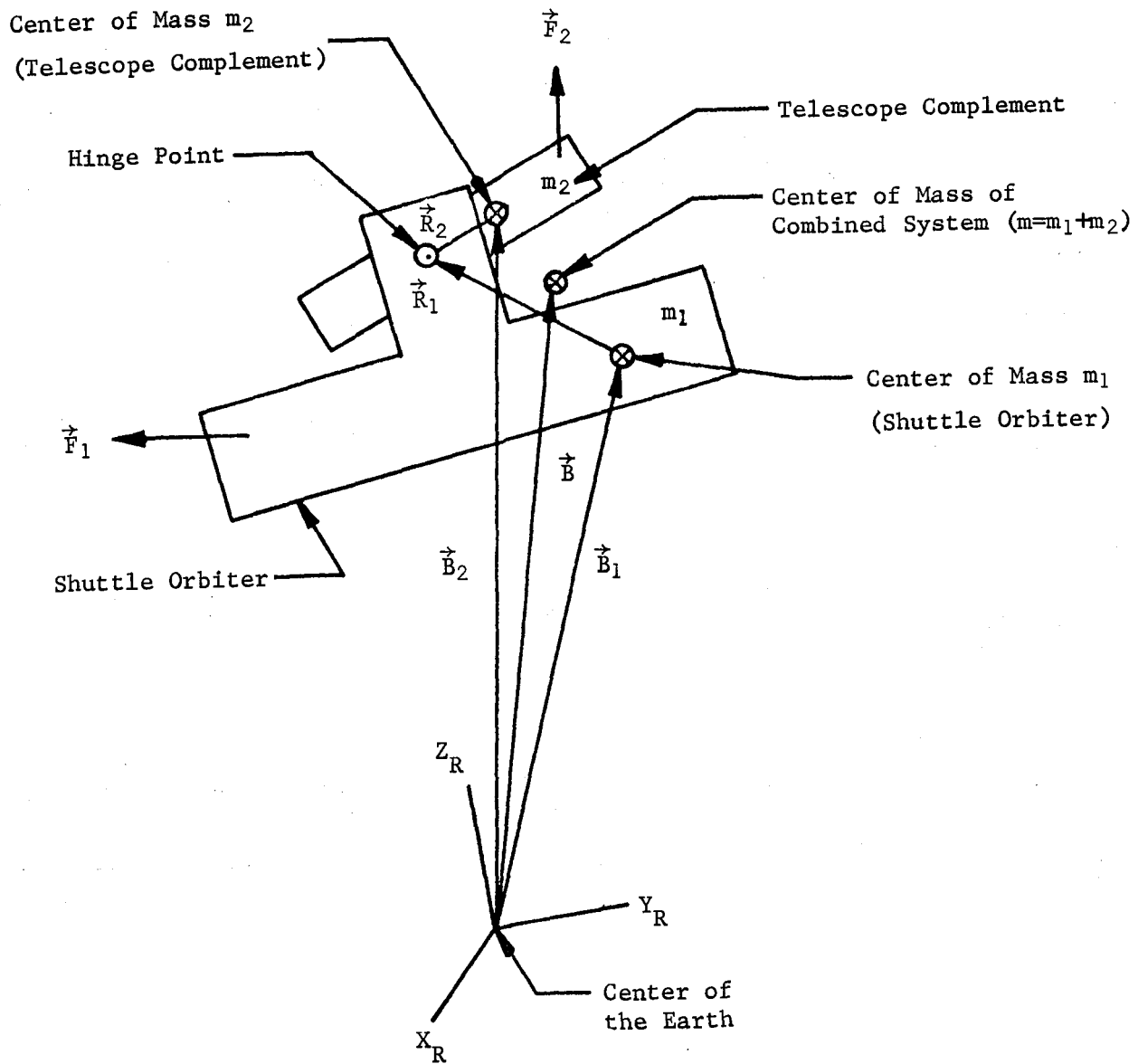


Fig. III-48 Orientation of Body 2 with Respect to Body 1

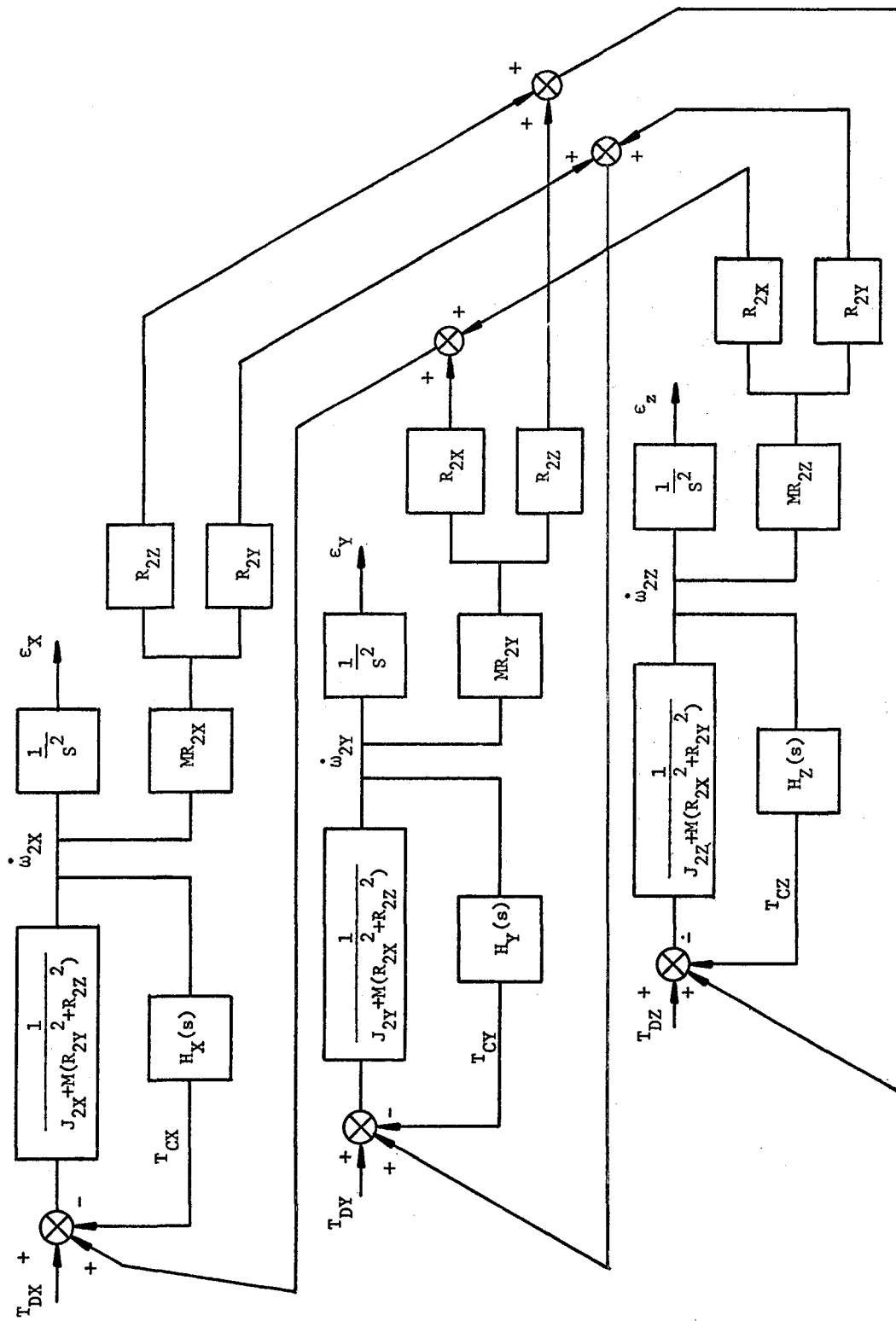


Fig. III-49 Block Diagram of Telescope Fine Stabilization System

This model was used to determine the gross stabilization capabilities of this system and to determine the effects of the telescope center of mass being offset from the intersection of three stabilization axes. The results of this analysis are presented in Appendix B3-4 and should not be considered to demonstrate the feasibility of this system. To demonstrate feasibility of this system, a more detailed model would be required. This new model should include: (1) the nonlinear cross-coupling terms deleted from the model shown in Fig. III-49; (2) a CMG Orbiter stabilization system with a detailed nonlinear CMG model; (3) all analog-to-digital (A/D) and all digital-to-analog (D/A) interfaces; (4) the bending modes associated with telescope complement and the Shuttle Orbiter; (5) more detailed fine stabilization actuator models including such nonlinearities as flex-pivot hysteresis characteristics; and (6) a detailed disturbance model including Shuttle Orbiter induced disturbances plus those generated by the telescopes themselves.

Using the model described in Fig. III-49, the experiment mass motion torque disturbance T_D shown in Fig. III-50 was applied to both the X and Y telescope fine stabilization axes ($T_{DX}=T_{DY}=T_D, T_{DZ}=0$). T_D is a projected worst-case experiment mass motion disturbance. This disturbance T_D was assumed to be periodic with a period of 1 sec. The computed rms stability of this system due to T_D is approximately 0.2 μ rad (0.04 $\overline{\text{sec}}$) about the X and Y telescope axes and zero about its Z roll axis. Although this stability is within the desired stability of this system 0.5 μ rad (0.1 $\overline{\text{sec}}$), it does not demonstrate the feasibility of this system, it only demonstrates that this system *may* be feasible.

In Appendix B3-4, it was recommended that: (1) the center of mass of the telescope complement should be carefully mounted as close as possible to the center of rotation of the telescope fine stabilization system; and (2) the Shuttle Orbiter stabilization system should be designed so that it will not generate any large Shuttle Orbiter rotational accelerations or translational forces during the ASM telescope experimentation periods. These recommendations are designed to minimize the disturbance coupling between the Shuttle Orbiter and the ASM telescopes.

2. ASM High-Energy Array Deployment and Pointing Systems

A high degree of hardware commonality exists between the baseline deployment and pointing systems for the high-energy arrays and telescope complement. Mechanically the deployment and basic pointing

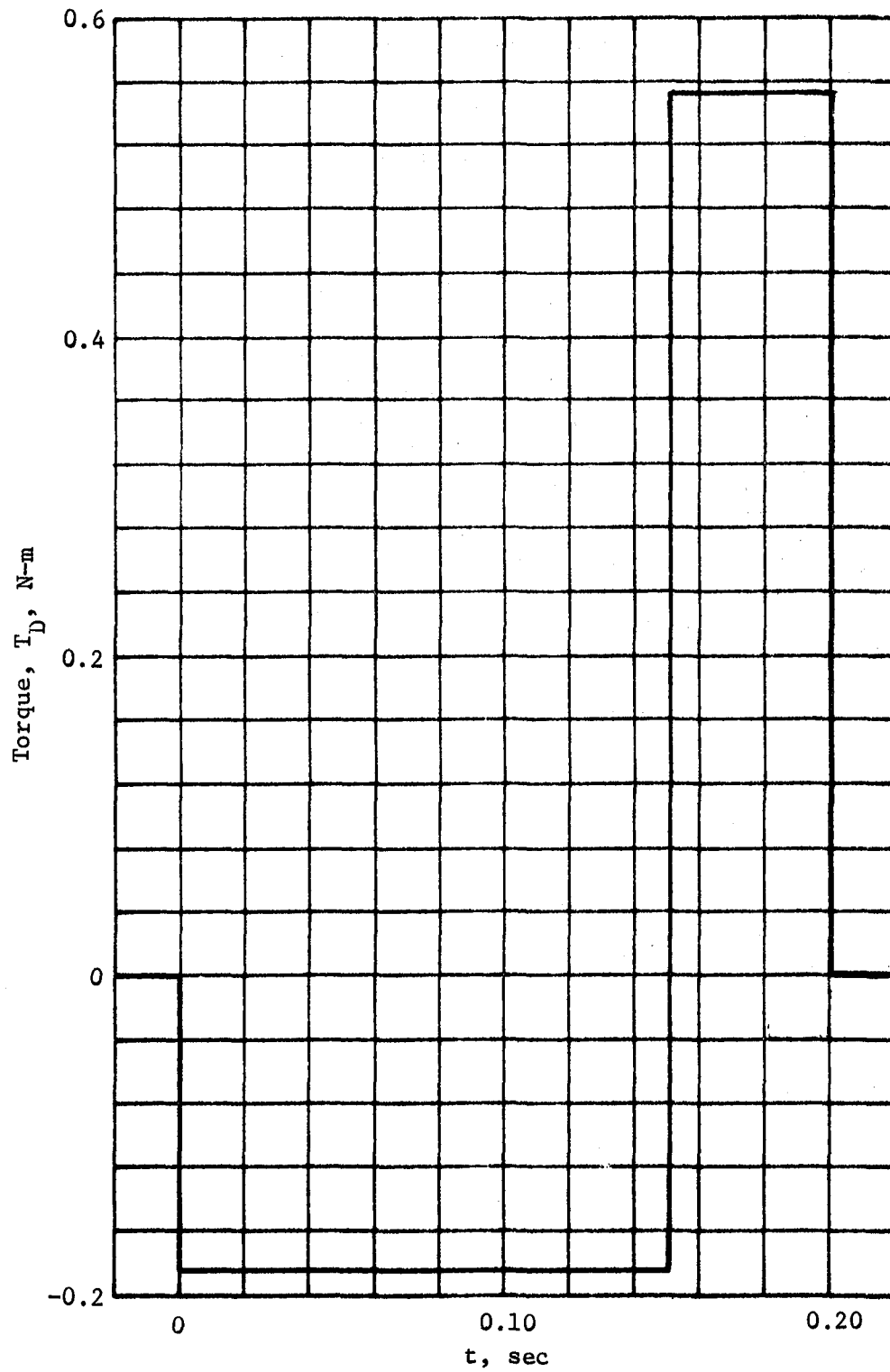


Fig. III-50 Experiment Mass Motion Distrubance Torque T_D

systems are identical. The telescope complement and high-energy arrays are both pointed in azimuth and elevation using two identical wide-angle gimbals. Mechanically the only difference is that the telescope requires a roll ring to point the telescopes in roll; such a requirement does not exist for the high-energy arrays.

The high-energy arrays are pointed by computing the appropriate wide-angle gimbal commands derived from knowing the relative orientation of the high-energy array gimbaling system with respect to the ASM pallet. The attitude of the pallet is computed using a strapdown IMU. This IMU consists of three rate gyros mounted to the pallet and uses the four star trackers mounted to the telescope complement to initialize and update this IMU. IMU strapdown equations are initialized and updated by transforming the attitude of the telescope complement as measured by the star trackers through the telescope gimbaling system to the pallet. The appropriate gimbal angles for pointing the high-energy arrays are then computed knowing the orientation of the high-energy array pointing system with respect to the pallet.

The pointing accuracy associated with this system is limited by (1) the misalignment errors between the telescope pointing system and the pallet; (2) the misalignment errors between the array pointing system and the pallet; and (3) the resolver errors associated with both systems. The resolvers are required to perform the transformations from the telescope to the pallet and from the pallet to the high-energy arrays. The inaccuracies of the star trackers will not significantly add to the inaccuracies of this system because their required accuracies of $5 \mu\text{rad}$ (1 sec) are much smaller than the arrays' pointing requirement of 0.3 mrad (1 min). If the combined system pointing error due to these misalignments and resolver errors are larger than the required pointing accuracy of 0.3 mrad (1 min), star trackers will have to be added to the arrays to perform fine pointing. These star trackers will be used as fine attitude reference sensors.

Normally after the arrays are pointed at the desired target, the wide-angle gimbals are locked because the estimated stability of the baseline CMG stabilized Orbiter is compatible with the stability required by the arrays. One high-energy array, the large modulation collimator, has a modulation requirement. One method of providing this modulation is by physically rotating the entire array back and forth through a small angular displacement using the two wide-angle gimbals. The experimenter onboard the Orbiter could control this modulation by selecting the appropriate gimbal commands. With this system, he could experiment with various modulations, such as sinusoidal and saw tooth.

3. ASM Stabilization and Control Subsystem Actuators

The ASM stabilization and control subsystem consists of two elements: (1) a telescope deployment, pointing, and fine stabilization system; and (2) a high-energy array deployment and pointing system. A great deal of hardware commonality exists between these two systems. The two deployment systems are identical. Each system performs experiment pointing in azimuth and elevation using two identical wide-angle gimbaling mechanisms. The only difference between the two pointing systems is that the telescope complement requires a roll ring for pointing the telescopes in roll axis. Due to the high stabilization requirements of the telescopes, an additional fine stabilization system is added to the telescope system. The high-energy arrays require no additional stabilization system because their stability requirements are compatible with the projected stability of the baseline CMG Shuttle Orbiter control system. Figure III-51 is a sketch of ASM telescope deployment, pointing, and fine stabilization system. The high-energy array deployment and pointing system is identical to that shown in Fig. III-51 with the exception that the flex-pivot/servoed roll ring fine stabilization system is deleted.

The ASM experiments are deployed out of the Shuttle bay using the deployment yoke shown in Fig. III-51. The deployment yoke is driven by a dc motor actuation system that uses a step down gear train to transfer torque from the motor to the yoke. This actuation system is designed to deploy the ASM experiments at a slow speed (0.02 μ rad/sec) to keep the electrical power requirements low. The deployment actuators consist of two redundant dc motors and potentiometers. The two potentiometers are used in an electrical slow down circuit to minimize dynamic loading. The potentiometers measure the position of the yoke, and when the yoke is fully deployed, the outputs of the potentiometers trigger the system's braking system. A face-type multitooth brake is used to hold the deployed yoke in a fixed position relative to the azimuth table shown in Fig. III-51. The jamming action of the clutch teeth should provide adequate stiffness.

The experiments are pointed in azimuth using the azimuth table shown in Fig. III-51. The table is rotated with respect to the pallet by using rolling element bearings. The azimuth table is driven by a direct drive redundant actuation system. The actuator consists of redundant dc motors, tachometers, and resolvers. The resolvers are used to measure the rotational displacement of the table with respect to the pallet.

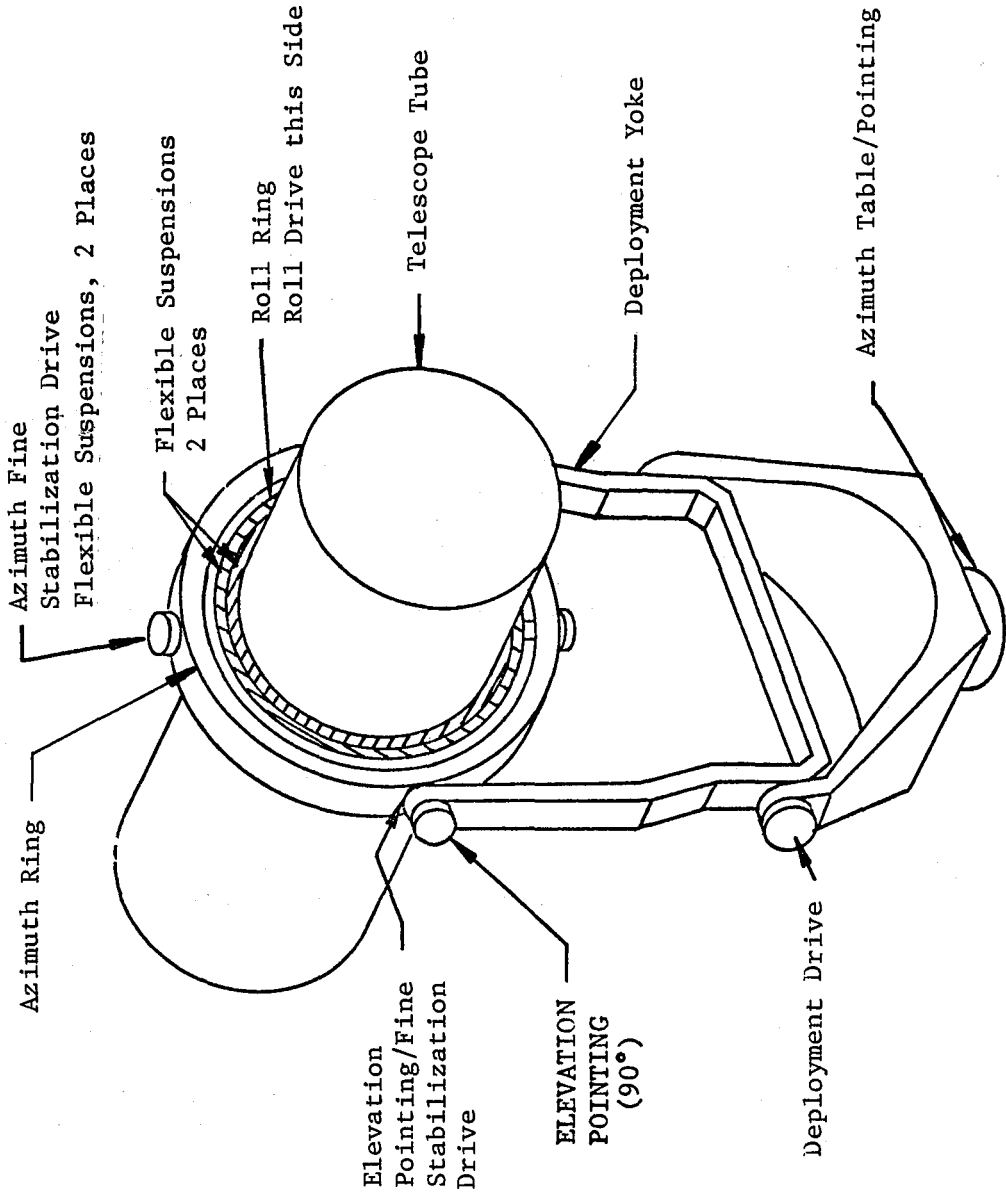


Fig. III-51 Baseline Telescope Deployment, Pointing, and Fine Stabilization System

Elevation pointing is achieved by the elevation gimbal shown in Fig. III-51. Like the azimuth pointing system, the actuators that drive the rolling element elevation gimbals are redundant. Identical actuators are mounted diametrically opposite each other on the deployment yoke. The actuators are direct drive devices identical to those used to drive the azimuth table. These actuators consist of two dc motors, two tachometers, and two resolvers.

For the ASM telescope system, a fine stabilization system is added to the deployment and pointing systems. The telescopes are stabilized in azimuth and elevation by flex-pivots and in roll by a rolling element roll ring. This roll ring is also used to point the telescopes in roll. The two elevation flex-pivot assemblies containing the direct drive dc torquers, dc tachometers, and position indicators are mounted on the inside of the elevation pointing shaft on the elevation stabilization shaft. The locations of these two shafts are shown in Fig. III-51. The mechanical output portion of the flex-pivot assemblies are attached to the azimuth stabilization gimbal ring. This gimbal ring acts as the flex-pivot's bearing support. In between the elevation pointing and stabilization shafts is a braking assembly that locks the pointing system when the stabilization system is operating and locks the stabilization system when the experiment is being pointed.

The azimuth flex-pivot stabilization assemblies are mounted to the azimuth ring diametrically opposite each other, as shown in Fig. III-51. The mechanical output portion of these flex-pivot assemblies are attached to the outer ring of the servoed roll ring assembly. A braking assembly is included to lock the flex-pivots to the azimuth ring during experiment pointing. The flex-pivot actuators used are the same as those used on the azimuth axis.

The roll ring shown in Fig. III-51 is used to point and stabilize the telescope complement in roll. One roll actuator, mounted to the outer roll ring, is used to drive this combined pointing and stabilization system. This actuator drives a spur gear that mates with a ring gear mounted on the inner roll ring to produce the required roll motion. The actuator contains redundant dc torquers, tachometers, and position indicators. A gear train is used to link the position indicator to the output actuator shaft to produce a one-to-one position correspondence.

All of the actuators used for pointing and stabilization utilize direct drive DC torque motors. The main characteristics of a direct-drive actuator are: (1) high coupling stiffness; (2) high torque-to-inertia ratio at the load shaft; (3) high resolution since dead zones and backlash associated with gear trains are eliminated; (4) high reliability; and (5) long life. The dc motors

are characterized by : (1) a fast response; (2) a slow operating speed capability; and (3) a linear operation within their operation region. The use of dc motors simplifies the design of the actuators because easily available dc power is used. The chief reasons for selecting direct-drive dc motors for driving the pointing and stabilization systems are their high torque capability, linearity, and high resolution capability.

A preliminary actuator design was performed. Table III-17 lists the various ASM actuators and their projected characteristics. Drawings of the actuators are included in Chapter IV of this volume.

4. Selected Shuttle Orbiter and ASM Experiment Pointing and Stabilization and Systems

Figure III-52 is a functional block diagram of the ASM guidance, navigation and control (GN&C) subsystem. The GN&C subsystem hardware complement consists of

- 1) Three double gimbal control moment gyros (DGCMGs);
- 2) Two inertial measurement unit (IMU) packages (three gyros per package);
- 3) Four strapdown star trackers;
- 4) One telescope fine attitude error sensor;
- 5) Two wide-angle gimbal experiment pointing systems (one for the telescopes and one for the high-energy arrays);
- 6) One telescope fine stabilization system (includes IMC where necessary).

a. *Double Gimbal Control Moment Gyros* - Three Skylab ATM DGCMGs are used to stabilize the Shuttle Orbiter in an X-POP attitude. The CMGs are desaturated using small angle gravity gradient desaturation maneuvers during the portion of the orbit when the telescope's primary celestial target is occulted by the earth.

Table III-17 ASM Gimbal System Actuators and Characteristics

Actuator	Torque Stall, lb-ft	NLS, rad/sec	Tach Sensor, V/rad/sec	Pos Ind Accuracy, μ rad	Motor Stall, CUR, Amps	Bearing System
Elevation Pointing	11.0	22	10.0	25	11.0	Rolling Element
Elevation Stabilization	7.0	27	25.0	25	8.7	Flex Pivot
Azimuth Table Pointing	11.0	22	10.0	25	11.0	Rolling Element
Azimuth Stabilization	7.0	27	35.0	25	8.7	Flex Pivot
Deployment	90	0.017	Open Loop or Rate Via Pos. Ind.	9 mrad	0.1	Rolling Element
Roll Ring	1.2	48	5.2	9 mrad	2.6	Rolling Element

Note: 1. Motor excitation = 28 Vdc.
 2. Deployment actuator motor has high voltage winding, excited at 28 Vdc to achieve low NLS and to simplify gear train.
 3. All actuators direct drive except deployment actuator.

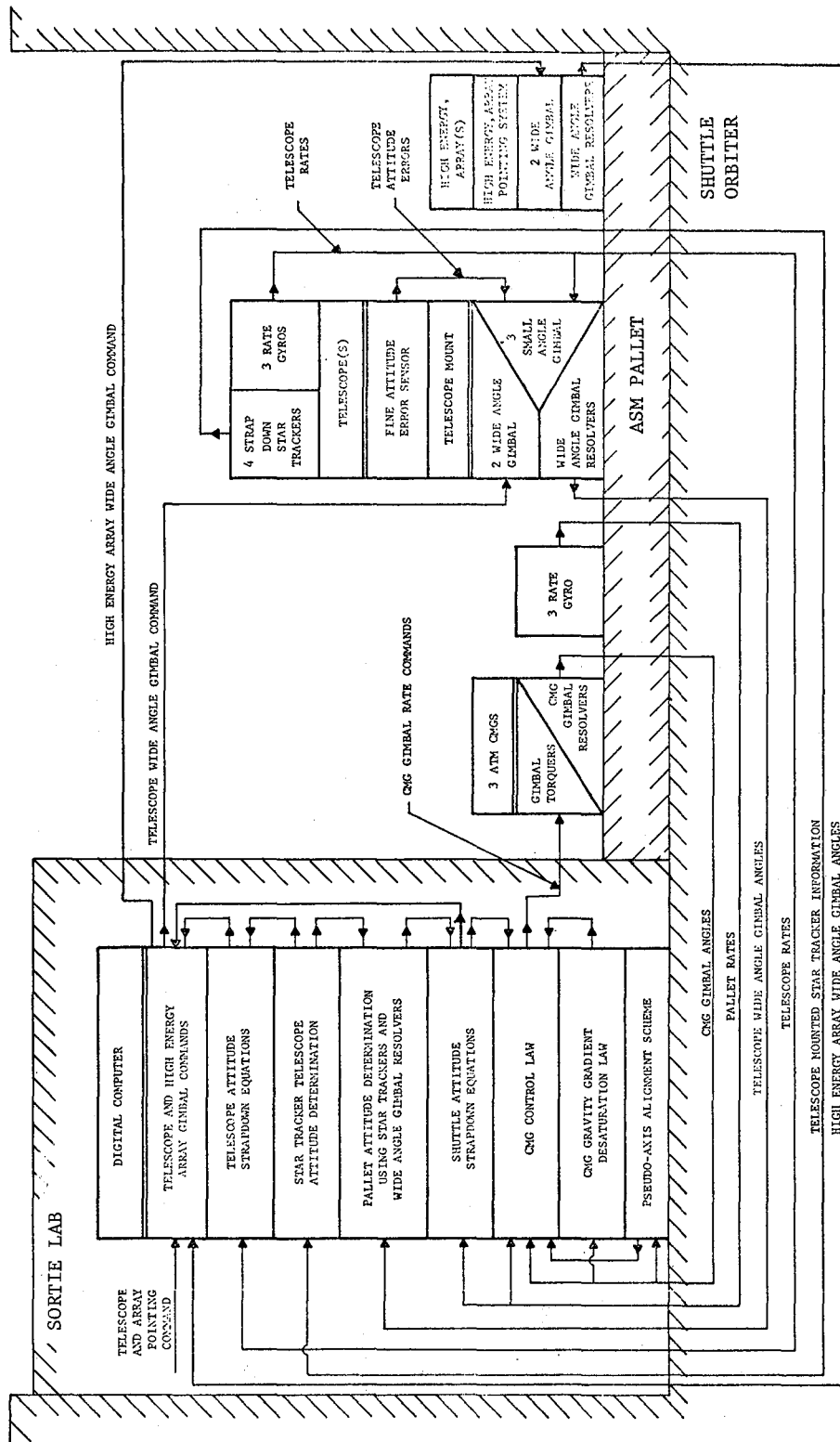


Fig. III-52 Functional Block Diagram of ASM Stabilization and Control Subsystem

The selection of a CMG system instead of a reaction control system (RCS) was primarily made on the basis of experiment contamination. CMGs are vituually contamination-free devices. An RCS system, on the other hand, provides vehicle control by expelling mass particles that are a source of experiment contamination. Due to the severe particulate experiment contamination requirements, it becomes highly undesirable to fire an RCS during an experiment. The contaminates from an RCS could degrade or cause the termination of some of the ASM experiments.

b. Inertial Measurement Unit (IMU) Packages - The ASM equipment complement consists of two IMU packages; one package is mounted to the ASM pallet and the other one is mounted to the telescope. The IMU mounted to the pallet senses Shuttle Orbiter body rates used by the CMG control system to stabilize the Orbiter and to input a set of strapdown equations for computing the Shuttle Orbiter attitude. This computed telescope attitude information is used by the telescope's wide-angle gimbal pointing system to point the telescope at its desired target. The outputs of these telescope-mounted IMUs, plus attitude errors derived from the telescope fine attitude sensor, are used by the telescope's fine stabilization system to furnish the additional stabilization required by the telescopes.

c. Strapdown Star Trackers - Four strapdown star trackers are mounted to the telescope and are used to determine the telescope's attitude. This telescope attitude information is used to update both the Shuttle Orbiter and telescope strapdown equations. The attitude of the Shuttle Orbiter is determined by transforming the attitude of the telescope as measured by the star trackers through the telescope's two wide-angle gimbals to the ASM pallet. To accurately point the telescopes, the accuracy of the star trackers must be within the $10 \mu\text{rad}$ ($2 \overline{\text{sec}}$) pointing requirement of the telescopes.

d. Telescope Fine Attitude Error Sensor - The telescope fine attitude error sensor is used to stabilize the telescope complement and to drive any image motion compensation system required. The scientific telescope or a separate boresighted sensor is used to derive the telescope attitude error information, depending on the telescope complement being flown.

e. *Two Wide-Angle Gimbal Experiment Pointing Systems* - The Shuttle Orbiter is stabilized in an inertial X-POP attitude. The ASM telescopes and high-energy arrays are then pointed with respect to the Shuttle Orbiter using two separate wide-angle pointing systems as shown in Fig. III-52. The two pointing systems consist of two wide-angle gimbals; one points the experiments in azimuth and the other one points them in elevation. The telescope pointing system requires an additional roll ring to point the telescopes in roll.

f. *Telescope Fine Stabilization System* - The stability of a CMG stabilized Shuttle Orbiter is estimated to be 0.3 mrad (1 $\overline{\text{min}}$). The telescope external body stabilization requirements are 0.5 μrad (0.1 $\overline{\text{sec}}$) in pitch and yaw and 25 μrad (5 $\overline{\text{sec}}$) in roll. To meet the above telescope stability requirements, an additional three-degree-of-freedom telescope fine stabilization is necessary. The telescopes must be completely isolated from Shuttle Orbiter perturbations in pitch, yaw, and roll. For the ASM high-energy arrays, no additional stabilization is required because the stability capabilities of the Shuttle Orbiter are sufficient.

g. *ASM GN&C Subsystem Interfaces* - The ASM GN&C subsystem has two system interfaces. The two system elements that interface with the ASM GN&C subsystem are:

- 1) CMG control law;
- 2) CMG gravity gradient desaturation law;
- 3) Pseudo-axis alignment scheme;
- 4) Shuttle Orbiter attitude strapdown equations;
- 5) Telescope attitude strapdown equations;
- 6) Telescope and high-energy array wide-angle gimbal pointing commands;
- 7) Star tracker telescope attitude determination;
- 8) ASM pallet attitude determination.

Table III-18 lists the functions and purposes of the above GN&C subsystem computer programs.

Table III-18 Function and Purpose of GN&C Subsystem
Digital Computer Programs

Programs	Function (to compute)	Purpose
CMG Control Law	CMG gimbal rate commands	To stabilize and maneuver Shuttle Orbiter
CMG Gravity Gradient Desaturation Law	Shuttle Orbiter maneuvers to be performed during CMG desaturation period	To desaturate CMGs
Pseudo-Axis Alignment Scheme	Shuttle Orbiter pseudo-axis alignment maneuvers to be performed at the end of the CMG desaturation period	To minimize angular momentum stored in CMGs
Shuttle Orbiter Attitude Strapdown Equations	Shuttle Orbiter attitude quaternions	To compute Shuttle Orbiter attitude
Telescope Attitude Strapdown Equations	Telescope attitude quaternions	To compute ASM telescope attitude
Telescope and High-Energy Array Wide-Angle Gimbal Pointing Commands	Telescope and high-energy array pointing gimbal rate commands	To point telescope and high-energy arrays with respect to the Shuttle Orbiter
Star Tracker Telescope Attitude Determination	Telescope attitude	To update telescope attitude strapdown equations
ASM Pallet Attitude Determination	ASM pallet attitude	To update Shuttle Orbiter attitude strapdown equations

D. ELECTRONIC SYSTEMS ANALYSIS

The electronic subsystems required to support the baseline Astronomy Sortie payloads include the controls and display (C&D) subsystem, the data management subsystem, and the electrical power subsystem. (An analysis of the stabilization and control system is included in Section C and is not repeated in this section.) Each scientific instrument and each payload combination established as a baseline in Volume II, Book 1, was analyzed to determine the type and amount of support required from these subsystems during the seven-day Sortie mission. Special emphasis has been placed on the operational modes of each payload combination. Function C&D requirements are satisfied by the recommended configuration and additions to the Sortie Lab C&D subsystem. Interfaces to the subsystem are through the data management subsystem for all interrelated operations and displays. Direct interfaces between the payloads and the C&D subsystem include caution and warning and alert signals and those functions related to initial setup and deployment. A significant portion of the scientific data from the primary (telescope) payloads is in the form of photographic film. Electronic data associated with these payloads is limited to instrument engineering, status, and control or command functions. Film cassettes tailored to the instrument and to the mission duration preclude the requirement for EVA during the limited data-taking period. Electronic data in the form of analog video for monitoring and all digital data to and from the payloads are handled through computer interface modules dedicated to each mission payload. The modules also receive the commands to control power to the payloads and related subsystems. Power from the Sortie Lab is provided on feeder lines to load center switches used with each payload and subsystem.

The Sortie Lab, in all cases, is assumed to be capable of providing the space to accommodate the payload-related controls and displays. The data management subsystem in the Sortie Lab will receive formatted digital data for recording and storage onto tape and for real-time display to the scientist-observer for monitoring and observation, or for near real-time transmission to the ground-based scientist. Power to the payloads and for pallet-mounted subsystems and subsystem components is derived from the Sortie Lab power subsystem.

1. Controls and Displays

The design of the C&D subsystem has developed based on the operational and design requirements levied by the experiment payloads, supporting subsystems, and crew systems. Those requirements, constraints, and program guidelines which are considered major drivers are:

- Payload C&D requirements limited to seven-day Sortie missions;
- Payload command and data functions managed via a centralized data management computer;
- Minimum hardware interface to the Sortie Lab C&D console;
- Minimal on-board processing of experiment data;
- Processing requirements not inclusive to C&D functional definition;
- Normal experiment operation by one unsuited crewman.

a. Experiment and Payload Requirements - The C&D subsystem in the Sortie Lab is required to provide for all of the mission payload controls and displays. It allows the scientific crewman to interface with the payload support subsystem and with the payload experiments. The basic functional control and display requirements are: experiment control, experiment checkout, experiment data monitoring, subsystem control, subsystem checkout, video monitoring and control, caution and warning displays and alarms, and audio distribution and control. The C&D functional and hardware requirements were established for each Astronomy Sortie experiment by analyzing proposed operational characteristics of the baseline telescopes and arrays. These functions and the display or component associated with the function are included in tables of each Baseline Experiment Definition Document (BEDD) found in Book 2 of Volume II.

An analysis of the C&D functional requirements provided commonality matrices for both the primary experiments (telescopes) and for the secondary experiments (high-energy arrays). These matrices present only those control and display requirement functions that are common among two or more telescopes or arrays. The matrix for the telescope is given in Table III-19. A total of 148 functions were initially identified from the BEDDs. Table III-19 shows that 83 of those functions are common between at least two experiments. This results in a 56% commonality between functions for the telescopes. The commonality matrix for the high-energy arrays is given in Table III-20. For the arrays, 74 functions were identified in the BEDDs and Table III-20 shows that 47 of these functions are common between at least two arrays.

Table III-19 Control and Display Commonality Matrix: Telescope

Function	Strato- scope III	X-Ray Tele- scope	IR Telescope	Photohelio- graph	XUV Spectroheli- ograph	WL Coronagraph Assembly
<u>1. General</u>						
Aperture Door	X	X	X	X	X	X
Launch Locks	X	X	X	X	X	
Thermal Control	X	X	X	X	X	X
Main Power	X	X	X	X	X	X
Intensity Data		X			X	
Mode Select					X	X
Mode Status					X	X
Primary Data Display	X			X	X	X
<u>2. Alignment and Focus</u>						
Translate X	X		X	X		
Translate Y	X		X	X		
Rotate X	X		X	X		
Rotate Y	X		X	X		
Focus	X		X	X		
Monitor HV		X		X	X	X
<u>3. Camera</u>						
Filter Select	X	X				
Mode Select	X			X		
Mode Status	X	X		X		
Frame Rate		X		X	X	
Frames Remaining		X		X	X	X
Filter Heater		X		X	X	
Camera Power				X	X	
<u>4. Spectrograph/ Spectrometer</u>						
Calibration	X	X	X			
Scans Completed	X	X				
Mode Status	X	X	X			
Scan Rate		X	X			
Slit Select	X	X				
Total	(17)	(16)	(12)	(17)	(13)	(8)

Table III-20 Control and Display Commonality Matrix: High-Energy Arrays

Function	Large Area X-Ray Detector	Low Background X-Ray Detector	Large Modulator Collimator	Gamma-Ray Spectrometer	Wide Coverage X-Ray Detector	Narrow Band Spectrometer-Polarimeter	Flat Crystal Spectrometer
Main Power	X	X	X	X	X	X	X
High Voltage Power	X	X	X	X	X	X	X
Calibration	X		X		X	X	X
Experiment Status	X	X	X	X	X	X	X
X-Ray Rate	X		X			X	
X-Ray (α or Crystal) Spectrum (PHA)	X	X	X	X	X	X	X
X-Ray Spectrum Select	X		X			X	
Gas Purge	X		X				
Exposure Duration	X		X				
PHA Resolution		X					X
Scan Mode Select	X						X
Total	10	5	9	4	5	7	7

This results in a 64% commonality between functions for the arrays. These commonality matrices and the unique requirements of each experiment are used as basic inputs to define the C&D console concepts in terms of size, weight, and power requirements.

b. Console Concept Analysis - Experiment functional requirements were reviewed for six telescopes and seven arrays. The C&D components necessary to perform the functions were defined and three console concepts were generated on the initial assumption of using one telescope and one array per payload. The concepts are discussed below with emphasis on the major advantages and disadvantages of each.

Mission Dedicated Console - To derive a concept for a mission dedicated console, each experiment functional requirement, control and/or display, number of components required, component weight, panel area required for installation (including nomenclature), and power requirements for that component were identified. For each experiment (both telescopes and arrays) the weight and area totals were adjusted to include necessary additional area requirements for component arrangement on the panels and estimated weights of console structure, wiring, cooling, etc. No additional power requirements were shown although some loss would occur. A grand total of weight, area, and power was derived for each experiment.

In addition to controlling and monitoring the experiment functions, the scientific crewman must also take care of the experiment supporting subsystems such as power, lighting, data management and recording, event timing, pointing and alignment, sensor information, thermal control, caution and warning, etc. From past experience, it can be shown that the controls and displays necessary to perform these functions can be considerable where each function requires a dedicated control or display. Based on a similar analysis conducted as part of the RAM study, the controls and displays for this additional experiment supporting subsystem have been estimated at 78.93 kg (174 lb), requiring a panel area of 0.24 m² (370 in.²).

The results of this assessment of dedicated controls and displays are presented in Table III-21. For each mission, a separate dedicated control and display console would have to be constructed. This console would encompass the controls and displays necessary to control the telescope, array, and support subsystems. The consoles will vary in weight from 141 to 196 kg (311 lb to 433 lb) and vary in panel area from 0.47 to 0.67 m² (728 to 1032 sq in.). The average console for all missions would weight 155 kg (342 lb) and have a panel face area of 0.55 m² (854 sq in.).

Table III-21 Mission Dedicated Console Requirements

Telescope Panel	Weight, lb	Panel Area, in. ²	Arrays	Weight, lb	Panel Area, in. ²
Stratoscope III	121	322	Large Area X-Ray Detector	63	140
X-Ray Telescope	179	402	Low Background X-Ray Detector	80	260
IR Telescope	79	218	Large Modulation Collimator	64	150
Photoheliograph	116	356	γ-Ray Spectrometer	64	162
XUV Spectroheliograph	91	254	Wide Coverage X-Ray Detector	80	174
Coronagraphs	81	234	Narrow Band Spectrometer/ Polarimeter	68	184
Estimated Experiment Support Subsystem C&D	174	370	Crystal Spectrometer	97	231
Worst Case = 433 lb, 1032 in. ²					
Best Case = 311 lb, 728 in. ²					
Average Console = 342 lb, 854 in. ²					
Note: Additional weight and panel arrangement factors are included.					

Common/Dedicated Console - The commonality analysis was reviewed to determine the effect of providing common panels to be shared by the various experiments from mission to mission. Some updating of the commonality matrix was necessary because the definition of components to perform functional requirements changed the degree of commonality in certain instances. Control and display component requirements were determined for common functions for both telescopes and arrays. As in the case of dedicated panels, the total component weight and area is adjusted to provide a console panel weight and area estimate.

The results of this portion of the study are summarized in Table III-22. For this concept, one C&D console would be constructed for the ASM. The console would have three panels that would remain the same for the total program and two panels that would change from mission to mission. The common telescope panel would weigh 52 kg (115 lb) and occupy 0.2 m² (325 in.²). The common array panel would weigh 29.5 kg (65 lb) and occupy 0.1 m² (151 sq in.²). The experiment support subsystem panel would be the same as is the dedicated concept: 79 kg (174 lb) and 0.24 m² (370 in.²). The two dedicated areas of the console were sized on the basis of the worst-case requirement. All of these requirements results in a console estimated to weigh 251 kg (554 lb) with a total panel face area of 0.865 m² (1297 in.²). Although the console would remain the same size for each flight, the weight could reduce because of the smaller number of dedicated components on some missions.

Although the console in this concept would be larger and heavier than in the completely dedicated concept, it should be more effective because only one console would need to be developed for the total program compared to six or more of the dedicated concepts. In addition to the standard console, it would be necessary to develop 13 additional chassis/panels to take care of the unique experiment requirements.

Table III-22 Common/Dedicated Console Requirements

Telescopes	Weight, lb	Panel Area, in. ²	Arrays	Weight, lb	Panel Area, in. ²																																				
Common Telescope Panel	115	325	Common Array Panel	65	151																																				
Unique Additional Panel Requirements			Unique Additional Panel Requirements																																						
Stratoscope III	15	35	Large Area X-Ray Detector	2	10																																				
X-Ray Telescope	156	296	Low Background X-Ray Detector	44	155																																				
IR Telescope	65	128	Large Modulation Collimator	3	21																																				
Photoheliograph	20	86	γ-Ray Spectrometer	20	71																																				
XUV Spectroheliograph	3	39	Wide Coverage X-Ray Detector	35	100																																				
WL Coronagraph	5	39	Narrow Band Spectrometer/ Polarimeter	8	59																																				
			Crystal Spectrometer	53	37																																				
Estimated Experiment Support Subsystem C&D	174	370																																							
<p>To accommodate all flights, the common dedicated concept must consist of the following:</p> <table style="width: 100%; border-collapse: collapse;"> <tr> <td style="width: 40%;">Common Telescope Panel</td> <td style="width: 10%;">-</td> <td style="width: 10%;">115 lb</td> <td style="width: 10%;">325 in.²</td> <td style="width: 10%;"></td> <td style="width: 10%;"></td> </tr> <tr> <td>Common Array Panel</td> <td>-</td> <td>65 lb</td> <td>151 in.²</td> <td></td> <td></td> </tr> <tr> <td>Worst Case Telescope Addition</td> <td>-</td> <td>156 lb</td> <td>296 in.²</td> <td></td> <td></td> </tr> <tr> <td>Worst Case Array Addition</td> <td>-</td> <td>44 lb</td> <td>155 in.²</td> <td></td> <td></td> </tr> <tr> <td>Exp Support Subsystems</td> <td>-</td> <td>174 lb</td> <td>370 in.²</td> <td></td> <td></td> </tr> <tr> <td colspan="3" style="text-align: center;">Total</td> <td style="border-top: 1px solid black;">554 lb</td> <td style="border-top: 1px solid black;">1297 in.²</td> <td></td> </tr> </table>						Common Telescope Panel	-	115 lb	325 in. ²			Common Array Panel	-	65 lb	151 in. ²			Worst Case Telescope Addition	-	156 lb	296 in. ²			Worst Case Array Addition	-	44 lb	155 in. ²			Exp Support Subsystems	-	174 lb	370 in. ²			Total			554 lb	1297 in. ²	
Common Telescope Panel	-	115 lb	325 in. ²																																						
Common Array Panel	-	65 lb	151 in. ²																																						
Worst Case Telescope Addition	-	156 lb	296 in. ²																																						
Worst Case Array Addition	-	44 lb	155 in. ²																																						
Exp Support Subsystems	-	174 lb	370 in. ²																																						
Total			554 lb	1297 in. ²																																					
<p><u>Note:</u> Additional weight and panel arrangement factors are included.</p>																																									

Hybrid Console - Only the ASM has been considered so far in this analysis. If the ASM is considered just one program in a larger group of Shuttle Sortie programs, then it is necessary to look for commonality on a much broader base. This has been done on a gross basis, as part of the RAM study contract. The RAM control and display concept trade study results show the most cost-effective control and display concept to be that of a hybrid universal/dedicated console. This concept requires the development of a single console to serve the requirements of all Sortie experiments. Primary control and monitoring of experiments and subsystems is performed through computer interface. The cathode ray tubes (CRTs) are capable of presenting both video and multiformat, computer-generated information. Computer data can be presented as either alphanumeric or graphically. Data entry is provided by keyboard or multi-axis hand controller. Through the keyboard the crewman can initiate or command experiment or subsystem functions, request more detailed information, or perform troubleshooting functions. Mission-to-mission differences are accommodated primarily through software routine adaptations rather than extensive hardware modification. However, to ensure complete interpayload flexibility, experiment-dedicated controls and displays can also be added to accommodate experiment-peculiar requirements. This is facilitated by the use of modularized interchangeable chassis. The hybrid console has a total panel area of 1.33 m² (2070 in.²) and is estimated to weigh 313 kg (690 lb). Although this is somewhat larger than the ASM common/dedicated console concept, it should be pointed out that the hybrid console also provides for the control and monitoring of module subsystems that are not considered in the present ASM study. These include such subsystems as RCS, ECS, TCS, OCS, control data management, electrical power, etc.

c. Recommended System - The recommended ASM payload control and display console is a hybrid configuration, combining computer interactive multipurpose controls and displays with conventional function-dedicated controls and displays. The interactive portion of the console consists of multipurpose CRT indicators and appropriate command and data entry keyboards interfaced with a central data management computer. The dedicated portion of the console comprises modular rack-type chassis that are provided based on specific unique payload control and display requirements. This concept provides a flexible cost-expedient C&D system that minimizes the impact of satisfying the requirements of the various ASM payloads. The versatility of the software-oriented interactive displays provides the capability of displaying information

in a multitude of formats. The optimum format for each instrument and support subsystem may be determined and implemented without impacting the basic hardware configuration of the system. Additionally, as greater amounts and more in-depth information may be displayed than with function/hardware dedicated controls and displays (such as the Skylab ATM control and display console), the crew dependence upon ground communications may be significantly reduced. Reconfiguration of the system to accommodate the differing requirements of the various payload configurations is implemented primarily by software formatting. Hardware modification of the console is required to accommodate the experiment mission-peculiar add-ons. These dedicated controls and displays are incorporated as modular add-ons within the console framework with power provided by the console electrical power distribution subsystem. The dedicated controls and displays are implemented via a hardwire interface with the payload, bypassing the data management computer, and provide the experimenter with an added degree of flexibility in the implementation of unique requirements.

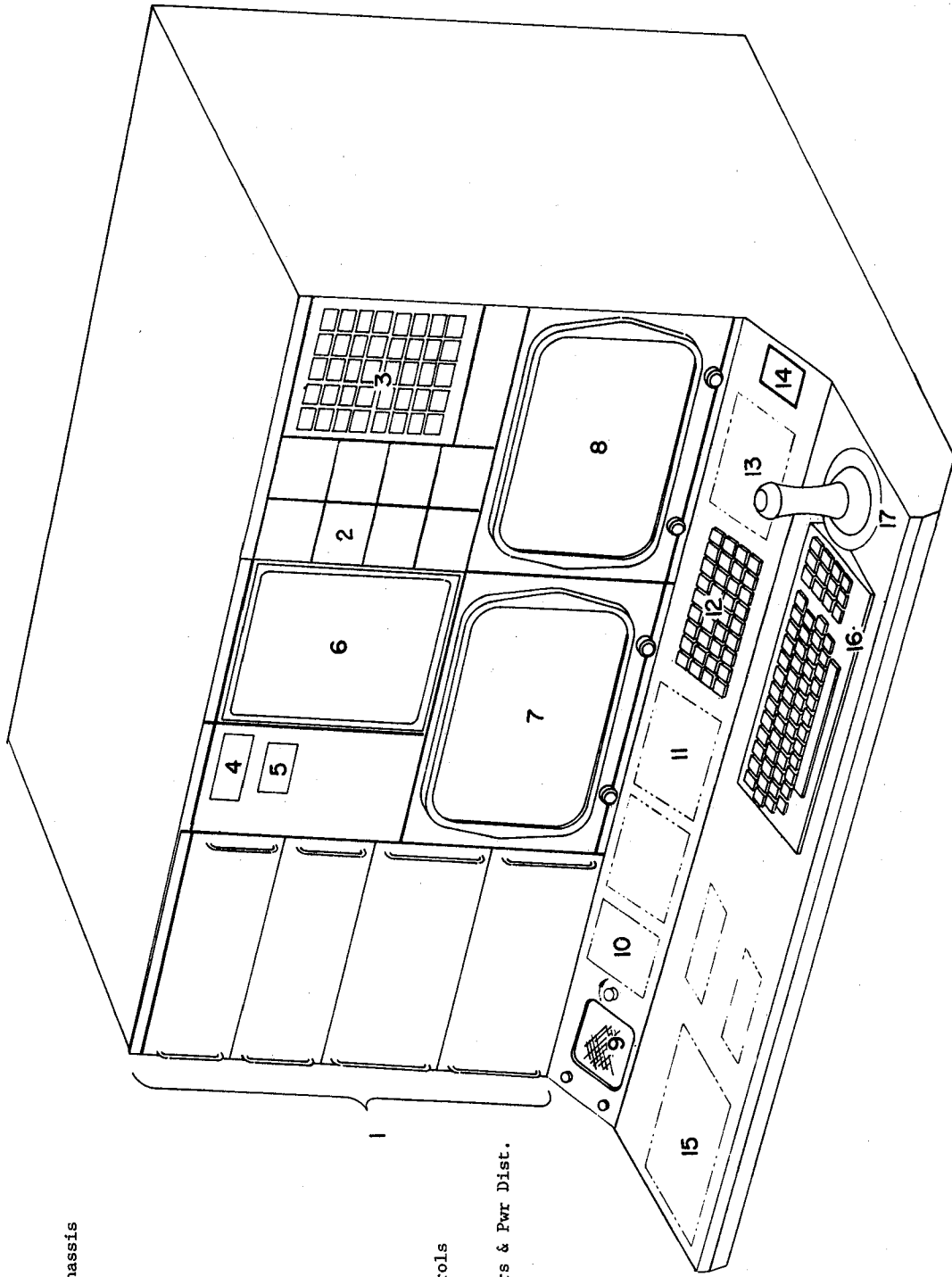
The ASM payload C&D console has been designed with a primary aim of satisfying the experiment and experiment support subsystems C&D requirements. A brief review of related study efforts indicates that both the Sortie Lab conceptual design and the Sortie RAM studies concluded that the module subsystems did not require continuous crew monitoring of parametric data and that monitoring should be accomplished at the experiment console. Considering that the current ASM baseline provides for a two-man crew, operating in shifts with a minimum of overlap, a more efficient use of crew timelines appears feasible if module subsystems are monitored and corrective actions initiated from the payload C&D console. Therefore, a caution and warning terminal and subsystems advisory indicators are included in the console to provide the scientific crewman with immediate visual cues of malfunctions without requiring translation to an alternative work station. In response to the malfunction cue, the crewman addresses the data system to provide the appropriate subsystem data display on one of the CRTs and commands corrective action via the keyboards.

The overall console configuration is illustrated in Fig. III-53. Outline and panel layout drawings of the console appear in Chapter IV. The console provides the command center for payload operation by a single crewman; however, two-crewman operation may be accommodated, with the second crewman limited to supporting activities, primarily associated with operation of the experiment-dedicated equipment chassis.

The center and right side areas contain the integrated portion of the console, which is common to all payloads. The interactive subsystem, the CRTs, and keyboards allow the display of information from a variety of sensors. The subsystem interfaces with the data management computer and with the experiment field monitors, allowing either CRT to display video and/or computer data in a variety of display combinations. Thus, for example, the left CRT may present experiment video information with limited computer data superimposed, such as digital readouts of intensity data while the right CRT presents a full alphanumeric display of experiment data. The balance of the upper console areas provides payload and module advisory indicators, a caution and warning terminal, mission and event timers, and a microfilm viewer for display of procedures. The lower portion of the console provides an intercom unit, console lighting controls, the function and alphanumeric keyboards, monitor select switches, payload power off emergency switch, console power distribution controls, and a three-axis hand controller for target acquisition.

d. System Interfaces

Data Management - The C&D console interface shown in Fig. III-54 provides a software-oriented interface, via a computer interface unit (CIU), with a centralized data management computer. This interface provides the primary path for the operation and monitoring of the ASM payloads, adapting to payload differences by software modification. Hardwire interfaces have been identified for the caution and warning subsystem and for the experiment-payload-unique controls and displays.



- 1 Dedicated Experiment Chassis
- 2 Advisory Experiment
- 3 Caution & Warning
- 4 Mission Time
- 5 Event Time
- 6 Microfilm Viewer
- 7 CRT 14" Experiment
- 8 CRT 14" Experiment
- 9 ICOM Speaker
- 10 ICOM Controls
- 11 Lighting
- 12 Function Keyboard
- 13 Monitor Selection Controls
- 14 Console Emergency Pwr
- 15 Console Circuit Breakers & Pwr Dist.
- 16 Alphanumeric Keyboard
- 17 3 Axis Controller

Fig. III-53 ASM Payload Control and Display Console

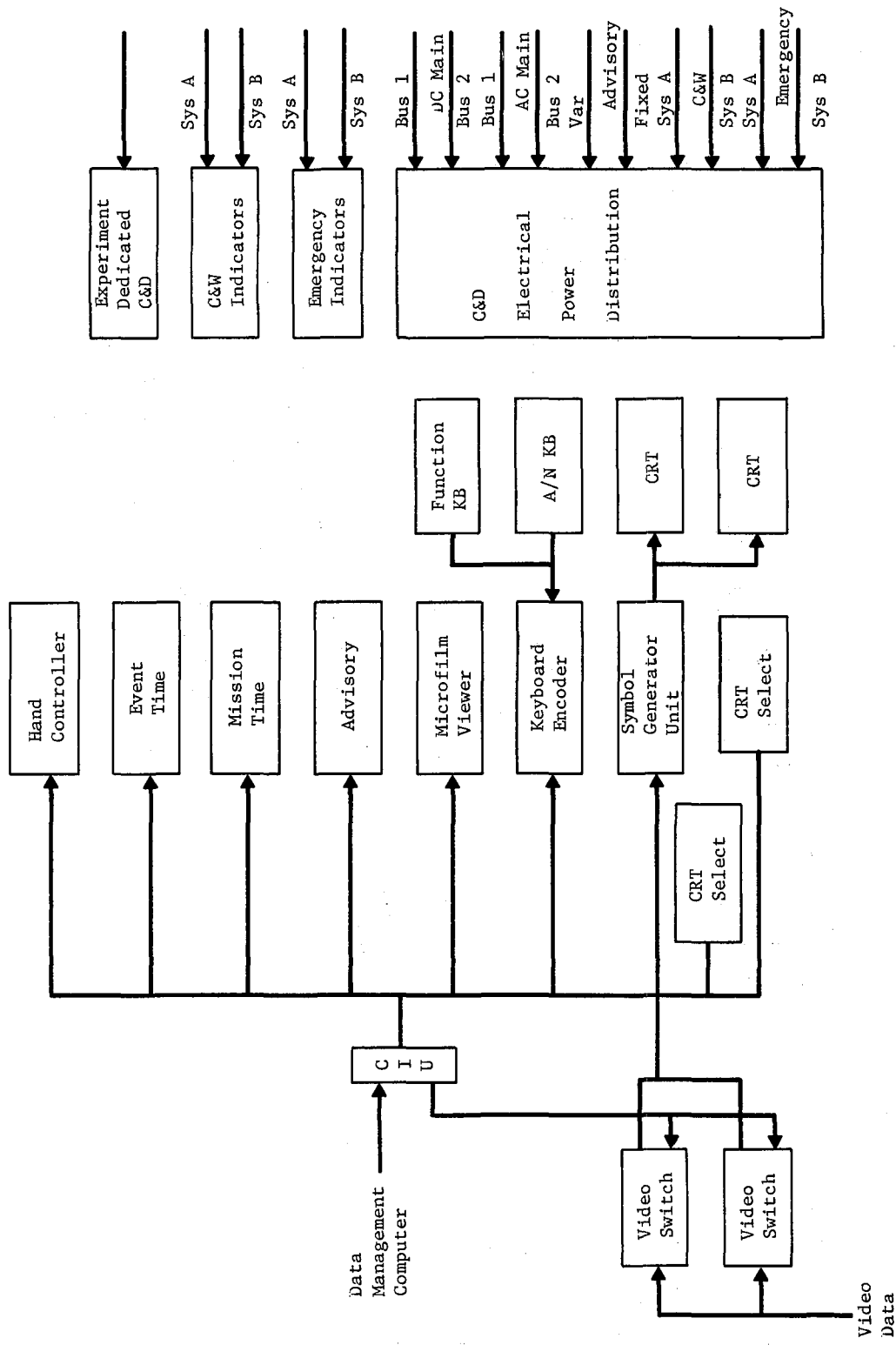


Fig. III-54 C&D Console Interface Diagram

The function and alphanumeric keyboards provide the means for command and data entry. Category selection made using the function keyboard provides addressing for the alphanumeric keyboard from which discrete commands and data entries are made. The symbol generator unit (SGU) provides two channels each of video computer data and drives the two CRT indicators. Both channels are identical, allowing all data to be presented on either CRT. Additional components interfacing with the CIU include the microfilm viewer, advisory indicators, mission and event timers, and a three-axis hand controller. Table III-23 summarizes the component computer interfaces.

Table III-23 C&D Console to CIU Interface

C&D Component	Quantity	Interface Description
Hand Controller	1	Analog, 28 V, 800 Hz
Event Timer	1	Discrete
Mission Timer	1	7 Digit BCD
Advisory	80	Discrete, 5 vdc Ground Return
Microfilm Viewer	1	Digital, 13-Bit Binary
Keyboard	1	Digital, 32-Bit Word
Symbol Generator	1	Digital, 12-Bit Data Word

Caution and Warning - A total of 30 caution and warning (C&W) parameters have been defined. To allow for growth, space has been allocated for 40 C&W indicators, master alarm memory, and the related power and test controls. The criticality of the subsystem dictates a redundant hardware interface providing for a system A and a system B signal to each indicator. Redundant buses, isolated from the console power distribution networks, are provided separately for the emergency and C&W indicators. The test controls allow the crewman to perform end-to-end verification of each redundant subsystem path. Isolation of malfunctioning indicators within the console is performed using the lamp test selector switch.

Electrical Power - The console electrical power interface assumes redundant bus feeds and cabling that are maintained internal to the console power distribution main and subbusses. Overload protection is provided at the interface by the console main circuit breakers.

Table III-24 lists, by component, the console power dissipation exclusive of the experiment mission-peculiar add-on C&D. The total power dissipation with all components energized is 565.1 W. The nominal dissipation is approximately 415 W, assuming that all components except the tone generator, C&W annunciators (three assumed energized), and advisory annunciators (eight assumed energized during mission experiment operations).

Thermal - Active management of the C&D console thermal environment will be required. Since the thermal load is concentrated essentially in four components--two CRT (125 W each), a symbol generator unit (90 W), and a microfilm viewer (40 W)--a fluid loop coolant system appears to be the more desirable method of heat transfer as opposed to a forced air system. The use of forced air would impact the module, requiring the addition of ducting to remove the warm air to a remote fluid heat exchanger, and as such may have a greater impact on the module atmospheric control system than a console fluid loop interface. Additionally, high heat density components for use in C&D space applications, such as the Skylab ATM CRTs (60 W), have traditionally been designed to allow thermal transfer via fluid cold plate interfaces.

e. Console Description

Functional Envelopes - The ASM C&D console is arranged to accommodate one crewman as a primary operator and a second crewman as a general observer. The console geometry is optimized for single operator operation.

It is assumed that the console operator will be foot and lap restrained only, thus allowing unrestricted freedom of the upper torso and shoulders during dynamic reach movements. The operator restraint device will have two degrees of freedom, permitting lateral end-to-end console travel and forward and aft pitching of the crewman seat. Without lateral movement the primary crewman has visual access to the CRT monitors, subsystem annunciators, and microfilm viewer. Also from a static position the computer input devices, i.e., keyboards, hand controller, and the dedicated manual operative controls located in the lower left quadrant of the

Table III-24 C&D Electrical Power Requirements

Component Nomenclature	No.	Power Dissipated, W									
		+28 Vdc		115 Vac		+5 Vdc		Isolated Voltages			
		Each	Total	Each	Total	Each	Total	Each	Total		
CRT	2			125	250						
Symbol Generator	1	90	90								
Keyboard Encoder	1	10	10								
Microfilm Viewer	1		40								
Event Timer	1	5	5								
Mission Timer	1	5	5								
Tone Generator	1	1.2	1.2								
Hand Controller	1							0.5	0.5		
Annunciator, C&W	42							1.7	71.4		
Annunciator, Advisory	80						1.15	92			
Console Total			151.2		250						71.9
Nominal Dissipation*			150		250						5.6

*Assumes all components on except tone generator, C&W annunciators (three assumed on), and advisory annunciators (eight assumed on).

console are positioned within the crewman's functional reach envelope. The controls can therefore be operated without lateral repositioning of the restraint system. However, for optimum functional operation and parallax free monitoring of chassis area, it would be advantageous for the crewman to translate directly in front of the dedicated portion of the console.

All static anthropometric dimensions are predicated on 5th and 95th percentile male measurements extrapolated for 1985. A static reach envelope of 78.6 cm (31.0 in.) (5th percentile male population) is referenced in the location of manually operative controls. With the primary operator positioned with his median plane perpendicular to the center point of the alphanumeric keyboard, the operator can statically reach all peripheral controls with exception of the outermost circuit breakers and the middle to upper chassis mounted controls (see Fig. III-55). In a dynamic reach position, i.e., lateral and forward extension of the upper torso and shoulders, the 5th percentile operator can easily reach and manipulate all controls located on the keyboard shelf and all but the uppermost peripheral area of the dedicated chassis.

The optimum vertical viewing envelope is 30 deg from the normal visual axis. Based on a 95th percentile eye height of 127 cm (50 in.) all primary displays are located within the optimum visual cone. At a 51 cm (20 in.) viewing distance, the maximum horizontal viewing envelope without head rotation is 70 deg. With the operator seated at the primary location the total visual angle subtended by the two CRTs is within the 70 deg envelope. Thus, the crewman can call up experiment information for single display monitoring or concurrent display monitoring with visual decrement.

The seating envelope was sized based on shoulder width tolerances specified for the 95th percentile male crewman (Fig. III-56). With the primary crewman positioned directly forward of the alphanumeric keyboard, a second 95th percentile crewman can maintain an operative position in front of the dedicated chassis. Crossover reach movements between the two crewmen are minimal, but considered adequate because of the decreased common responsibility for the observer crewman.

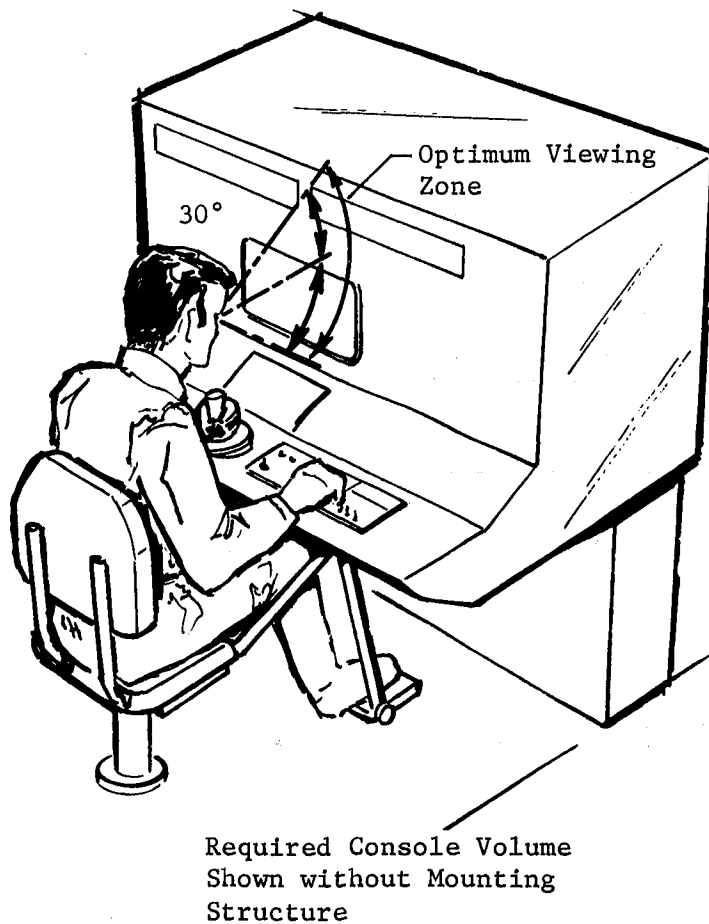


*Fig. III-55 Vertical Reach and Viewing Envelope
(Fifth Percentile Crewman)*

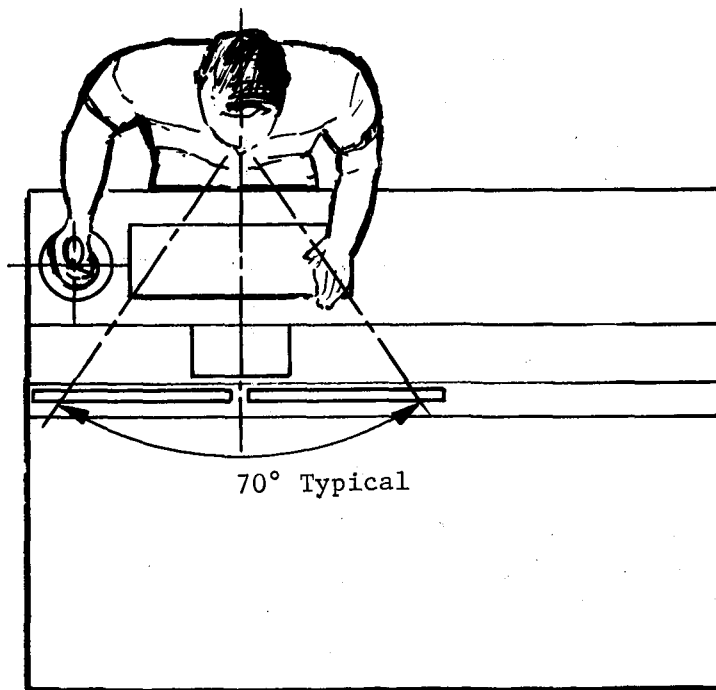


Fig. III-56 Lateral Work and Visual Envelope
(95th Percentile Crewman)

Layout Arrangement - The arrangement of the C&D components and the functional characteristics of a primarily integrated display system significantly reduces hand and eye link distances. The adjacent CRT locations permit nearly simultaneous monitoring of both monitors with head and eye movement limited to a horizontal scan of less than 70 deg. The microfilm viewer, which has a high use rate, is optimally located with respect to the visual axis and the "horizontal" plane. Scan time between the viewer and main displays is minimized due to their adjacent spatial location. The experiment/subsystem advisory and C&W annunciators are located in the optimum visual zone (30 deg) of the primary crewman and are also observable from the observer's crew station.

The experiment dedicated controls and display will, in general, be part of a self-contained unit. However, some monitoring and command functions will also be required via the main displays and keyboards. Link distances between the upper chassis and the

monitor and keyboards will be relatively large and may require two crewmen for performance of certain tasks; however, to reduce viewing and reach links, the lower chassis are assumed to house units that require critical visual monitoring.

Human engineering criteria were instrumental in the definition of alphanumeric characteristics. A standard Leroy font is assumed for characters. The symbol height was computed at 0.42 cm (0.17 in.). This is based on the symbol subtending a visual angle of 20 min at a viewing distance of 51 cm (20 in.). A symbol width of 0.32 cm (0.125 in.) or 75% of symbol height, was selected and considered optimum for symbol legibility. Symbol spacing, i.e., distance between vertical tangents erected at the outer limits of adjacent symbols, was computed at 0.21 cm (0.083 in.), which is 50% of the symbol height.

f. Component Description - The recommended hybrid display panel combines Sortie Lab subsystems and experiment functions onto one panel. An interface diagram of the control and display subsystem was shown in Fig. III-54. Mass property data for the C&D console and integral major components are provided in Table III-25. Salient functional and technical information for the primary C&D components is provided in the following paragraphs.

CRT Indicator - Two CRT indicators provide the display capability for the integrated portion of the ASM display system. The indicators display complete ASC II Code alphanumerics, dynamic and static graphics, vectors, circles, and special symbols. The CRT is a self-contained unit that includes deflection amplifiers, video amplifiers, and all required low- and high-voltage power supplies. Each unit also includes an automatic brightness control and built-in test (BIT) features.

Symbol Generator Unit - The symbol generator unit (SGU) provides the video and computer data interface to the CRTs. Two channels of video and data formatting allow the simultaneous display of independent data on each CRT. Video inputs are presented in a raster/scan mode with symbols generated by the symbol makers superimposed by stroke writing techniques during the vertical retrace time.

Table III-25 C&D Console Mass Properties

Unit Nomenclature	No. Units	Unit Dimensions, in. WxHxD	Volume, ft ³		Weight, lbs		Notes
			Unit	Total	Unit	Total	
<u>Components</u>							
CRT	2	14.5x12.5x17.25	1.8	3.6	50	100	
Symbol Generator	1	13.0x11.0x18.0	1.5	1.5	30	30	
Function Keyboard	1	7.5x3.5x2.0	0.3	0.3	2	2	
Alpha/Numeric Keyboard	1	16.5x5.5x2.0	1.0	1.0	3	3	
Keyboard Encoder	1	6.0x4.0x4.0	0.05	0.05	10	10	
Microfilm Viewer	1	9.5x11.5x13.0	0.8	0.8	20	20	
Event Timer	1	3.25x1.75x4.25	0.01	0.01	2	2	
Mission Timer	1	4.0x1.75x3.75	0.01	0.01	2	2	
Tone Generator	1	7.0x5.25x4.0	0.08	0.08	5	5	
Three-Axis Controller	1	4.5x4.5x4.0	0.05	0.05	5	5	
Advisory Bank (10 Indicators)	8	3.25x2.75x1.0	0.005	0.04	0.3	2.4	
C&W Panel (42 Indicators)	1	7.0x8.75x1.0	0.04	0.04	6	6	
ICOM Speaker	1	4.0x4.0x3.0	0.03	0.03	1.5	1.5	
Switches, Toggle	25				0.11	2.8	
Switches, Rotary	6				0.78	4.7	
Circuit Breaker	18				0.10	1.8	
Potentiometer	3				0.10	0.3	
Distributor	1	24.0x6.0x9.0	0.8	0.8	40	40	Unit and Cabling
<u>Structure</u>							
Main	1	50.0x35.5x20.0	20.6	20.6	97	97	Does not include collant lines and cold plates
Keyboard Ledge	1	50.0x6.0x13.5	2.3	2.3	36	36	
Panel Area	1					52	
Total Console				22.9		423.5	

Data inputs for the symbol makers are received by interfacing circuitry and transferred to the appropriate SGU channel under the control of a timing and control section. This section also provides the timing to synchronize the symbol makers to the video displays. Two channels of a single frame memory and symbol makers are independent and may generate any of the formats provided by the bulk data storage section, with updates provided by CIU data. Routing of signal outputs to the CRTs is performed by the switching network as directed by the CIU.

Keyboards - A function keyboard and an alphanumeric keyboard are provided at the C&D console. The function keyboard represents the basis of the man-computer syntax. The buttons allow the crewman to configure the experiments and subsystems into desired operating modes. A particular operation is initiated by performing a series of events in a predetermined hierarchical scheme. Functions performed via the keyboard include: category selection, function selection, mode selection, status selection, and the common keyboard entry functions, e.g., enter, clear, execute, etc. Physically the keyboards use solid-state buttons and are compatible with MOS encoding. Activation of the function buttons assigns meaning to the alphanumeric keyboard commands. Through the alphanumeric keyboard the crewman can enter discrete commands, i.e., manual mode, modify existing programs, or enter new programs. Each activated key represents a command for the computer to perform a particular task. The keyboards are standard ASC II typewriter type with solid-state keys and MOS encoding.

Three-Axis Controller - A three-axis multifunction hand controller is provided at the C&D console and is used primarily for instrument pointing and initial target acquisition. For pointing tasks, the unit is used to coarse point to a target accuracy of approximately 5 $\overline{\text{sec}}$. Fine pointing is accomplished by computer command.

Microfilm Viewer - The microfilm viewer provides the majority of read-only, procedural-type data to the operator. These data include experiment and subsystem operational procedures, on-board checkout procedures, simplex schematics, etc. The data are cassette loaded on dual-track 16-mm film with each cassette containing 5200 frames. Information is retrieved either by a manual slewing control or from the computer.

Timers - Two timing devices are provided at the C&D console. The four-digit event timer displays the time remaining or expended for a particular event. Second and minute slewing switches are provided for setting in desired time sequences. The timer is capable of operating either in a countup or countdown mode and provides discrete event start and stop commands via the CIU for experiments requiring operational time sequencing. The seven-digit mission timer provides a time reference in Greenwich Mean Time with 1-sec update rate. Time is maintained via the data management computer. Both displays are solid-stage light emitting diode (LED) units. The digits are generated from 5 x 7 dot matrices and are 0.635 cm (0.250 in.) in height.

Advisory Annunciators - Eight dual annunciator banks are shown on the C&D console. The annunciators provide a visual alert cue when a low priority malfunction occurs in any of the onboard experiments or module subsystems. Appropriate nomenclature identifies which subsystem or instrument requires attention. The crewman, by addressing the computer via the keyboards, may obtain detailed status information of the malfunction on either CRT.

Caution and Warning Indicators - An emergency, caution, and warning subsystem terminal is provided in the console. This subsystem has the following characteristics:

<u>Function</u>	<u>Quantity</u>	<u>Indicator</u>
Emergency	3	Flashing red - redundant filaments
Warning	10	Red
Caution	17	Amber
Master Alarm	1	Flashing red - redundant filaments Reset switch - redundant switch contacts
Memory	1	White - redundant filaments
Spare	10	Amber or red

The master alarm and memory indicators are activated when any emergency, caution, or warning is detected. The master alarm reset switch resets the emergency, caution, and warning subsystem leaving only the memory indicator illuminated. The memory indicator must be manually reset following corrective action.

Intercom - An intercom unit, located on the lower left side of the console provides a communications link between the Sortie Lab and the Shuttle. Two hardwired channels of audio service are provided via the fixed speaker/microphone or the two headset connectors. The fixed speaker/microphone provides a simplex voice link with the Shuttle and the ground via the Shuttle while the headsets provide a duplex link. Controls are provided for speaker volume control, channel and mode select, call, transmit or intercom, and voice record. Caution and warning tone signals are routed to the unit and will override any intercom message, bypassing the volume control.

2. Data Management

The Sortie Lab data management subsystem operating in conjunction with the control and display subsystem and crew will perform all onboard formatting, storage command, control sequencing, and telescope field monitoring. Specific support functions of the data management subsystem include:

Processing (for real-time display) of both scientific and engineering data;

Storage of scientific and engineering electronic data;

Real-time command, control, sequencing, and video monitoring;

Receipt, storage, and distribution of command data from the ground;

Generation and distribution of onboard timing.

These electronic data handling functions are accomplished by using interface electronics modules, a master command decoder/multiplexer, and a data bus to interface with the pallet-mounted instruments and subsystems. Each interface module is located near the scientific instrument or support subsystem that it manages.

Assumptions made or derived from the nature of a Shuttle Sortie mission and in keeping with defined operational concepts include the following:

Mission derived data are recorded on film and on magnetic tape for physical return at mission end;

Processing of payload data is limited to functions essential to the control of instrument operation;

Operational data required on the ground for mission control and principal investigator monitoring will be transmitted in real time or near-real time using the Shuttle communications subsystem.

a. Experiment and Payload Requirements - The baseline payload combinations consisting of the solar telescopes or one stellar telescope (primary) experiment and one or more array (secondary) experiments were analyzed to determine the operational data rates and total data generated during the Sortie mission. Baseline Experiment Definition Documents (BEDDs) for each scientific instrument were reviewed and the data rate information was combined with support subsystem data rates to establish payload data timelines for the on-orbit operational sequences. These timelines were used to determine the data management requirements and data handling components for the Shuttle pallet.

All telescopes except the infrared telescope provide hard copy photographic outputs. The scientific data interface becomes quite simple for these telescopes because sufficient film will be carried with each telescope to delete any requirement for inflight servicing during the seven-day mission. The arrays and subsystems generate relatively low bit rate data and are readily accommodated by the Sortie Lab data recorders. An analysis of the baseline payloads provided the data summaries for each payload shown in Table III-26. These summaries define the tape requirements for the Astronomy Sortie mission and an estimated data rate for monitor and control onboard or at the Space Astronomy Control Facility. Additionally, the capabilities of both the original and updated Shuttle data management subsystem were reviewed to determine the transmission time required to provide field monitoring information to the ground-based observer. A single frame of standard 525 TV line resolution information was to be provided each orbit for both the X-ray telescope and the XUV spectroheliograph. Detailed data analysis of each payload is included in Appendix B1, Volume III, Book 2 of this report.

Table III-26 Digital Data Rates, Storage, and Telemetry Requirements

	Baseline Payload	Maximum Data Rate, kbps	Onboard Storage, 10^9 bits	Telemeter - During Mission, 10^6 bits
Solar	1-2	4.0	1.76	743
Stratoscope III Payloads	3AB	4.2	2.04	210
	3AC	8.3	4.30	235
	3AD	4.4	2.20	225
	3AE	8.6	4.43	251
IR Telescope Payloads	4AB	4.5	2.00	157
	4AC	8.6	4.30	181
	4AD	4.8	2.15	172
	4AE	8.9	4.43	198

b. *Data Handling Concept* - Managing of the commands and controls to the pallet and storage or monitoring of the scientific and engineering data from the pallet are functions provided by the Sortie Lab data management subsystem. The concept of handling data between the baseline payloads and support subsystems and the Sortie Lab consists of using: (1) data busses (digital and analog) between the Sortie Lab and pallet; (2) a master command decoder and multiplexer located on the pallet; (3) data bus interface units (DIUs) associated with each payload and pallet-mounted subsystem; and (4) a data processor or remote multiplexing unit dedicated to interfacing each instrument to the DIU. A block diagram of the data handling interfaces is shown in Fig. III-57. The digital data bus provides control signals to each experiment and subsystem and low bit rate data are returned to the Sortie Lab along the same bus. A master command decoder and multiplexer determines the routing of signals for the forward payload and gibal, aft payload and gibal, and for the support subsystem

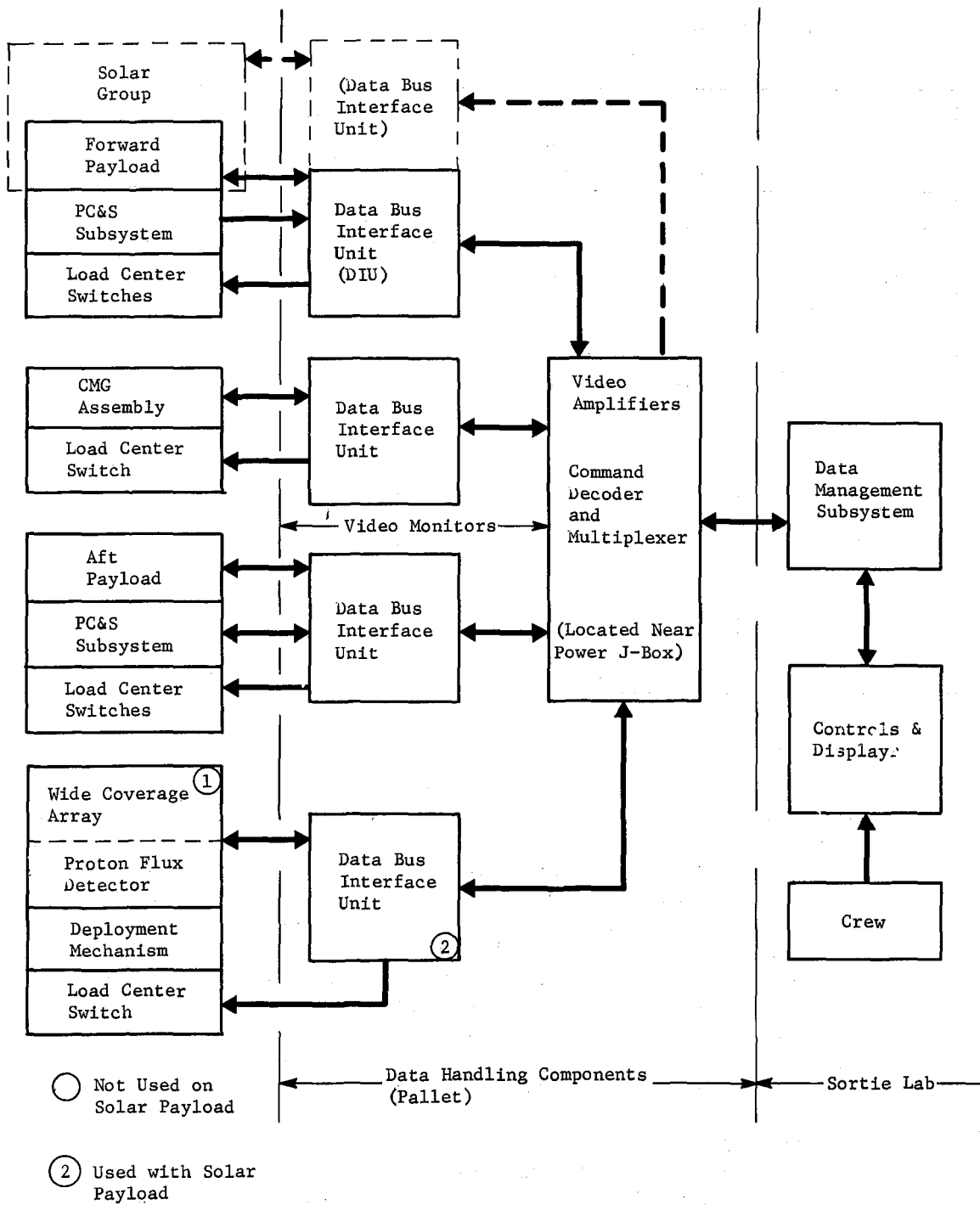


Fig. III-57 Data Handling Interface Components

components (i.e., the IMU, CMGs). The DIU for each payload or subsystem is the direct interface providing decoded commands to the payload, to the load center switch for each payload, or to the support subsystem.

The total digital data storage is accommodated onboard the Sortie Lab with a single 14-in. reel of 1-in. tape. Two recorders are used to allow separate uninterrupted recording of data for each of the two payloads. Data from pallet-mounted subsystems and from common instruments such as the wide coverage X-ray detector and the proton flux detector can be recorded onto both storage tapes for data correlation by the principal investigator.

A single frame of 525 TV line resolution information, quantized to 8-bit resolution will require approximately 11.5 min to transmit the digitized data to ground at a 5 kbps rate. This time is reduced to approximately 10 sec when the frame data can be transmitted at 256 kbps. Data links with capabilities as low as 51.2 kbps require 50 sec to send the single frame to a receiving ground station. Variations in TV picture line resolution and time required to transmit a single frame over selected RF or ground data links is shown parametrically in Fig. III-58. A "nominal" station contact time of 7 to 9 min will provide an adequate margin to send the field monitoring information to ground at data rates above 25 kbps. The Shuttle RFP identifies 25 kbps available for the payloads.

c. Recommended System - The recommended data handling components provide data transfer and operational control in modular packaging. The addition of experiment data processors interfacing with DIUs permit system expansion with minimum impact on the existing system. The overall system consists of the data busses, four data bus interface units, source data processors, video amplifiers for field monitoring, and a master command decoder and multiplexer.

The data bus accepts a unique modulation scheme for the transmission of data and routing addresses and is adaptable to any digital system. Communications along the bus is asynchronous, random access, and noncued. Data bus interfaces are in parallel through the master command decoder and multiplexer and direct data exchange between any two interfaces must be routed through the Sortie Lab data management subsystem.

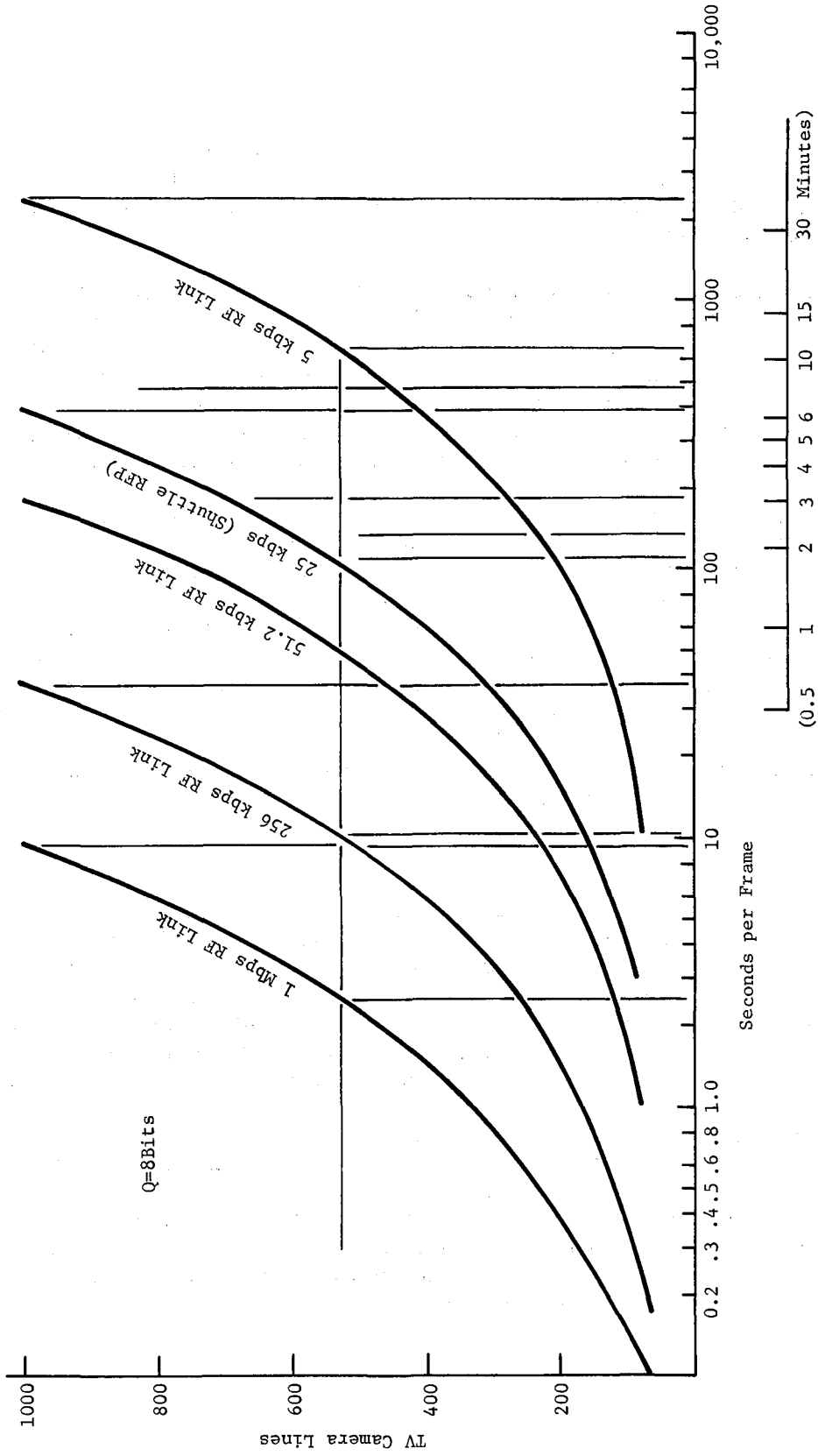


Fig. III-58 Single Frame Transmission Time

Data bus interface units (DIUs) are of modular design to allow adaptation to various pallet requirements. The units provide all of the signal functions required to transfer data and instructions to and from the command decoder and multiplexer. Discrete or analog measurement points are monitored in any combination under direction of a central controller such as the Sortie Lab data management subsystem. For normal operations, the DIU performs data multiplexing and routine sequencing using stored data and programmed routines. Specified routines can be interrupted by the scientific crewman on command. Each DIU consists of a transmitter and a receiver section. The transmitter section contains a parity generator, shift registers for data storage and conversion, controller for wake-up and coding, clock for the shift registers, and line drivers. The receiver section consists of threshold detectors, data converters and parity detectors, shift registers, unique word and receiver decoders, and control logic.

Source data processors provide the direct interface between the experiment detectors and instrument and the DIUs. The processors are used to: monitor and report the state of discrete functions or events; measure analog voltages and perform analog-to-digital conversion; and provide "circuit closure" type functions to operate relays, solenoids, camera mechanisms, and other on-off circuits.

Video amplifiers are included on the Shuttle pallet to ensure impedance matching and sufficient signal to the field monitors located within the Sortie Lab.

The master command decoder and multiplexer transmits commands to the DIUs as programmed and performs all data routing and processing for Shuttle data management subsystem compatibility.

3. Electrical Power

Each payload and pallet-mounted support subsystem or support equipment requires continuous power while on orbit. Peak power demands occur during camera film changes, initial deployment, and final stowing. These peak demands are short compared with the overall mission duration and are considered negligible for derivation of total energy requirements.

a. *Experiment and Payload Requirements* - The electrical power requirements for the baseline mission payloads have been analyzed for the operational (on-orbit) mode. Support subsystem requirements are included to generate the power requirements for the seven-day mission. The input power for the individual experiments of each mission payload was obtained from the updated Baseline Experiment Definition Documents of Volume II, Book 2 (Appendix). Support equipment such as correlation trackers, bore-sight trackers, fine sun sensors, and field monitoring vidicons are added to the respective payload. The operational pointing and control subsystems modified for solar or stellar payloads and the electrical supporting subsystems complete the overall mission payload power requirements. The electrical supporting subsystems include the data and power handling components mounted on the pallet and the hybrid control and display console located in the Sortie Lab. The average power requirement for each baseline mission payload is given in Table III-27.

Table III-27 *Electrical Power Requirements for Mission Payloads, W*

<u>Payload</u>	<u>Instruments</u>	<u>Stabilization Systems</u>	<u>Support Electronics (DM/C&D/Elec)</u>	<u>Total</u>
<u>SOLAR</u>	348	650	482	1480
<u>SIII</u>				
3AB	410	475	467	1352
3AC	338	475	467	1280
3AD	441	475	467	1383
3AE	502	475	467	1444
<u>IRT</u>				
4AB	350	475	392	1217
4AC	278	475	392	1145
4AD	381	475	392	1248
4AE	442	475	392	1309

b. Recommended System Components - The pallet-mounted interfacing unit that provides operating power to the payloads and supporting subsystems consists of dual redundant power busses, the master junction box, and load center switches. Direct current power is provided by the Sortie Lab to the junction box. The box provides the common tie point for the instruments and subsystems and reduces the number of cables interfacing with the Sortie Lab. The same box structure is used to house the master command decoder and multiplexer, the video amplifier for the telescope monitors, and the multipin connectors for hardwire analog and control signals. Each payload and support subsystem is connected to the master junction box through a dedicated load center switch. Power is applied through a relay network to the payload or support subsystem under control of the data-bus interface unit located near the payload or subsystem. A fail-safe circuit and a relay driver are included in each switch. The block diagram for the pallet-mounted power distribution system is shown in Fig. III-59.

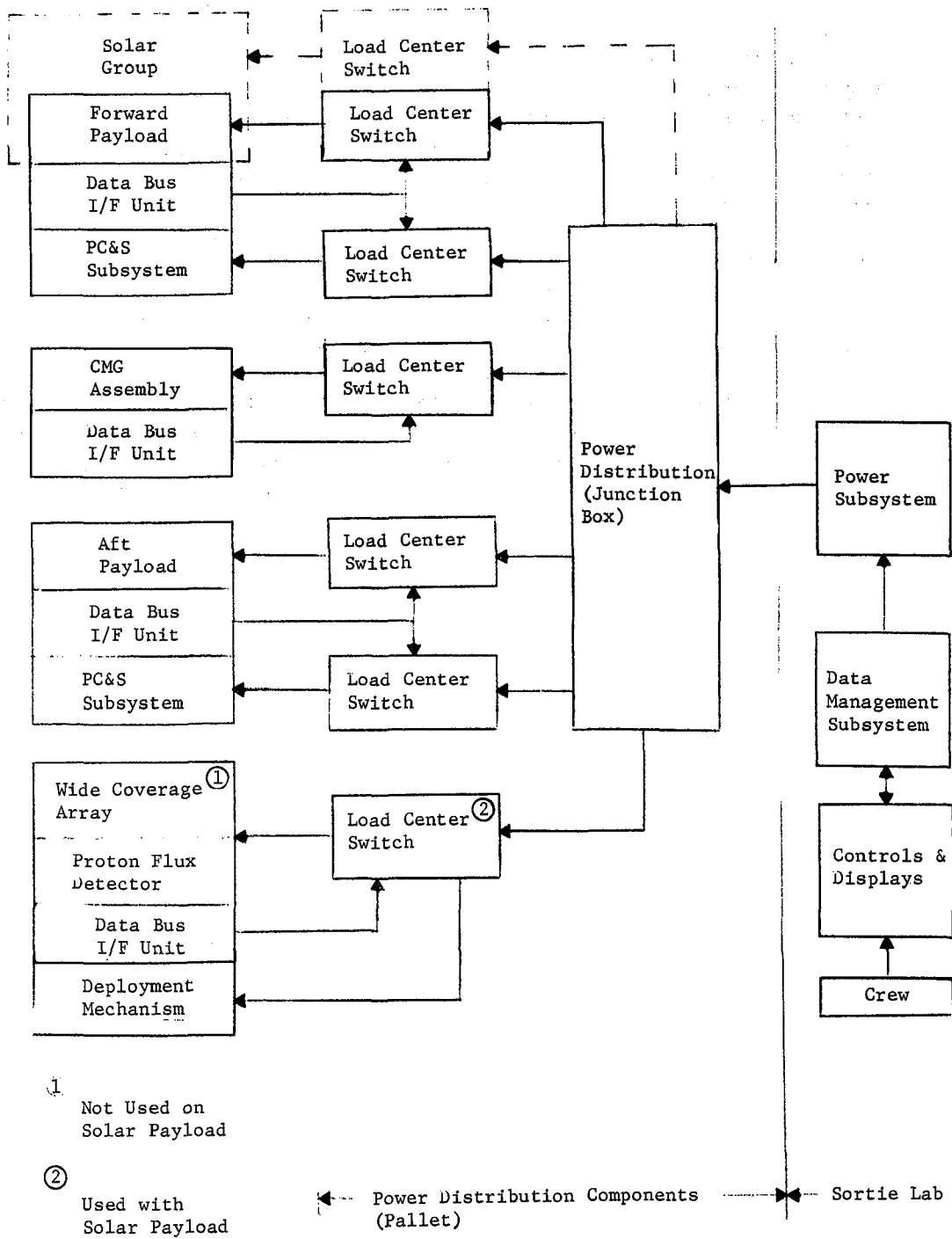


Fig. III-59 Power Distribution Interface Diagram

E. REFERENCES

The following documents are referenced in this chapter.

- III-1. "Martin Marietta Corporation Orbiter/Payload Thermal Environment Model." S-72-46593-04.
- III-2. "Martin Thermal Radiation Analyzer Program." Engineering Department Technical Manual. Martin Marietta Corporation, September 1970.
- III-3. "Martin Interactive Thermal Analysis System." Engineering Department Technical Manual. Martin Marietta Corporation, November 1971.
- III-4. R. P. Warren: "Cryogenic Cooling System for a One Meter IR Telescope." Memorandum, Martin Marietta Corporation, July 1972.
- III-5. M. Zemansky: *Heat of Thermodynamics*. 4th Edition, 1957.
- III-6. M. M. Saffren, D. D. Elleman, and T. C. Wang: "Low Gravity Superfluid Helium Cooling Systems," presented at the Cryogenic Workshop, Huntsville, Alabama, 1972 (to be published in the proceedings).
- III-7. A. Elsner and G. Klipping: "Control System for Temperatures and Liquid Level Between 4.2° and 1°K." *Advances in Cryogenic Engineering*. Vol 14, 1969.
- III-8. *Large Space Telescope System Definition Study*. Technical Report, Itek Optical Systems Division, December 1971.

IV. PRELIMINARY DESIGN

The ASM concept, selected, analyzed, and defined earlier in this study, is presented in pictorial form in this chapter. Beginning with the establishment of layout criteria and guidelines, a layout drawing was developed showing the payload accommodations capable of supporting the experiment complements of all nine ASM payloads. This drawing illustrates the results of the adopted design approach, which stressed the maximization of commonality of hardware. Where complete commonality could not be achieved, payload-peculiar hardware is identified. Using this drawing as the baseline, layout drawings were developed that show the experiment complements of the nine ASM payloads, and the required configuration of the accommodations installed in the Shuttle Orbiter. Subsystem and telescope configuration drawings were prepared, showing details of these items. System-level schematics, emphasizing interfaces, are shown for each of the nine ASM payloads.

A. SYSTEM LAYOUT DRAWINGS

Layout criteria and guidelines were developed to assure that the layouts would represent feasible arrangements, reflecting consideration of accessibility requirements, simplicity of interfaces, etc. System level layout drawings are presented that show the payload accommodations, and each of the complete payloads installed in the payload bay of the Shuttle Orbiter. Major subsystems are located and the structural concepts of the various experiment mounts are illustrated. Launch and operational configurations are shown, with critical clearances and overall dimensions. Mass properties were calculated for each of the payloads and the centers of gravity (cg) for the nine ASM payloads are shown superimposed on a plot of the Orbiter's cg limits. All payloads fall within the Orbiter cg constraints, as shown in Fig. IV-1.

1. Layout Criteria and Guidelines

Criteria and guidelines were developed for use in layout activities. Levels of detail were set by the level of definition presented in the layouts.

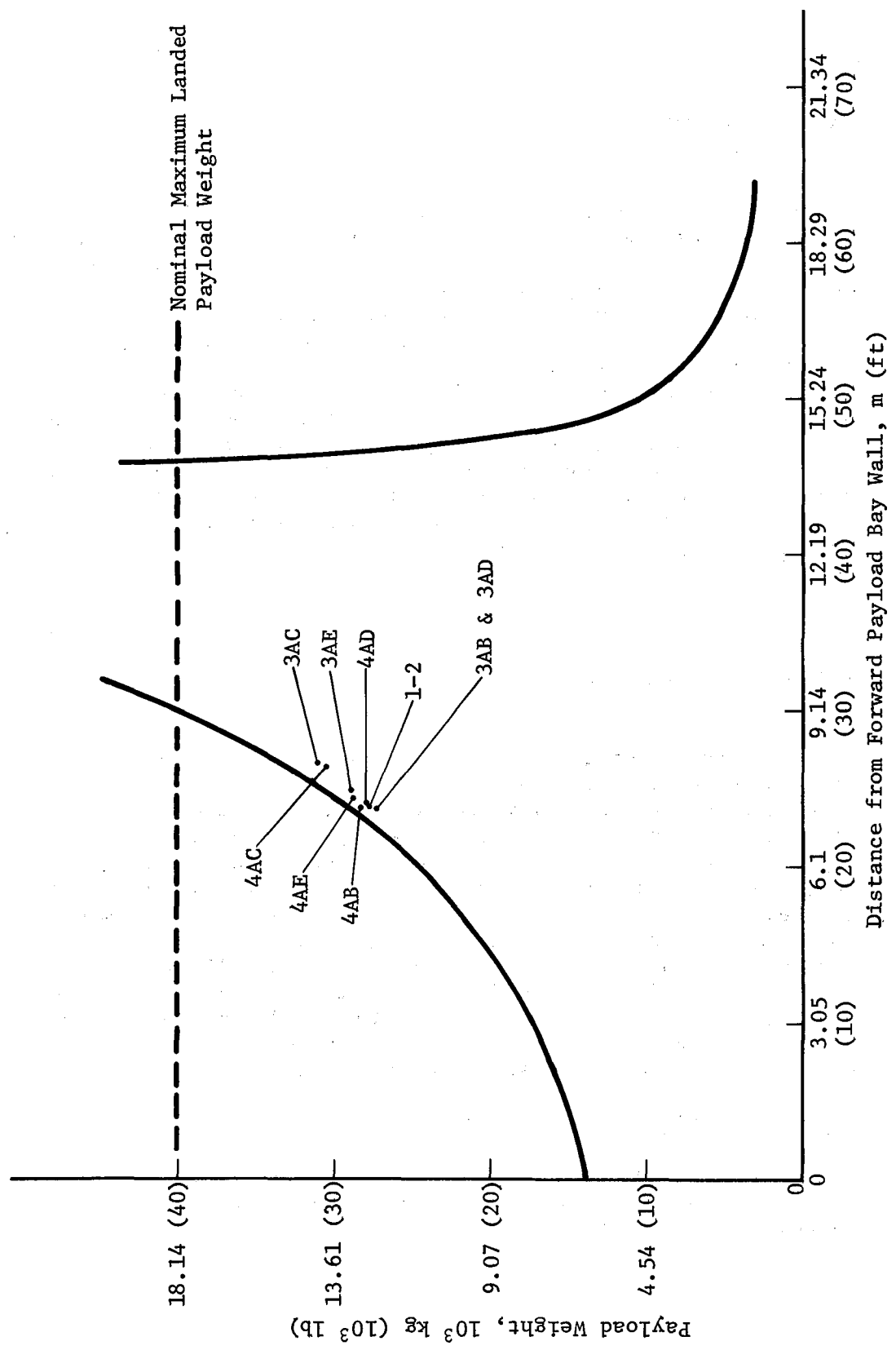


Fig. IV-1 Payload vs Shuttle Orbiter eg Constraints

a. Shuttle Constraints

Payload Envelope - The overall payload envelope with the Orbiter doors closed is a 4.58 m (15.0 ft) diameter x 18.29 m (60.0 ft) long cylinder.

Orbiter Configuration - The Grumman Orbiter configuration will be used for determining clearances and viewing obstructions.

Jettisoning Provisions - All objects that extend beyond the payload envelope specified above, and that would prevent the payload bay doors from closing for Orbiter reentry will be jettisonable.

Sortie Lab and Pallet - The MSFC definition of the Sortie Lab and pallet will be used.

b. Experiment Viewing - The experiment viewing requirements specified in the Baseline Experiment Definition Documents (BEDDs) will be satisfied to the greatest extent possible. These BEDDs are included in Volume II, Book 2 of this report.

c. Interfaces - Physical interfaces between the payload experiments and subsystems mounted on the pallet and the Shuttle Orbiter will be through the Sortie Lab and pallet. All interfaces will be designed for easy ground accessibility for maintenance and refurbishment. Electrical interfaces will be conveniently grouped, consistent with requirements for proper spacing of power and data cables.

d. Accessibility - All crew activities on the pallet will be accomplished on the ground. Therefore, no EVA provisions are required. The following documents shall be used as design guides:

- 1) MSFC-STD-267A, *Human Engineering Design Criteria*;
- 2) MIL-STD-1472, *Human Engineering Design Criteria for Military Systems*.

The man-machine interfaces involving the C&D console, located in the Sortie Lab, and discussed in Section III.D.1 of this volume.

e. Subsystems - The subsystem definitions presented in Chapters III and IV of this volume will be used in the layouts.

2. Payload Accommodation Layout Drawing

An overall layout showing those items that are required to accommodate all nine ASM payload combinations is presented in Fig. IV-2. This accommodation concept is compatible with the Sortie Lab/pallet and the Shuttle Orbiter, and adheres to the layout criteria and guidelines identified in subsection 1, Layout Criteria and Guidelines. Commonality, simplicity of interfaces, and maximization of experiment viewing capabilities were achieved, and the feasibility of the concept selected earlier in this study has been established.

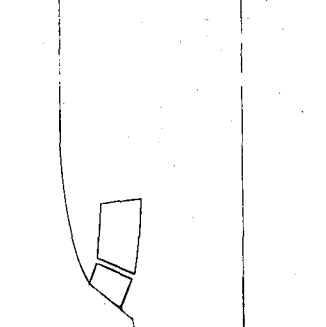
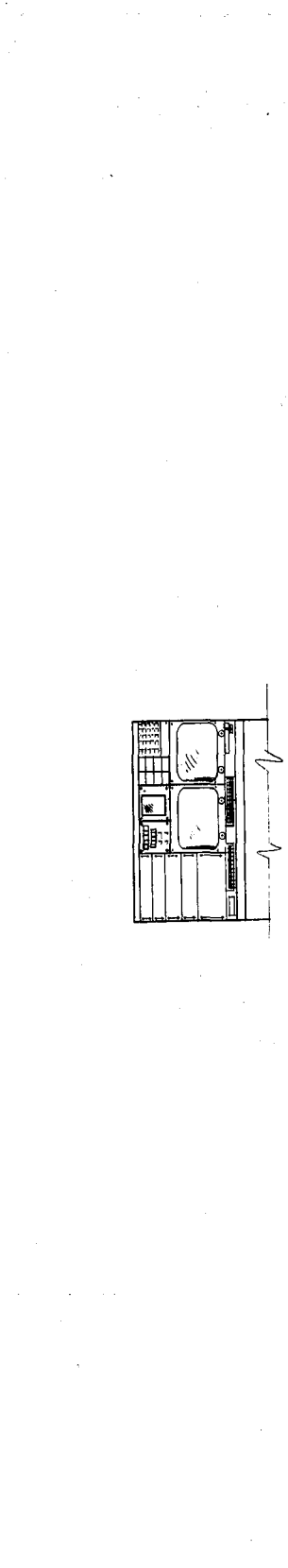
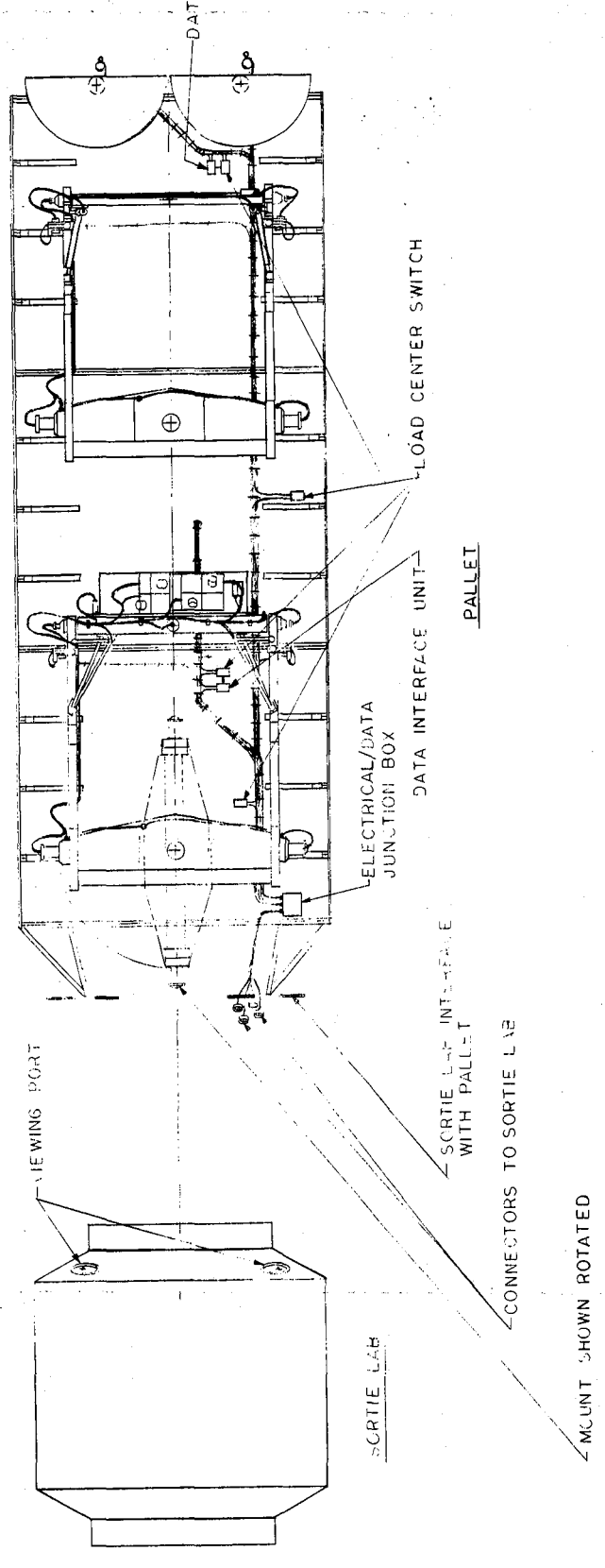
All payload combinations use the Sortie Lab and pallet and the subsystem support available from them. Other equipment items used for all payloads are the pallet-mounted CMGs and IMU, the electrical/data junction box, the data interface and load center switches, the Sortie Lab/pallet connectors, essentially all of the cordage shown, and the C&D console located in the Sortie Lab.

The telescope mount, including components mounted on the telescope P&C platform, which is located just aft of the Sortie Lab, is also used for all payloads except Payload 1-2. This payload includes two telescope groups and no array group, thus requiring the addition of a second telescope mount. The array mount is converted into the second telescope mount by replacing the array platform assembly and elevation pointing actuators with a telescope gimbal assembly and associated elevation pointing/stabilization actuators. The mounts that support the wide coverage X-ray detector arrays, along with the attached proton flux detector, are not installed for Payload 1-2 flights. The pallet-mounted deployment launch locks are common for both telescope and array mounts for all payloads.

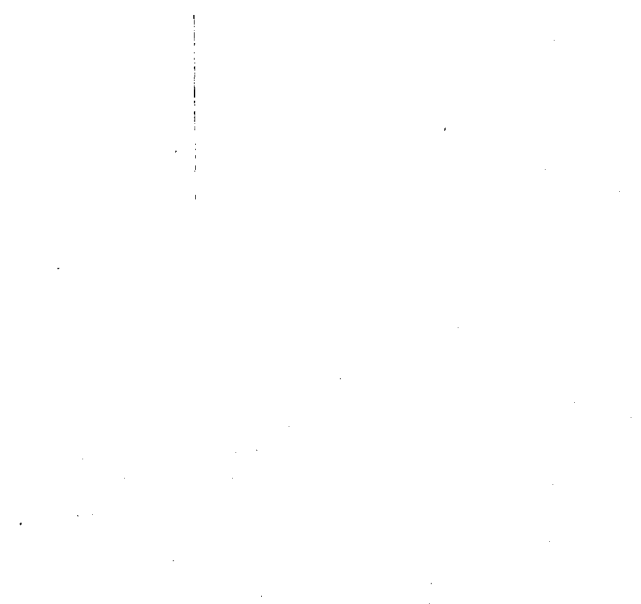
3. Payload Layout Drawings

Layout drawings, showing the nine ASM payloads installed in the Shuttle Orbiter, are presented. These layouts were based on and developed in conjunction with the Payload Accommodation drawing, Fig. IV-2.

a. Payload 1-2 - This payload (Fig. IV-3) is entirely devoted to solar-oriented telescopes. Three telescopes, the XUV spectroheliograph, X-ray telescope, and the inner-outer coronagraphs are integrated into a single housing, supported by the forward telescope mount. The aft telescope mount supports the photoheliograph.



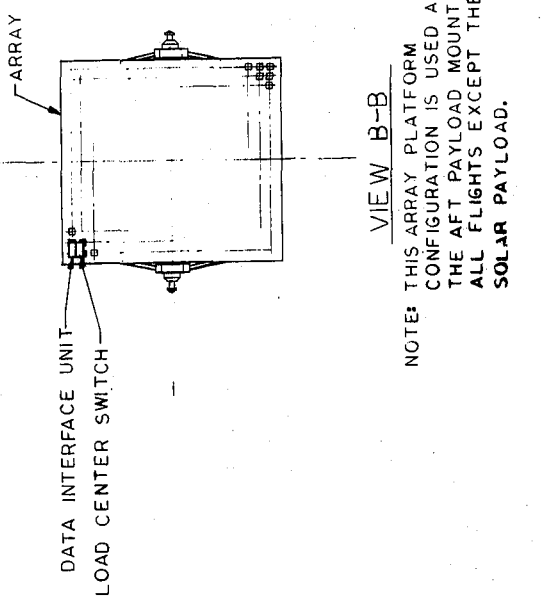
VIEW A-A
NOTE: THIS TELESCOPE GIMBAL CONFIGURATION IS USED AS THE FORWARD PAYLOAD MOUNT ON ALL FLIGHTS, AND ALSO THE AFT MOUNT FOR THE SOLAR PAYLOAD.



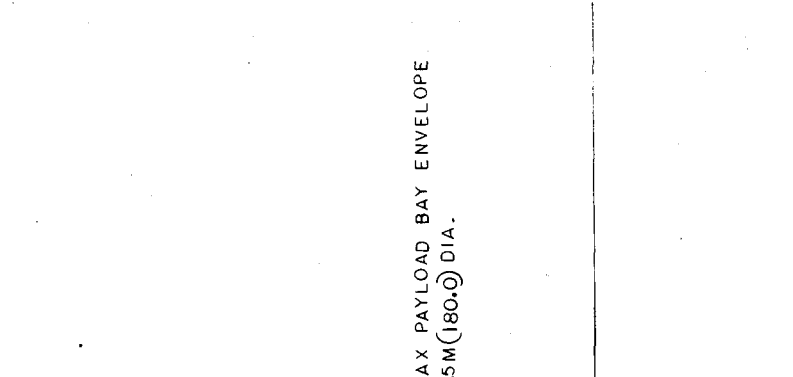
VIEW B-B
NOTE: THIS ARRAY PLATFORM CONFIGURATION IS USED AS THE AFT PAYLOAD MOUNT ON ALL FLIGHTS EXCEPT THE SOLAR PAYLOAD.



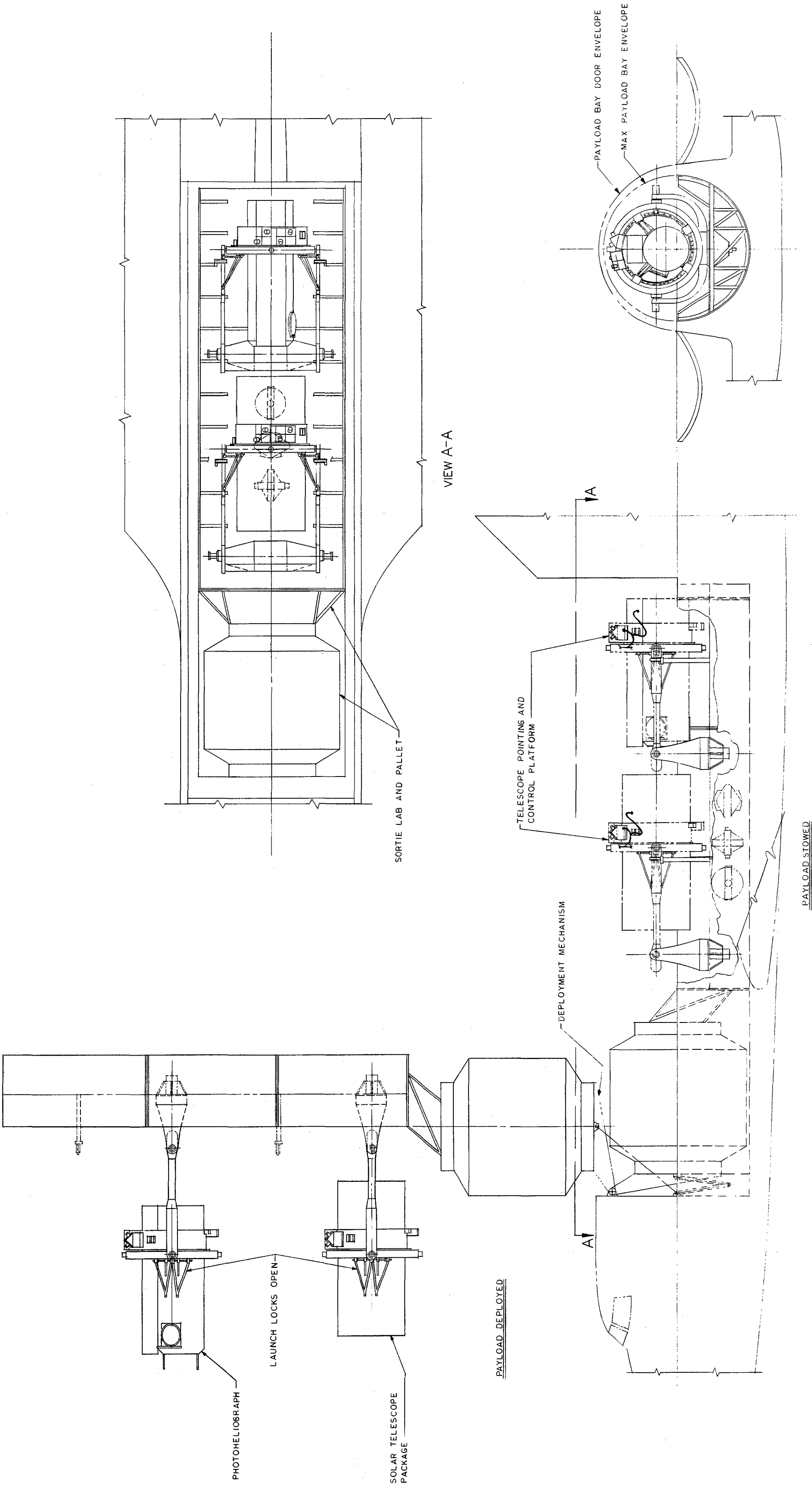
TELESCOPE MOUNT
ARRAY MOUNT
PROTON FLUX DETECTOR (2)
(FLOWN ON ALL PAYLOADS EXCEPT SOLAR)



SORTIE LAB AND PALLET IN SPACE SHUTTLE
(GIMBALS IN OPERATING POSITION)
(NO EXPERIMENTS SHOWN)



WIDE COVERAGE X-RAY DETECTOR MOUNTS ON ALL PAYLOADS EXCEPT SOLAR
25M (100)
MAX PAYLOAD BAY ENVELOPE 45M (180.0) DIA.

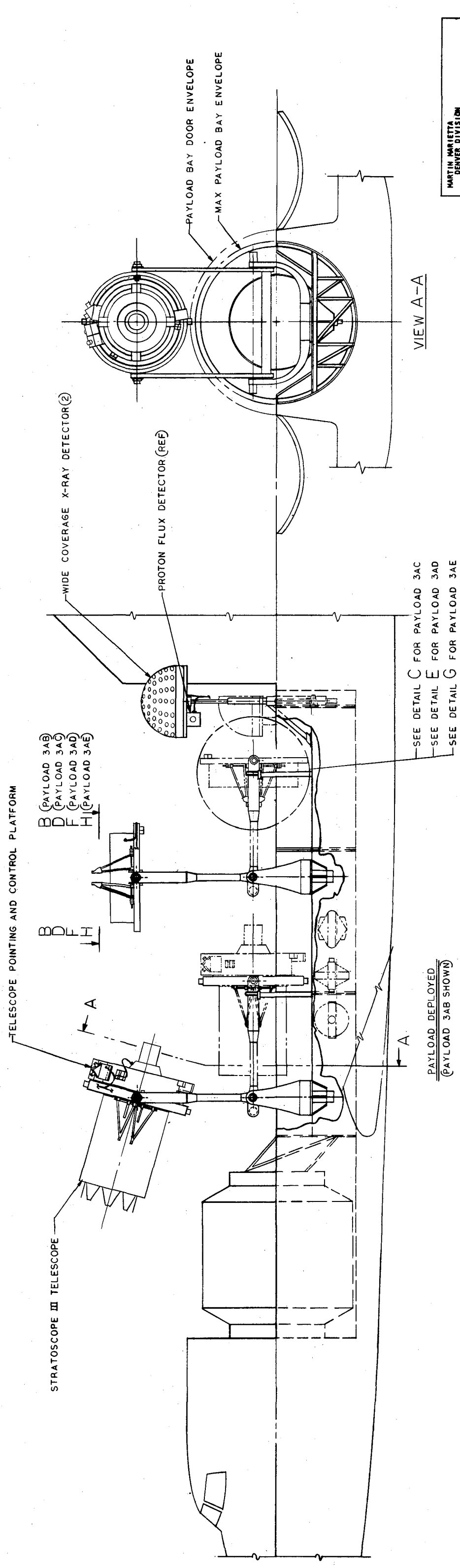
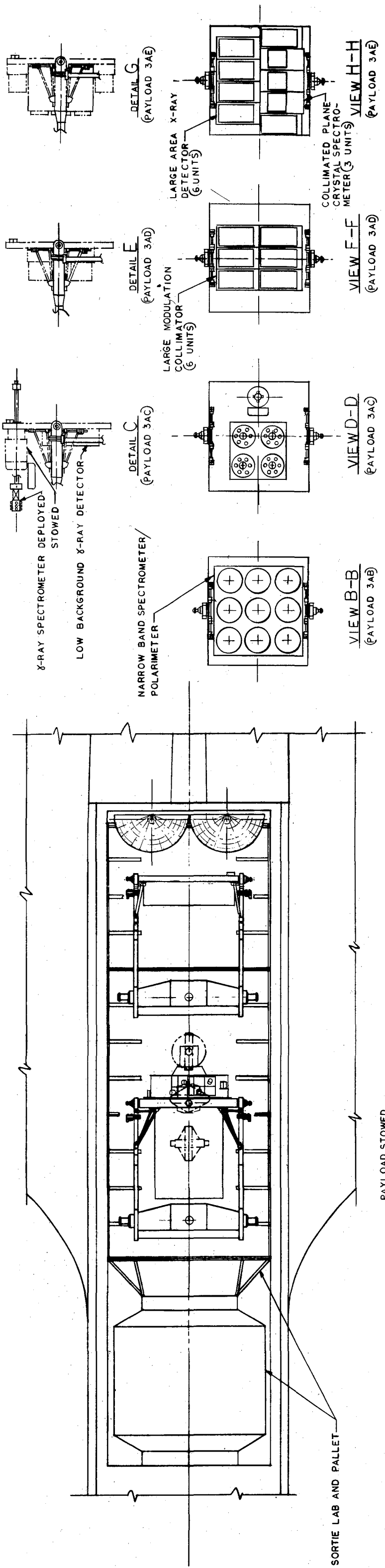


These telescopes all need to simultaneously view the sun. To accomplish this, the Sortie Lab and pallet are rotated 90 deg out of the Orbiter payload bay and fixed in this position for viewing. This is done to allow simultaneous viewing with the Orbiter in X-POP altitude and at high orbital inclinations required for continuous viewing of the sun.

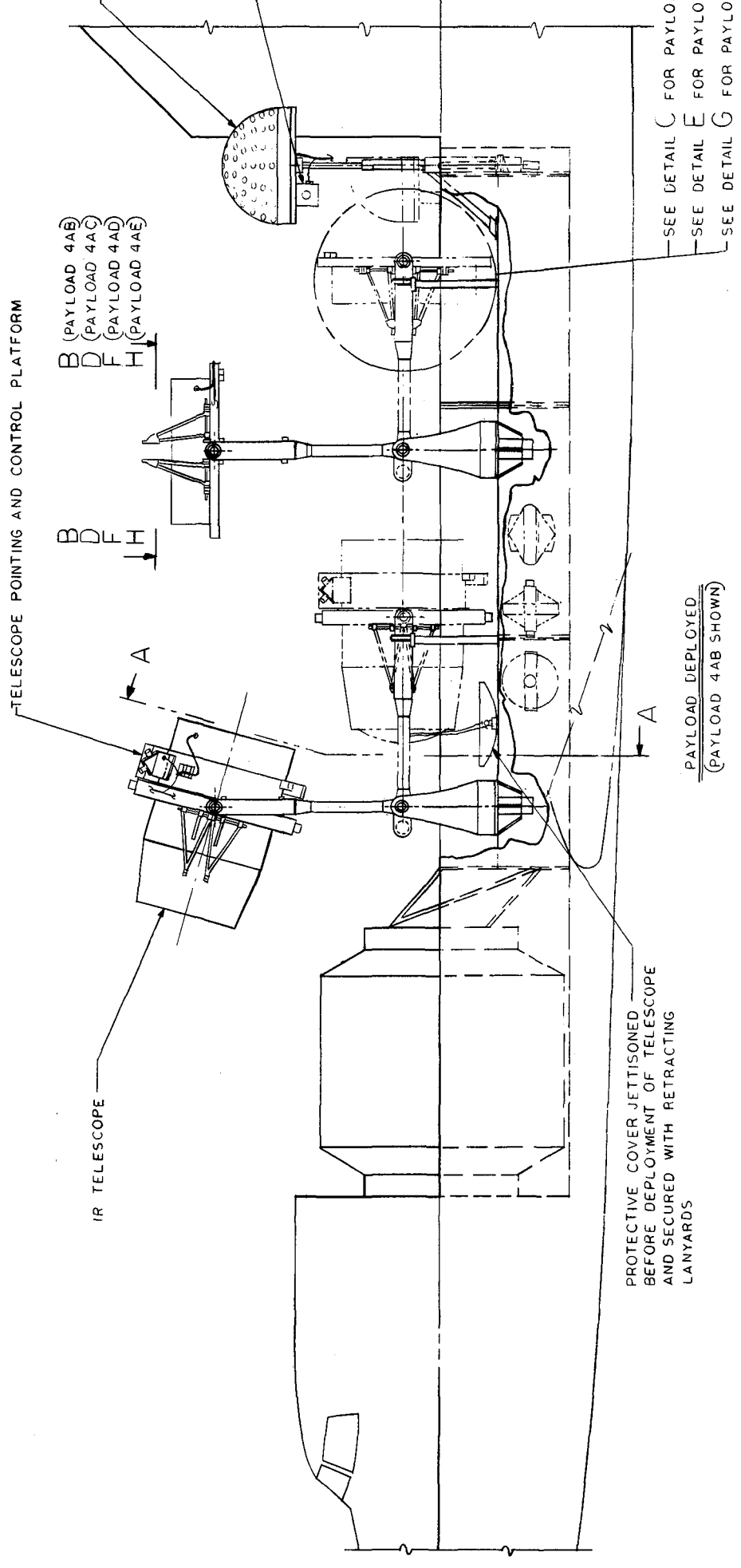
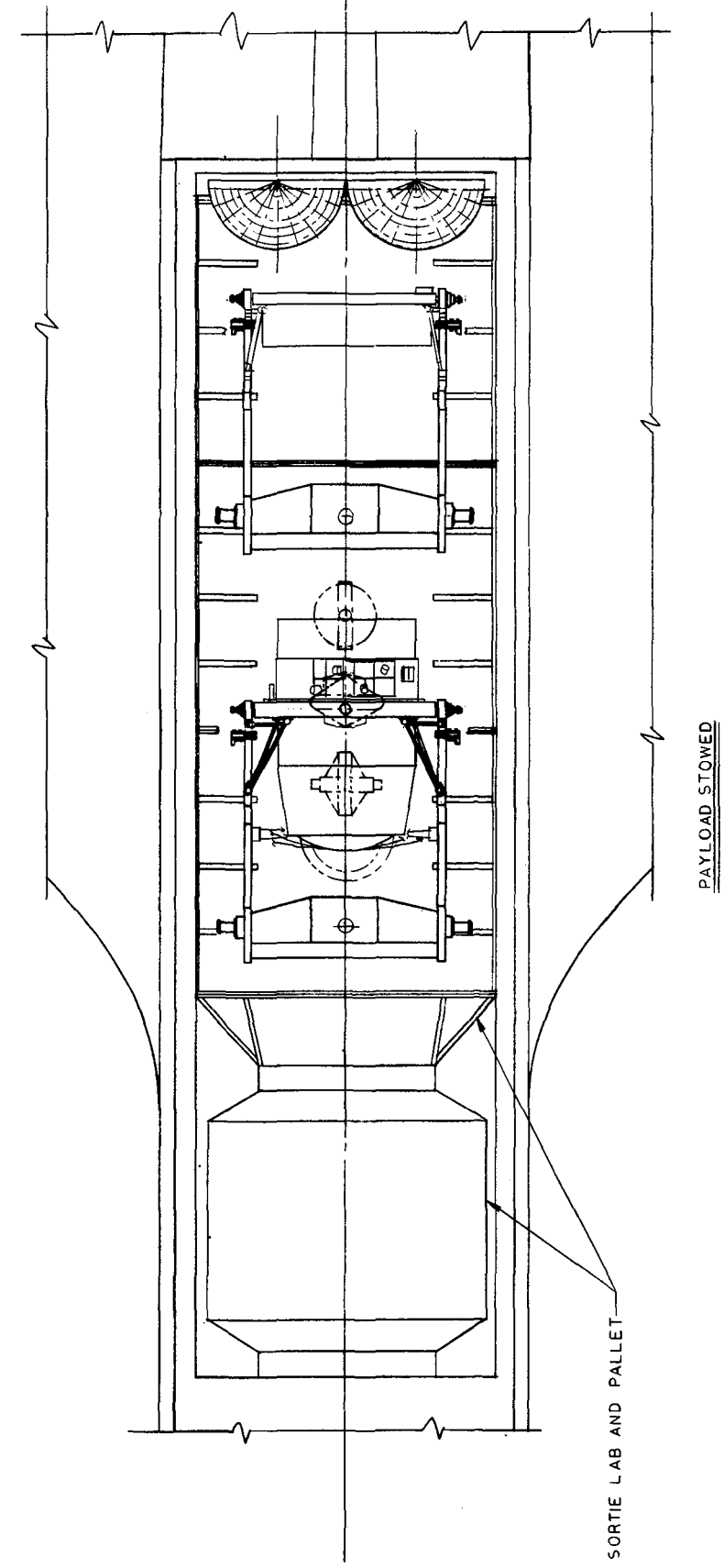
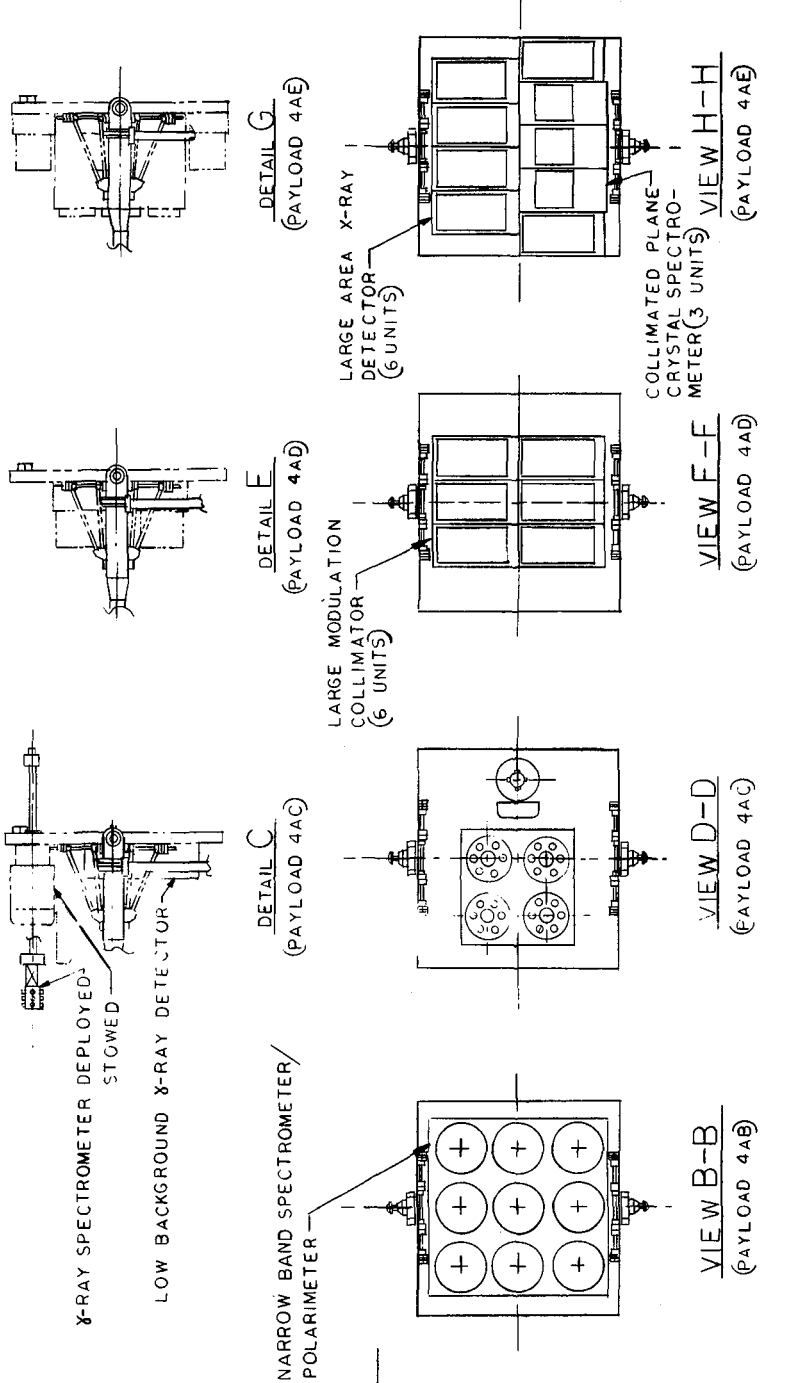
b. Payloads 3AB, 3AC, 3AD, and 3AE - Due to the similarities between these four payloads, all are shown in Fig. IV-4. These stellar-oriented payloads all include the Stratoscope III telescope and the wide coverage X-ray array. Note that this array has been divided into two identical assemblies. This was done due to the large size of the complete hemispherical array, and to eliminate the viewing blockage imposed by the vertical tail of the Shuttle Orbiter. The aft-located array mount accommodates the array groups shown for each of the four payloads.

c. Payloads 4AB, 4AC, 4AD, and 4AE - Again due to similarities, these four stellar-oriented payloads are shown on a single drawing, Fig. IV-5. All payloads include the IR telescope and the wide coverage X-ray array, with the aft-located array mount accommodating the array groups shown for each of the four payloads.

This page intentionally left blank.



MARTIN MARIETTA DENVER DIVISION	
ASM PAYLOAD 3AB, 3AC, 3AD AND 3AE	
SCALE: 1/50	FIG. NO. IV-4
DATE: 8/11/72	IV-11 & IV-12



MARTIN MARIETTA DENVER DIVISION	
ASM PAYLOAD 4A, 4AC, 4AD AND 4AE	
SCALE: 1/50	FIG. NO: IV-13
DATE: 8/17/50	IV-13 & IV-14

d. *Mass Properties* - Mass properties for each of the nine ASM baseline payload combinations were developed using a mass properties computer program. Figure IV-6 defines the Orbiter payload bay reference datum system used in these calculations. Calculations for each payload group referenced to its own datum system were made using a programmable desk top computer. These were then input into the overall payload program as a single card entry, allowing flexibility of location of each group. While only launch and recovery conditions have been included in this report, flexibility built into the program data inputs will allow calculations of deployed condition mass properties.

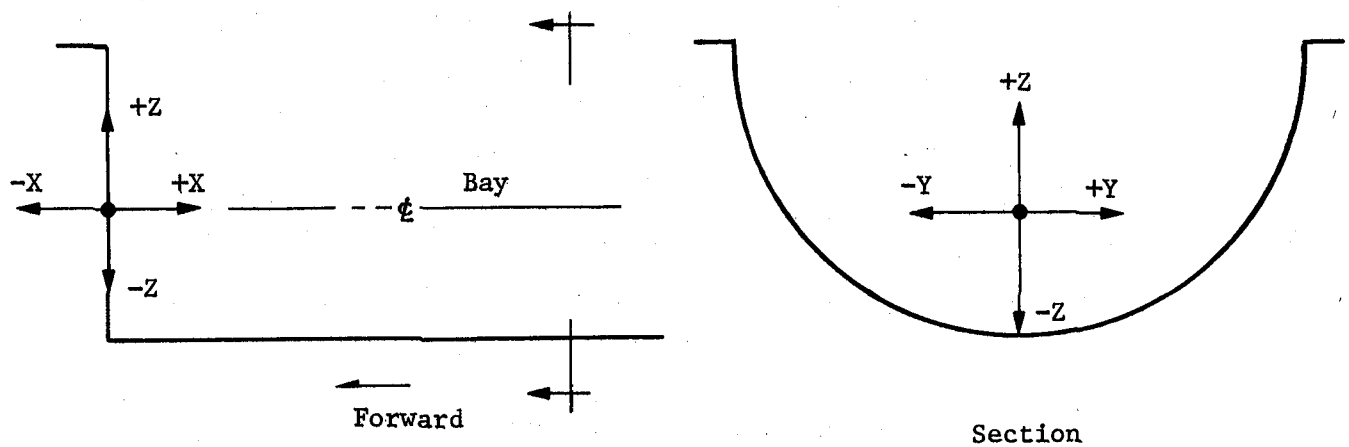


Fig. IV-6 Orbiter Payload Bay Reference Datum System

A detailed computer printout of Payload 1-2 (Solar) mass properties is included in Appendix C1, Volume III, Book 2. Summary sheets are provided for the other eight ASM payloads.

B. SUBSYSTEM AND INSTRUMENT LAYOUTS

Configuration drawings of major subsystem elements and of the telescopes, are presented in this section. Mass properties were developed for these elements and for the ASM arrays. In addition, system level schematics for each of the payloads are included.

1. Subsystem Configuration Drawings

The ASM C&D console, experiment pointing and control actuators and sensors, and the CMGs are shown in this section.

a. *C&D Panel* - The ASM C&D console, discussed in detail in Section D of Chapter III, is shown in Fig. IV-7 thru IV-10.

b. *CMGs* - An outline drawing of one of the pallet-mounted CMGs is shown in Fig. IV-11. Chapter II.A of this volume discusses, in detail, the use of the CMGs.

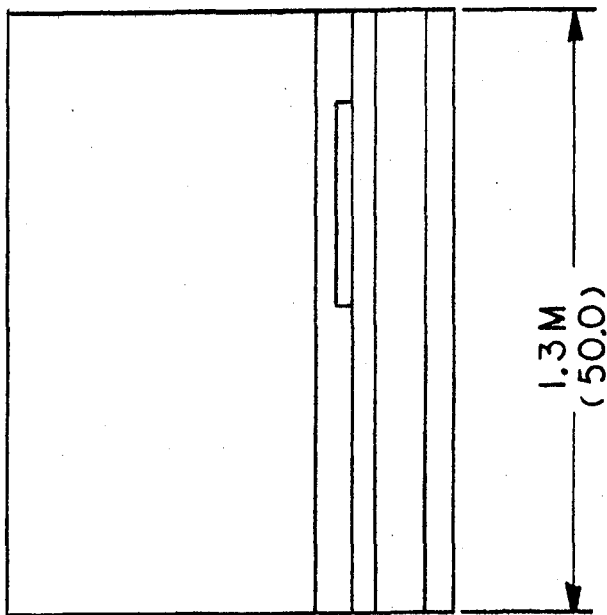
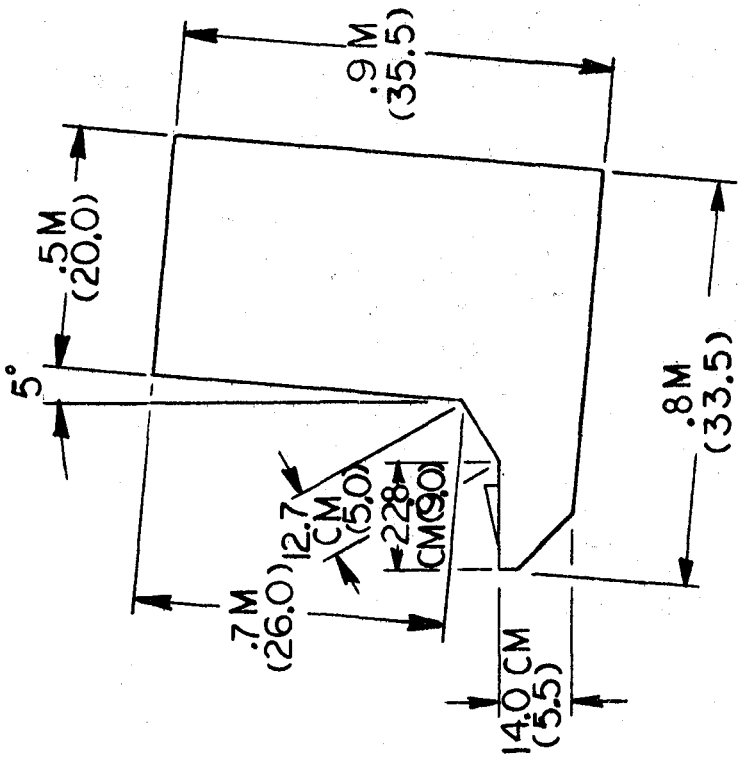
c. *Pointing and Control* - Figures IV-12 thru IV-17 depict the telescope and array mount pointing and stabilization actuators, described in detail in Section C.4 of Chapter III. Figures IV-18 and IV-19 show the telescope P&C sensors located on the telescope and array mounts.

d. *Mass Properties* - Subsystem and support data may be found in the detail computer printout in Appendix C1, Volume III, Book 2. Interconnecting cabling running up the mounts, however, is included in the weight of those elements to simplify center of gravity and inertia calculations.

2. Telescope Layout Drawings

Configuration drawings of each of the ASM telescopes are presented here, along with mass properties of the telescopes and the arrays.

a. *Telescopes* - Figures IV-20, IV-21, and IV-22 show the X-ray telescope, inner and outer coronagraphs, and the XUV spectroheliograph, respectively. Figure IV-23 shows these telescopes packaged together in a common structure, along with supporting sensors and electronic equipment. This package is located in the forward telescope mount for solar Payload 1-2. Figures IV-24 and IV-25 depict the photoheliograph and Stratoscope III telescopes. The IR telescope has been shown and discussed previously in Section III.B of this volume. All of the telescopes that are mounted individually on the telescope mount, as well as the package of telescopes mentioned above, interface with the inner roll ring of the telescope gimbal assembly. This is accomplished by means of adapters that allow attaching the telescopes to a multiple point pattern on the roll ring.

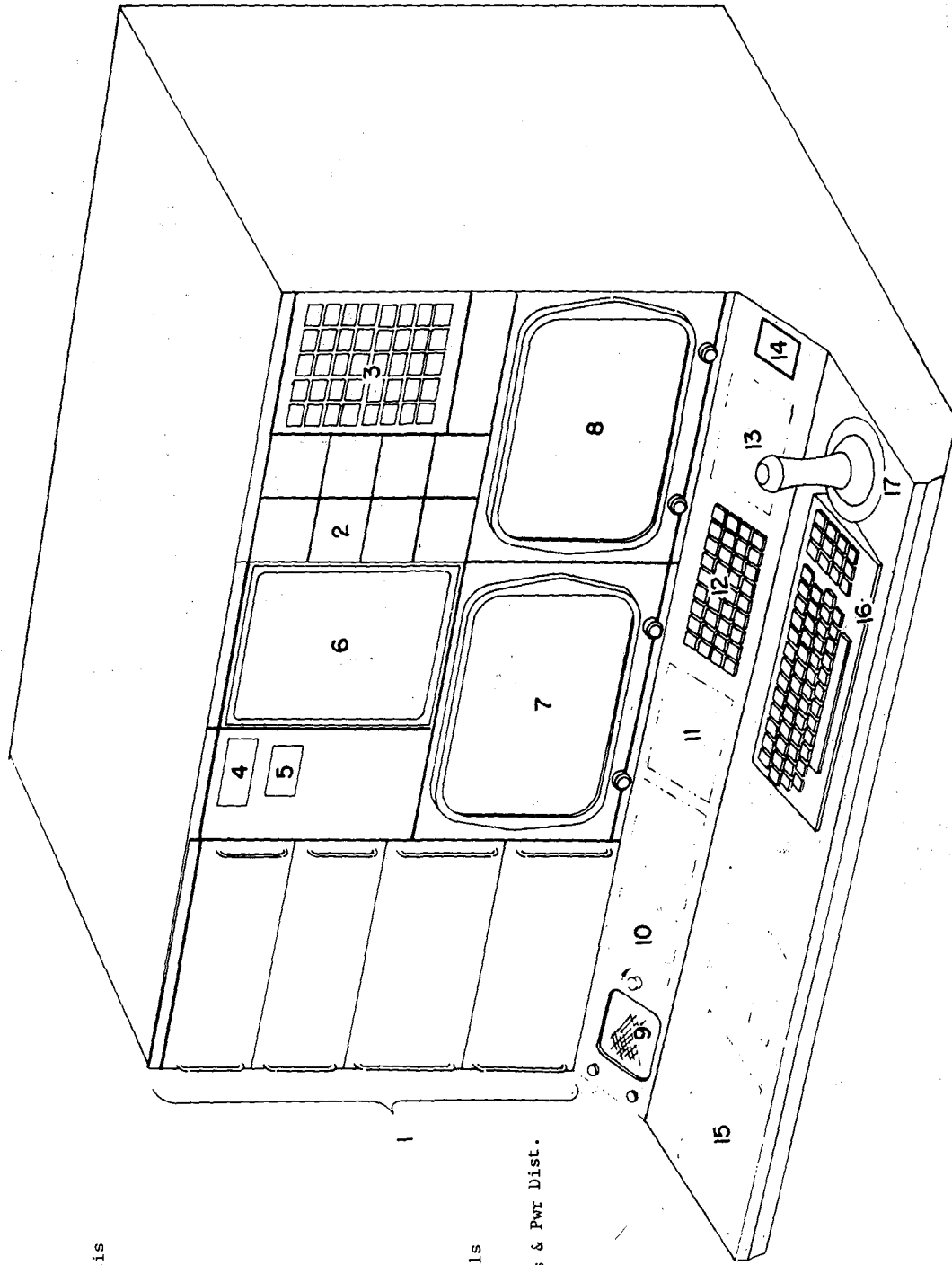


The Bendix Corporation
 Navigation & Control Division
 Teaneck, New Jersey 07608

ASM C&D CONSOLE
 OUTLINE DRAWING

FIG. IV-7

- 1 Dedicated Experiment Chassis
- 2 Advisory Experiment
- 3 Caution & Warning
- 4 Mission Time
- 5 Event Time
- 6 Microfilm Viewer
- 7 CRT 14" Experiment
- 8 CRT 14" Experiment
- 9 ICOM Speaker
- 10 ICOM Controls
- 11 Lighting
- 12 Function Keyboard
- 13 Monitor Selection Controls
- 14 Console Emergency Pwr
- 15 Console Circuit Breakers & Pwr Dist.
- 16 Alphanumeric Keyboard
- 17 3 Axis Controller

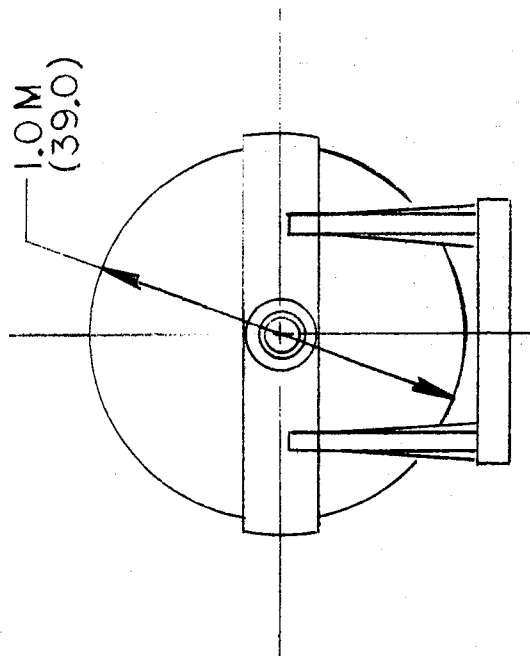


The Bendix Corporation
 Navigation & Control Division
 Teterboro, New Jersey 07608

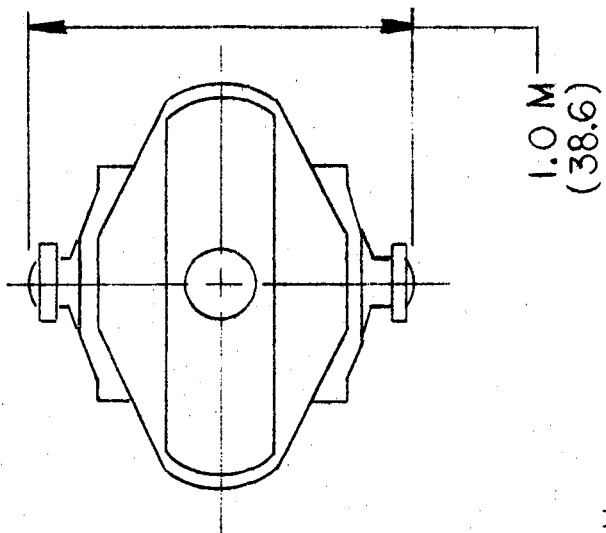
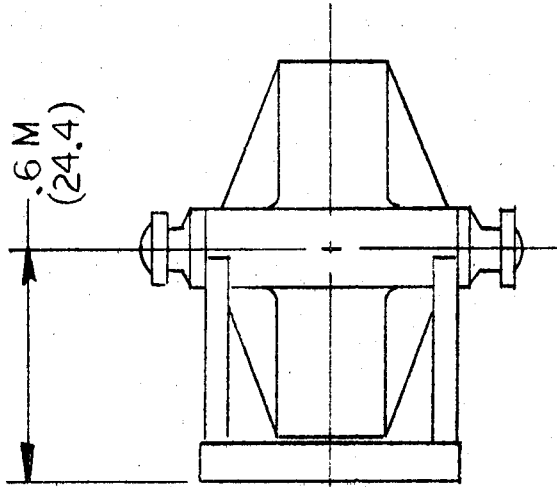
ASM C & D CONSOLE

FIG. IV-8

1.0 M
(39.0)



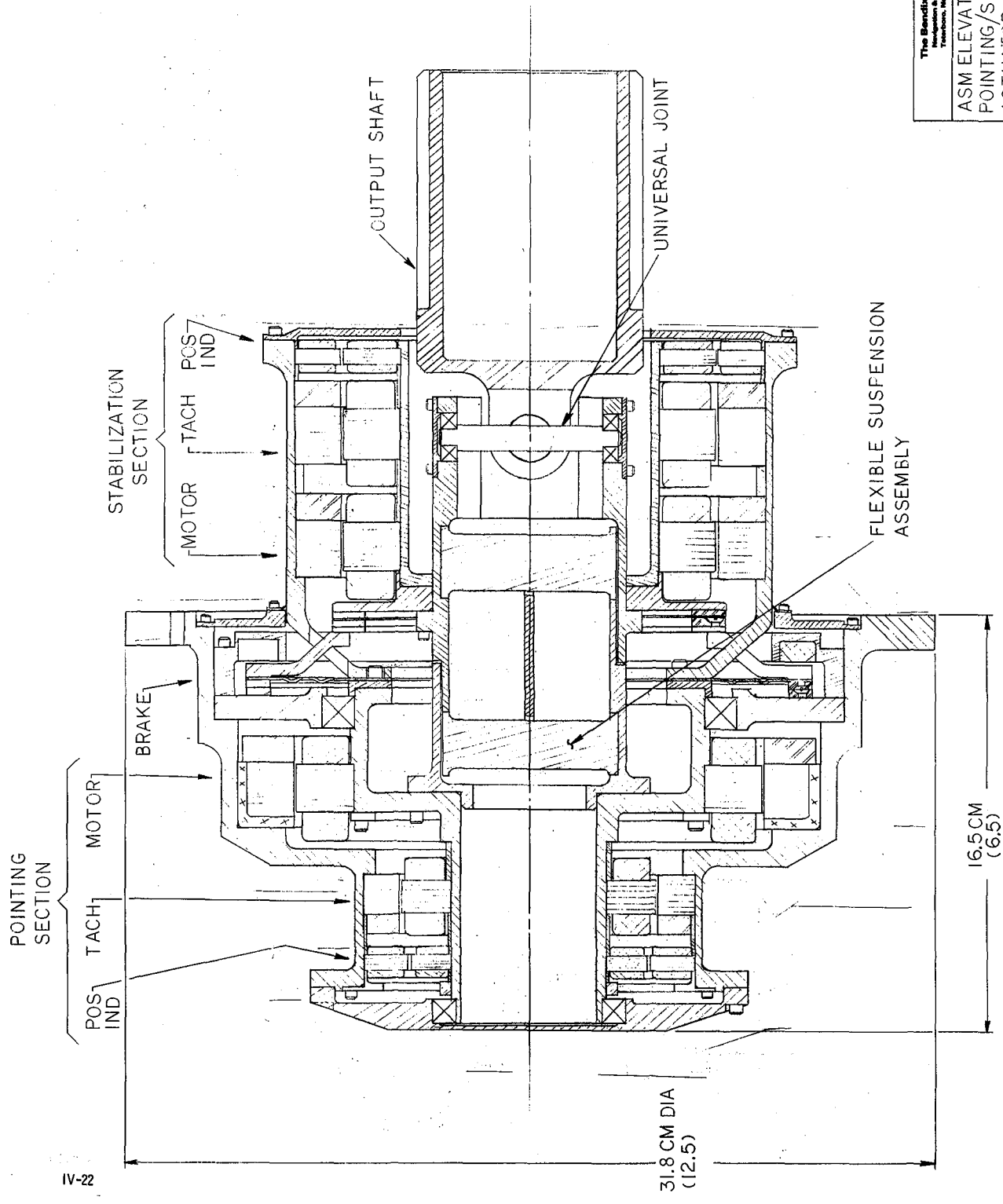
.6 M
(24.4)



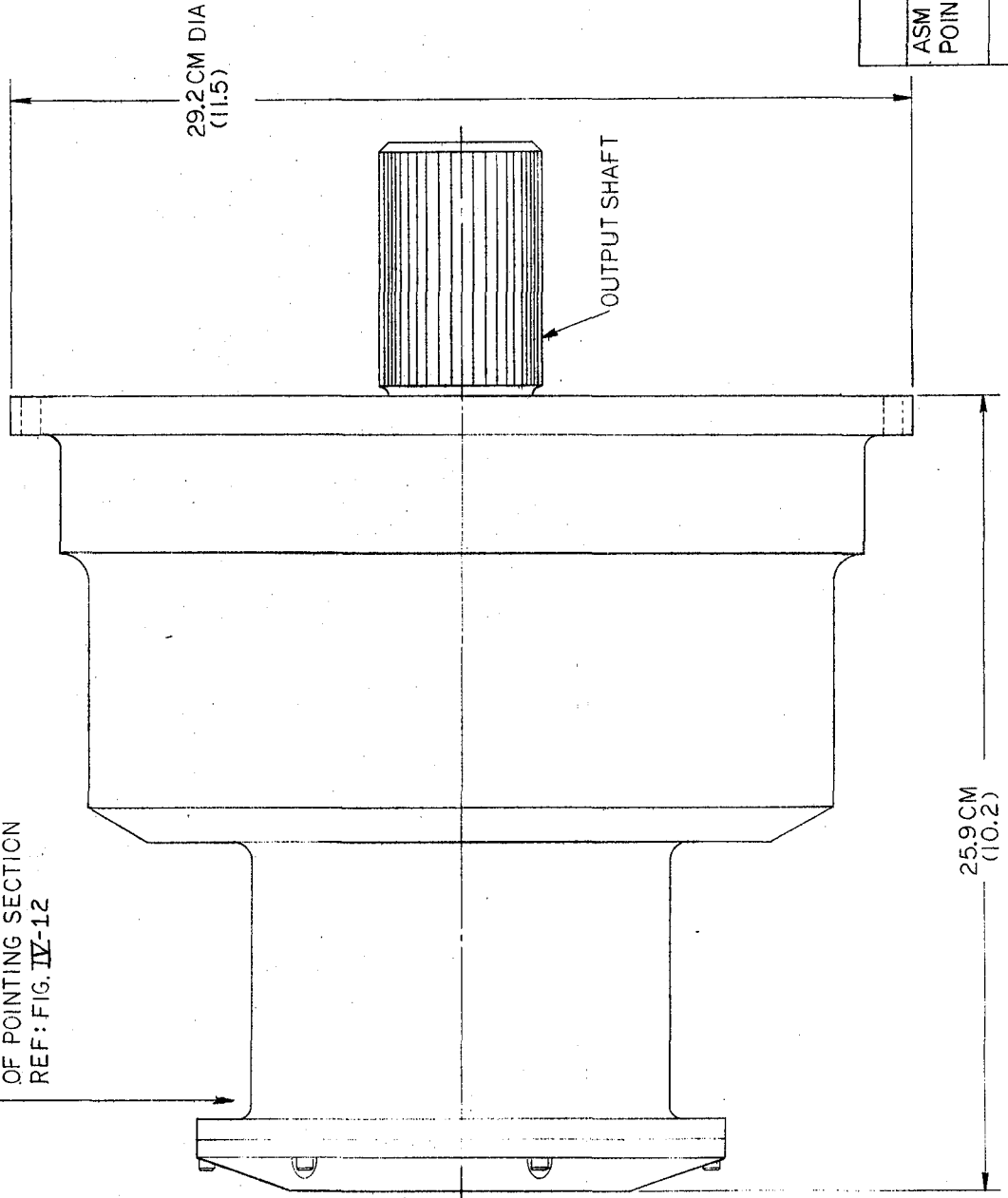
The Bendix Corporation
Navigation & Control Division
Teterboro, New Jersey 07608

**ASM CMG OUTLINE
DRAWING**

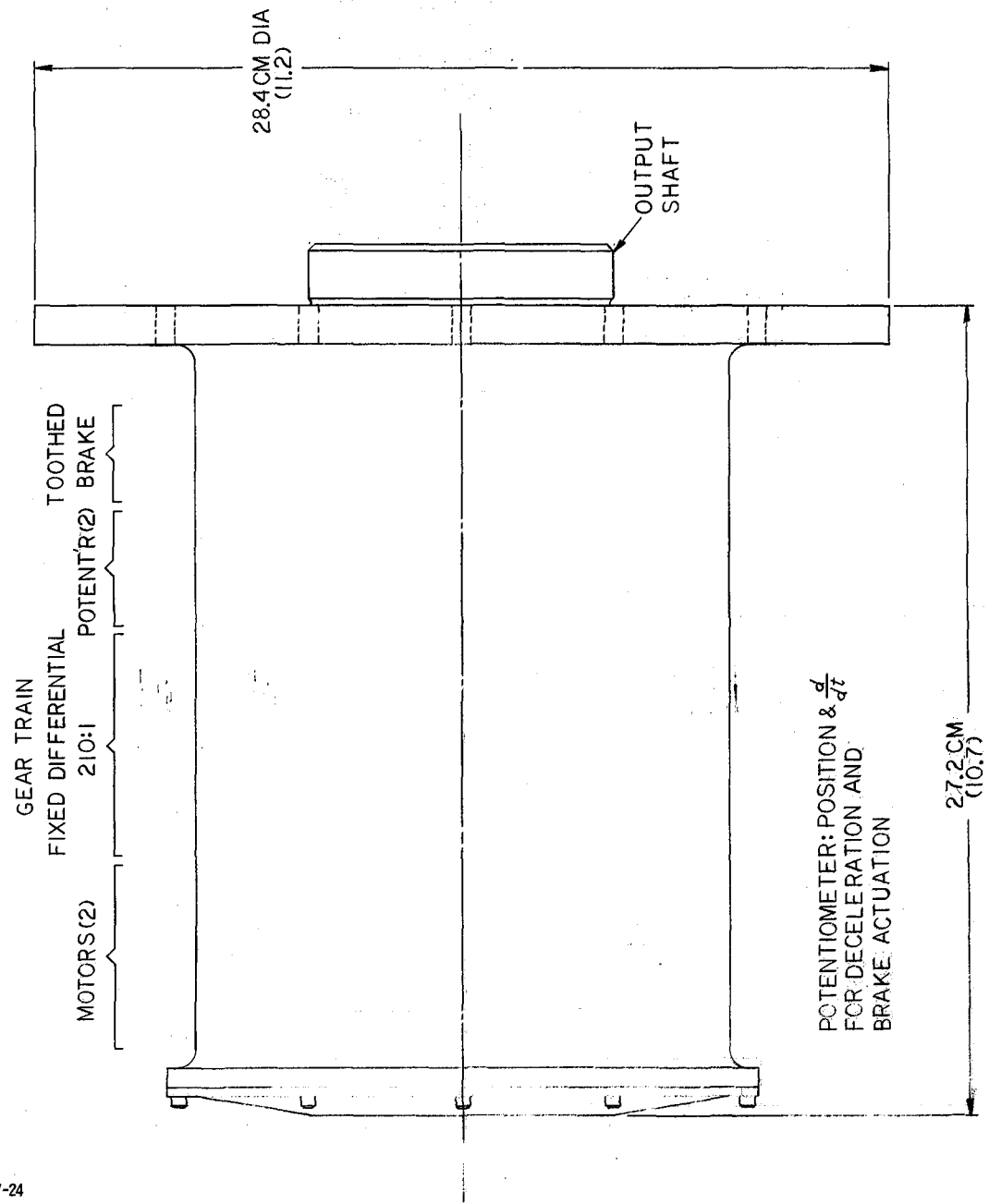
FIG. IV-11



INTERNAL MECHANISM PER
ELEVATION POINTING/STAE.
ACTUATOR EXCEPT
REDUNDANT MOTOR, TACH.,
& POSITION INDICATOR
OF POINTING SECTION
REF: FIG. IV-12

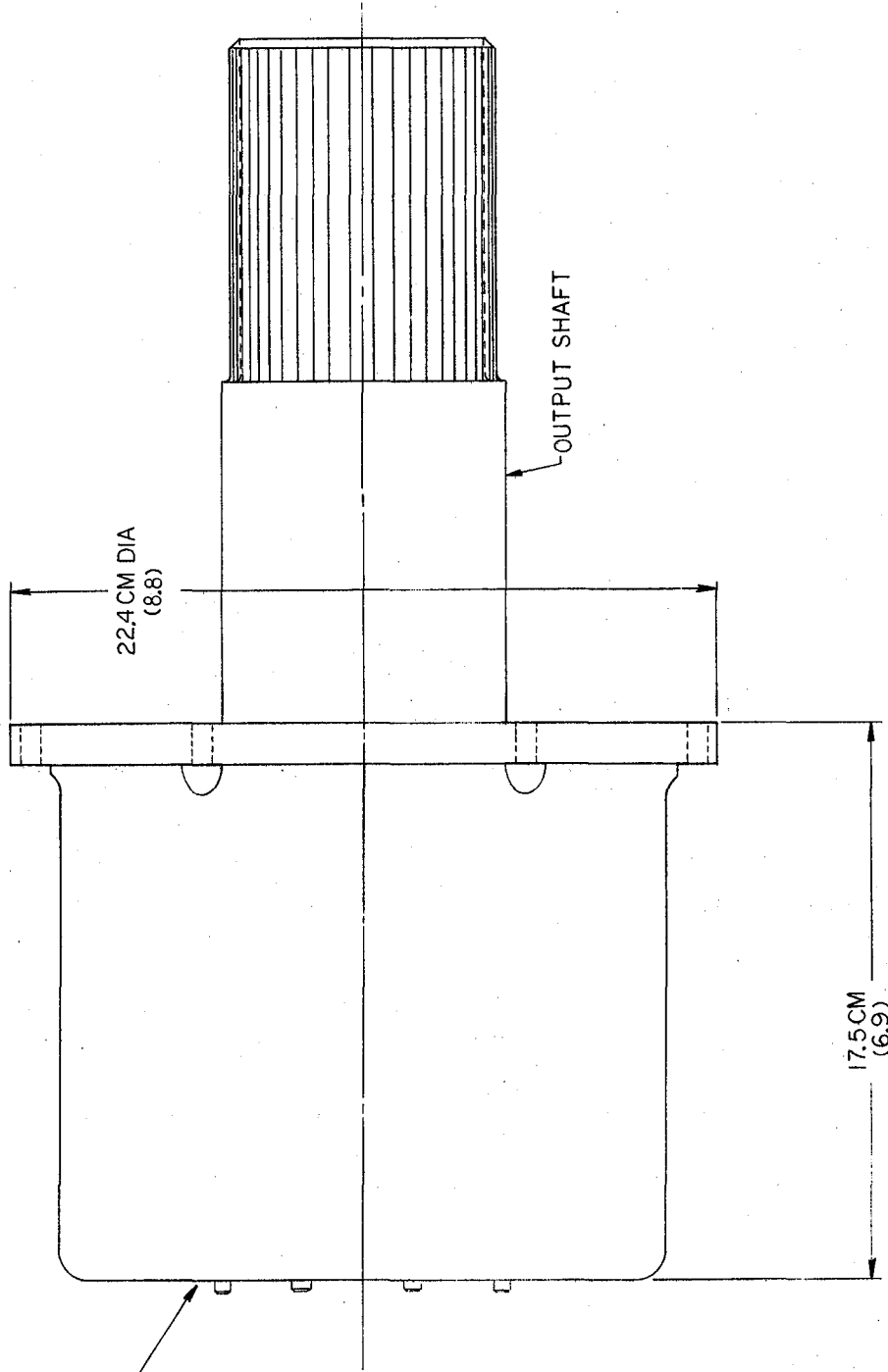


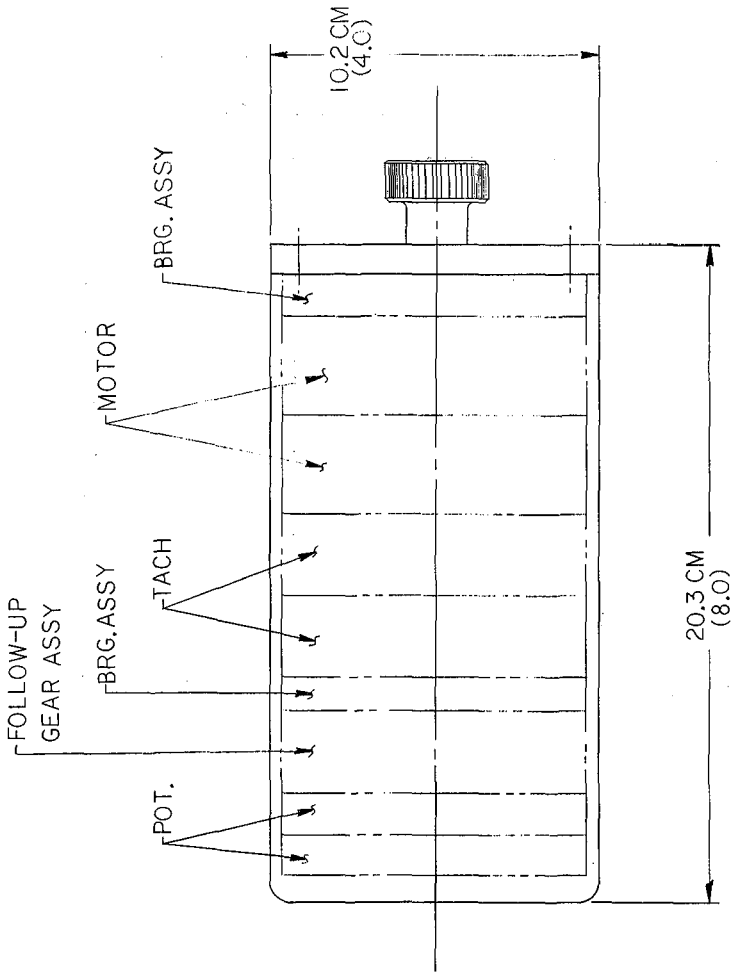
The Bendix Corporation Manufacturing & Control Division Troy, Michigan 48060
ASM AZIMUTH TABLE POINTING ACTUATOR
FIG. IV-13



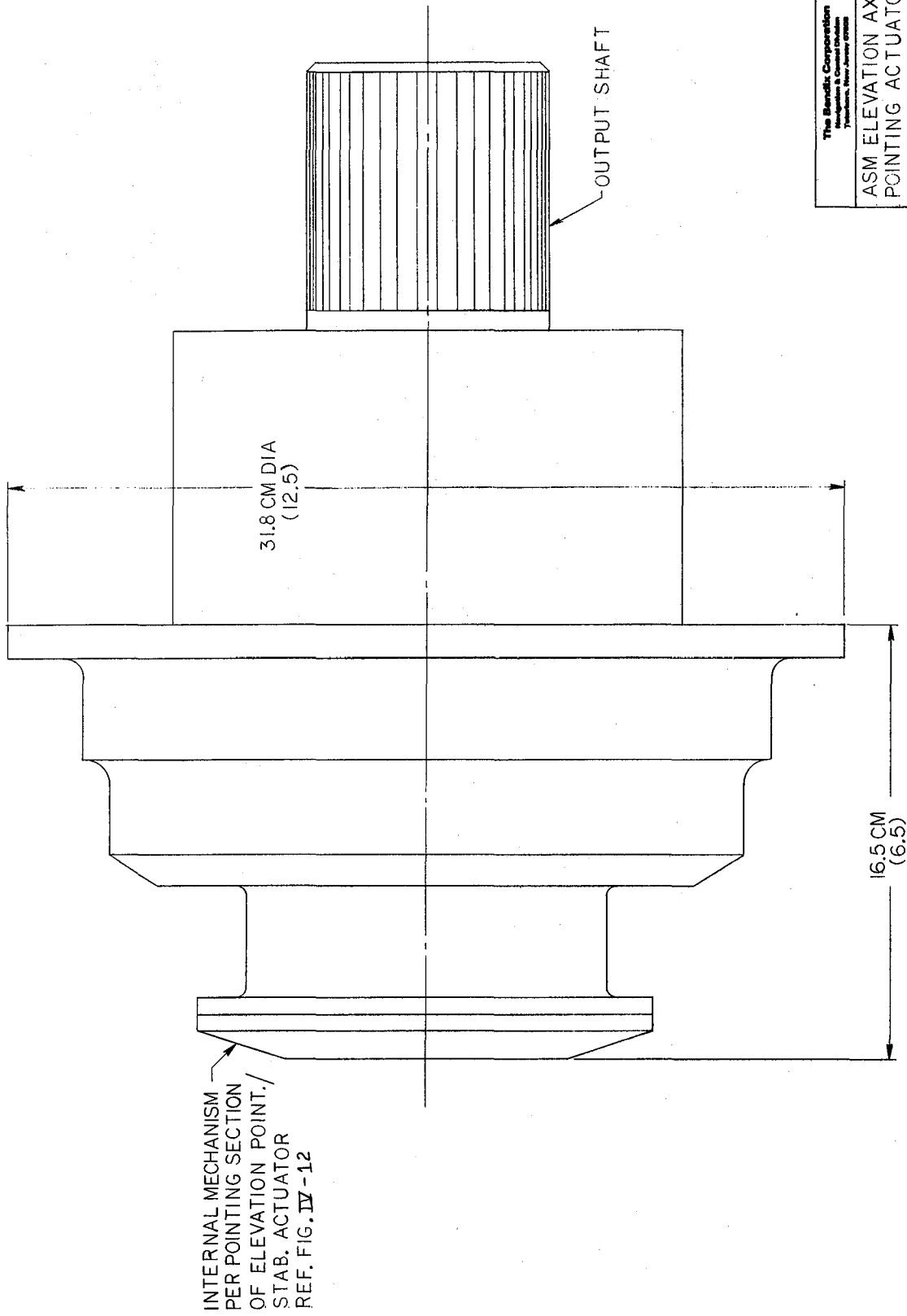
The Sherrill Corporation Manufacturing Division P.O. Box 1000 Cincinnati, Ohio 45201
ASM DEPLOYMENT ACTUATOR
FIG. IV-14

INTERNAL MECHANISM PER STABILIZATION
SECTION OF ELEVATION POINTING/STAB.
ACTUATOR (INCLUDES SMALLER DIA.
BRAKE FOR POINTING MODE)
REF.: FIG. IV-6

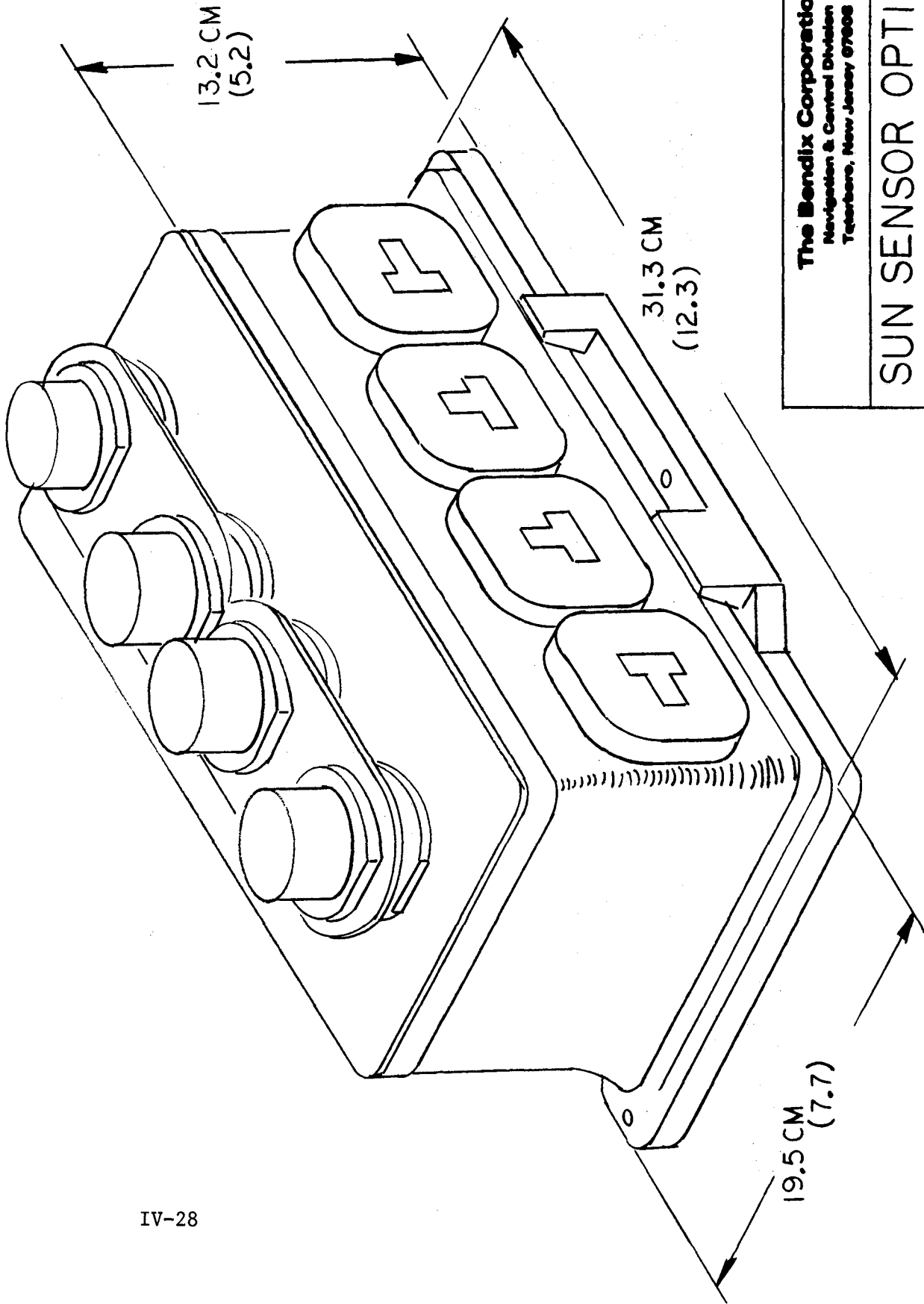




The Benditt Corporation Navigation & Control Division Washington, D.C. 20546
ASM ROLL POINTING/ STABILIZATION ACTUATOR
FIG. IV-16



The Benditt Corporation Manufacture & Control Division Tulsa, Oklahoma	
ASM ELEVATION AXIS POINTING ACTUATOR	
FIG. IV-17	

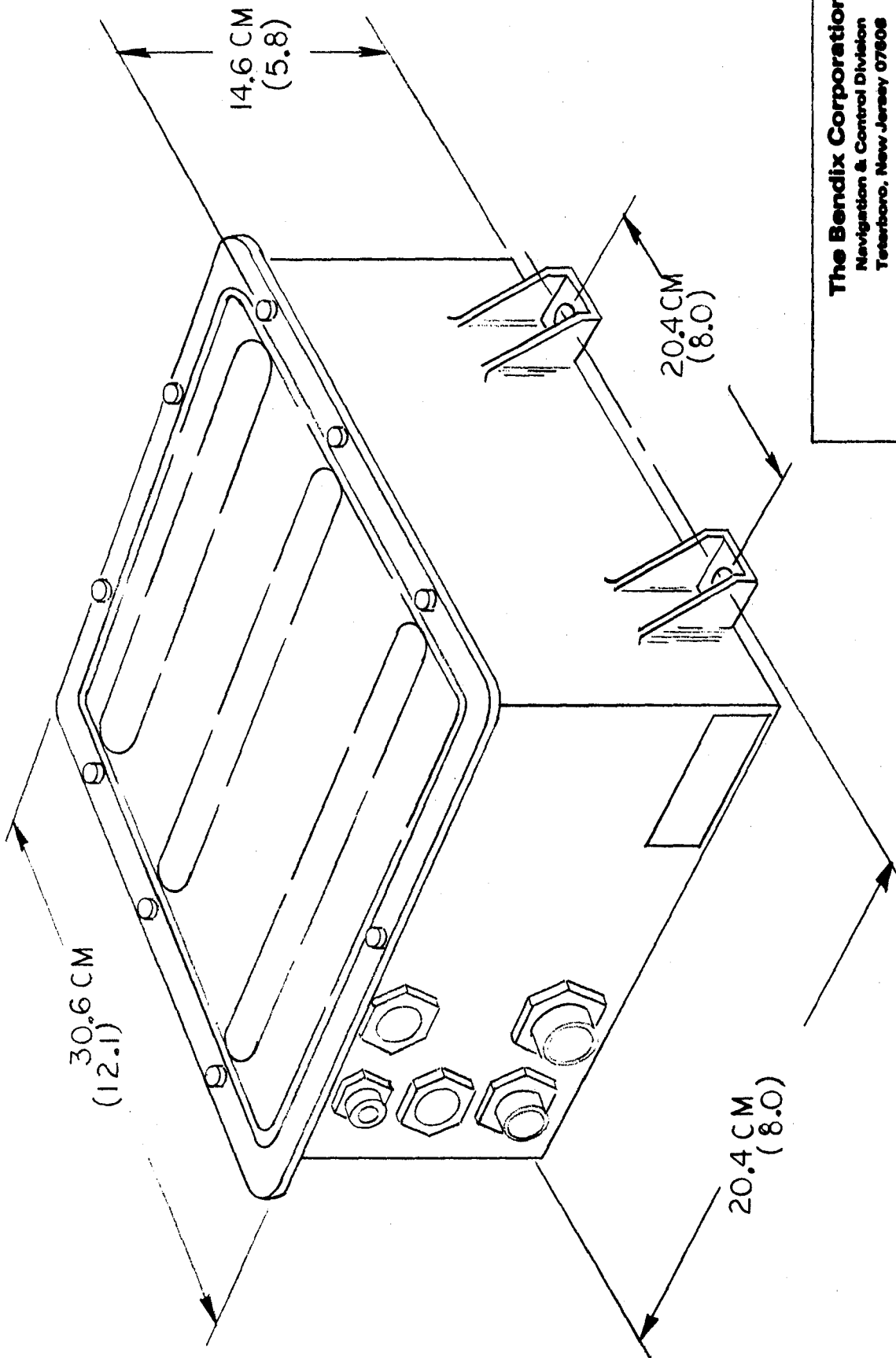


IV-28

The Bendix Corporation
Navigation & Control Division
Teterboro, New Jersey 07608

SUN SENSOR OPTICAL-
MECHANICAL ASSY

FIG. IV-18

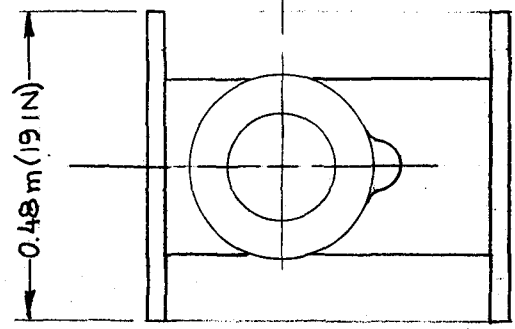
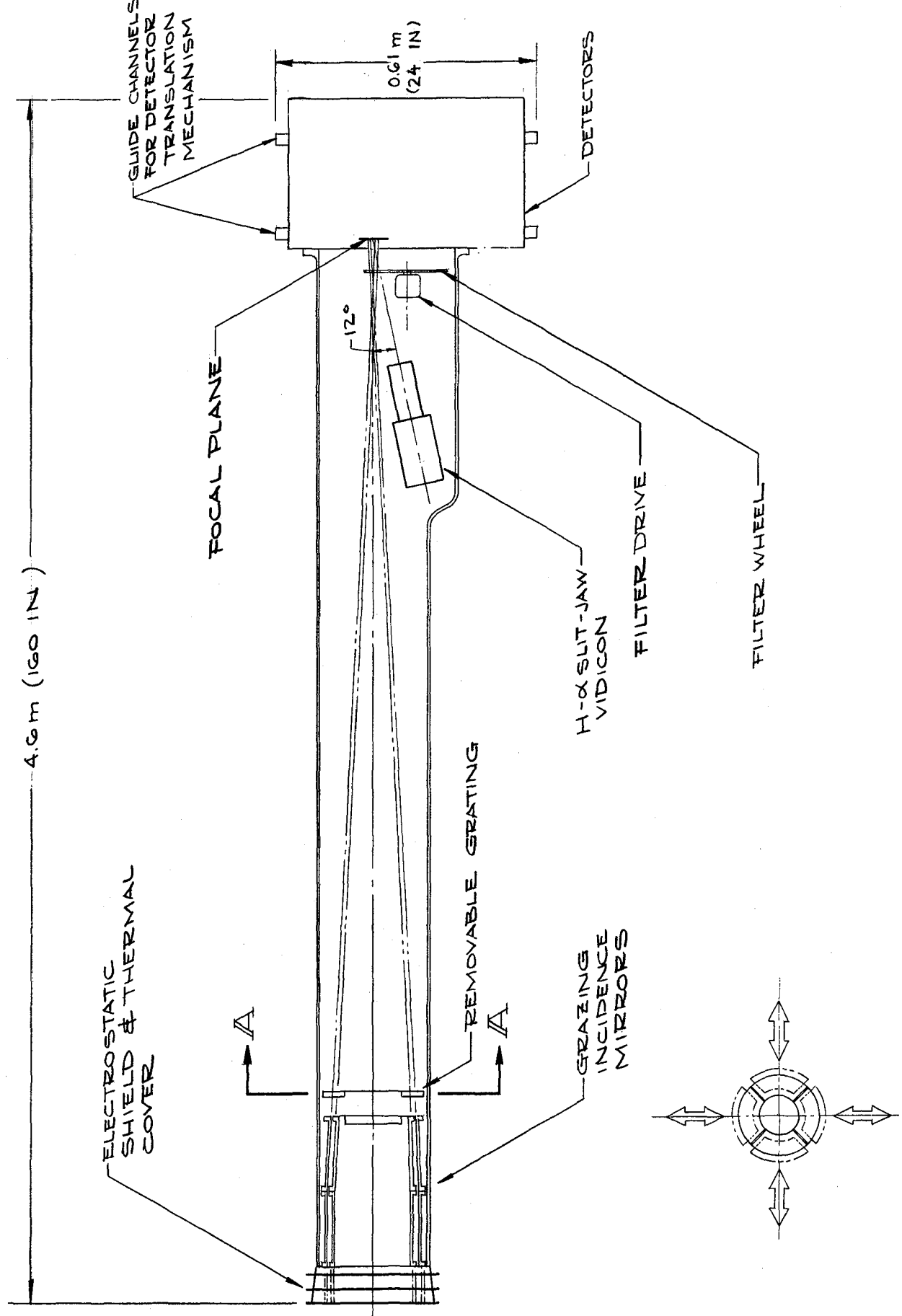
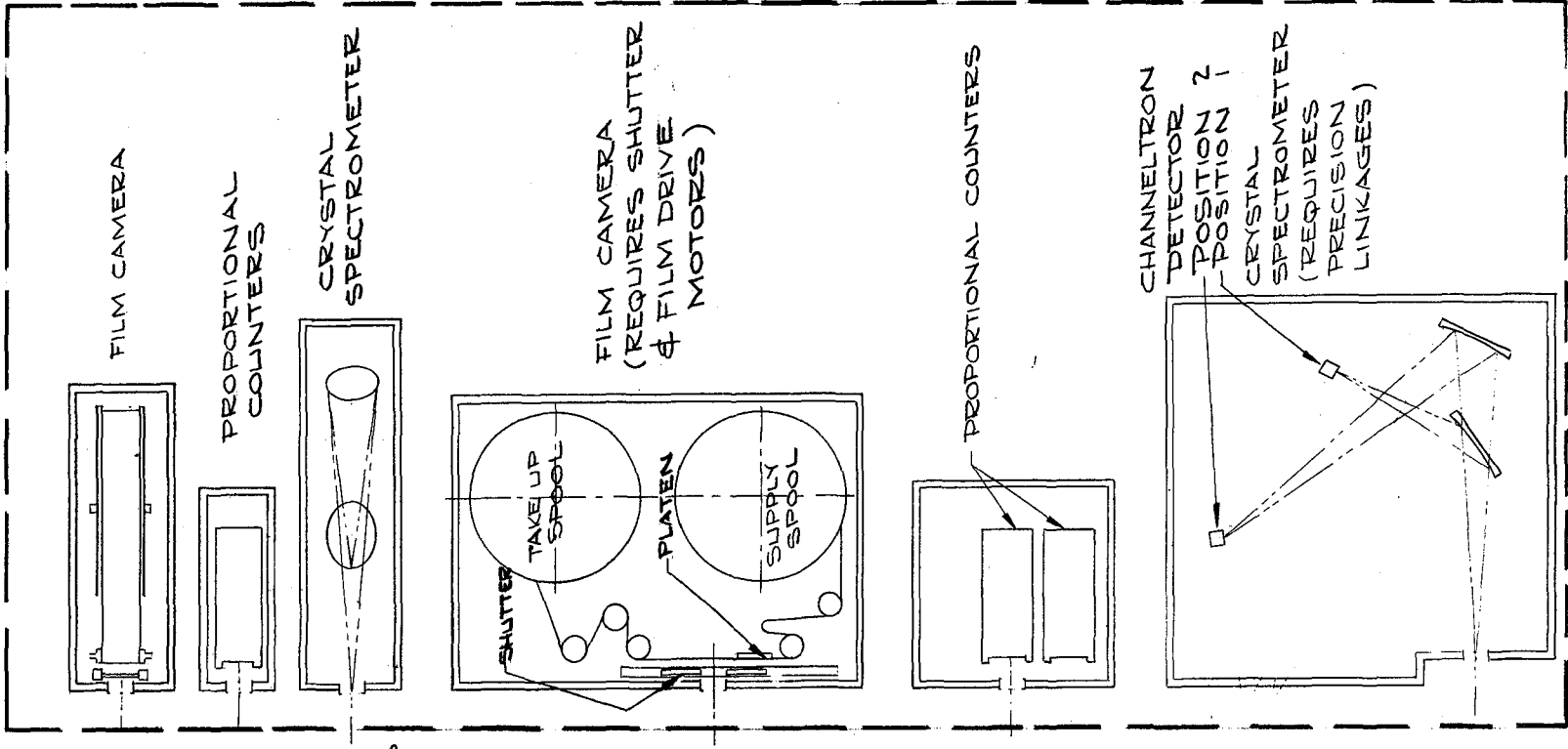


The Bendix Corporation
 Navigation & Control Division
 Teterboro, New Jersey 07608

IMU PACKAGE

FIG. IV-19

This page intentionally left blank.

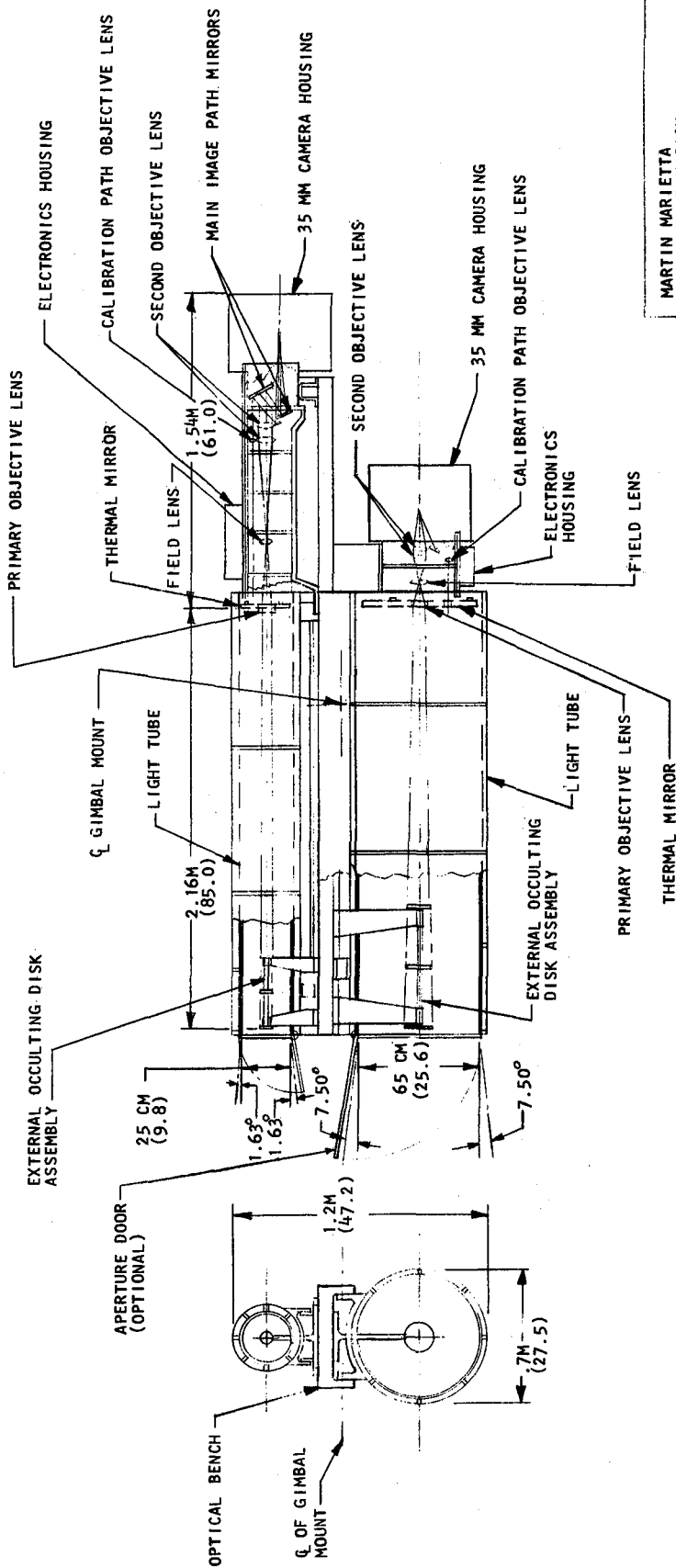


SECTION A-A
GRATING INSERTION/REMOVAL MOTION

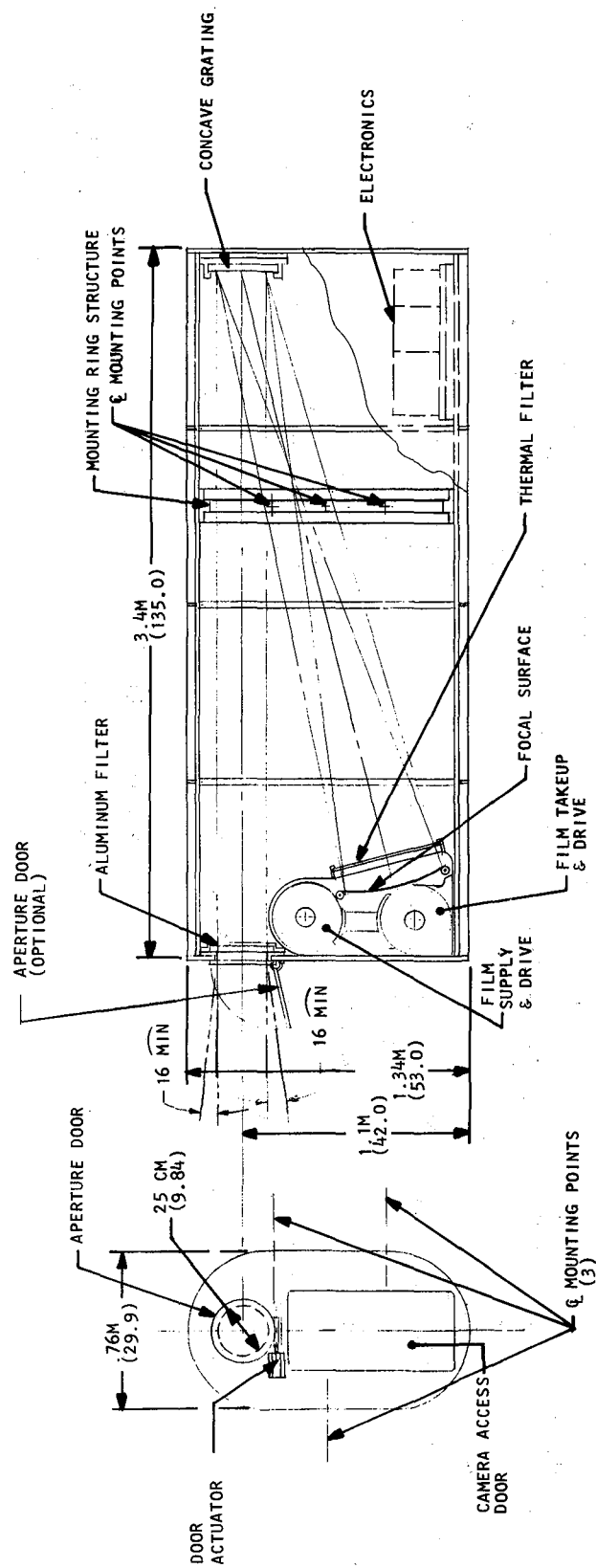
The Bendix Corporation
Navigation & Control Division
Teterboro, New Jersey 07608

X-RAY
TELESCOPE

FIG. IV-20



MARTIN MARIETTA
 DENVER DIVISION
 INNER AND OUTER CORONAGRAPHS
 FIG. NO. IV-21



MARTIN MARIETTA DENVER DIVISION
25 CM XUV SPECTROHELLOGRAPH
FIG. NO. IV-22

AFT VIEW SHOWING
 LOCATION OF
 ELECTRONIC PACKAGES

FINE SUN SENSOR SIGNAL
 CONDITIONER

FINE SUN SENSOR CONTROL ELECTRONICS
 ASSY

FINE SUN SENSOR PRE-AMP ASSY

XUV CAMERA CONTROL UNIT
 (OPPOSITE SIDE OF BULKHEAD)

XUV SPECTROHELIOGRAPH

X-RAY TELESCOPE

INSULATION BLANKET

METEOROID SHIELD WITH
 FIBERGLASS STANDOFFS

INNER GIMBAL ROLL RING(REF)

EXTERNAL RING FRAME(TYP)

VIEW D
 SCALE: 1/4

MULTILAYER INSULATION

INNER GIMBAL ROLL RING(REF)

ADAPTER FITTING

METEOROID SHIELD

FIBERGLASS STANDOFF

SHELL

EXTERNAL FRAME

FORWARD

SECTION C-C
 SCALE: 1/4
 (TYP DOOR MECHANISM)

X-RAY TELESCOPE

X-RAY TELESCOPE MONITOR

INNER CORONAGRAPH

CORRELATION TRACKER

FORWARD CLOSURE WITH
 APERTURE DOORS

INNER CORONAGRAPH

52°

78°

90°

80°

112°

FRONT VIEW
 (SHOWS OPERATIONAL
 MOVEMENT OF DOORS)

SECTION A-A
 NOTE: CROSS HATCHING DENOTES
 APERTURE OPENING

X-RAY TELESCOPE

X-RAY TELESCOPE MONITOR

INNER CORONAGRAPH

CORRELATION TRACKER

INNER CORONAGRAPH

OUTER CORONAGRAPH

FINE SUN SENSOR

XUV SPECTROHELIOGRAPH

XUV MONITOR

SECTION B-B

INTERNAL STRINGER(TYP)

2.13 M (6.97)

2.1 M (6.89)

EXTERNAL FRAME

GIMBAL RING ATTACH BRACKET
 (5 PLACES)

INNER GIMBAL ROLL RING

VIEW E
 SCALE: 1/4
 (C-OC INDEPENDENT
 GIMBAL; ±.5° TRAVEL
 EACH AXIS)

PITCH DRIVE
 MOTOR

CORONAGRAPH
 MOUNT

WORM AND WORM
 GEAR DRIVE

MOUNTING PLATE

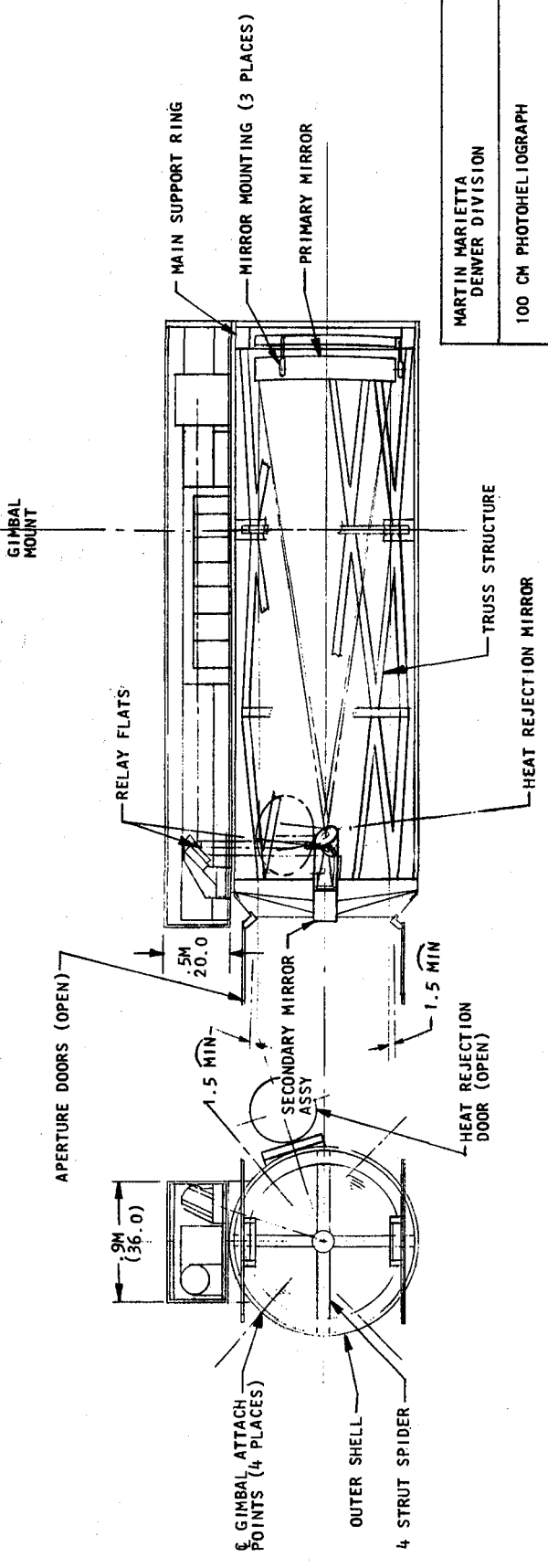
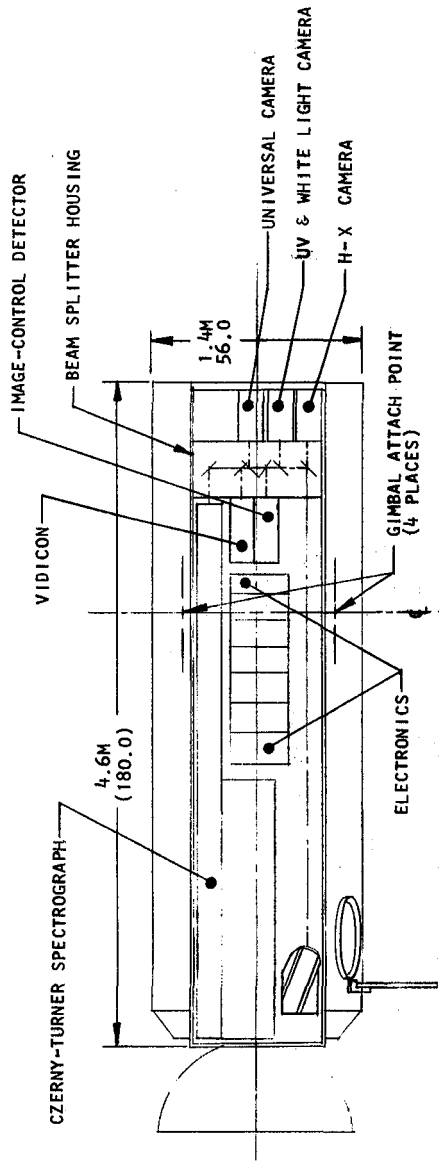
OFFSET ROLLERS (3)

SKIN OMITTED FOR CLARITY

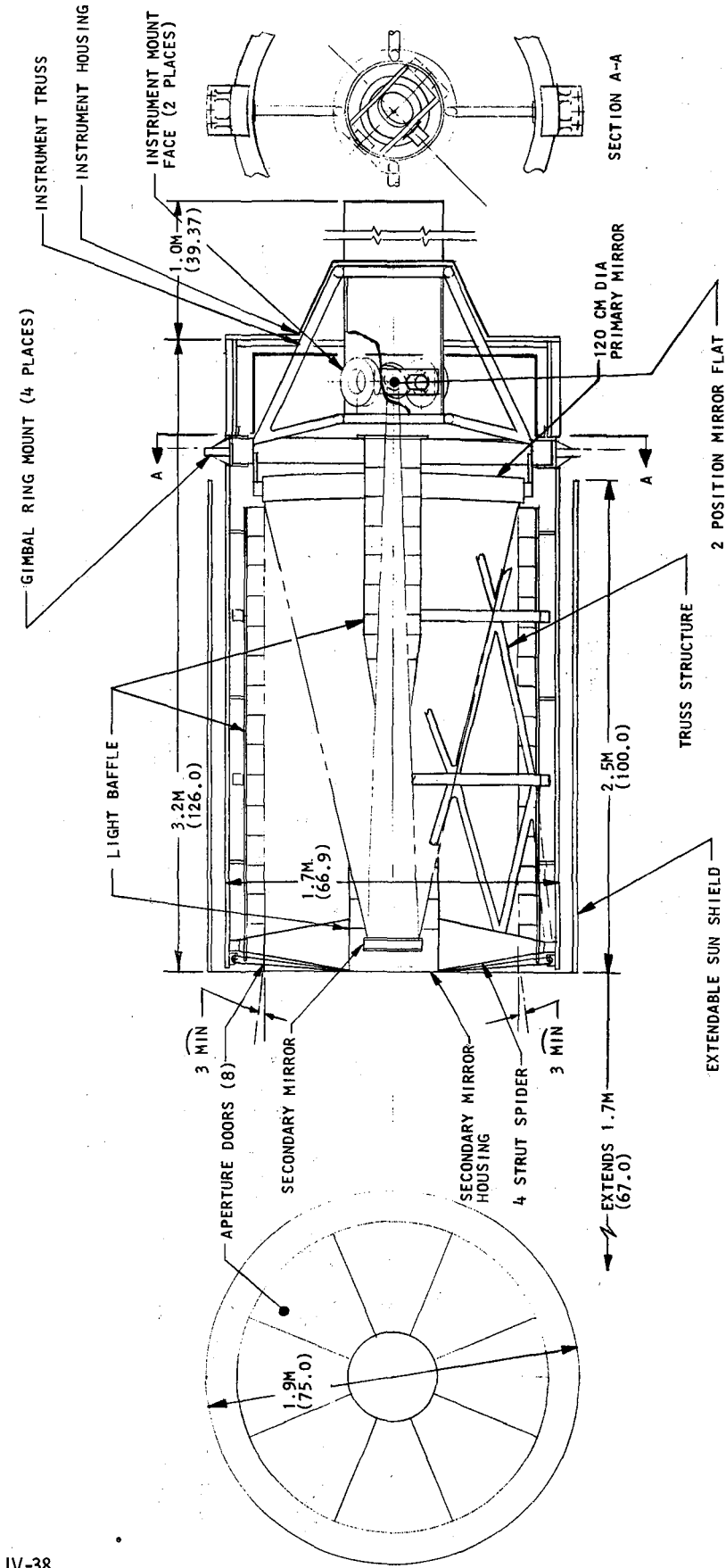
WORM AND WORM
 GEAR DRIVE

INTERNAL STRINGER(TYP)

INTERNAL



MARTIN MARIETTA DENVER DIVISION	
100 CM PHOTOHELIOGRAPH	
FIG. NO. IV-24	



MARTIN MARIETTA DENVER DIVISION
STRATOSCOPE III - 120 CM TELESCOPE
FIG. NO. IV-25

b. *Mass Properties* - Individual telescope and array installations were calculated using desk top computer routines. Copies of the work sheets used for these calculations form good summary statements for each payload group. These are shown in Appendix C2, Volume III, Book 2.

To simplify calculations, parts such as truss structure, insulation, baffles, etc, have been combined into a single entry.

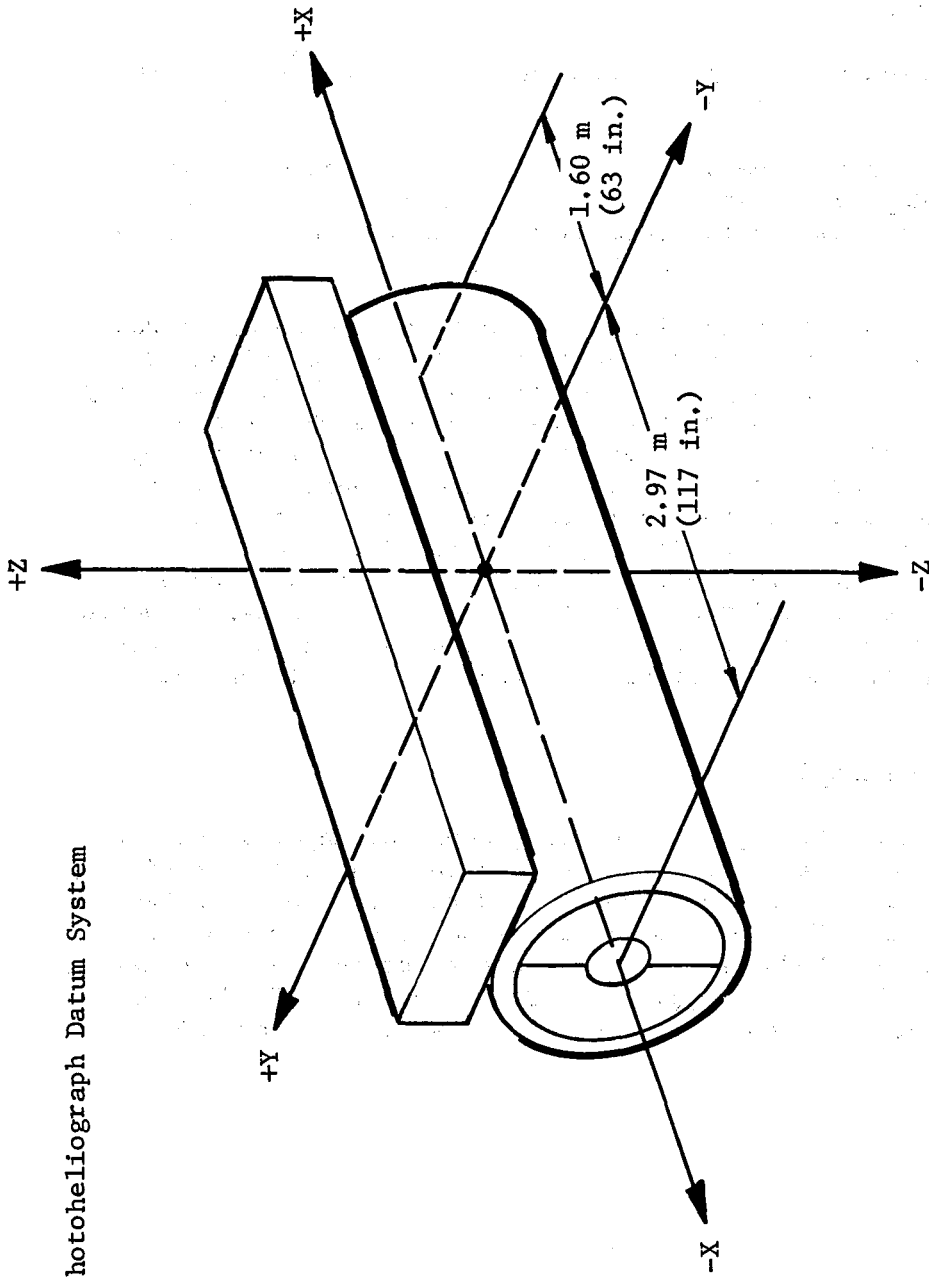
Each experiment reference datum is set up within the experiment to provide an independent reference that can be used for future calculations of instruments in deployed positions. These reference systems are shown in Fig. IV-26 thru IV-30.

By modifying input cards and instructions to the computer it was possible to develop mass characteristics felt by each gimbal drive motor. Some telescope payloads have already been shifted slightly to bring their centers of gravity closer to the gimbal plane. Because these data were developed late in the program no attempt was made to evaluate the effect on the drive actuators or whether it would be necessary or desirable to shift the telescope center of gravity. Some cg correction may be achieved by equipment rearrangement or slight relocation of attachment points. Further correction could be achieved by ballast, however, ballasting would increase moment of inertia, which may be less desirable for actuator operation than centers of gravity that do not fall on the gimbal centerline.

3. System Level Schematics

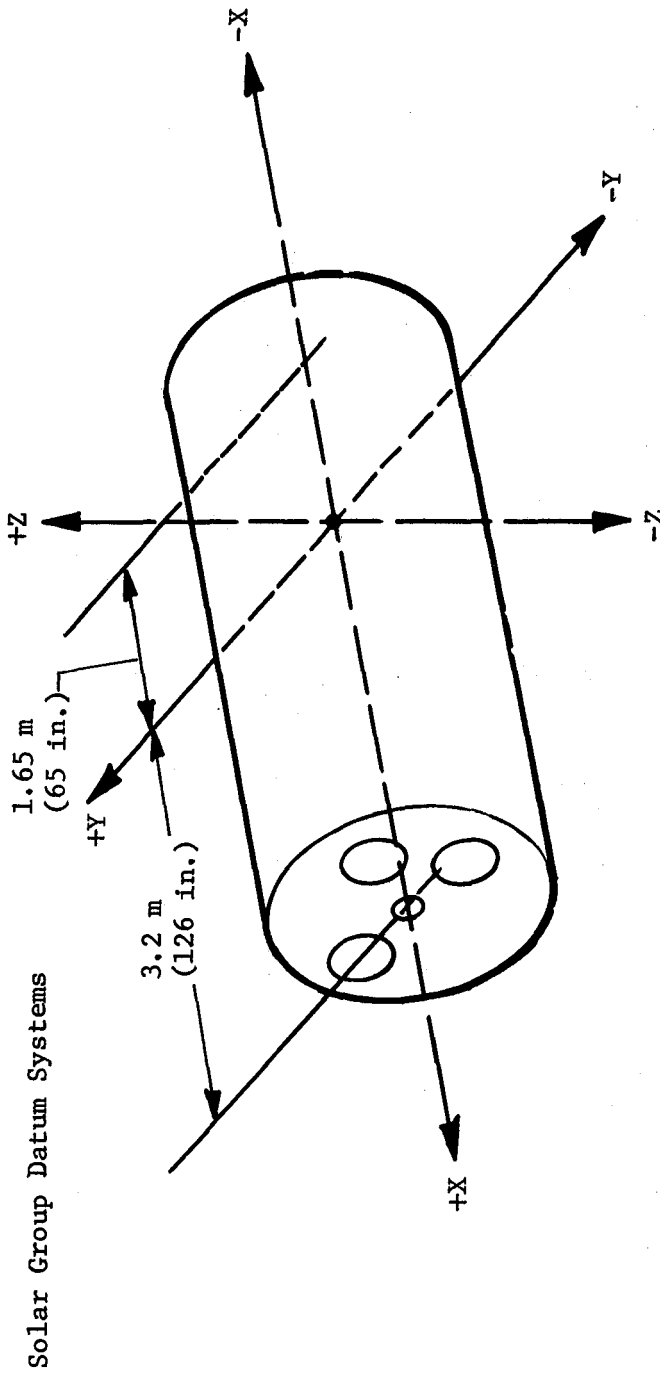
System level schematics presented here, show the major interfaces between the payload and the Sortie Lab/pallet, the relationship of the subsystems to the experiments, and the relationships between subsystems. Figure IV-31 is the schematic for Payload 1-2. Figures IV-32 and IV-33 each present schematics for four similar ASM payloads. The former applies to Payloads 3AB, 3AC, 3AD, and 3AE, while Fig. IV-33 covers Payloads 4AB, 4AC, 4AD, and 4AE.

Photoheliograph Datum System



Weight: 1000 kg (2200 lb)	Inertia, kgm^2 (slug-ft ²)	Radius of Gyration, m (in.)
Xcg : -14.5 cm (-5.7 in.)	Iox 304.0 (224.4)	Kx 0.551 (21.7)
Ycg : 0.76 cm (0.3 in.)	Ioy 2428.9 (1793.1)	Ky 1.559 (61.4)
Zcg : 30.2 cm (11.9 in.)	Ioz 2302.1 (1699.5)	Kz 1.519 (59.8)

Fig. IV-26 Mass Properties Data, Photoheliograph

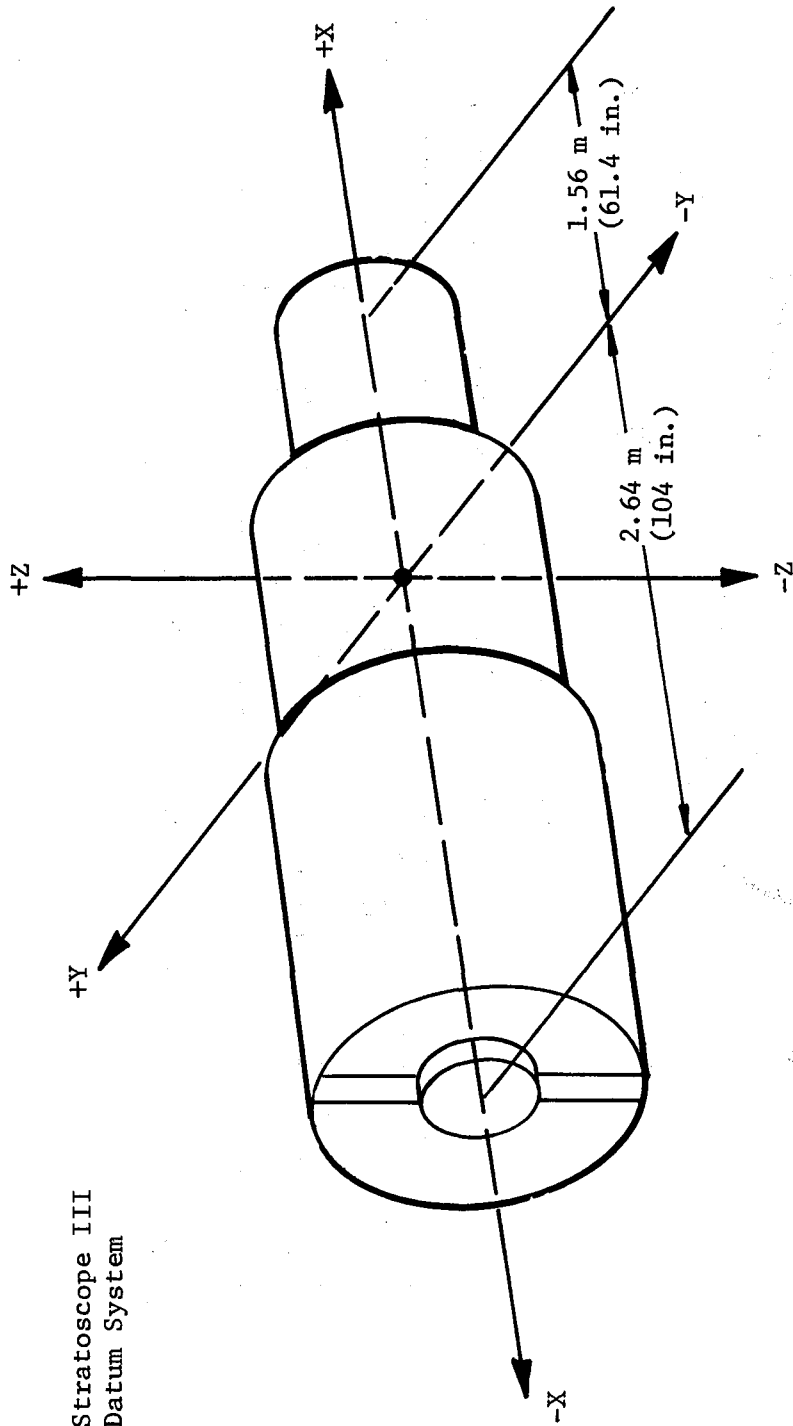


Solar Group

(XUV Spectroheliograph; X-Ray Telescope; Coronagraphs)

Weight: 1967 kg (4337 lb)	Inertia, kgm^2 (slug-ft ²)	Radius of Gyration, m (in.)
Xcg : 68.1 cm (-26.8 in.)	Iox 1219.7 (900.4)	Kx 0.787 (31.0)
Ycg : -6.86 cm (-2.7 in.)	Ioy 4471.0 (3300.6)	Ky 1.506 (59.3)
Zcg : 3.56 cm (1.4 in.)	Ioz 4530.2 (3344.3)	Kz 1.516 (59.7)

Fig. IV-27 Mass Properties Data, Solar Group

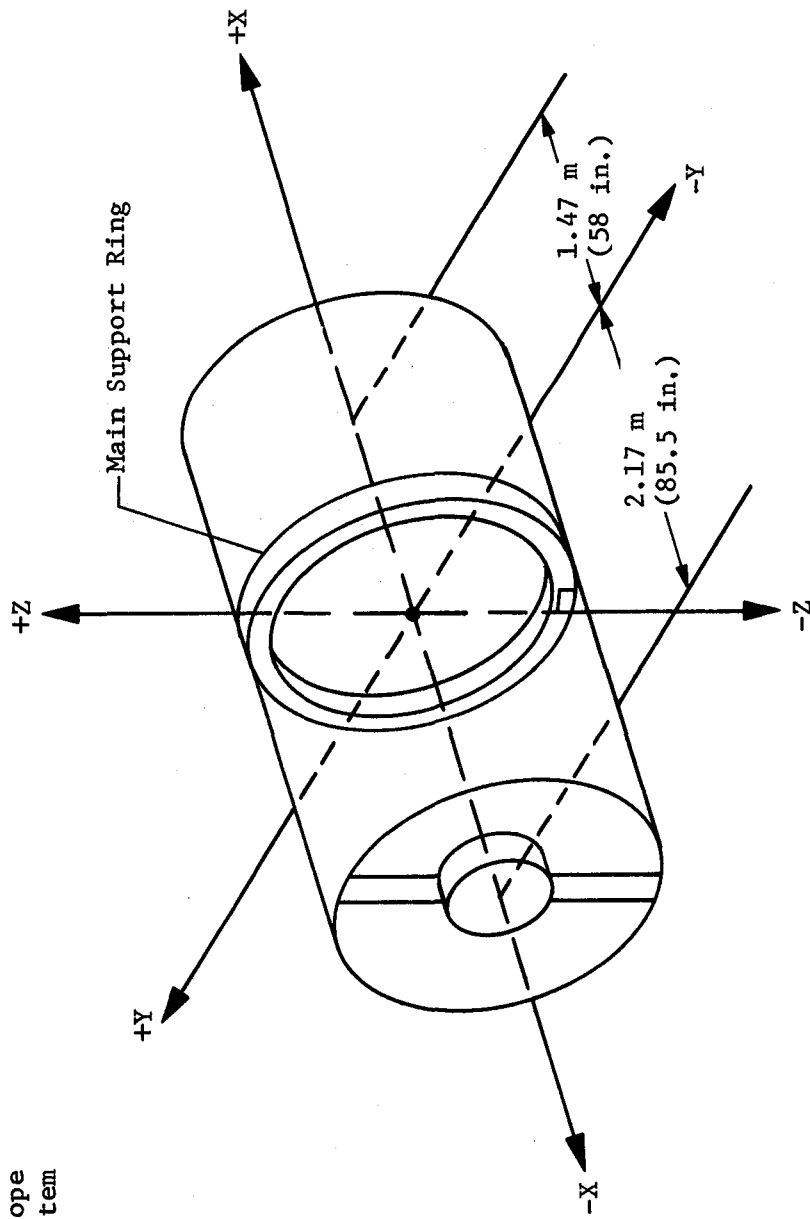


Stratoscope III
Datum System

Weight: 1792 kg (3951 lb)		
Xcg : -10.4 cm (-4.1 in.)		
Ycg : 0 (0)		
Zcg : 0 (0)		
Inertia, kgm ² (slug-ft ²)		Radius of Gyration, m (in.)
Iox 616.7 (455.3)		Kx 0.588 (23.1)
Ioy 3025.1 (2223.2)		Ky 1.295 (51.0)
Ioz 3025.1 (2223.2)		Kz 1.295 (51.0)

Fig. IV-28 Mass Properties Data, Stratoscope III

IR Telescope
Datum System



Weight:	1988 kg (4383 lb)		
Xcg :	1.27 cm (0.5 in.)		
Ycg :	0 (0)		
Zcg :	0 (0)		
Inertia, kgm^2 (slug-ft ²)			Radius of Gyration, m (in.)
Iox	1478.5 (1098.1)		Kx 0.864 (34.0)
Ioy	2420.9 (1787.2)		Ky 1.102 (43.4)
Ioz	2420.0 (1786.5)		Kz 1.102 (43.4)

Fig. IV-29 Mass Properties Data, IR Telescope

Array	Weight, kg (lb)	Center of Gravity, cm (in.)			Moment of Inertia kgm ² (slug-ft ²)			Radius of Gyration, m (in.)		
		X	Y	Z	I _{ox}	I _{oy}	I _{oz}	K _x	K _y	K _z
A. Wide Coverage X-Ray	436 (962)	-30.7 (-12.1)	-1.02 (-0.4)	15.0 (5.9)	783.1 (578.1)	375.0 (276.8)	560.4 (413.7)	1.339 (52.7)	.927 (36.5)	1.133 (44.6)
B. Narrow Band Spec/Polar	549 (1210.5)	-13.0 (-5.1)	-1.27 (-0.5)	0 (0.0)	581.7 (429.4)	323.2 (238.6)	323.6 (238.9)	1.029 (40.5)	.767 (30.2)	.767 (30.2)
C. X-Ray Spec & Low Background	1869 (4121)	-37.59 (-14.8)	-2.25 (-0.1)	14.73 (5.8)	1623.2 (1198.3)	1499.1 (1106.7)	617.4 (455.8)	.932 (36.7)	.894 (35.2)	.574 (22.6)
D. Lg Mod Collimator	581 (1281)	-18.29 (-7.2)	-2.29 (-0.9)	0 (0.0)	568.0 (419.3)	345.1 (254.8)	289.5 (213.7)	.988 (38.9)	.770 (30.3)	.706 (27.8)
E. Lg Area X-Ray & Coll Pn Crystal	781.5 (1723)	-34.29 (-13.5)	-14.48 (-5.7)	-5.1 (-0.2)	841.9 (621.5)	571.4 (421.8)	531.4 (392.3)	1.036 (40.8)	.853 (33.6)	.823 (32.4)

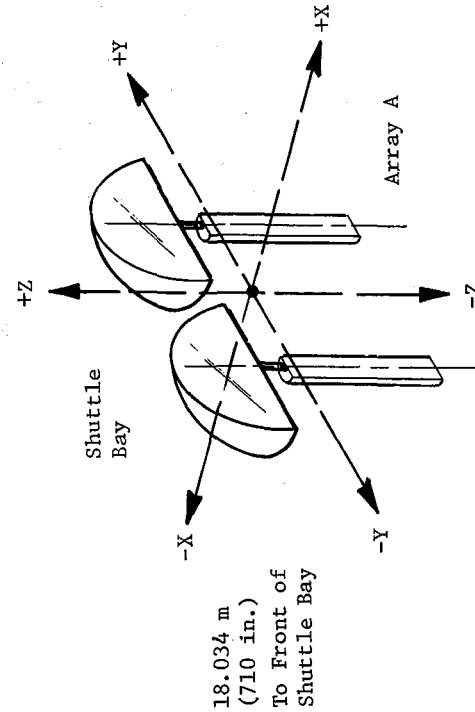
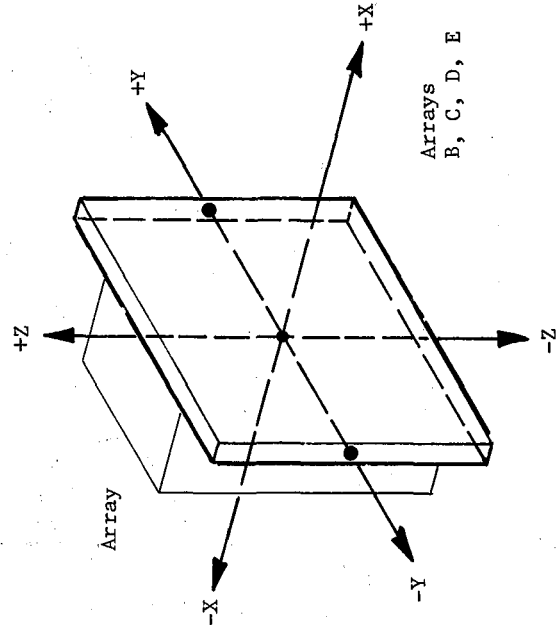
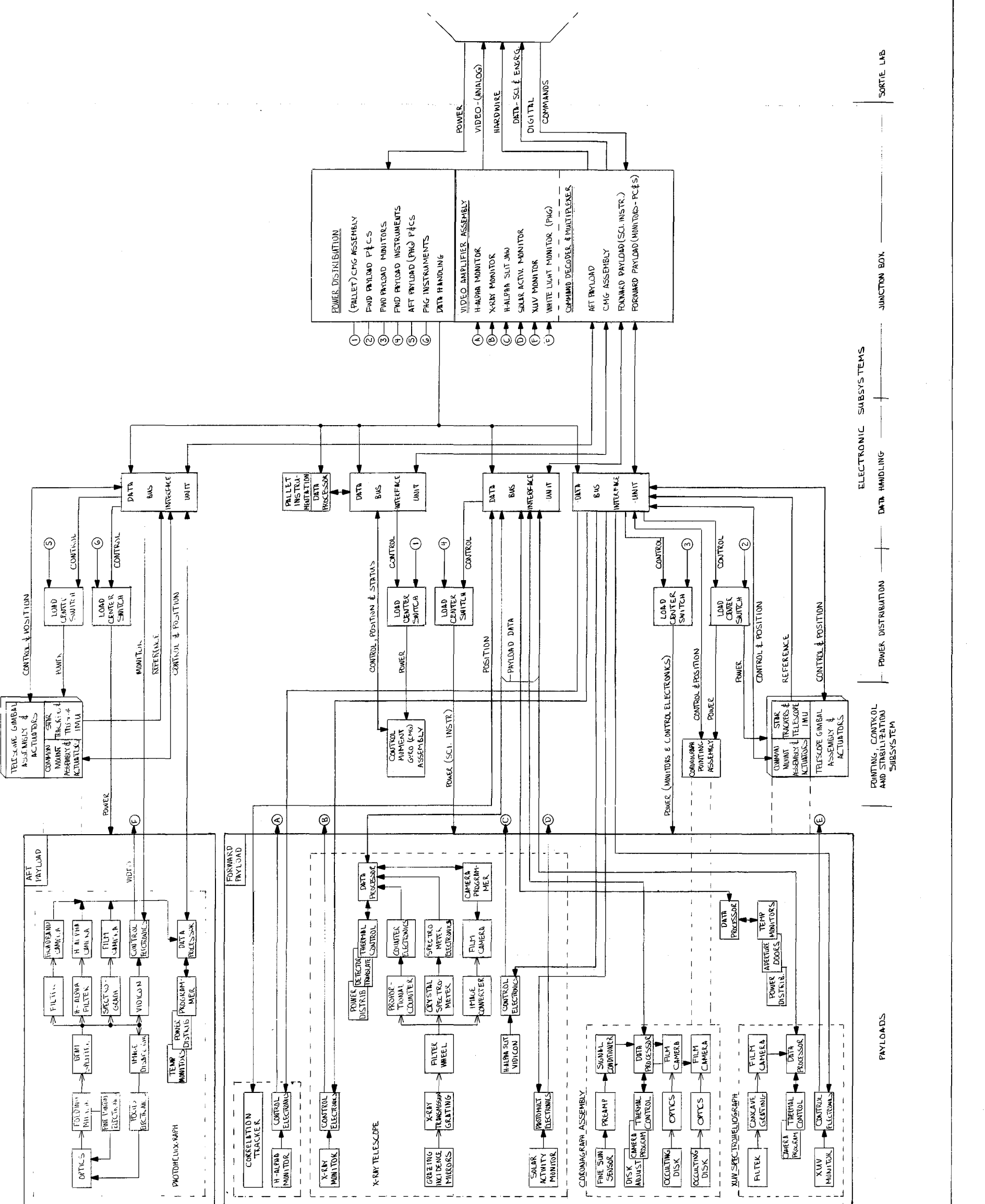
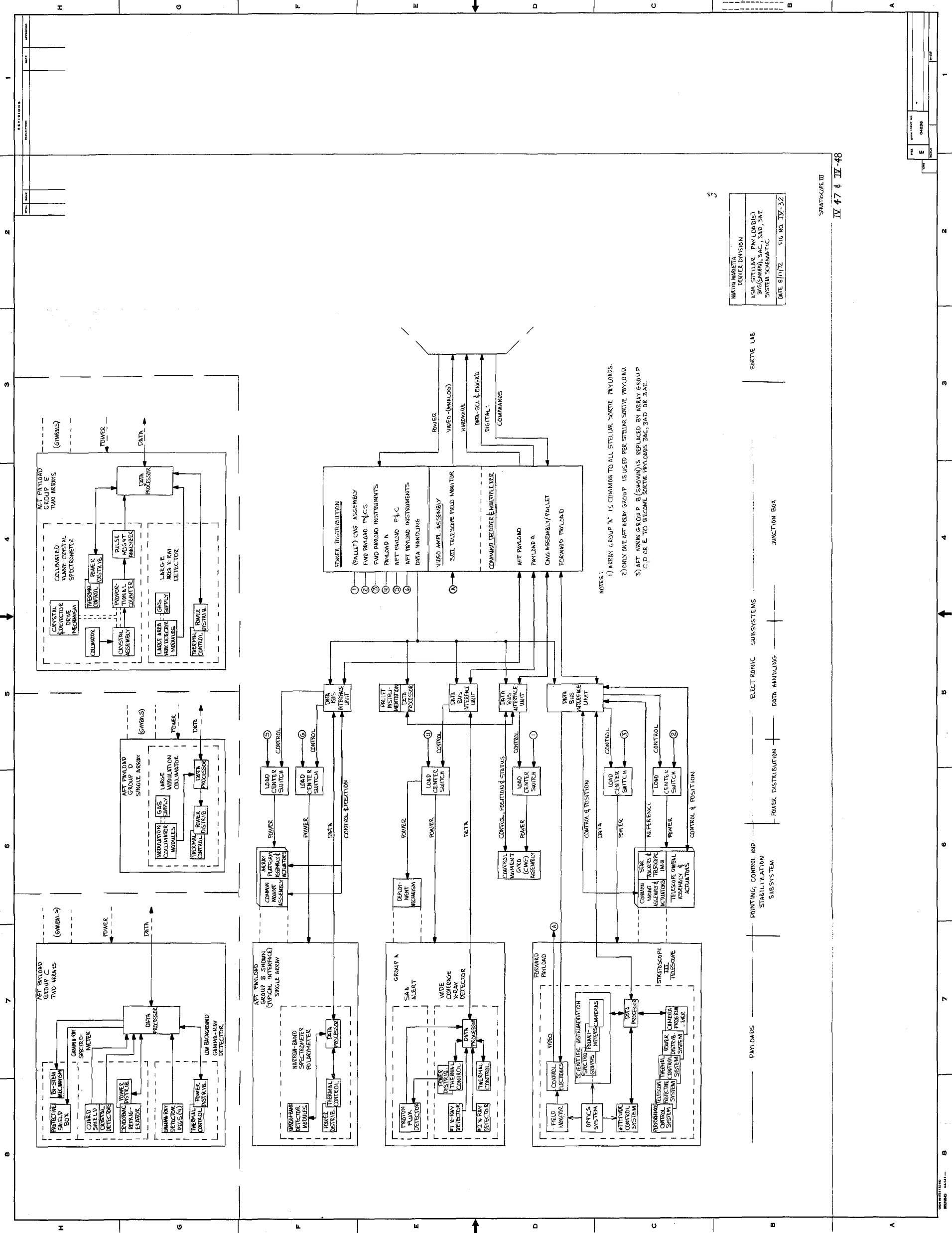


Fig. IV-30 Mass Properties Data, High-Energy Arrays



MARTIN MARIETTA
 DENVER DIVISION
 ASH (SALAR) PAYLOAD 1-2
 SYSTEM SCHEMATIC
 DATE: 8/10/72 FIG. NO. III-31
AS 715775 1000
 81 4/14/72 W.S.



- NOTES:
- 1) ARRAY GROUP 'A' IS COMMON TO ALL STELLAR SORTIE PAYLOADS.
 - 2) ONLY ONE AFT ARRAY GROUP IS USED PER STELLAR SORTIE PAYLOAD.
 - 3) AFT ARRAY GROUP B (SHOWN) IS REPLACED BY ARRAY GROUP C/D OR E TO BECOME SORTIE PAYLOADS 3A-C, 3A-D OR 3A-E.

MITCHELL
DENVER DIVISION
AFT STELLAR PAYLOAD(S)
3A(C/D/E), 3A-C, 3A-D, 3A-E
SYSTEM SCHEMATIC
DATE 8/17/72 FIG NO. IV-32

SYNOPSIS III
IV 47 4 IT-48

REV	DATE	DESCRIPTION
1		
2		
3		
4		
5		
6		
7		
8		

V. INTERFACES

The results of this study indicate that the Astronomy Sortie Mission concept is feasible. However, the study results are very dependent on the interfaces defined for the Space Shuttle and Sortie Lab. This chapter provides a summary of the interface capabilities and constraints that were used in performing the study analyses.

A. SPACE SHUTTLE INTERFACES

Interfaces between the Astronomy Sortie mission payloads and the Shuttle are those involving orbital parameters (such as payload capability, orbit inclination, orbit altitude, and vehicle attitude and stability), payload bay environment (such as acoustics and thermal) and physical constraints such as allowable payload center of gravity and the payload envelope. Other interfaces to the Shuttle, including communications and mechanical attachment, will be through the Sortie Lab and pallet.

1. Payload Capability

The level 1 ground rule baselined for this study was that the payload weight could not exceed 80% of the Shuttle capability. The mission analyses performed during the study established the orbital parameters for the baseline Astronomy Sortie missions as:

Solar Payload -

- Inclination - 1.38 to 1.57 radians (79 to 90 deg),
- Altitude - 470 to 418 km (254 to 226 n mi),
- Time of Year - February 20 to April 19 and August 25 to October;

Stellar Payloads

- Inclination - 0.5 to 1.57 radians (28.5 to 90 deg),
- Altitude - 463 to 370 km (250 to 200 n mi),
- Time of Year - Anytime.

Figure V-1 shows the Shuttle payload capability as a function of altitude and inclination for 80% of the baseline capability. This figure assumes that the air breathing engine system (ABES) is not installed on the Orbiter. Also shown on the figure are the estimated weights for the nine sortie mission payloads. In each case, a Sortie Lab weight of 5760 kg (12,688 lb) and a pallet weight of 1390 kg (3060 lb) were used.

From the figure it can be seen that the Astronomy Sortie payloads are marginal at the higher inclinations. The solar payload requires an altitude of 418 km (226 n mi) for an inclination of 1.57 radians (90 deg) to provide continuous sun for the seven-day mission. This requirement exceeds the baseline Shuttle payload capability (80% of total) slightly, and emphasizes how the large payload capability of the Shuttle is reduced at the higher inclinations.

2. Operational Constraints

The operational constraints in the following paragraphs were assumed or derived during the study.

Attitude Constraint - It was assumed that there were no attitude constraints on the Shuttle and that an X-POP inertial attitude could be maintained for the seven-day sortie mission. Should the Shuttle have attitude constraints, it would be necessary to reevaluate the CMG stabilization system proposed for the Shuttle and the on-orbit operations of the astronomy experiments.

Air Breathing Engines - The ABES is not required because the Astronomy Sortie mission is not a passenger mission and there are sufficient deorbit opportunities within the 1100-n mi crossrange capability. Should ABES be baselined for the Astronomy Sortie missions, all of the payloads would exceed the Shuttle capabilities at inclinations greater than approximately 0.87 radian (50 deg). This would seriously affect the scientific objectives of the astronomy experiments.

Launch Time - A 24-hr launch capability was assumed. Should the launch times be restricted, it would be necessary to increase the launch inclinations required for the 1.57 radians (90 deg) beta angle.

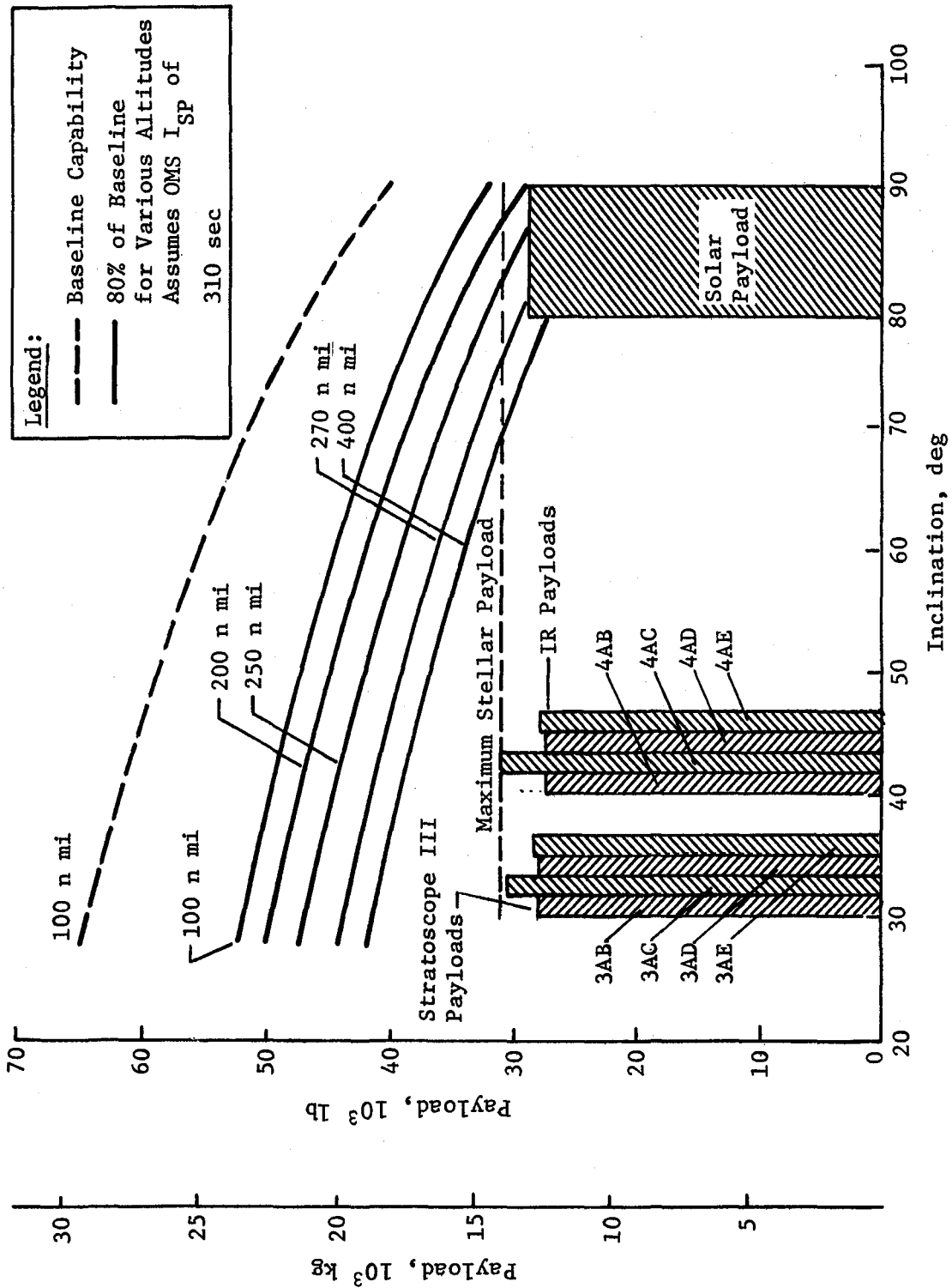


Fig. V-1 Shuttle Payload Capability

Space Shuttle Stabilization - This study recommends the use of three control moment gyros (CMGs) to stabilize the Shuttle in an X-POP inertial attitude. Should the CMG system not be possible for the Astronomy Sortie missions it would be necessary to reevaluate the study results in terms of payload weights, pointing and control system requirements, and the effects of contamination on the telescopes.

Orbit Inclination - To satisfy the experiment objectives, orbit inclinations from 0.5 to 1.57 radians (28.5 to 90 deg) are required. Should any constraints be imposed on the orbit inclinations available, it would be necessary to reevaluate the mission parameters selected for the astronomy experiments.

3. Acoustic Levels

The acoustic spectrum and overall sound pressure level (OASPL) used as a baseline for this study is presented in the top curve of Fig. V-2. These data were extracted from the document *Payload Design Requirements for Shuttle/Payload Interface* (Ref V-1). Based on the results of Titan III test data, it was recommended that the OASPL should not exceed approximately 140 dB for the astronomy experiments. The lower curve in Fig. V-2 shows the expected acoustic spectrum and OASPL for the addition of 9.76 kg/m² (2.0 lb/ft²) of acoustic material. As shown on the figure the OASPL is down to 140 dB with this protection. Calculated wall densities including insulation and meteoroid shielding for the telescopes are:

Photoheliograph	- 18.6 kg/m ² (3.83 lb/ft ²)
Stratoscope III	- 26.1 kg/m ² (5.35 lb/ft ²)
IR Telescope	- 66.3 kg/m ² (13.6 lb/ft ²)
Container for Other Solar Telescopes	- 9.77 kg/m ² (2.04 lb/ft ²)

While the tolerances of the various instruments are not defined, it is anticipated that the Shuttle cargo bay acoustic environment will cause only localized problems on extremely delicate components of the instruments.

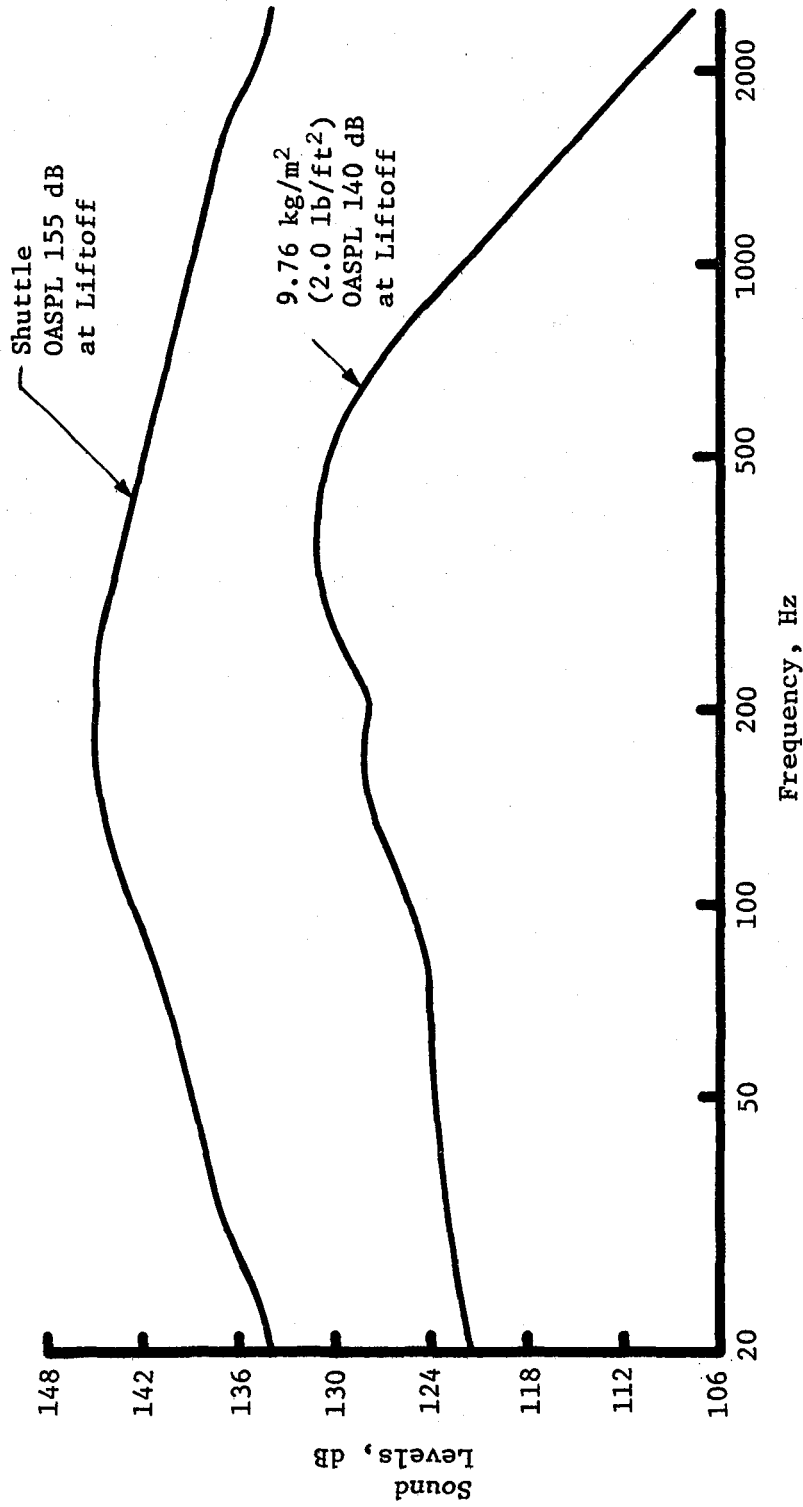


Fig. V-2 Shuttle Cargo Bay Acoustic Environment

The Space Shuttle RFP (Ref V-2) specifies an OASPL for the cargo bay of 145 dB. This reduction in OASPL in conjunction with the acoustic protection provided by the instruments themselves should minimize the effects of the acoustical environment for the astronomy payloads.

4. Thermal Environment - The Space Shuttle thermal environment used for this study was based on the results of in-house activities. In analyzing the effects on the astronomy payloads during ascent and prior to opening the cargo bay doors, the environment shown in Fig V-3 was used. The Shuttle RFP defined a thermal environment (Table V-1) that was not severe as the one used during this study.

The results of the thermal analysis for the ascent phase of the mission are shown in Fig. V-4 for a simplified model of a typical telescope. As can be seen from the figure, the thermal environment has little effect on the internal temperatures of the telescope. Two insulation conductances are shown. Case "A" reflects a good thermal insulation that is typical of the Multiple Docking Adapter (MDA) on Skylab. Case "B" reflects an insulation with five times the number of penetrations as Case "A". Both conductances result in very small temperature changes during the first 2 hr of mission time.

Table V-1 Payload Bay Wall Thermal Environment (Adiabatic Payload Bay Wall)

Condition	Minimum, °F	Maximum, °F
Prelaunch	+40	+120
Launch	+40	+150
On-Orbit (door closed)	-100	+150
On-Orbit (door open)	-	-
Entry and Postlanding	-100	+200

During the on-orbit phase of the mission, the Grumman Shuttle Orbiter configuration and characteristics were used in the thermal analysis. Table V-2 identifies the orbital and environmental conditions that were used in the detailed analysis of the IR telescope.

Environmental Parameters

- q Solar = 457 Btu/ft²-hr
- Albedo = 0.48
- q Earth = 95 Btu/ft²-hr
- Orientation, $\beta = 90^\circ$

Thermal Properties

- Microquartz Insulation
- Density = 3.5 lb/ft³
- Sp Heat = 0.18
- Thermal Conductivity = 0.005 Btu/ft-hr-°F (in vacuum)

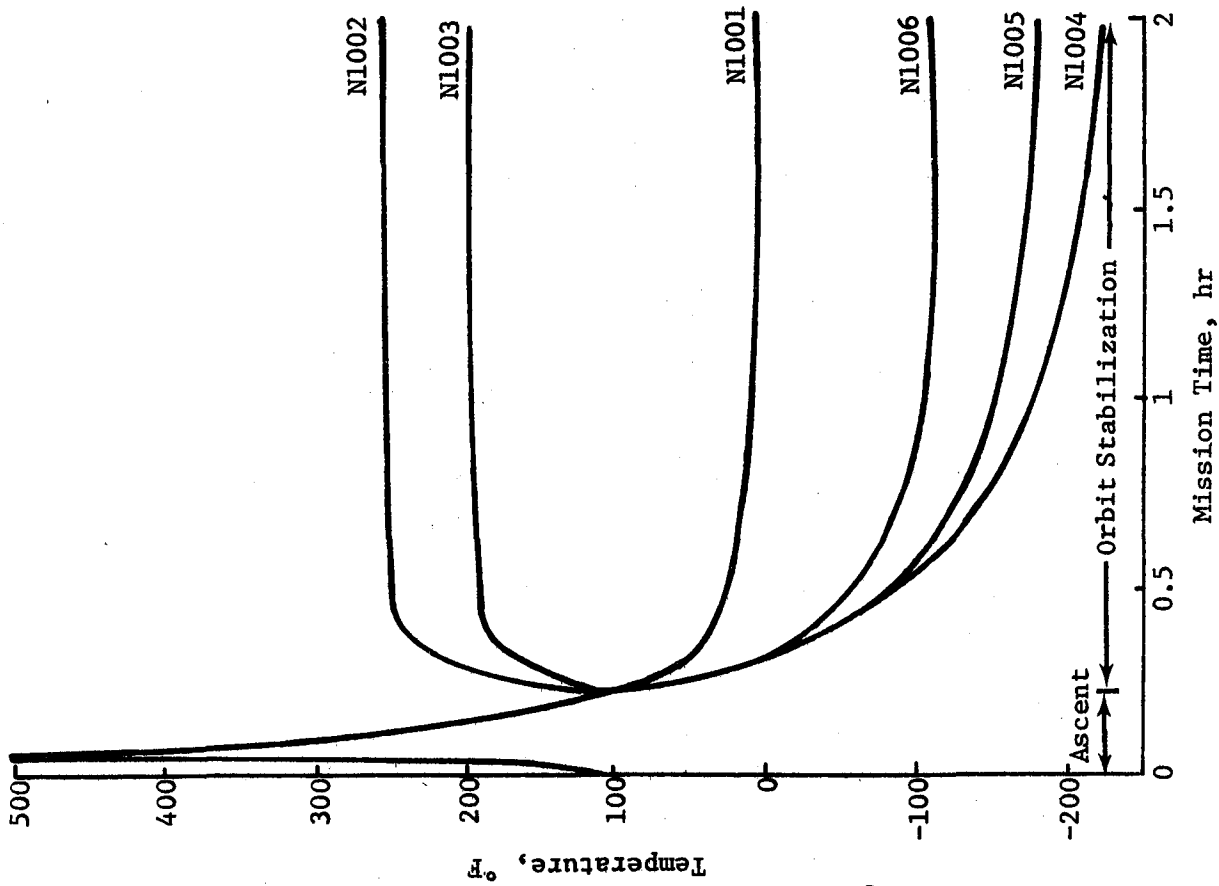
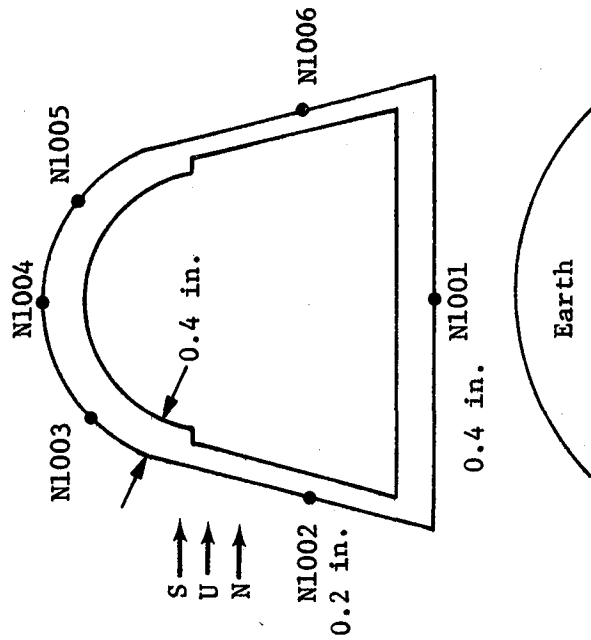
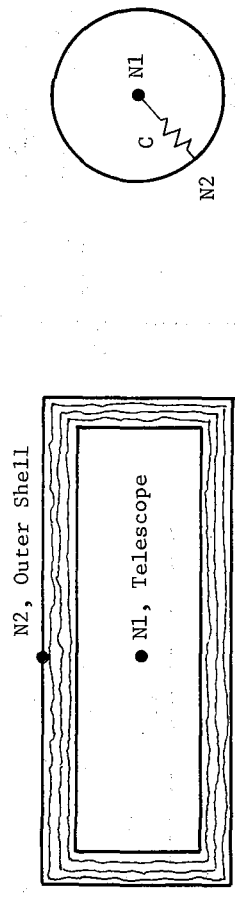
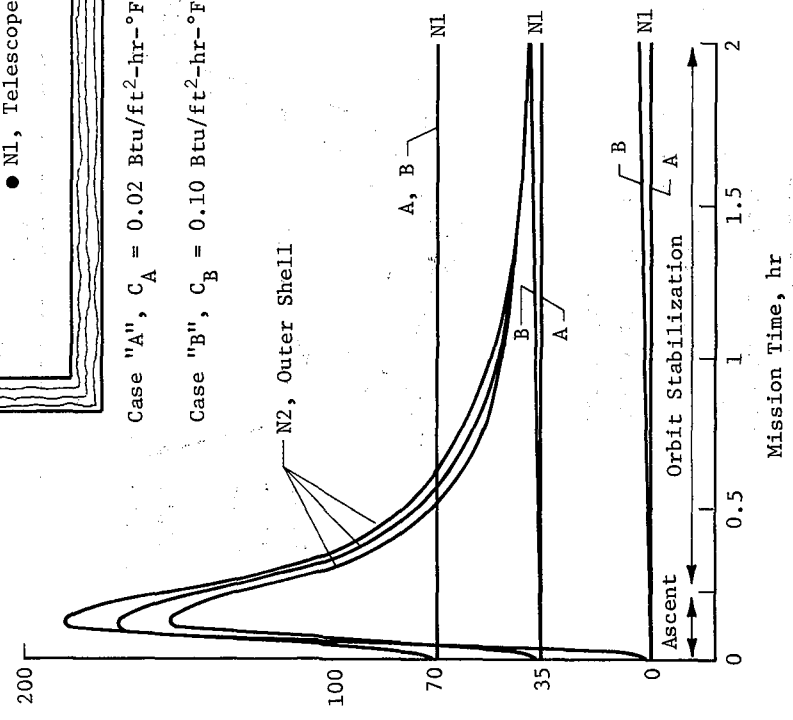


Fig. V-3 Shuttle Thermal Environment



Case "A", $C_A = 0.02 \text{ Btu/ft}^2\text{-hr-}^\circ\text{F}$, Thermal Time Constant = 180 hr

Case "B", $C_B = 0.10 \text{ Btu/ft}^2\text{-hr-}^\circ\text{F}$, Thermal Time Constant = 36 hr



Initial Temp, °F	Insulation Conductance, C	Telescope, N1	
		Max Temperature, °F	Final Temp, °F
0	Case "A" 0.02	0.7	0.7
35	Btu/ft ² -hr-°F	35.3	35.3
70		70.2	70.0
0	Case "B" 0.1	3.0	3.0
35	Btu/ft ² -hr-°F	36.5	36.5
70		70.8	70.0

Fig. V-4 Telescope Temperature During Ascent

Table V-3 shows the absorbed flux, equivalent space sink temperature, and viewfactor to space for the Shuttle configuration and the orbital and environmental conditions specified above. For comparison purposes, the same parameters are shown for a free-flying module in the same orbit. As can be seen from the table, the Space Shuttle cuts down on the telescope viewfactor to space, and results in a sink temperature that is 29°F warmer than an equivalent free-flying telescope. The absorbed fluxes are averaged around the telescope cylindrical surface for one orbit period.

5. Center of Gravity Constraint

The center of gravity (cg) constraints defined by the Shuttle RFP (Ref V-2) for the payloads within the Shuttle bay are shown in Fig. V-5. Current estimates of the Astronomy Payload weights and cg are also plotted. All payloads are within the constraints.

6. Shuttle Bay Size

All of the payloads are within a payload bay envelope of 4.57 m (15 ft) diameter 18.23 m (60 ft) long.

7. Communication

Table V-4 summarizes the communication requirements for the nine astronomy payloads. The data quantities show the totals that must be transmitted to the ground during the seven-day mission.

8. Mechanical

Mechanical attachment to the Shuttle will be through the Sortie Lab and pallet. The solar payload (Payload 1-2) requires that the Sortie Lab and pallet be deployed (rotated up 90°) from the payload bay by a payload deployment mechanism assumed part of Shuttle.

Table V-2 On-Orbit Thermal Characteristics

Orbital Conditions	
Orbit Altitude	235 n mi
Beta Angle	90 deg
Orientation	Solar Oriented
Environmental Conditions	
Solar Constant	458 Btu/hr-ft ²
Albedo	0.4
Planetary Emission	78 Btu/hr-ft ²
Surface Coating Properties, α/ϵ	
Orbit	0.9/0.9
Orbiter Radiator	0.1/0.9
Pallet/Payload	0.2/0.9

Table V-3 IR Telescope Thermal Environment Summary

Heat Source	Absorbed Flux (Btu/ft ² -hr)	
	Orbiter Deployed	Free Flying
Solar	29.2	29.4
Albedo	0.243	0.95
Earth IR	13.3	22.3
Reflected	1.9	0
Orbiter/Payload IR	-1.9	0
Total	42.74	52.6
↳ to space	0.55	0.88
Equivalent Space Sink Temperature	1°F	-28°F

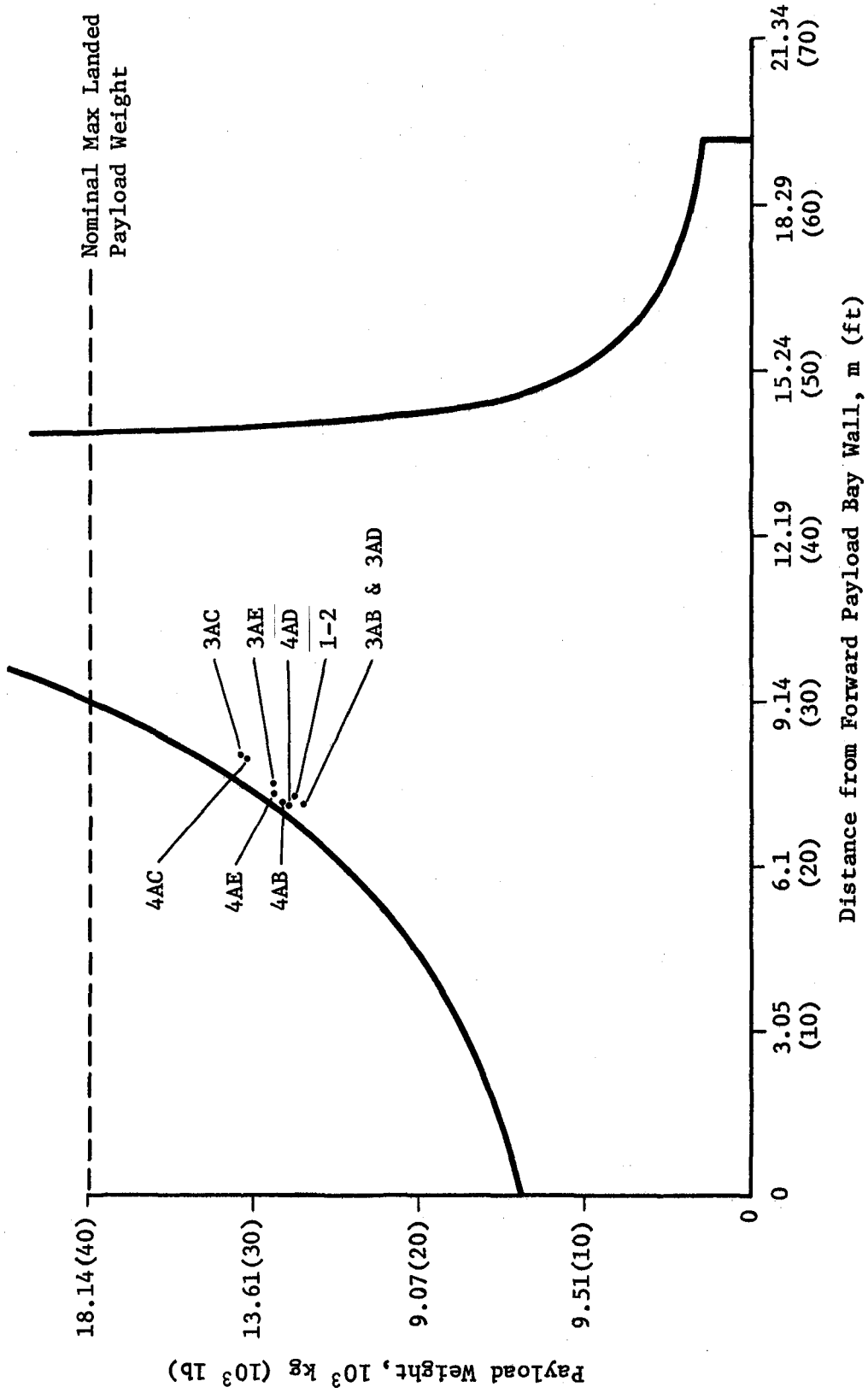


Fig. V-5 Center of Gravity Constraint

Table V-4 Telemetry Requirements

Baseline Payload	Telemeter - During Mission, 10 ⁶ bits	
Solar 1-2	743	
Stratoscope Payloads	3AB	210
	3AC	235
	3AD	225
	3AE	251
IR Payloads	4AB	157
	4AC	181
	4AD	172
	4AE	198

B. SORTIE LAB AND PALLET INTERFACES

Primary interfaces for the Astronomy Sortie mission program are between the experiments with their mount, data, and control systems and the Sortie Lab and pallet. These interfaces are both electrical and mechanical in nature. Design emphasis has been placed on commonality of interfaces for the nine astronomy payloads. This is accomplished by a common modification of the baseline pallet, which will then accommodate each of the payloads by a physical interchange of hardware and reprogramming or junction box rewiring of control, data and power systems.

The Sortie Lab and pallet definition used for this study are summarized in Fig. V-6. These data were extracted from the MSFC document *Sortie Can Conceptual Design* (Ref V-3).

1. Quantity of Sortie Labs and Pallets

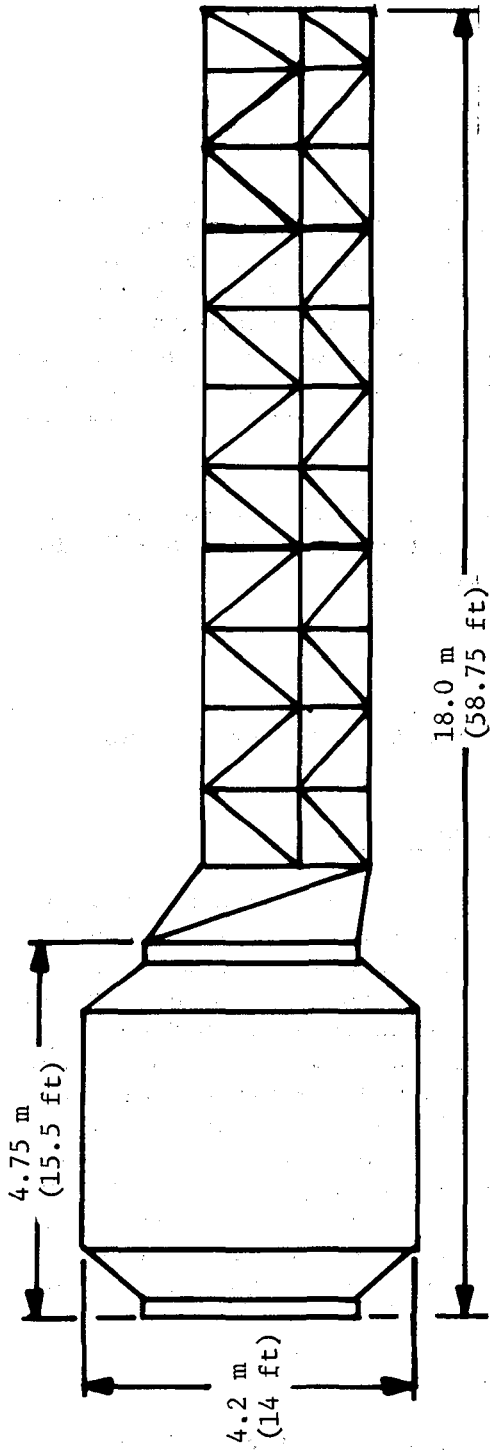
To satisfy the maximum baseline flight schedule of eight astronomy sortie missions per year, a total of two Sortie Labs and two pallets are required.

2. Sortie Lab and Pallet Physical Characteristics

To provide adequate space for arrangement of the selected payload groups a 4.7 m (186 in.) long Sortie Lab and a 13.2 m (519 in.) pallet, of which 12.2 m (480 in.) is flat bed structure are required. The pallet floor or plane of azimuth table attachment is 1 m (40 in.) below the centerline of the Shuttle payload bay. Overall length of Sortie Lab and pallet is 18.0 m (705 in.). When the wide coverage X-ray detector is attached the overall assembly length is increased to 18.2 m (715 in.). A 4.27 m (14 ft) diameter Sortie Lab was used for this study, however, a larger diameter within the maximum limit of the payload bay would not interfere with instrument viewing. In calculating the mass properties of the astronomy payloads, the cg assumed for the Sortie Lab and pallet were 2.29 m (90 in.) and 11.3 m (444 in.) from the forward end of the Shuttle cargo bay.

3. Mechanical Interface

There are two types of mechanical interfaces to the pallet: (1) those structural attachments that are major load-carrying interfaces and/or require a high degree of alignment; and (2) equipment supports.



Sortie Lab Weight	5,760 kg (12,688 lb)
Pallet Weight	<u>1,390 kg (3,060 lb)</u>
Total	7,150 kg (15,748 lb)

Subsystem Support to Experiments

Power	~ 1.5 kW Avg
EC/LS	~ Autonomous System - 2 Men for 7 Days
Thermal	~ 15,000 Btu/hr (Nondeployed); 51,000 Btu/hr (Deployed)
Data	~ Record at 100 kbps
Comm	~ Voice & 5 kbps through Shuttle; 10 kbps Uplink (through Shuttle)
C&D	~ Multifunction Control & Display; Computer Controlled

Fig. V-6 Baseline Sortie Lab and Pallet

Major structural attachments are required for:

- 1) Control moment gyros (3);
- 2) Pallet inertial measurement unit (IMU);
- 3) Azimuth tables (2);
- 4) Deployment locks (4);
- 5) Wide coverage X-ray Detector mounts (2).

Equipment supports are required for:

- 1) Control input box;
- 2) Inverters (3);
- 3) Ordnance package;
- 4) Interface junction box;
- 5) Experiment control, data, and power junction boxes (3);
- 6) Cabling;
- 7) Cable cutters (3).

The mechanical interfaces to the Sortie Lab are the umbilical plate and the structural attachment for the experiment control and display console.

4. Power Interface

Electrical power interface between the ASM cabling system and the Sortie Lab will be at the interface junction box. The average power requirements for the experiments are summarized in Table V-5. This power is the average power required by the experiments and experiment support equipment, including the control and display console located in the Sortie Lab.

Table V-5 Payload Power Requirements

Payload	Average Power, W
Solar Payload 1-2	1480
Stratoscope III Payloads	
Payload 3AB	1352
Payload 3AC	1280
Payload 3AD	1383
Payload 3AE	1444
IR Telescope Payloads	
Payload 4AB	1217
Payload 4AC	1145
Payload 4AD	1248
Payload 4AE	1309

5. Data Interface

Experiment data output consists of film and digital format. The film remains in the instrument for the duration of the mission. Digital data are transferred to the Sortie Lab in coax cables. Table V-6 summarizes the digital data requirements. The table lists the maximum data rate transferred to the Sortie Lab, the data storage required during the seven-day sortie mission, and the data that must be transmitted to the ground in real time or near real time.

The data system defined for the Astronomy Sortie missions uses the Sortie Lab data management system for all computational requirements, storage requirements, formatting, etc.

6. Control and Display

The C&D concept identified for the Astronomy Sortie missions is a separate hybrid C&D console that interfaces with the Sortie Lab C&D and data management systems. The Astronomy Sortie C&D does require hardwire interconnections to the experiments located on the pallet. These hardwire connections will provide for the experiment-peculiar analog signals, video monitors, and caution and warning circuits.

7. Thermal

The astronomy equipment located on the pallet will not require a fluid interface. Thermal control will be provided using electrical energy or it will be incorporated into the telescope designs. The C&D console in the Sortie Lab will require the dissipation of approximately 447 W of electrical power.

Table V-6 Digital Data Requirements

Baseline Payload	Maximum Data Rate, kbps	Onboard Storage, 10 ⁹ bits	Telemeter - During Mission, 10 ⁶ bits
Solar 1-2	4.0	1.76	743
Stratoscope III 3AB Payloads	4.2	2.04	210
3AC	8.3	4.30	235
3AD	4.4	2.20	225
3AE	8.6	4.43	251
IR Payloads 4AB	4.5	2.00	157
4AC	8.6	4.30	181
4AD	4.8	2.15	172
4AE	8.9	4.43	198

C. REFERENCES

- V-1. *Payload Design Requirements for Shuttle/Payload Interface*. MSFC, November 5, 1971.
- V-2. Space Shuttle Program, Request for Proposal, No. 9-BC421-67-2-40P, MSC.
- V-3. *Sortie Can Conceptual Design*, ASR-PD-DO-72-2, NASA/MSFC, March 1, 1972.

VI. IR TELESCOPE ON-ORBIT DETECTOR ACCESS

A controversial issue that surfaced during this study was the desirability of the scientific community to have on-orbit shirt-sleeve access to the focal plane of the telescopes. The concept defined in this study does not provide this capability because the entire telescope is located external to the Sortie Lab.

The NASA/MSFC, COR directed that during the study several alternative configurations be examined that would provide the capability for on-orbit access to the IR telescope focal plane. The results are presented in this chapter.

A. GROUND RULES AND ASSUMPTIONS

The following ground rules and assumptions were used in the evaluation:

- 1) The same payload configuration was assumed for each of the alternative configurations (i.e., a cryogenically cooled IR telescope plus a group of high-energy arrays);
- 2) The changes to the telescope f/number and optical configuration were not analyzed, but it was assumed that the designs shown would be feasible;
- 3) The IR viewing constraints used in the analyses were 1.57 radians (90 deg) from sun and 0.79 radian (45 deg) from earth;
- 4) IR payloads were assumed to fly orbits between $\beta = 0$ and $\beta = 1.57$ radians (90 deg), at an altitude of 463 km (250 n mi);
- 5) It was assumed that the Shuttle would be stabilized using control moment gyros (CMGs);
- 6) It was assumed that the Shuttle could maneuver at a rate of 0.1 rad/min (6 deg/min) about the longitudinal axis (X-axis) and 0.02 rad/min (1 deg/min) about the Y and Z axes.

B. ANALYSIS

Figures VI-1 thru VI-5 present five alternative IR telescope configurations that were evaluated and the salient features of each concept. All of these configurations, with the exception of Fig. VI-1, provide on-orbit shirt-sleeve access to the detectors through an airlock. The configurations in Fig. VI-1 and VI-2 use mechanical gimbals for the telescope pointing system, while the configurations in Fig. VI-3 thru VI-5 use a gas bearing system. A conceptual design for the gas bearing system is shown in Fig. VI-6.

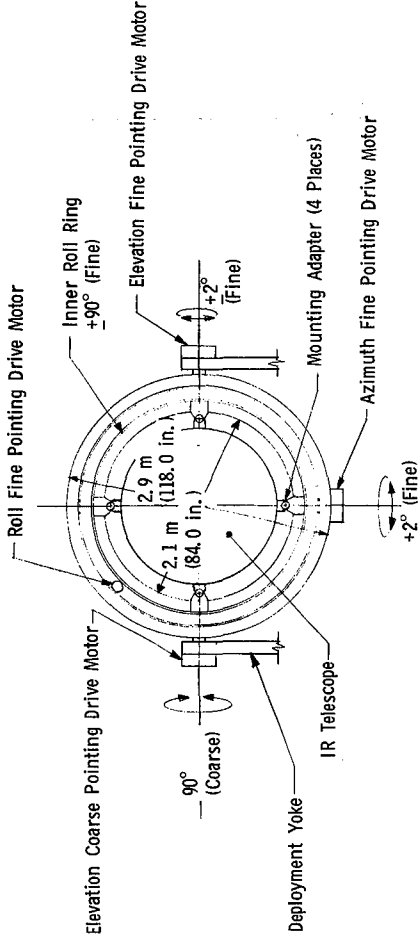
Figure VI-7 presents the observation time percentage as a function of the slew rate. These observation time percentages are based on the large slew angles that would be required because of the IR telescope 1.57 radians (90 deg) constraint on viewing the sun and 0.79 radian (45 deg) constraint on viewing the earth.

With these constraints, it is necessary to slew the telescope approximately 2.3 radians (132 deg) to view two targets per orbit and twice this to view three targets per orbit. This assumes that each target would be viewed a maximum of 31.4 minutes.

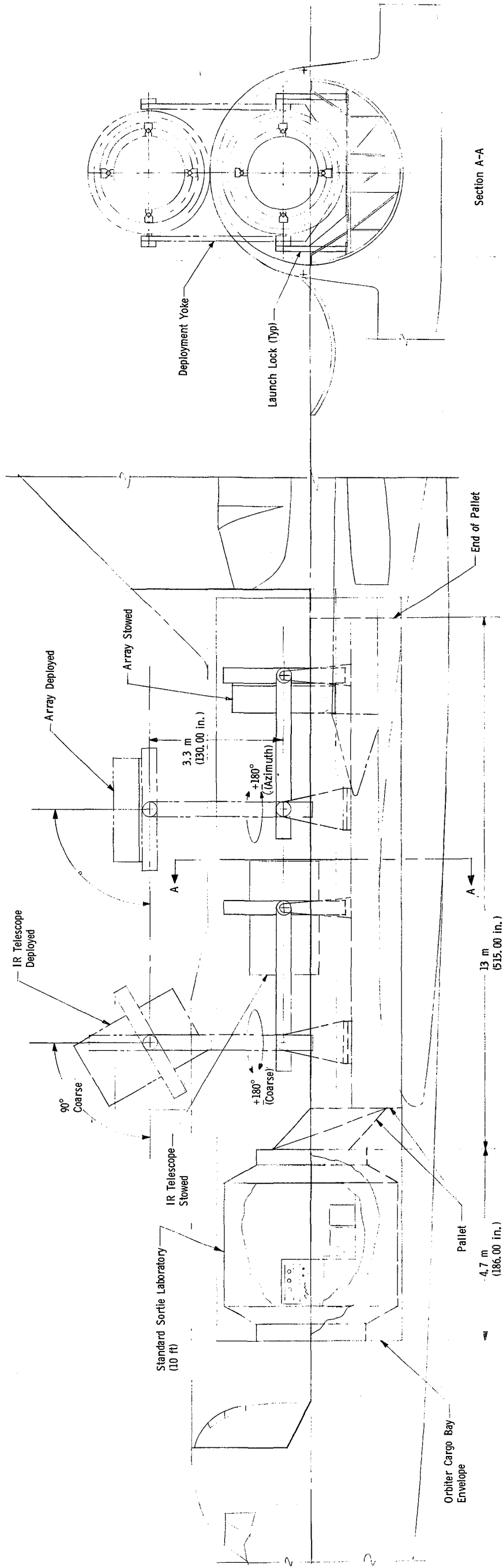
With these large slew angles, maneuvering of the Shuttle with the CMG system is very restricted. Using the Shuttle moments of inertia, a maneuver of 0.02 rad/min (1 deg/min) in the Shuttle Y and Z axes and 0.1 rad/min (6 deg/min) in the X-axis requires approximately 2450 N-m-s (1800 ft-lb-sec) of momentum. This amount of momentum is about equal to the capability of an ATM CMG. To increase the Shuttle maneuver rate by a factor of 2 would require an additional CMG; by a factor of 3 would require two additional CMGs, etc. Each of the ATM CMGs weigh approximately 227 kg (500 lb), so it can be seen that to increase the Shuttle maneuver rate would be very expensive. To obtain operating efficiencies of 60 to 70%, it would be necessary to slew the Shuttle at rates of .42 to 1 rad/min (24 to 60 deg/min). To provide this capability with CMGs would require an additional 4 to 10 CMGs.

Another disadvantage of maneuvering the Shuttle to obtain sky-coverage is the requirement to maintain an X-IOP inertial attitude. When CMGs are used to maintain X-IOP, approximately one half of the orbit is required to dump the momentum build-up in the CMGs using the gravity gradient torques. During this half orbit, the Shuttle would be under a constant maneuver (to obtain correct gravity gradient torques) and it would not be possible to take astronomy observations.

- Note: 1) Sorite Lab & Pallet Data Extracted from NASA/MSC Document ASR-PD-00-72-2, Sorite Can Conceptual Design, March 1, 1972.
- 2) Hemispherical Coverage Available with Wide Angle Azimuth and Elevation Gimbal.
- 3) Approximately 0.02 rad/sec (deg/sec) Slew Rate Available with Mechanical Wide Angle Gimbal.
- 4) Shuttle Would Be Stabilized in X-POP Inertial Attitude Best Inertial Attitude for Gravity Gradient Torques.
- 5) Payload Weight of 11,400 to 12,570 kg (25,100 to 27,700 lb) Depending on Which Array Group Is Flown with the Telescope.
- 6) Observation Time Efficiency of Up to 70%. This Is Possible Because of the Fast Slew Rate 0.02 rad/sec (1 deg/sec) of the Mechanical Gimbal.
- 7) Telescope Support Hardware Is Common to Solar Payloads.
- 8) No On-Orbit Access to Detectors for Maintenance.
- 9) No Eyepeice for Viewing the Telescope Field.

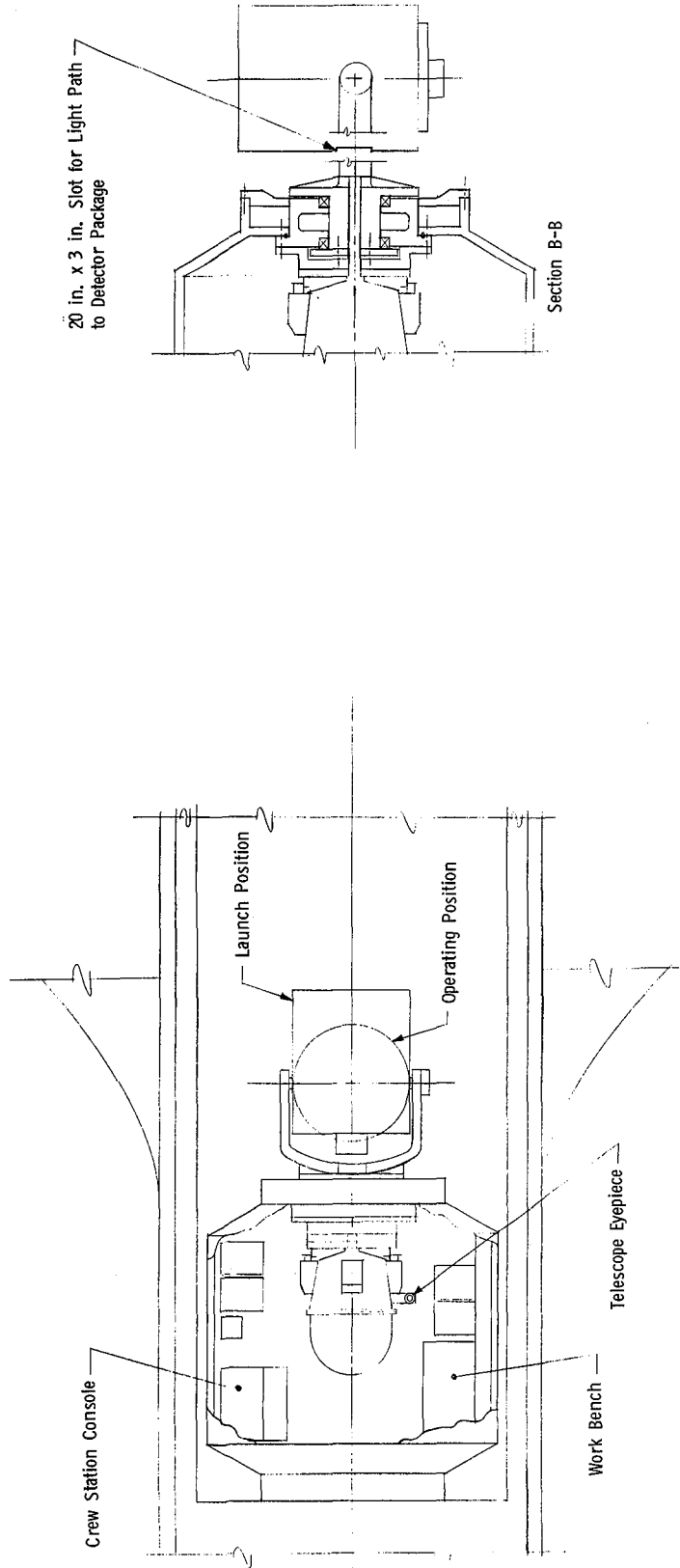


Fine Pointing System
(Gimbal Mount-Telescope Only)

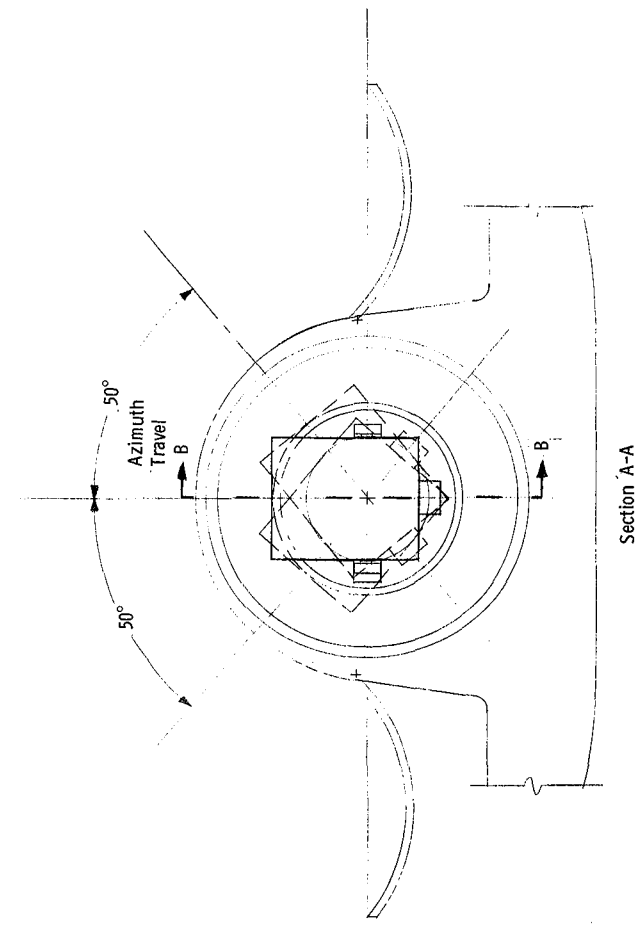
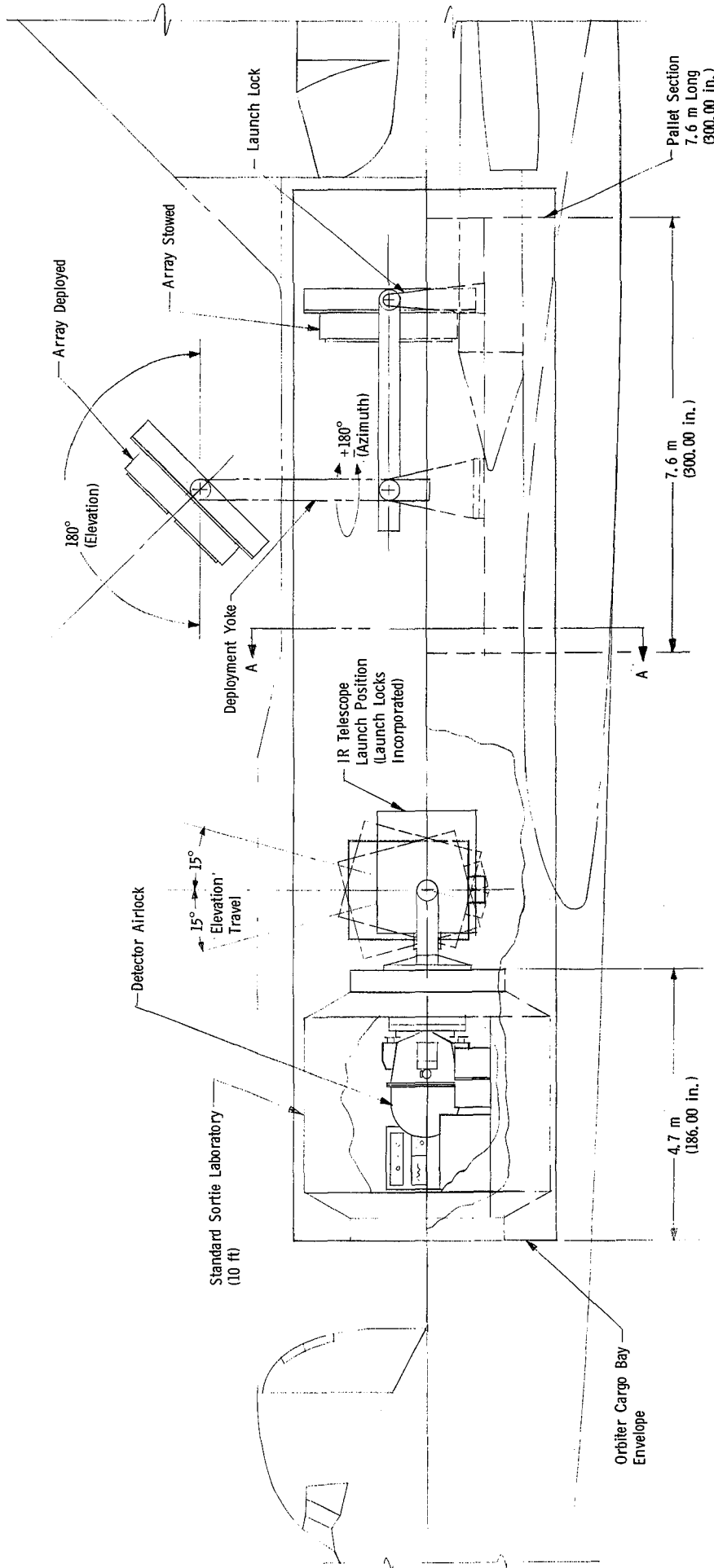


Wide Angle Gimbal Mounts Shown on Sorite Pallet in Orbiter

IR Telescope
Configuration No. 1
Fig. VI-1



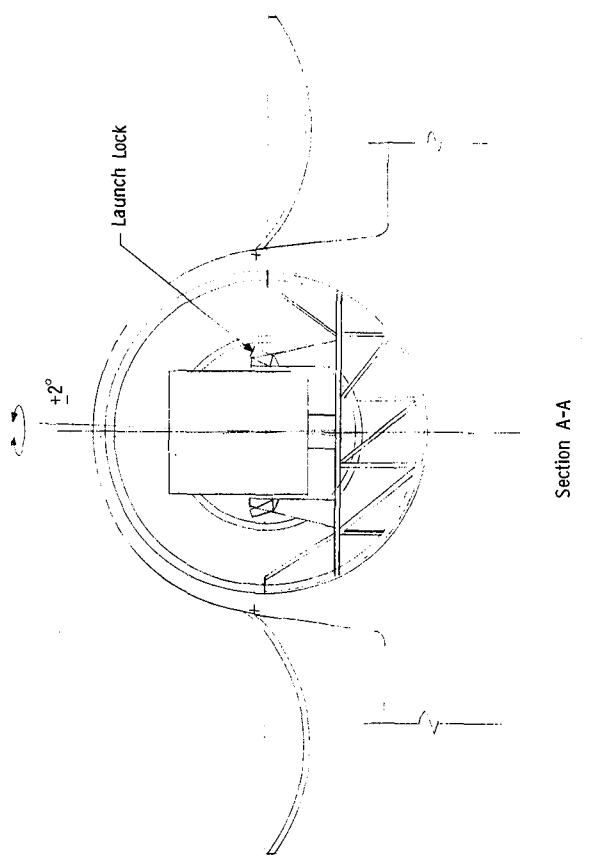
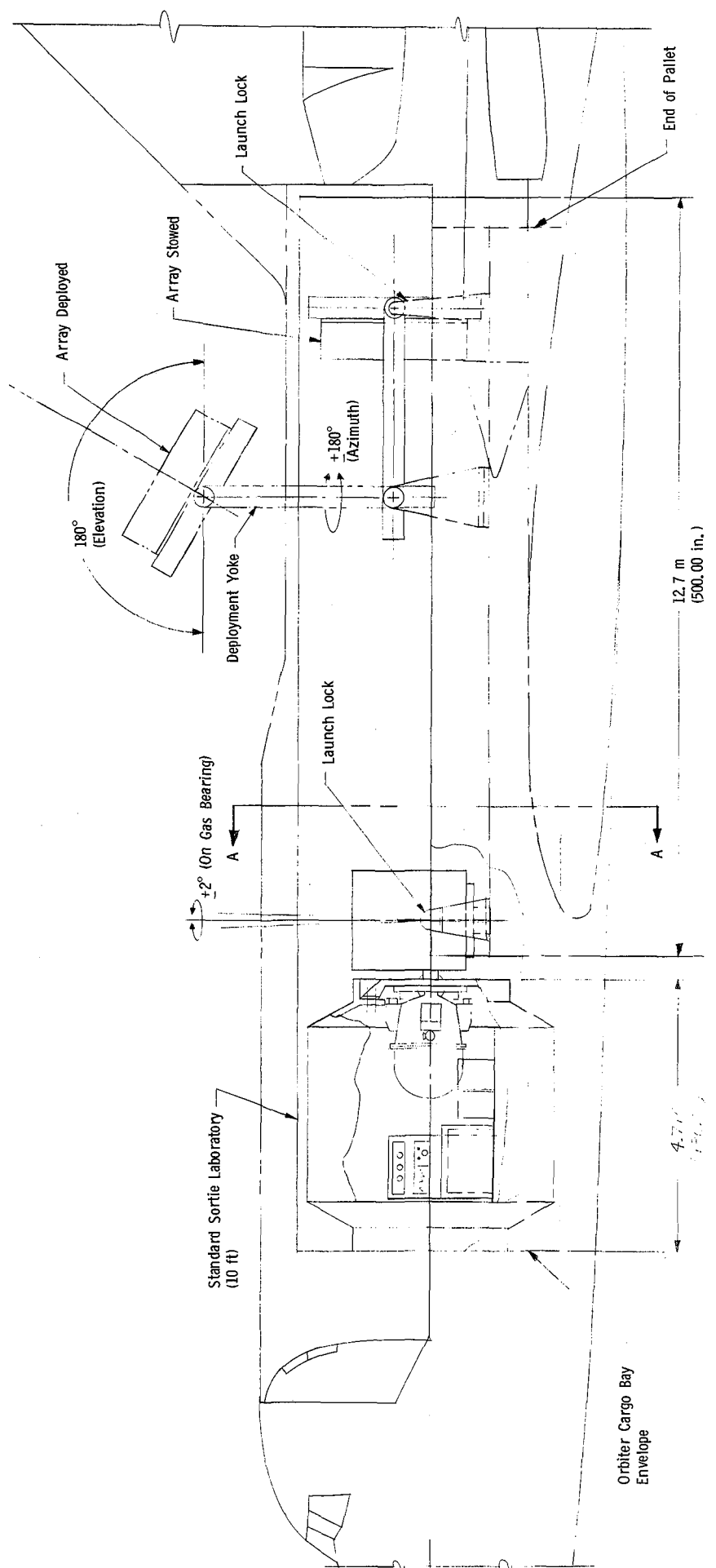
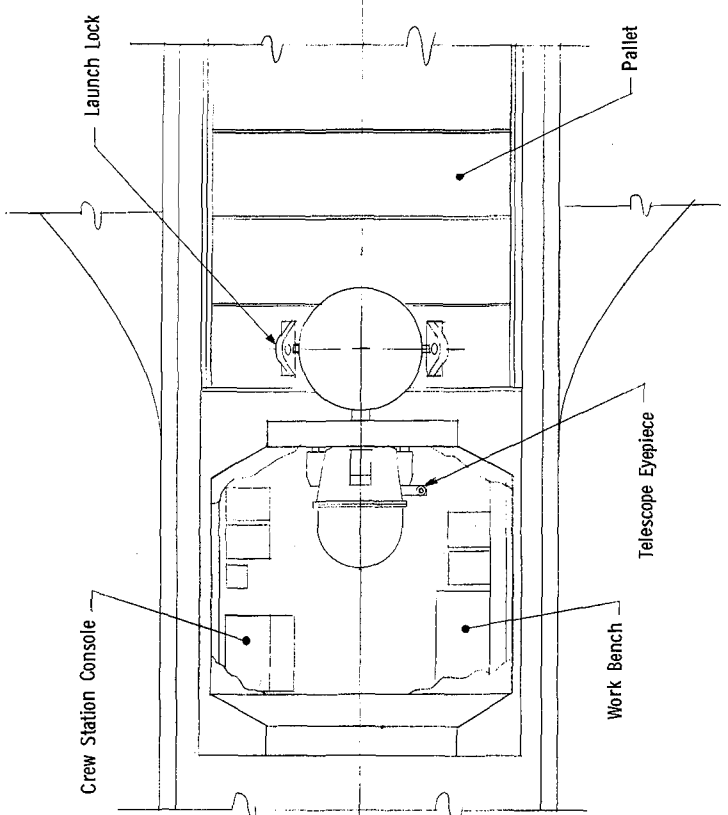
- Note:
- Sortie Lab & Pallet Data Extracted from MASAMSC Document ASR-PD-DO-72-2, Sortie Can Conceptual Design, March 1, 1972.
 - Limited Mechanical Gimbal Provides $+0.28$ radian (15 deg) in Elevation and $+0.87$ radian (50 deg) in Azimuth.
 - On-Orbit Access of Detectors Possible through Airlock.
 - Eyepiece Available for Viewing Telescope Field.
 - Special Pointing & Stabilization System Required for IR Telescope.
 - Minor Modification Required to Sortie Lab & Pallet.
 - Payload Weight of 11,650 to 12,800 kg (25,700 to 28,300 lb) Depending on Which Array Group Is Flown with the IR Telescope.
 - Telescope Overall f Number Longer (f20).
 - Moving Component in Optical Path (Tertiary Mirror Moves through $+0.13$ radian (7.5 deg) Angle.
 - Shuttle Must Be Stabilized in X-10P to Provide the Pointing Capability.
 - Shuttle Maneuvering Would Be Required, approximately 0.1 rad/min (6 deg/min).
 - Observing Time Efficiency of Approximately 32% Because of the Maneuvering Time Required.



Payload Mounted in Shuttle

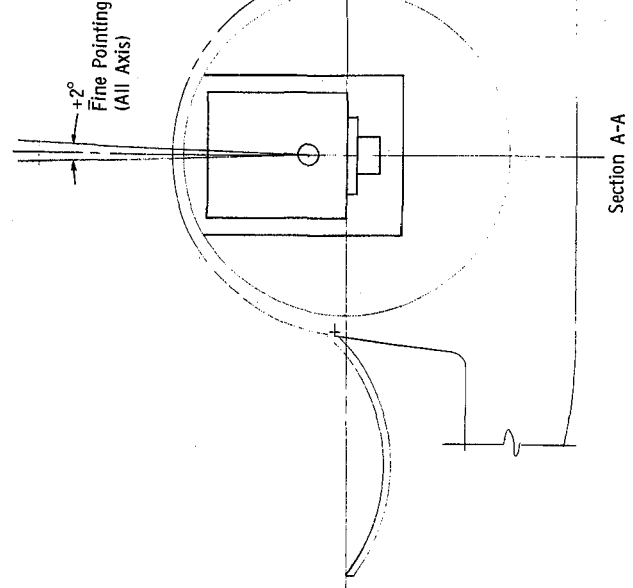
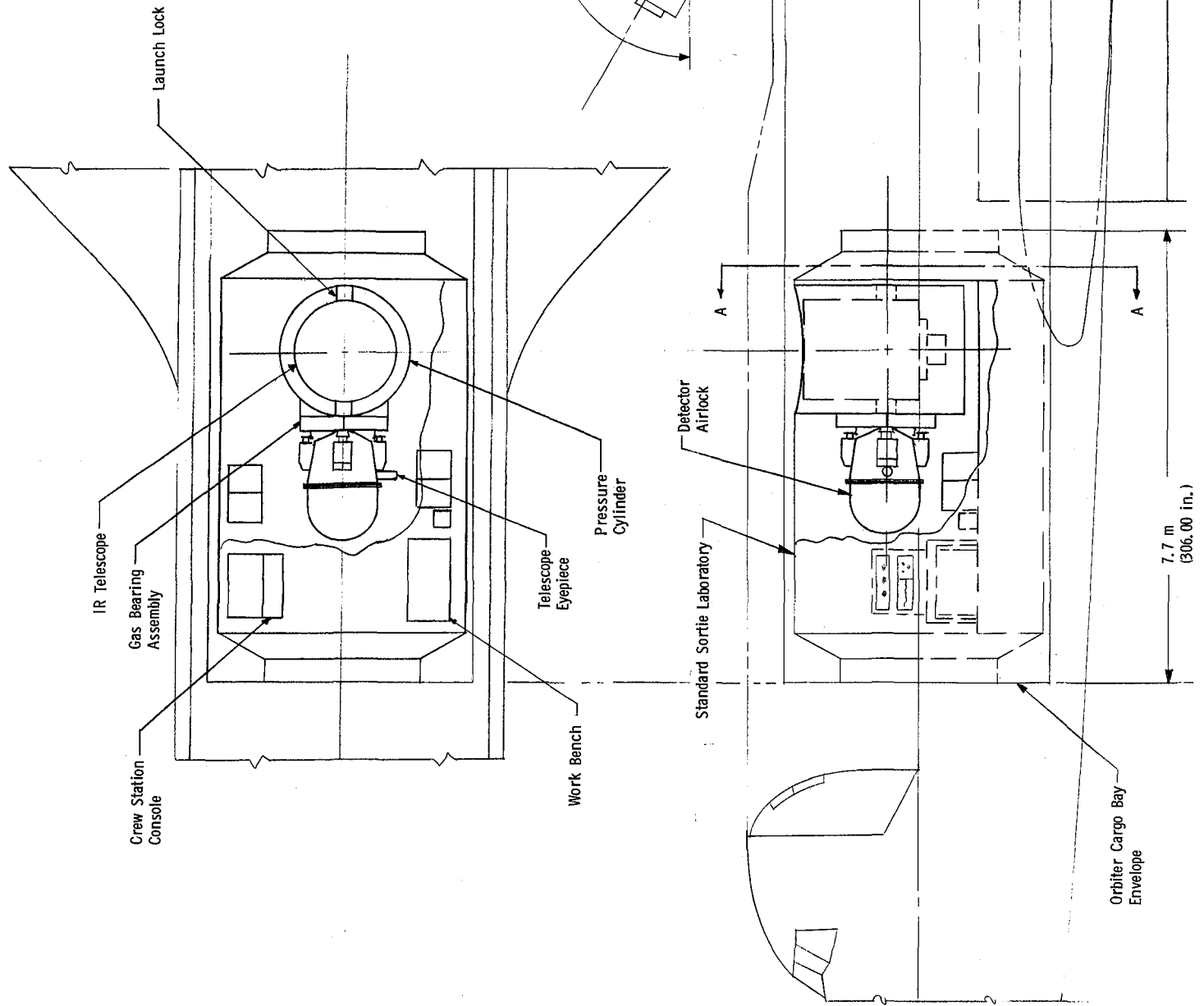
IR Telescope Configuration No. 2
Fig. VI-2

- Note:
- 1) Sortie Lab & Pallet Data Extracted from NASA/MSFC Document ASR-PD-DO-72-2, Sortie Can Conceptual Design, March 1, 1972
 - 2) On-Orbit Access of Detectors Is Possible through an Airlock.
 - 3) An Eyepiece Is Available for Viewing the Telescope Field.
 - 4) Special Stabilization System Required for IR Telescope, & Little Commonality Exists with the Solar Payloads Support Hardware.
 - 5) The Shuttle Must Maneuver to Point the Telescope Approximately 0.1 rad/min (6 deg/min).
 - 6) The Shuttle Must Maintain an X-IOP Inertial Attitude to Provide the Pointing Capability.
 - 7) Observing Time Efficiency of Approximately 32%.
 - 8) Payload Weight of 14,200 to 15,400 Kg (31,300 to 33,900 lb) Depending on Which Array Group Is Flown with the IR Telescope.
 - 9) Longer f/Number Telescope (Approximately f/20).
 - 10) Tertiary Mirror Added to Optical Path.



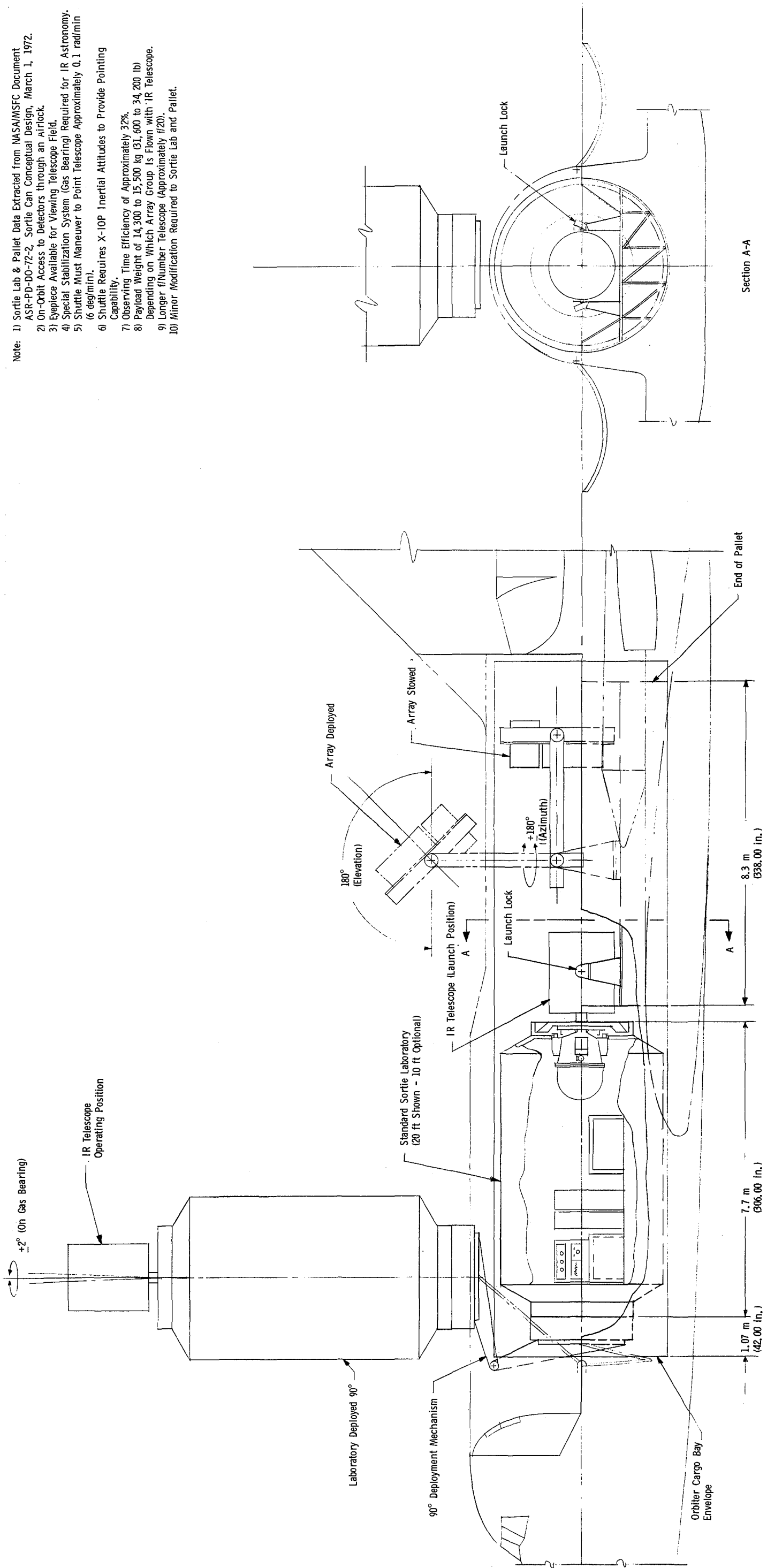
IR Telescope Mounted in Shuttle

- Note: 1) Sortie Lab & Pallet Data Extracted from NASA/MSFC ASR-PD-00-72-2, Sortie Can Conceptual Design, March 1, 1972.
- 2) On-Orbit Access to Detectors Provided through an Airlock.
 - 3) Eyepiece Available for Viewing Telescope Field.
 - 4) Special Stabilization System (Gas Bearing) Required for IR Telescope, and Very Little Commonality Exists with Solar Payloads.
 - 5) Sortie Lab Requires Major Modification to Mount Telescope.
 - 6) Shuttle Must Maneuver to Point Telescope Approximately 0.1 rad/min (6 deg/min).
 - 7) Shuttle Requires X-10P Inertial Attitude to Provide Pointing Capability.
 - 8) Observing Time Efficiency of Approximately 32%.
 - 9) Payload Weight of 15,500 to 16,600 kg (34,100 to 36,700 lb) Depending on Which Array Group Is Flown with IR Telescope.
 - 10) Longer f/Number Telescope (Approximately f/20).
 - 11) Tertiary Mirror Required in Optical Path.
 - 12) Long Sortie Laboratory Required (20-ft Cylindrical Section).



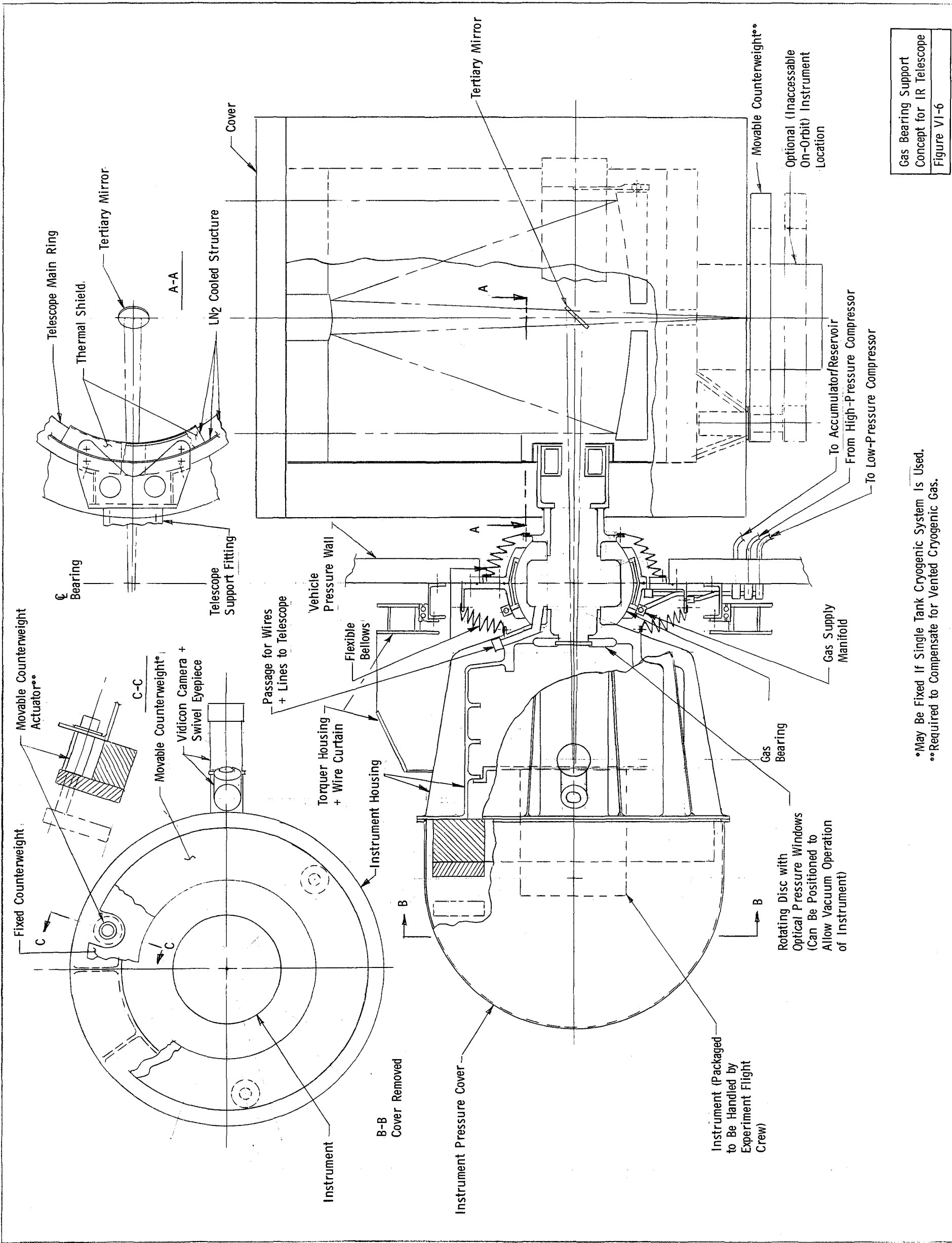
IR Telescope Configuration No. 4
Figure VI-4

- Note:
- 1) Sortie Lab & Pallet Data Extracted from NASA/MSFC Document ASR-PD-DO-72-2, Sortie Can Conceptual Design, March 1, 1972.
 - 2) On-Orbit Access to Detectors through an Airlock.
 - 3) Eyepiece Available for Viewing Telescope Field.
 - 4) Special Stabilization System (Gas Bearing) Required for IR Astronomy.
 - 5) Shuttle Must Maneuver to Point Telescope Approximately 0.1 rad/min (6 deg/min).
 - 6) Shuttle Requires X-10P Inertial Attitudes to Provide Pointing Capability.
 - 7) Observing Time Efficiency of Approximately 32%.
 - 8) Payload Weight of 14,300 to 15,500 kg (31,600 to 34,200 lb) Depending on Which Array Group Is Flown with IR Telescope.
 - 9) Longer f/Number Telescope (Approximately f/20).
 - 10) Minor Modification Required to Sortie Lab and Pallet.



Payload Mounted in Shuttle

IR Telescope Configuration No. 5
Figure VI-5



Gas Bearing Support
 Concept for IR Telescope
 Figure VI-6

*May Be Fixed If Single Tank Cryogenic System Is Used.
 **Required to Compensate for Vented Cryogenic Gas.

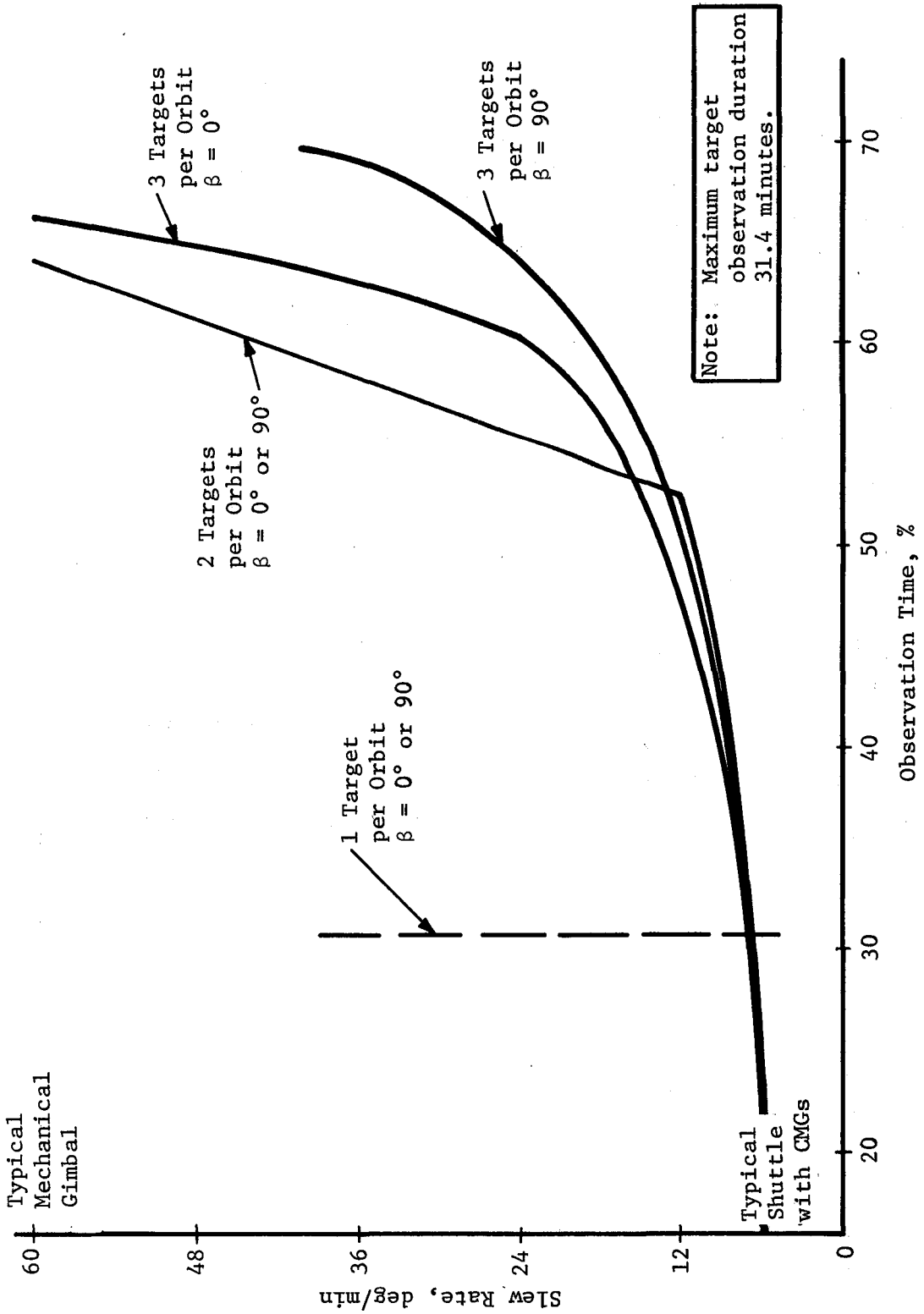


Fig. VI-7 IR Telescope Observation Time

For the above reasons, the maximum observing time shown on Fig. VI-1 thru VI-5 for those IR telescopes using Shuttle pointing was 32%. This corresponds to one target per orbit for a maximum of 34.4 minutes. It would be possible to view several targets in the same general area of the celestial sphere, but the total observing time would be approximately 34.4 min.

Table VI-1 summarizes the operational parameters for the five alternatives. The primary advantages and disadvantages for each of the five alternatives are listed below.

Table VI-1 Operation Parameters

Parameter	Config 1	Config 2	Config 3	Config 4	Config 5
Slew Rate	0.02 rad/sec (1 deg/sec)	0.1 rad/min (6 deg/min)			
No. of Targets/Orbit	3 max	1 max	1 max	1 max	1 max
Time per Target (max)	31.4 min	31.4 min	31.4 min	31.4 min	31.4 min
Operating Efficiency	70%	32%	32%	32%	32%
Monitor	Vidicon thru Aux Telescope	Eyepiece or Vidicon	Eyepiece or Vidicon	Eyepiece or Vidicon	Eyepiece or Vidicon
On-Orbit Access to Detectors	None	Thru Airlock	Thru Airlock	Thru Airlock	Thru Airlock
Shuttle Inertial Attitude	X-POP	X-IOP	X-IOP	X-IOP	X-IOP
Telescope Pointing	Az & El Gimbal	Shuttle	Shuttle	Shuttle	Shuttle
Telescope Adjustments	Remote Cont	Remote Cont	Remote Cont	Remote Cont	Remote Cont

CONFIGURATION NO. 1

ADVANTAGES:

- 1) Hemispherical coverage available with wide angle gimbal
- 2) Fast slew rate with mechanical gimbal 0.02 rad/sec (1 deg/sec)
- 3) Telescope support hardware common to solar payloads
- 4) No modifications required to Sortie Lab and pallet
- 5) Minimum weight configuration - 11,400 to 12,570 kg (25,100 to 27,700 lb)
- 6) X-POP shuttle inertial attitude possible
- 7) High-speed telescope f/10 system
- 8) Maximum observation time - up to 70% efficiency

DISADVANTAGES:

- 1) No on-orbit access to detectors
- 2) No eyepiece for viewing the telescope field

CONFIGURATION NO. 2

ADVANTAGES:

- 1) On-orbit access of detectors through an airlock
- 2) Eyepiece available for viewing telescope field
- 3) Limited gimbal provides ± 0.28 radian (15 deg) in elevation and ± 0.87 radian (50 deg) in azimuth
- 4) Payload weight 11,650 to 12,800 kg (25,700 lb to 28,300 lb)

DISADVANTAGES:

- 1) Special pointing and stabilization system for IR telescope
- 2) Longer system f/number (approximately f/20)

- 3) Moving component in optical path; tertiary mirror tracks
+ 0.13 radian (7.5 deg)
- 4) Primary mirror would see hot structure thru light path slit
(approximately 3 X 20 in. slit)
- 5) Shuttle must be stabilized in X-IOP attitude
- 6) Shuttle maneuvering would be required; approximately 0.1 rad/
min (6 deg/min)
- 7) Telescope would be limited to viewing one area of the cele-
stial sphere because of limited maneuver rate of Shuttle with
CMGs. Observing time efficiency $\approx 32\%$
- 8) Minor modifications required on Sortie Lab to mount telescope
in aft closure
- 9) Sortie pallet will require minor modifications to adapt to
new tie down points

CONFIGURATION NO. 3

ADVANTAGES:

- 1) On-orbit access of detectors through an airlock
- 2) Eyepiece available for viewing telescope field

DISADVANTAGES:

- 1) Special stabilization system (gas bearing) required for IR
astronomy
- 2) Shuttle must maneuver to point telescope; approximately 0.1
rad/min (6 deg/min)
- 3) Shuttle inertial attitude of X-IOP required
- 4) Observing time efficiency of approximately 32%
- 5) Payload weight 14,200 to 15,400 kg (31,300 to 33,900 lb)
- 6) Longer f number telescope (approximately f/20)

- 7) Tertiary mirror added to optical path
- 8) Minimum commonality with solar payloads
- 9) Minor modifications required on Sortie Lab and pallet

CONFIGURATION NO. 4

ADVANTAGES:

- 1) On-Orbit access of detectors through an airlock
- 2) Eyepiece available for viewing telescope field

DISADVANTAGES:

- 1) Special stabilization system (gas bearing) required for IR astronomy
- 2) Major modifications required to sortie laboratory
- 3) Shuttle must maneuver to point telescope; approximately 0.1 rad/min (6 deg/min)
- 4) Shuttle inertial attitude of X-IOP required
- 5) Observing time efficiency of approximately 32%
- 6) Payload of 15,550 to 16,600 kg (34,100 to 36,700 lb)
- 7) Longer f number telescope (approximately f/20)
- 8) Tertiary mirror added to optical path

CONFIGURATION NO. 5

ADVANTAGES:

- 1) On-orbit access of detectors through an airlock
- 2) Eyepiece available for viewing telescope field
- 3) No tertiary mirror required

DISADVANTAGES:

- 1) Special stabilization system (gas bearing) required for IR astronomy
- 2) IR telescope must be deployed from cargo bay
- 3) Shuttle must maneuver to point telescope; approximately 0.1 rad/min (6 deg/min)
- 4) Shuttle inertial attitude of X-IOP required
- 5) Observing time efficiency of approximately 32%
- 6) Payload weight of 14,300 to 15,500 kg (31,600 to 34,200 lb)
- 7) Longer f/number telescope (approximately f/20)
- 8) Minor modifications to Sortie Lab and pallet

C. RECOMMENDED CONFIGURATIONS

Based on this preliminary examination of the alternative concepts, it was recommended that the Astronomy Sortie Mission Definition Study maintain the current baseline configuration for the IR telescope, which is configuration No. 1 shown in Fig. VI-1.

The desirability for on-orbit shirt-sleeve access to the telescope detectors has been expressed several times by UV and IR astronomers. This subject should be addressed in some detail by a separate study to determine what the costs and benefits are and a firm position established for the Astronomy Sortie missions.